UNIVERSITÀ DI PARMA

UNIVERSITA' DEGLI STUDI DI PARMA

DOTTORATO DI RICERCA IN NEUROSCIENZE

CICLO XXXVII

Surface-based analysis of cortical FLAIR intensity. Clinical application in epilepsy surgery and its translational potential for basic neuroscience research.

Coordinatore:

Chiar.mo Prof. Luca Bonini

Tutore:

Chiar.mo Prof. Pietro Avanzini

Dottorando: Dr. Francesco Cardinale

Anni Accademici 2021/2022 – 2023/2024

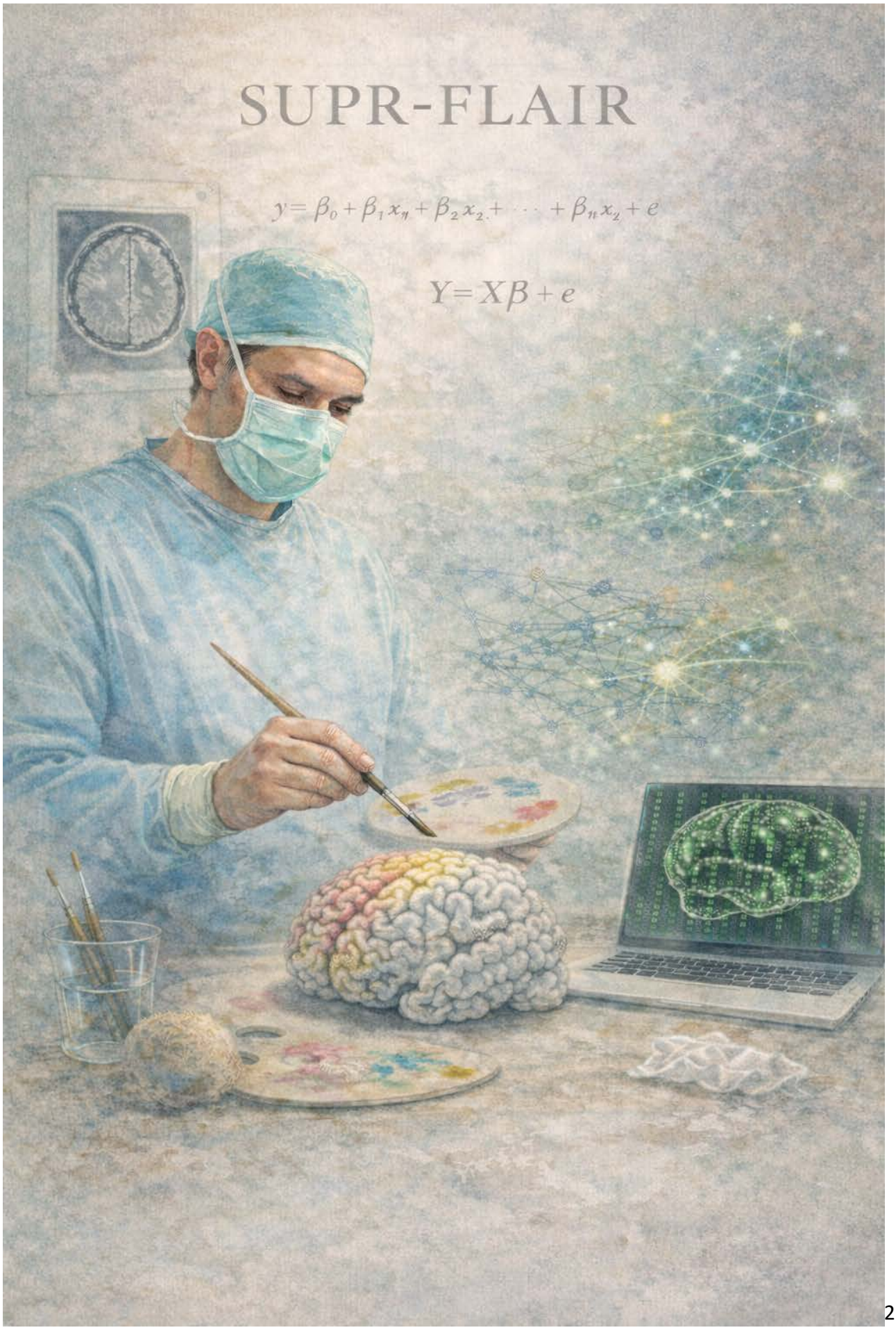
SUPR-FLAIR
$y = \beta_0 + \beta_1 x_1 + \beta_2 x_2 + \cdots + \beta_n x_2 + e$
$Y = X\beta + e$

To my family, who accepted that I could be at home and absent at the same time, and loved me anyway

ABSTRACT AND ABBREVIATIONS

Abstract

Background. Epilepsy surgery critically depends on accurate delineation of the epileptogenic zone (EZ). While the presence of an MRI-visible lesion is a strong predictor of postoperative seizure freedom, many drug-resistant patients are MRI-negative on conventional inspection. Focal Cortical Dysplasia (FCD) and other subtle cortical abnormalities potentially leave a signature on cortical FLuid Attenuated Inversion Recovery (FLAIR) signal. This thesis introduces and evaluates a surface-based framework for the analysis of cortical FLAIR intensity, SUrface-PRojected FLAIR (SUPR-FLAIR) and its statistical extension (SUPR-FLAIR-sa), both as tools for advanced diagnostic work-up and surgical planning, and as probes of cortical functional organization.

Methods. We implemented a pipeline combining T1w–FLAIR coregistration, voxel-wise normalization of FLAIR to the white-matter median, and "projection" of normalized intensities onto FreeSurfer brain surfaces (SUPR-FLAIR). Vertex-wise generalized linear models (GLMs) were then applied for single-patient versus control comparisons (SUPR-FLAIR-sa) and for group-level analyses, adjusting for covariates where appropriate. Chapter I presents a pilot study and illustrative clinical cases (FCD, Hippocampal Sclerosis —HS—, tumor-related epilepsy) in which SUPR-FLAIR/SUPR-FLAIR-sa were integrated into multimodal 3D planning for StereoElectroEncephaloGraphy (SEEG) and resections. Chapter II reports a retrospective cohort of 29 MRI-negative, presumed Temporal Lobe Epilepsy (TLE) patients who underwent temporal surgery, including a diagnostic-performance analysis in a subset of 21 patients and 30 healthy controls. Chapter III investigates the translational potential of SUPR-FLAIR in 95 healthy volunteers through: (experiment A) "between-subjects" analyses relating cortical FLAIR patterns to language lateralization and handedness/dexterity; and (experiments B–D) "within-subject" paired analyses testing short-timescale task- or state-locked modulations (finger tapping, eye-movement paradigms, eyes-open rest vs. eyes-closed rest).

Results. In surgical cases, SUPR-FLAIR proved useful for rapidly visualizing MRI-visible cortical lesions on the surface and embedding them into multimodal 3D scenes. SUPR-FLAIR-sa reliably detected MRI-visible FCDs and, in selected MRI-negative patients, uncovered subtle lesional clusters that were concordant with SEEG-defined EZ and histology. In the MRI-negative temporal cohort, SUPR-FLAIR-sa achieved an estimated sensitivity of ~54% and specificity of ~45% under conservative case

definitions, with resection of the peak cluster associated with higher seizure-freedom rates, particularly when concordant with SUPR-PET-sa. Across multiple etiologies, SUPR-FLAIR-sa also revealed extra-lesional hyperintense territories that mapped onto epileptic networks and could partially normalize or reconfigure after surgery, suggesting dynamic network-level effects.

In healthy volunteers, between-subjects analyses showed that cortical FLAIR intensity patterns vary with hemispheric language dominance and handedness, yielding bilateral but asymmetric differences across language areas, occipito-temporal streams, sensorimotor regions, and the cingulate cortex. "Within-subject" experiments demonstrated small but consistent increases in normalized FLAIR signal in task-relevant regions (e.g., hand-knob and Supplementary Motor Area (SMA) during finger tapping; visual and oculomotor areas during visual/eye-movement conditions; occipital cortex in eyes-open vs. eyes-closed rest), despite very small effect sizes and limited samples.

Conclusion. SUPR-FLAIR and SUPR-FLAIR-sa provide a flexible surface-based framework that augments conventional MRI in epilepsy surgery by improving lesion visualization, supporting presurgical hypothesis generation, and offering additional localization cues even in MRI-negative cases. At the same time, the observed trait- and state-dependent patterns in healthy brains indicate that cortical FLAIR signal is not purely structural but also reflects aspects of functional organization and transient physiological states. Together, these findings argue for SUPR-FLAIR as a promising bridge between structural and functional imaging, with both immediate clinical utility and substantial potential for future basic neuroscience research, provided that technical limitations (notably scanner specificity and small effect sizes) are addressed in larger, rigorously designed studies.

Abbreviations

- ^{18}F-FDG-PET: FluoroDeoxyGlucose F-18 Positron Emission Tomography
- 2D: Bi-Dimensional
- 3D: Three-Dimensional
- ADC: Apparent Diffusion Coefficient
- ASST GOM Niguarda: Azienda Socio-Sanitaria Territoriale Grande Ospedale Metropolitano Niguarda
- BASH: Bourne Again Shell

- BBB: Blood–Brain Barrier
- BCI: Brain-Computer Interface
- BOLD: Blood Oxygen Level Dependent
- CBF: Cerebral Blood Flow
- CSF: Cerebro-Spinal Fluid
- CCEP: Cortico-Cortical Evoked Potentials
- CSV: Comma-Separated Values (file format)
- CWP: Cluster-Wise Probability
- DICOM: Digital Imaging and COmmunications in Medicine
- DTI: Diffusion Tensor Imaging
- EC: Eyes Closed
- ECR: Eyes Closed Rest
- EEG: ElectroEncephaloGraphy
- EM: Eyes Moving
- EO: Eyes Open
- EOR: Eyes Open Rest
- EZ: Epileptogenic Zone
- f-MRI: functional MRI
- FEF: Frontal Eye Field
- FN: False Negative
- FP: False Positive
- FCD: Focal Cortical Dysplasia
- FFE: Fast Field Echo
- FLAIR: FLuid Attenuated Inversion Recovery (a software package)
- FlaT1: a junction and extension z-score map based on 3D-T1w, 3D-Flair, and a mean template (software tool provided by SWANE software package)
- FLIRT: FMRIB's Linear Image Registration Tool (a software tool)
- FMRIB: Functional Magnetic Resonance Imaging of the Brain
- FSGD: FreeSurfer Group Descriptor (file format)
- FSL: FMRIB Software Library
- FT: Fiber Tracking

- G_postcentral: Gyrus postcentralis (Destrieux atlas)
- G_precentral: Gyrus precentralis (Destrieux atlas)
- GLM: Generalized Linear Model
- GMV: Gray Matter Volume
- GWMI: Gray/White Matter Interface
- HS: Hippocampal Sclerosis
- L: left-hander
- Lat_Fissure-post_sgt: Lateral Fissure – Posterior Segment (Destrieux atlas)
- lh_langdom: subject with left-hemisphere dominance for language
- IQR: Inter-Quartile Range
- M1: Primary Motor Cortex
- MAP18: Morphometric Analysis Program 18 (software package)
- MELD: Multi-centre Epilepsy Lesion Detection (software package)
- MGH: Massachusetts General Hospital (file format, with MGZ as compressed variant)
- MRI: Magnetic Resonance Imaging
- MPR: MultiPlanar Reconstruction
- MTPlus (Middle Temporal area, or MT/V5 complex)
- MTLE: Mesial Temporal Lobe Epilepsy
- NIfTI: Neuroimaging Informatics Technology Initiative
- NKA: Na^+/K^+ ATPase pump
- NODDI: Neurite Orientation Dispersion and Density Imaging
- NPV: Negative Predictive Value
- PRC: Peri-Rolandic Cortex
- PET: Positron Emission Tomography
- PHANTOMS (script): PHysiology and ANaTOmy Management for Surgery (a software tool)
- PLNTY: Polymorphous Low-Grade Neuroepithelial Tumor of the Young
- PPV: Positive Predictive Value
- PT: Planum Temporale
- PVR: Per-Vertex Regressor
- QDEC: Query, Design, Estimate, Contrast (a software tool provided by FreeSurfer)
- R: right-hander

- rh_langdom: subject with right-hemisphere dominance for language
- RHFT: Right-Hand Finger Tapping
- RFTC: Radio-Frequency Thermo-Coagulation
- RZ: Resection Zone
- S_calcarine: Sulcus calcarine (Destrieux atlas)
- S_occipital_ant: Sulcus occipitalis anterior (Destrieux atlas)
- S_occipital_superior: Sulcus occipitalis superior (Destrieux atlas)
- SBA: Surface-Based Analysis
- SD: Standard Deviation
- SEEG: StereoElectroEncephaloGraphy
- SENSE: SENSitivity Encoding
- SMA: Supplementary Motor Area
- SNR: Signal-to-Noise Ratio
- SUPR-FLAIR: SUrface-PRojected-FLAIR
- SUPR-FLAIR-sa: SUPR-FLAIR statistical analysis
- SUPR-PET: SUrface-PRojected-PET
- SUPR-PET-sa: SUPR-PET statistical analysis
- SWANe: Standardized Workflow for Advanced Neuroimaging in Epilepsy (software package)
- T1w: T1 weighted
- TE: Time of Echo
- TLE: Temporal Lobe Epilepsy
- TN: True Negative
- TP: True Positive
- TR: Time of Repetition
- TSE: Turbo Spin-Echo
- V1: Primary Visual Area
- V3: Visual Area 3
- VBM: Voxel-Based Morphometry
- zsh: Z shell of Apple Mac computers

TABLE OF CONTENTS

INTRODUCTION

Epilepsy surgery is an established treatment for drug-resistant epilepsy (Wiebe et al., 2001), grounded in the concept of the EZ, defined as “the site of the beginning and of primary organization of the epileptic seizures” (Munari & Bancaud, 1985). The presence of an MRI-visible lesion is a strong positive predictor of postoperative seizure freedom (Spencer & Huh, 2008; Téllez-Zenteno et al., 2010). Among MRI-negative, drug-resistant epilepsies, FCD is the most frequent underlying substrate (Wang et al., 2013). Accordingly, multiple post-processing strategies have been developed to enhance MRI sensitivity for subtle FCDs, including Voxel-Based Morphometry (VBM), voxel-wise intensity analysis, sulcal morphometry, computational modeling, diffusion MRI, and functional imaging approaches (Huppertz et al., 2005; Duncan, 2010; Bernasconi et al., 2011; Dorfer et al., 2015). Surface-Based Analyses (SBA) of common morphometric metrics have been reported (Thesen et al., 2011; Ahmed et al., 2015), as has an automated classifier leveraging surface-derived features of FCD morphology and intensity (Hong et al., 2014). More recently, mixed-method platforms have also been introduced (Sone et al., 2021; Spitzer et al., 2022; Wagstyl et al., 2022; Genovese et al., 2024).

A preliminary automated reconstruction of the cortical surface provided the basis for vertex-wise analyses in many of these studies. FreeSurfer (Dale et al., 1999; Fischl, 2012) remains the most widely used package for automated 3D cortical surface reconstruction and vertex-wise statistical mapping of morphometric properties. It is typically applied to investigate physiological and pathological conditions by comparing groups of subjects nonlinearly registered to a common space. At the “Claudio Munari” Center for Epilepsy Surgery, ASST GOM Niguarda, Milan, FreeSurfer has been integrated into the presurgical workflow since 2008, primarily because automated cortical surface models facilitate surgical planning (Cardinale et al., 2012, 2013, 2015). Multimodal 3D imaging, encompassing surface models (pial surface, cerebral vasculature, and intracerebral electrodes) and volumetric datasets — structural MRI, functional MRI (f-MRI), FluoroDeoxyGlucose F-18 Positron Emission Tomography (^{18}F-FDG-PET), Diffusion Tensor Imaging, and Fiber Tracking (FT) —, is routinely employed to support advanced diagnostics and planning for SEEG or resections. Most FreeSurfer-based investigations have leveraged its surface reconstruction and morphometry pipelines. Several capabilities have been validated against ex vivo data (Rosas et al., 2002; Cardinale et al., 2014), supporting the reliability of this software. Over time, we have expanded the set of

FreeSurfer tools incorporated into our presurgical workflow. The projection of signal intensity from FLAIR sequences onto the cortical surface has proved useful for planning resections of MRI-visible lesions. We also found that visual inspection of cortical surfaces with scalar FLAIR overlays can facilitate detection of subtle regions with increased FLAIR signal. In addition, we explored SBA to identify subtle FCDs, and we investigated whether the same framework could highlight subtle "static" or "dynamic" variations in cortical FLAIR intensity linked not to overt structural abnormalities but to anatomo–physiological features or events.

The aim of the present work is twofold: first (chapter I), to synthesize our first findings (some previously published), and second, to present two new studies (chapters II-III), one assessing the diagnostic performance of SUPR-FLAIR-sa in the clinical context of epilepsy surgery, and another evaluating the translational potential of this technique for basic neuroscience research. Therefore, chapters I–III will present the aims, methods, results, limitations, and principal conclusions separately for each main study, whereas a unified, overarching discussion will be provided in chapter IV.

CHAPTER I: THE DAWN OF SUPR-FLAIR AND FIRST MOUNTING EVIDENCE

Our first data include the cohort reported in a pilot study (Cardinale et al., 2015) together with some subsequent case studies. Therefore, the method and the results reported in this chapter predate the doctoral study period.

The birth of an idea for clinical application in epilepsy surgery

The initial objective was pragmatic: leverage FreeSurfer tools, already embedded in our workflow for assembling multimodal 3D scenes to manage SEEG implantations and craniotomy-based resections, to delineate the location and contours of hyperintense cortical epileptogenic lesions on FLAIR scan. We routinely constructed these scenes in 3D Slicer (Pieper et al., 2004; Fedorov et al., 2012), importing volumetric images already co-registered with FLIRT (FMRIB's Linear Image Registration Tool), an FSL (FMRIB Software Library) tool (Jenkinson et al., 2001, 2012), alongside surfaces estimated by FreeSurfer. To streamline the substantial image-processing workload, we developed an in-house BASH (Bourne Again SHell) pipeline, namely PHANTOMS (PHysiology and ANaTOmy Management for Surgery). Because manual slice-by-slice contouring of MRI-visible lesions is time-consuming, we extended PHANTOMS to project voxel-wise FLAIR intensities onto cortical surfaces (pial, Gray/White Matter Interface —GWMI—, or inflated), thereby accelerating and facilitating lesion visualization.

SUPR-FLAIR (SUrface PRojected FLAIR): “painting” the cortical surface with FLAIR signal

We termed this procedure SUPR-FLAIR: a surface-projection method that maps voxel-wise FLAIR intensity onto the cortical sheet (pial, GWMI, or inflated surfaces), effectively “painting” the brain surface to highlight candidate hyperintense cortical abnormalities.

Methods

MRI acquisition. MRI data were acquired on a Philips Achieva 1.5 T scanner (Philips Healthcare, Best, The Netherlands) using an eight-channel head coil and SENSE (SENSitivity Encoding) parallel imaging.

Two sequences essential to the study were obtained in all patients: (a) a 3D Fast Field Echo (FFE) T1w volume —contiguous axial sampling; reconstructed matrix 560 × 560; voxel size 0.46 × 0.46 × 0.90 mm; no interslice gap; Time of Repetition (TR)= 7.3 ms; Time of Echo (TE)= 3.3 ms — and (b) an axial Turbo Spin-Echo (TSE) FLAIR sequence (matrix 288 × 288; voxel size 0.87 × 0.87 × 3.0 mm; 0.6 mm interslice gap; TR= 11 ms; TE= 140 ms). These sequences formed part of our routine diagnostic protocol (Colombo et al., 2012).

Data processing. All datasets were originally processed with FSL 5.0.9 and FreeSurfer 5.3.0 on Apple Mac Pro workstations (2 × 2.26 GHz Quad-Core Intel Xeon; macOS 10.11.1). Processing focused on cortical surface reconstruction and FLAIR-to-surface mapping. Multimodal 3D scenes were assembled with 3D Slicer 4.5.0-1.

File format conversion. DICOM (Digital Imaging and COmmunications in Medicine) images were converted to NIfTI (Neuroimaging Informatics Technology Initiative) or MGH (Massachusetts General Hospital) format using FreeSurfer's `mri_convert`.

Image registration. Within-subject linear registrations were performed with FSL's FLIRT. The FLAIR volume was automatically registered to the 3D T1w-FFE dataset using a six-degree-of-freedom metric, mutual-information cost function, and sinc interpolation for resampling. After completion of the FreeSurfer pipeline (see below), inter-subject nonlinear registrations were carried out with `mri_cvs_register`, aligning each subject to the `fsaverage` template to enable vertex-wise statistical analyses (see SUPR-FLAIR-sa).

FLAIR intensity normalization. The white-matter mask was generated with FreeSurfer-derived brain masks to remove extracerebral misclassifications. This white-matter mask was then applied to the FLAIR volume registered to T1w-FFE. Finally, each FLAIR voxel intensity was normalized by dividing by the median intensity of white-matter voxels. Masking, arithmetic operations, and summary statistics were performed with FSL tools (`fslmaths`, `fslstats`).

Brain surface estimation. The 3D T1w-FFE dataset was processed with FreeSurfer's `recon-all` surface-based stream, including affine registration to Talairach space, intensity nonuniformity correction, and skull stripping. Hemispheric separation, brainstem and cerebellar removal were followed by estimation of the GWMI and pial surfaces. GWMI and pial reconstructions were visually

inspected and manually corrected as needed in all subjects. All datasets were processed with the same FreeSurfer version and operating system to avoid version-related variability (Gronenschild et al., 2012; Chepkoech et al., 2016).

Projection of normalized FLAIR onto the brain surface. Normalized FLAIR signal was sampled along the surface normal using FreeSurfer's `mri_vol2surf`, restricting sampling to cortical-ribbon voxels. The resulting scalar file provides vertex-wise normalized FLAIR intensities, effectively projecting FLAIR onto the cortical sheet for subsequent visualization and analysis.

The workflow described above is summarized in Figure 1, Figure 2, and Figure 3.

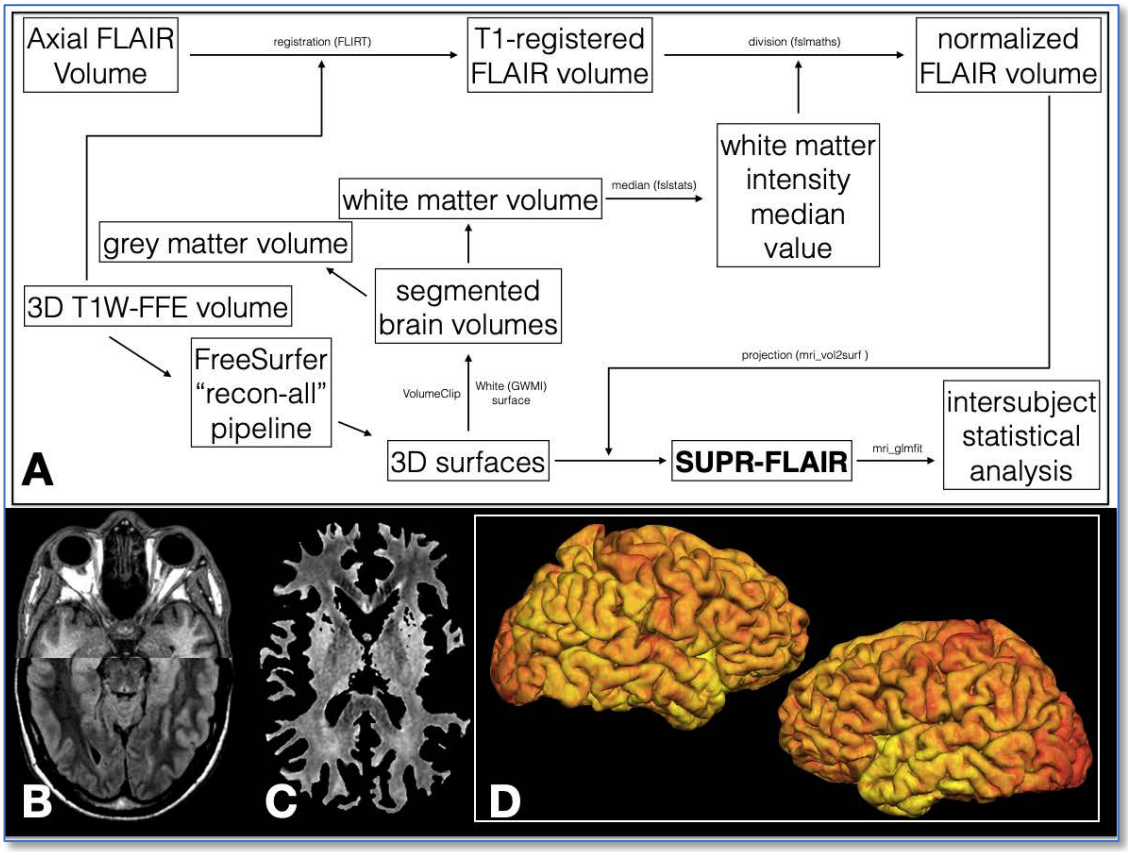

Figure 1: Image processing workflow.
(A*) Schematic of the processing pipeline. The version presented here is slightly updated compared with the one published in 2015 (Cardinale et al., 2015). (B) Registration: axial FLAIR aligned to the 3D T1w-FFE volume (split overlay view). (C) Normalization: the median intensity of the white-matter segmentation is used to normalize the axial FLAIR (each voxel divided by the WM median), yielding a unitless map (see also Figure 2). (D) SUPR-FLAIR: bilateral lateral views of the pial surface in a healthy subject, overlaid with vertex-wise normalized cortical FLAIR intensity. A heat colormap is used (red→ yellow = lower→ higher values). Note that cortical FLAIR intensity is not spatially uniform and varies in a manner consistent with known cytoarchitectonic patterns, for example, relatively lower values in the central and occipital regions bilaterally (see also Figure 20). Software tool: from FSL, we used FLIRT for linear registration, fslmaths for image arithmetic, and fslstats for summary statistics. From FreeSurfer, we used recon-all to run the core surface-based pipeline, mri_vol2surf to sample volumetric values onto cortical vertices, and mri_glmfit for vertex-wise generalized linear modeling. VolumeClip is a 3D Slicer extension for volumetric clipping/mask generation, available via Extension Manager or from Github website (https://github.com/PerkLab/SlicerVolumeClip).*

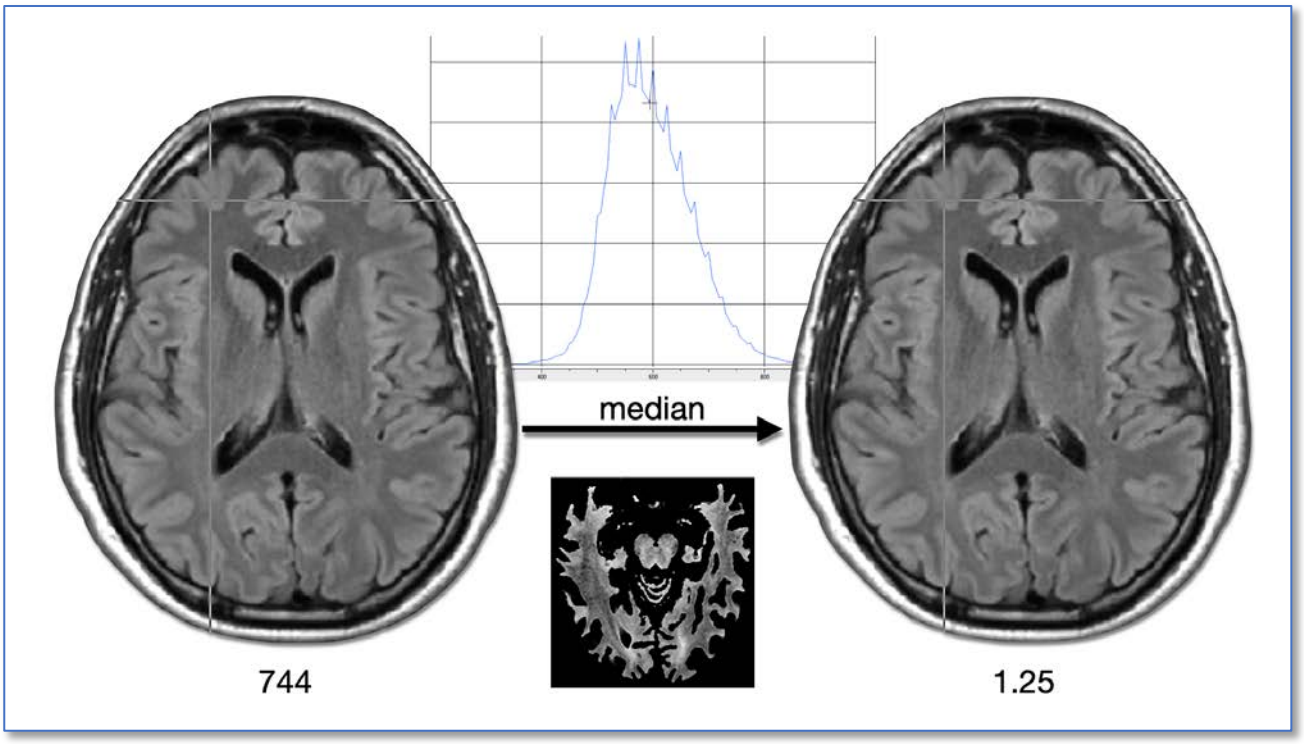

Figure 2: Intensity normalization.
The median intensity value of white matter voxels (shown in the central panel) is used as a divisor for the intensity of all voxels in the FLAIR dataset. The same voxel indicated by the cursor has an intensity of 744 in the original dataset (left) and 1.25 in the normalized dataset (right). As expected, on visual inspection the two datasets appear essentially identical, because intensity ratios are preserved by the normalization process.

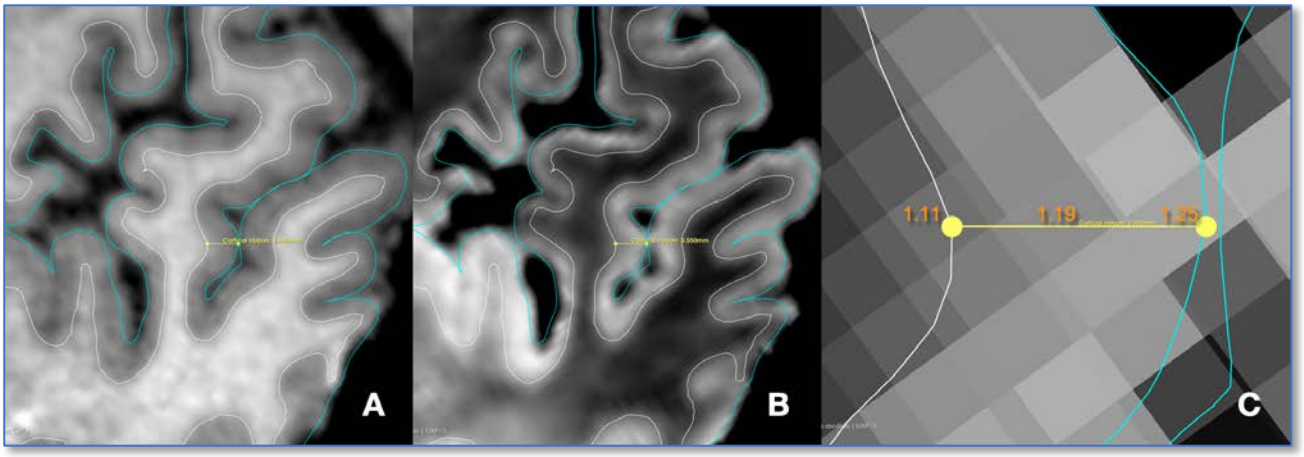

Figure 3: Scalar computation.
In all three panels of the figure, one can see the intersection of the pial surface (cyan) and the GWMI (white) with the 2D viewing plane, as well as a segment (yellow) connecting vertices with the same ID on the two surfaces. The 2D views have been reformatted to align with this segment. The correspondence between the estimated surfaces and the MRI is evident in panels A and B (showing the 3D T1w-FFE and 3D FLAIR sequences, respectively). Panel C shows a strong magnification of the FLAIR image resampled into FreeSurfer space (voxel conforming, downsampling to 1 × 1 × 1 mm). The scalar projected onto the surface is obtained by averaging the normalized intensity values of voxels along the surface normal (1.11, 1.19 and 1.25 in this example), restricted to the cortical ribbon.

Planning surgery for lesions evident on visual examination of the MRI scan - Illustrative case

Figure 4 depicts the case of Pt-01, a patient with an MRI-visible FCD. Accurate surgical planning is essential in this case, as the lesion lies deep within the central sulcus and in close proximity to eloquent sensorimotor cortex.

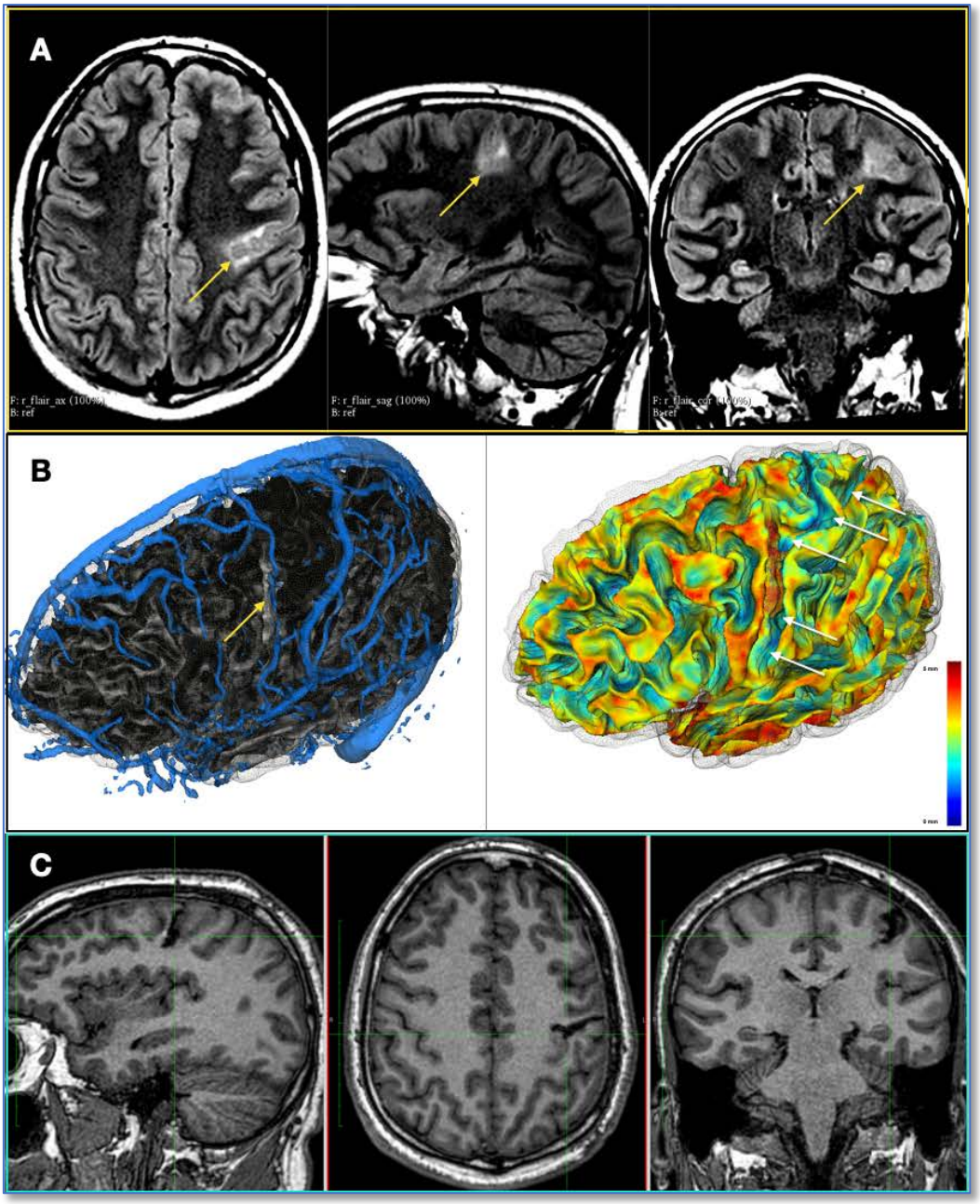

Figure 4: Pt-01. MRI and surface -based mapping in focal cortical dysplasia (FCD IIb).
A 39-year-old patient with a histologically confirmed FCD type IIb centered at the fundus of the left Rolandic sulcus. (A): multiplanar FLAIR reconstructions depict a focal cortical–subcortical hyperintensity (yellow arrows). (B): On the left, FLAIR signal projected onto the white-matter surface, localizing the lesion to the bottom of the central sulcus (yellow arrow) and supporting surgical planning. On the right, cortical-thickness map: using a cold-to-hot color scale, the primary somatosensory cortex (S1), characteristically thinner than adjacent cortex, appears as a blue band along the posterior bank of the central sulcus (white arrows), corroborating sulcal identification relative to the lesion. (C): postoperative multiplanar images show the extent of resection.

SUPR-FLAIR-sa: enhancing the visualization of difficult-to-see lesions

After establishing the utility of SUPR-FLAIR for planning resections of MRI-visible lesions, we asked whether the same technique could also aid visualization of lesions that are only subtly hyperintense and not readily identifiable by eye on FLAIR images. As shown in Figure 1 and Figure 20, FLAIR signal intensity is not uniform across the cortical surface, which complicates the detection of faint hyperintensities. We therefore adopted a statistical comparison with normative data, fitting a vertex-wise generalized linear model, after appropriate surface-based smoothing, with group membership (patient - healthy control) as the explanatory variable. In practice, we used FreeSurfer to compare two cohorts, the individual patient with 101 healthy volunteers, implementing a leave-one-out strategy.

Subjects and methods

Control group. The control group included 101 healthy volunteers (49 males). Mean age ± Standard Deviation (SD) was 32.9 years ± 14.9 (range, 8 - 65 years). All subjects were neurologically and neuropsychologically normal; none had any history of neurologic or psychiatric disease.

Statistical analysis. It followed the completion of the pipeline already described for SUPR-FLAIR (see Figure 1, Figure 2, and Figure 3). First, the patient and healthy controls were nonlinearly registered to FreeSurfer's spatial template, fsaverage. The SUPR-FLAIR maps were then transformed into this common space, enabling statistical analysis. Statistical modeling was performed with QDEC (Query, Design, Estimate, Contrast) FreeSurfer's graphical interface. A vertex-wise GLM was fitted, using cortical surface vertices as observational units and the normalized SUPR-FLAIR intensity as the outcome variable. GLM significance values were mapped onto the fsaverage surface as –log(10)P. By convention, a positive sign was assigned where the patient's cortical intensity exceeded that of healthy controls, and a negative sign in the opposite case.

Validation with MRI-visible lesions – Illustrative cases

The method was then applied to images of two patients with FCD visible on MRI in order to verify the correctness of the method.

Pt-02 (Figure 5) is a left-handed woman, 38 years old at the time of surgery, already presented in Cardinale et al., 2015. Seizure onset at age 5, ictal episodes occurred predominantly during sleep.

MRI showed a deep-seated lesion at the fundus of the right central sulcus. f-MRI demonstrated right-hemispheric language dominance. After lesionectomy, she experienced transient aphasia and hand paresis over the first postoperative days, with full recovery in the following weeks. She remains seizure-free 11 years postoperatively without antiseizure medication. Histopathology: FCD type IIb.

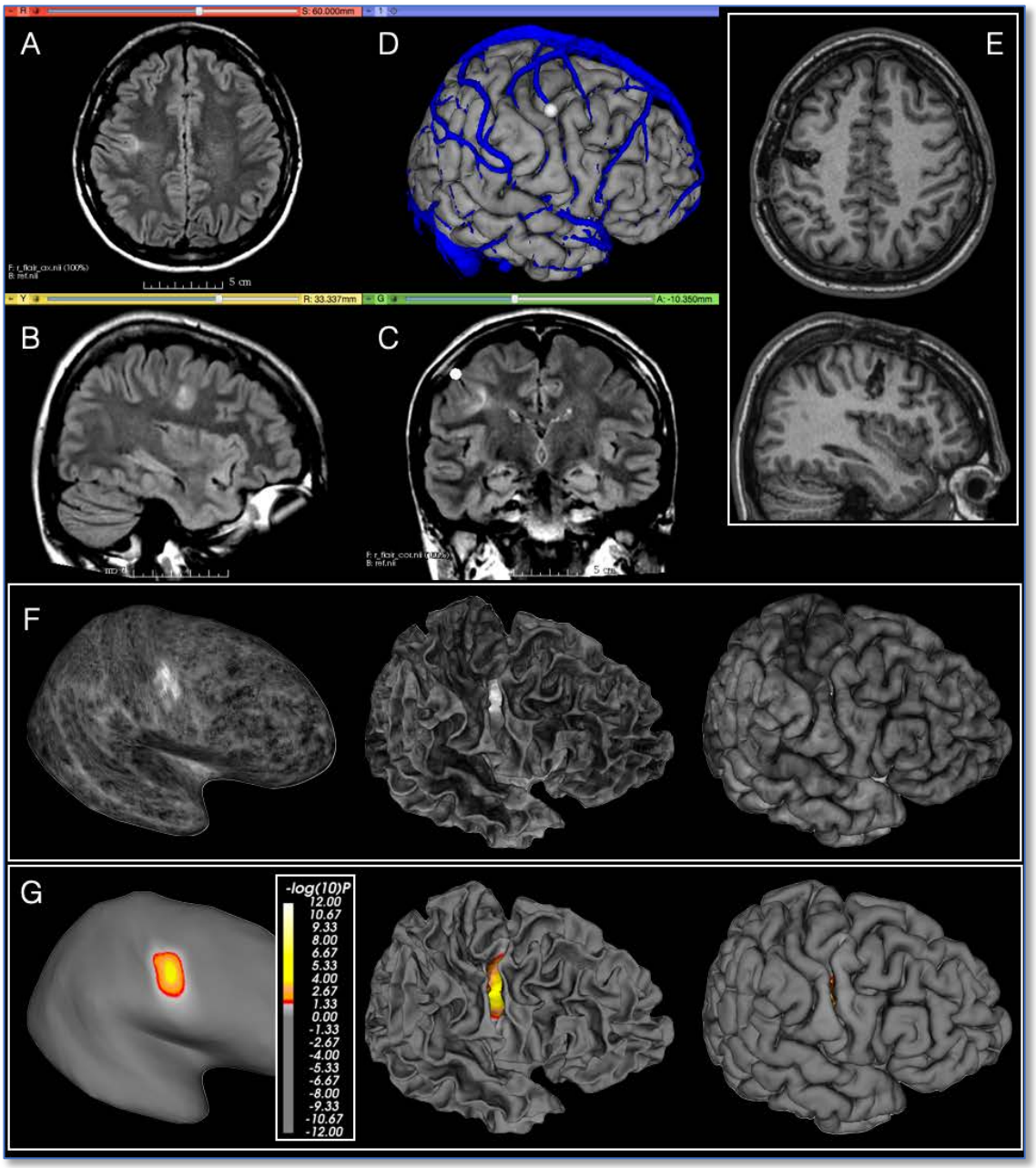

Figure 5: Pt-02. Multiplanar and surface-based mapping of a central-sulcus FCD.
(A–C) MultiPlanar Reconstructions (MPRs) of FLAIR dataset. (D) 3D multimodal rendering for presurgical topographic analysis; a white spherical marker denotes the central-sulcus entry in coronal and 3D views, highlighting the lesion's concealed location. (E) Postoperative cavity on axial and sagittal images. (F) SUPR-FLAIR projected onto the individual inflated, GWMI, and pial surfaces (left →right) localizes dysplastic tissue to the sulcal fundus. (G) Vertex-wise statistics across the three surfaces: the peak (minimum-P) vertex lies at the sulcal fundus; maps are shown as signed –log10(P) with a heat colormap (lighter = more significant).

Pt-03 (Figure 6) is a right-handed man, 38 years old at the time of surgery, already presented in Cardinale et al., 2015. Seizures began at age 6 and occurred several times per week. MRI revealed a deep-seated lesion along the infero-lateral left fronto-orbital cortex. He underwent lesionectomy without neurological deficit and is seizure-free 10 years after surgery; antiseizure therapy has been stopped. Histopathology: FCD type IIb.

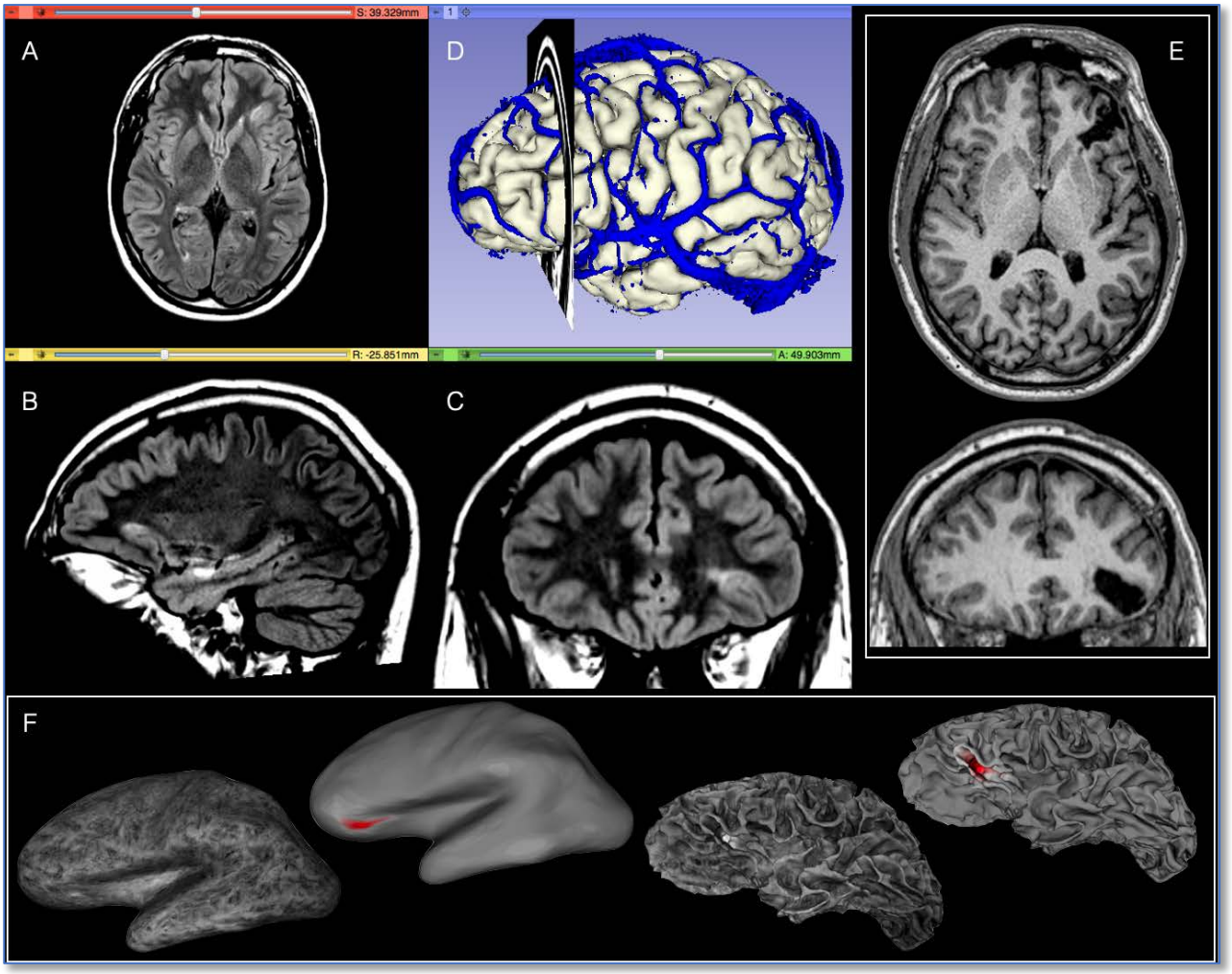

Figure 6: Pt-03. Fronto-orbital FCD with SUPR-FLAIR and statistical mapping.
(A–C) FLAIR MPRs. (D) 3D multimodal rendering. (E) Postoperative cavity on axial and coronal views. (F) SUPR-FLAIR and vertex-wise statistics projected onto the individual GWMI and inflated surfaces localize dysplastic tissue to the fundus of an abnormal sulcus in the inferolateral left orbito-frontal cortex.

Planning surgery for hidden lesions – Illustrative cases

After validating the method in patients with MRI-visible hyperintense lesions, we tested and subsequently applied it to MRI-negative cases. The principal utility of SUPR-FLAIR-sa was to flag cortical regions with the highest suspicion for FCD, thereby optimizing the topographic strategy for SEEG electrode implantation. We therefore present two illustrative MRI-negative cases evaluated with SEEG and treated by cortical resection, in which histopathology confirmed type II FCD.

Pt-04 (Figure 7) is a 32-year-old man at the time of surgery, already presented in Cardinale et al., 2015. A right temporo-frontal SEEG exploration was performed. Seizure onset localized to the anterior superior temporal gyrus (contacts 1 and 2 of electrode T), with posterior propagation through the remaining temporal lobe and into the orbito-frontal cortex. The cluster with highest vertex significance closely overlapped the Resection Zone (RZ). As the P-value threshold was progressively lowered, the suprathreshold cluster expanded posteriorly across the lateral temporal cortex and anteriorly into the orbitofrontal region, mirroring the ictal spread observed on SEEG. Histopathological examination diagnosed a type IIa FCD located at the level of the superior temporal gyrus.

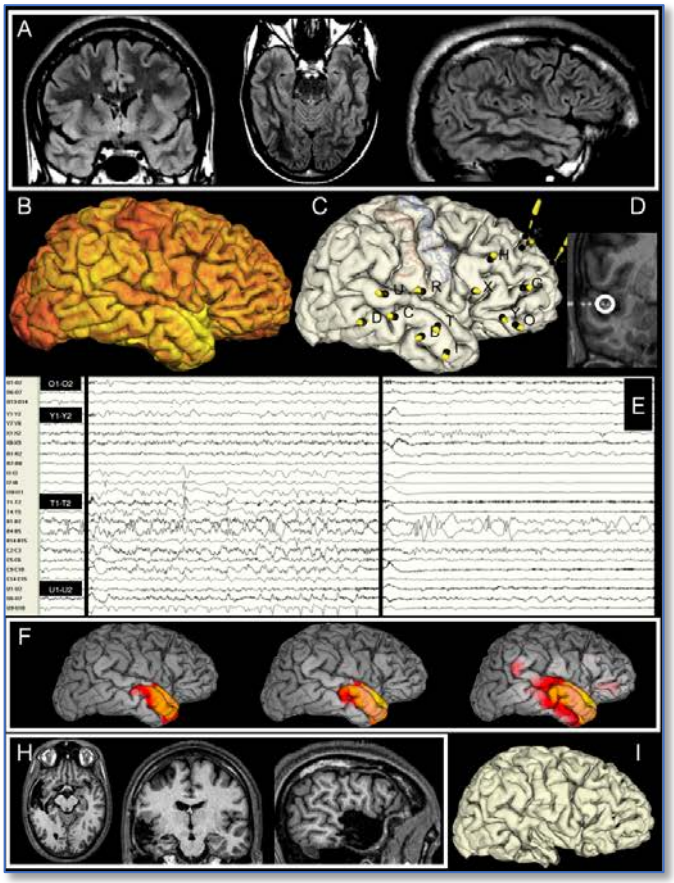

Figure 7: Pt-04. MRI-negative case with SUPR-FLAIR/SUPR-FLAIR-sa localization.
(A)–(C) Coronal, axial, and sagittal FLAIR MPRs show no discernible lesion; sections are aligned through the vertex of peak significance. (B) In contrast, SUPR-FLAIR on the pial surface reveals a focal hyperintensity in the anterior superior temporal gyrus. (C) SEEG electrode trajectories reconstructed on the patient's pial surface. (D) Contacts T1–T2 (white circle) mark the SEEG-defined epicenter of the epileptogenic zone. (E) Representative ictal SEEG: bipolar channel pairs are listed on the left; lower contact numbers indicate deeper contacts. At the left vertical marker, mid-voltage fast activity emerges in T1–T2, O1–O2, Y1–Y2, persists for ~8 s, and rides on theta slow waves. At the right marker, tonic low-voltage fast activity appears on T1–T2 with rapid propagation to O1–O2, Y1–Y2, U1–U2, and more subtly to additional temporal and frontal channels. (F) The most significant cluster is shown as a heat-map overlay on the pial surface.
Progressively lowering the significance threshold (left→right) enlarges the cluster, extending posteriorly across the lateral temporal cortex and anteriorly into the orbitofrontal region. (I–J) Postoperative cavity on MPRs and 3D reconstruction.

Pt-05 (Figure 8 and Figure 9) is a 31-year-old right-handed woman working in finance who was evaluated in our hospital at outpatient visit. Her seizures began at age five, with immediate initiation of carbamazepine; at presentation they occurred weekly. Typical events featured auditory illusions ("voices and overlapping noises in both ears"), a sudden sensation of fear and warmth, impaired language (affecting both comprehension and expression), loss of awareness, and oroalimentary automatisms. Postictally, language disturbance persisted for at least 10 minutes. The neurological examination was normal.

Awake EEG showed bursts of bilateral, diffuse slow waves with greater amplitude over the left hemisphere. During sleep, epileptiform activity included not only right-sided spikes but also independent left temporal spikes, along with a pseudo-rhythmic spike–wave and slow-wave sequence confined to the left hemisphere. Structural MRI was unremarkable. ^{18}F-FDG-PET demonstrated apparent hypometabolism in the right superior temporal gyrus and at both temporal poles. Notably, SUPR-FLAIR-sa localized the most significant cluster to the same right superior temporal region identified as hypometabolic on PET.

Given these findings, SEEG was planned with the following objectives: (i) to determine whether the ^{18}F-FDG-PET hypometabolic zone, despite no obvious FLAIR hyperintensity on visual inspection and no GWMI blurring on MAP18 (Morphometric Analysis Program 18) (Huppertz et al., 2005), represented dysplastic cortex; (ii) to delineate the relationship between the putative FCD and adjacent structures (temporal pole, mesial temporal regions, and operculo-insular cortex); (iii) to demonstrate that the left hemisphere, despite frequent and independent epileptiform EEG features, did not participate in the epileptogenic zone; (iv) to confirm that the right hemisphere was not language-dominant in a patient who was clearly aphasic during and after seizures, with limited f-MRI lateralization and a neuropsychological profile suggestive of dominant-hemisphere involvement; and (v) to perform multiple radio-frequency thermal ablations if appropriate. SEEG confirmed an FCD within the right superior temporal gyrus. The patient subsequently underwent a right temporal lobectomy with generous extension onto the superior temporal gyrus. Histological examination revealed a type-IIb FCD. The patient is completely seizure free 6 years after the resection and the drug therapy has been totally discontinued.

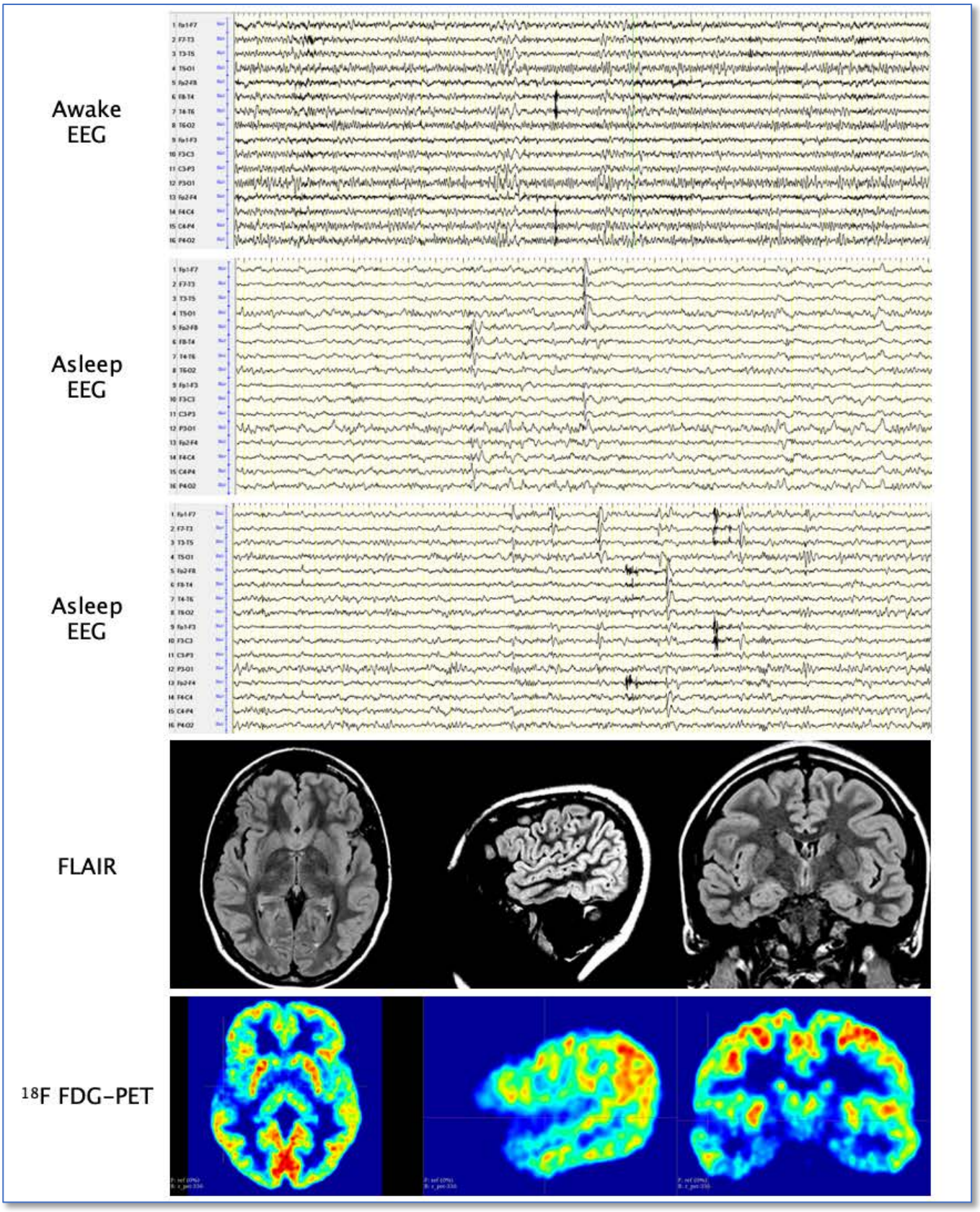

Figure 8: Pt-05 (part 1). FCD type IIb of the right superior temporal gyrus.
EEG and conventional imaging. Awake EEG showed bilateral diffuse slowing, maximal over the left hemisphere. During sleep, independent left temporal spikes were present in addition to right-sided spikes, and a pseudo-rhythmic spike–slow-wave pattern was confined to the left hemisphere. Structural MRI was unremarkable, whereas ^{18}F-FDG PET demonstrated focal hypometabolism in the right superior temporal gyrus.

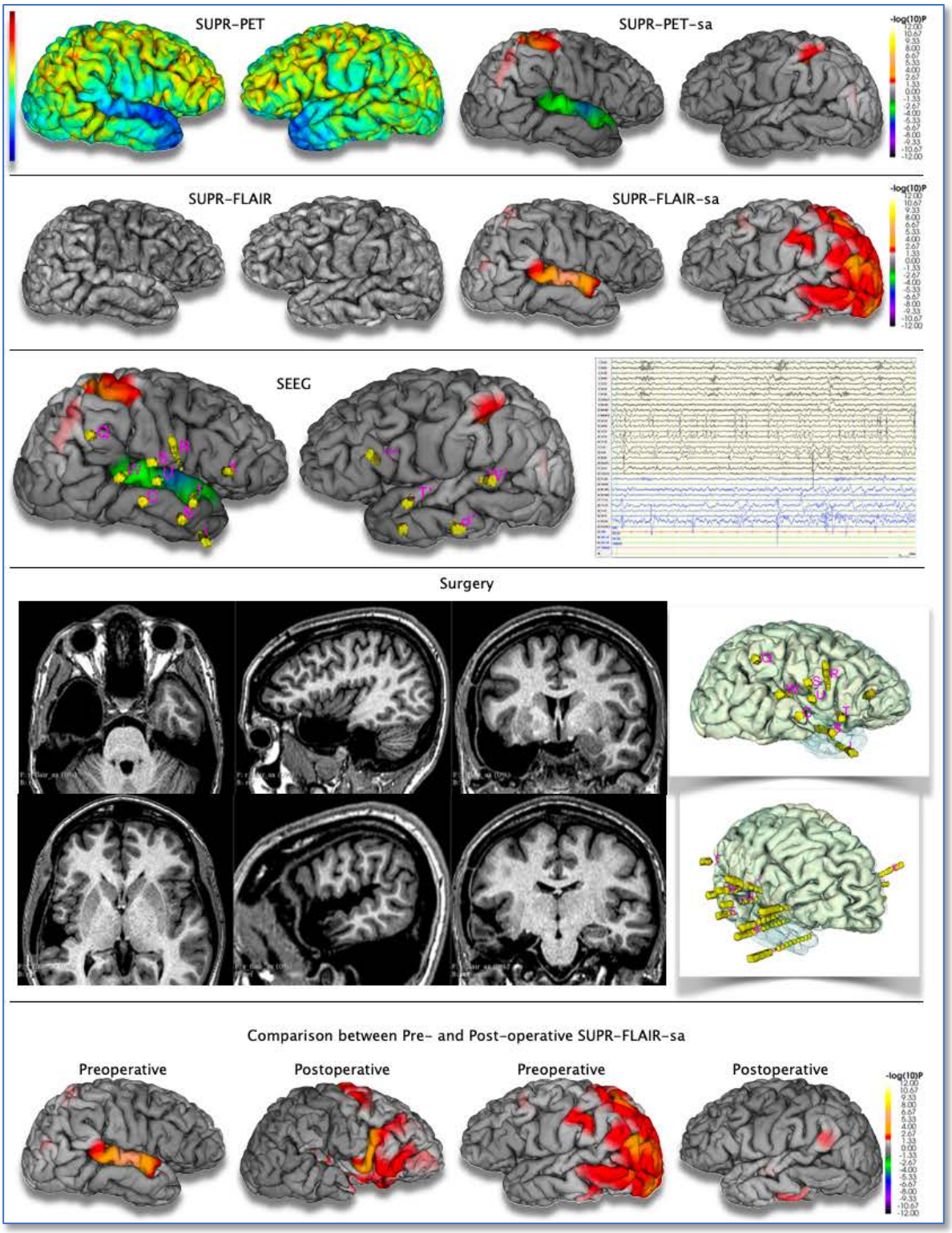

Figure 9: Pt-05 (part 2). Image processing and surgery.
SUPR-PET (SUrface-PRojected PET)[1] sharply delineated hypometabolism in the right superior temporal gyrus. An apparent bilateral relative hypometabolism was also noted at the temporal poles. In contrast, SUPR-PET-sa (SUPR-PET statistical analysis) enhanced the right superior temporal deficit while suppressing the temporal-pole findings bilaterally, consistent with normative values when compared with controls. Conventional SUPR-FLAIR added little beyond standard 2D FLAIR review, whereas SUPR-FLAIR-sa highlighted, with highest statistical significance, the same right superior temporal cluster identified by ^{18}F-FDG-PET. A broad swath of left parieto-occipital cortex also showed increased signal at lower significance. SEEG implantation was bilateral with a right-sided emphasis and electrophysiologically confirmed FCD. The patient underwent a right temporal lobectomy with generous extension over the lesional zone. Postoperative SUPR-FLAIR-sa demonstrated contralateral normalization, with new hyperintense clusters in the right premotor region, consistent with postoperative change.

Evidence of extra-lesional areas of subtle cortical FLAIR hyper-intensity: can we highlight also non-structural modulation of FLAIR signal?

As shown in Figure 8, Figure 9 and Figure 10, SUPR-FLAIR-sa can reveal subtly hyperintense, likely extra-lesional clusters, including contralateral areas, and postoperative study demonstrate a reconfiguration of these patterns, with some areas disappearing and others emerging.

To explore whether such extra-lesional signals might reflect non-structural changes, we present now five patients (Pt-06 … Pt-10) with MRI-visible, histologically proven HS (Figure 10 and Figure 11). All five patients, already presented in Cardinale et al., 2015, had a typical mesial temporal lobe epilepsy history. After a standard noninvasive presurgical work-up, each underwent an uneventful antero-mesial temporal lobectomy; histopathology confirmed HS. All remain seizure-free with 10–15 years of follow-up and are off antiseizure medication. Figure 10 summarizes the radiological findings and SUPR-FLAIR-sa results. Conventional MRI showed HS with temporopolar atrophy and gray–white junction blurring. Despite the absence of visually appreciable FLAIR hyperintensity, in every case the most significant SUPR-FLAIR-sa cluster localized to the temporal pole ipsilateral to HS[2]. No additional polar structural abnormalities beyond gray–white blurring was identified histologically.

In Figure 11, using a more permissive statistical threshold, additional cortical regions of relative FLAIR hyperintensity emerge, particularly within sectors of the cingulate gyrus known to be connected with mesial temporal structures.

[1] SUPR-PET and SUPR-PET-sa are the ^{18}F-FDG-PET counterparts of SUPR-FLAIR and SUPR-FLAIR-sa. In our workflow, the only substantive difference concerns the reference cohort: instead of healthy volunteers, the “control” group comprises patients with epilepsy who either have small, heterogeneous lesions or no visible lesion. We deliberately exclude individuals with temporal lobe epilepsy, owing to their relatively stereotyped metabolic patterns, and patients with large lesions that markedly distort brain anatomy. This choice reflects regulatory constraints in Italy that preclude performing PET examinations in healthy volunteers.

[2] The hippocampus is excluded from SUPR-FLAIR-sa in FreeSurfer because it is modeled as a subcortical structure rather than part of the cortical ribbon; accordingly, hippocampal signal is not captured by the surface-based statistics.

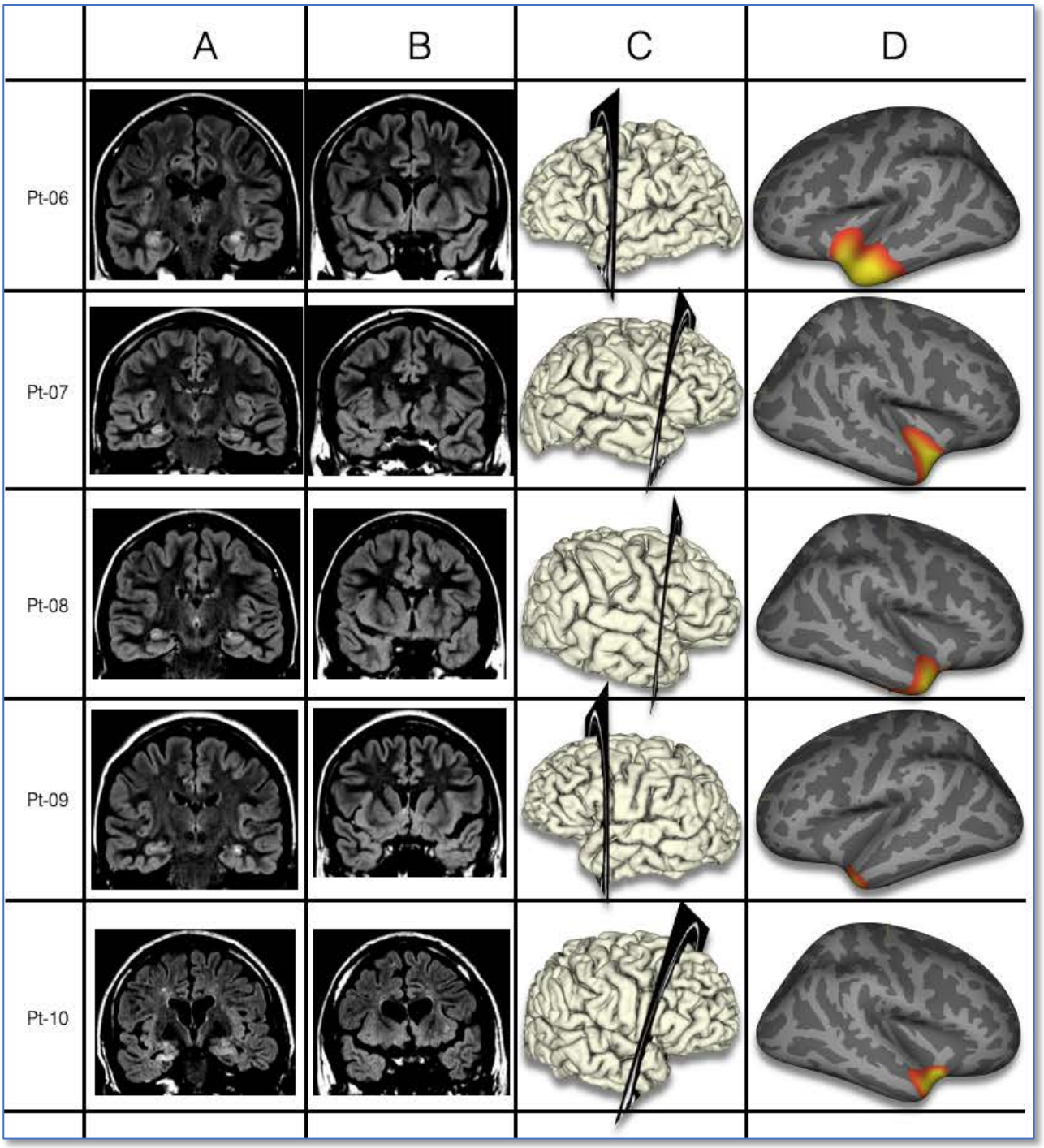

Figure 10: Pts 06–10. Coronal FLAIR and surface-based statistics in hippocampal sclerosis.
(A) Coronal FLAIR at the hippocampal level. (B) Coronal FLAIR at the temporal-pole level. (C) Locator images indicating the slice positions for (B). (D) SUPR-FLAIR statistical maps in template space. Column (A) shows a clearcut hippocampal hyperintensity. By contrast, visual inspection of (B) does not reveal the subtle temporo-polar hyperintensity that emerges on the surface-based statistics in (D).

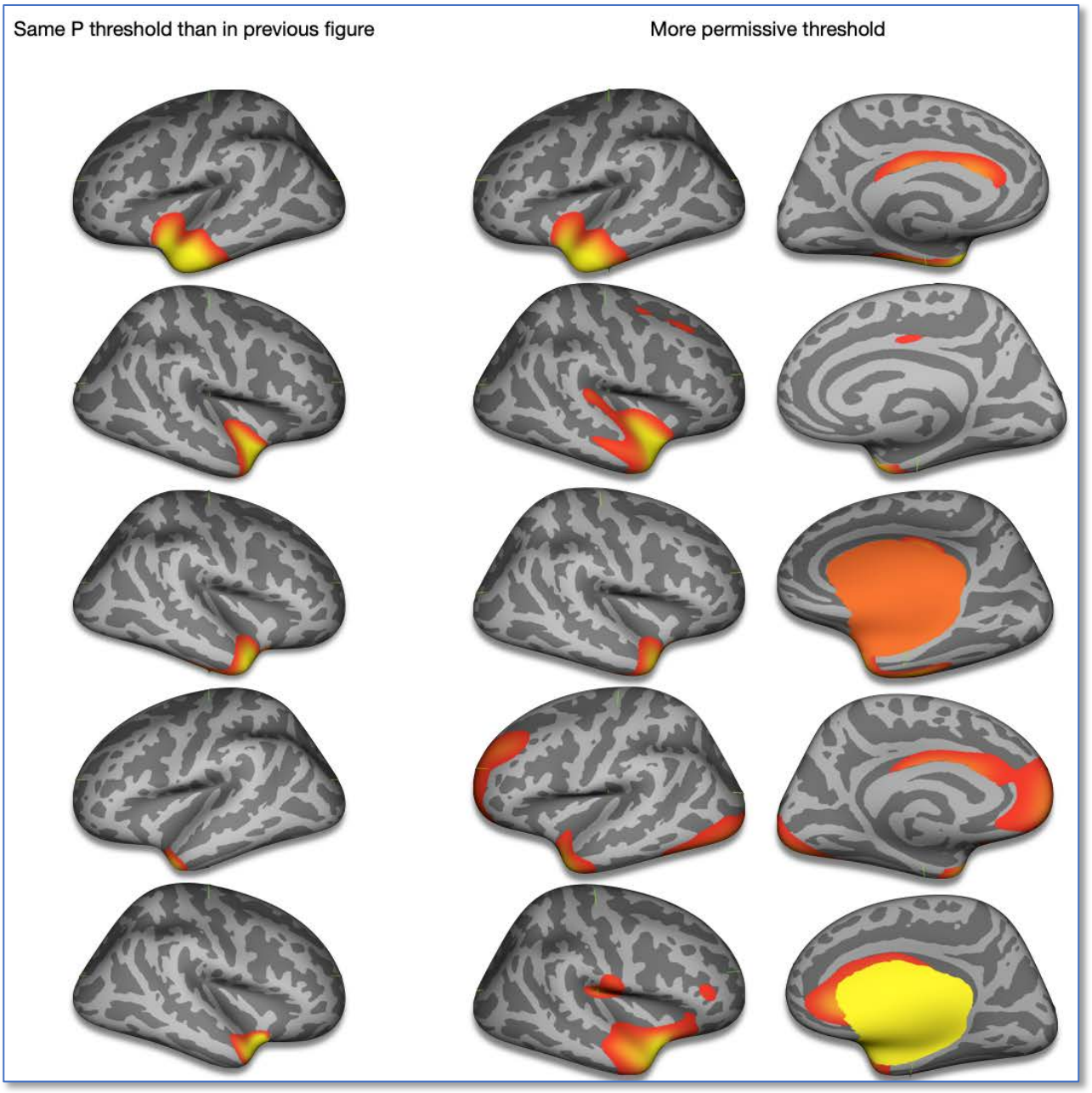

Figure 11: SUPR-FLAIR highlighting possible cortico-cortical connectivity.
Left panels replicate the SUPR-FLAIR-sa results shown in Figure 8. Right panels display maps computed with a more liberal P-value threshold, revealing additional significant clusters along the mesial surface. Notably, portions of the cingulate gyrus, functionally connected to the hippocampus, appear hyperintense.

Further along the line of SUPR-FLAIR-sa as a potential tool for studying cortical connectivity, we present two more illustrative cases.

Pt-11 (Figure 12, Figure 13, Figure 14, and Figure 15) is an eight-year-old boy with a major neurocognitive disorder and associated behavioral difficulties attends second grade with special educational support. Seizures began at age seven and manifest in two clinical patterns. The “minor”

episodes start without warning: he abruptly disengages, staring eyes with a slight leftward deviation of the head and eyes. There are no automatisms. Awareness is impaired, and he resumes baseline within 10–15 seconds without postictal deficit. The “major” episodes begin with a tonic phase characterized by generalized hypertonia, apnea, and pallor, followed by a hypotonic phase. These events last approximately 20–30 seconds. Recovery is slower and is accompanied by chewing automatisms.

Video-EEG monitoring (Figure 12): background asymmetry with a better-structured rhythm in the right hemisphere; abundant slow activity over the left hemisphere. Multifocal epileptiform abnormalities predominating on the left, with independent right-hemispheric involvement as well. Nocturnal sleep was poorly organized, especially in the initial phase, with a marked increase in epileptiform activity and a tendency toward synchronization. Epileptiform abnormalities remained predominantly left parietal. Two electroclinical events were captured (one in wakefulness, one in sleep), minimally symptomatic, each associated with a non-focal EEG discharge.

MRI (Figure 13) demonstrated a probable glio-neuronal tumor of the left temporal pole. The patient underwent an antero-mesial temporal lobectomy with total removal of the lesion. SUPR-FLAIR-sa revealed bilateral, diffuse cortical hyperintensity, with peak significance at both temporal poles.

The patient has remained seizure-free since surgery (follow-up > 5 years); the EEG has normalized, and nearly all cortical FLAIR hyperintensity has resolved.

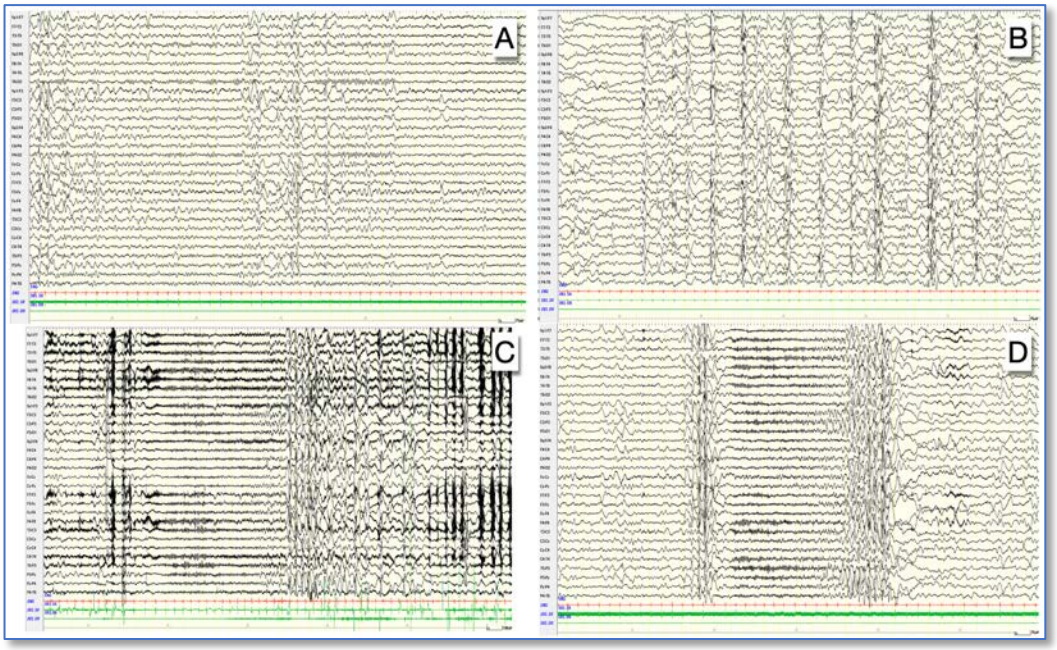

Figure 12: Pt-11 (part 1). Video-EEG Monitoring.
(A): Interictal EEG during wakefulness. (B): Interictal EEG during sleep. (C): Ictal EEG during wakefulness. (D): Ictal EEG during sleep. Epileptiform anomalies are non-focal.

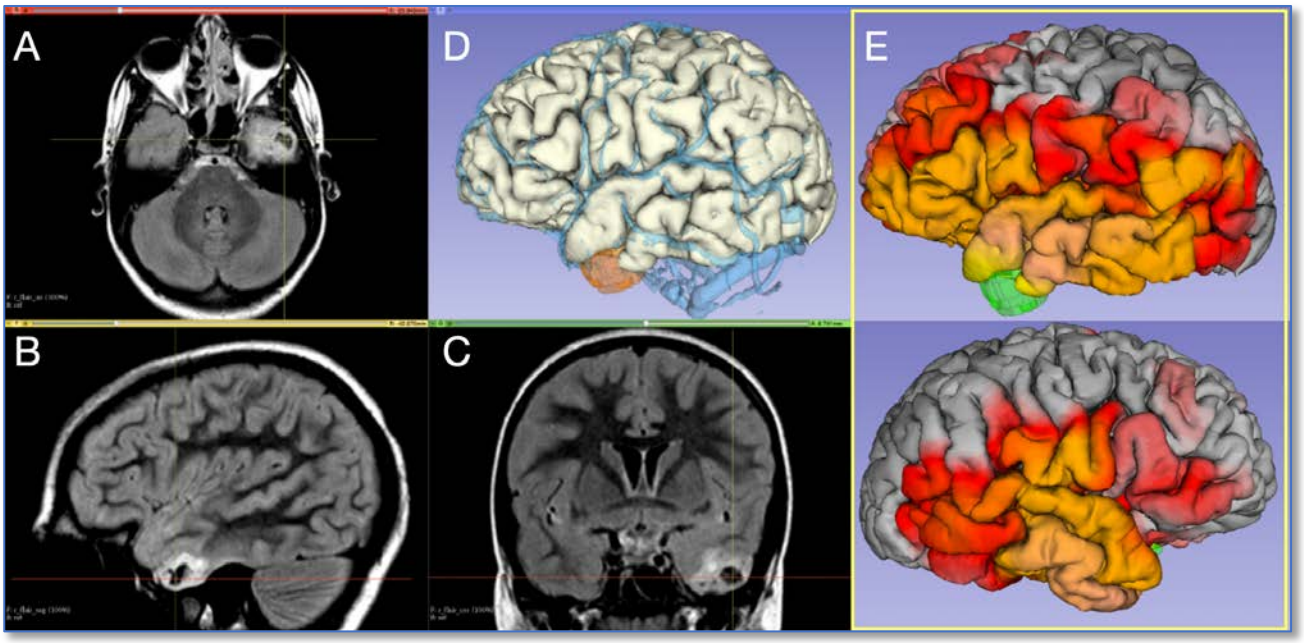

Figure 13: Pt-11 (part 2). Left temporo-polar tumor (Polymorphous Low-Grade Neuroepithelial Tumor of the Young — PLNTY), imaging and processing.
(A–C) FLAIR MPRs. (D) 3D multimodal rendering. The tumor segmentation is rendered in orange. (E) SUPR-FLAIR-sa showing diffuse bilateral hyperintensity. Here the tumor segmentation is rendered in green.

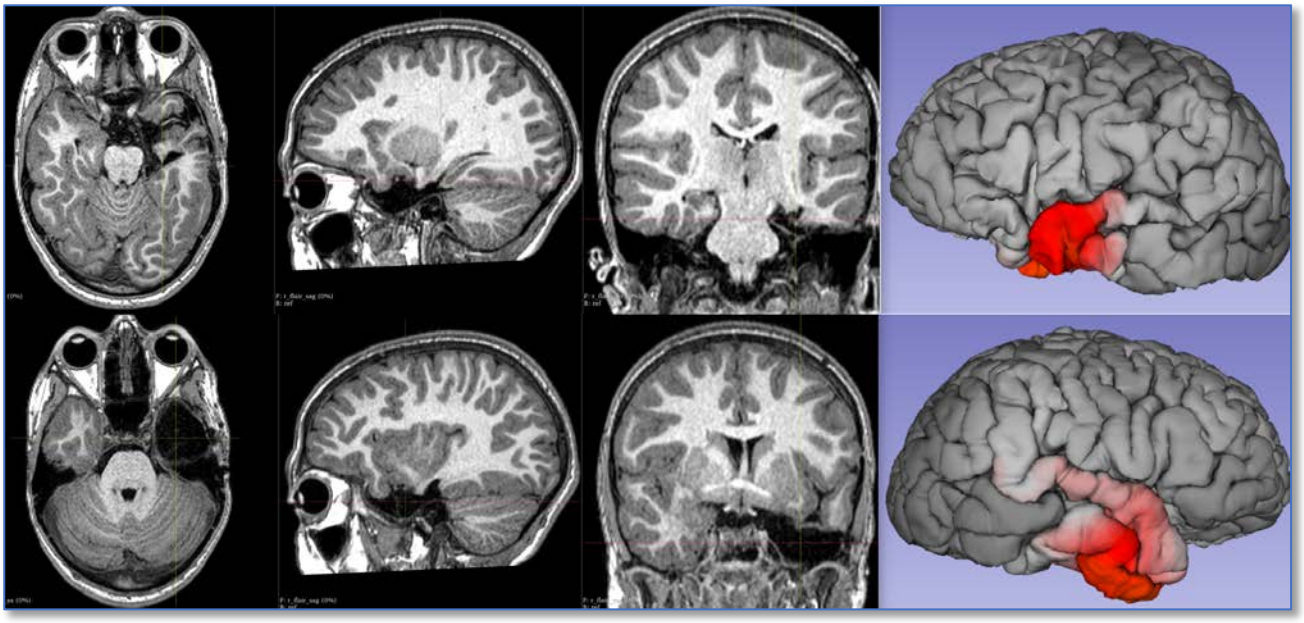

Figure 14: Pt-11 (part 3). Postoperative imaging.
Postoperative MRI demonstrates the resection cavity following antero-mesial temporal lobectomy. SUPR-FLAIR-sa performed on the postoperative study shows near-complete normalization of cortical FLAIR signal.

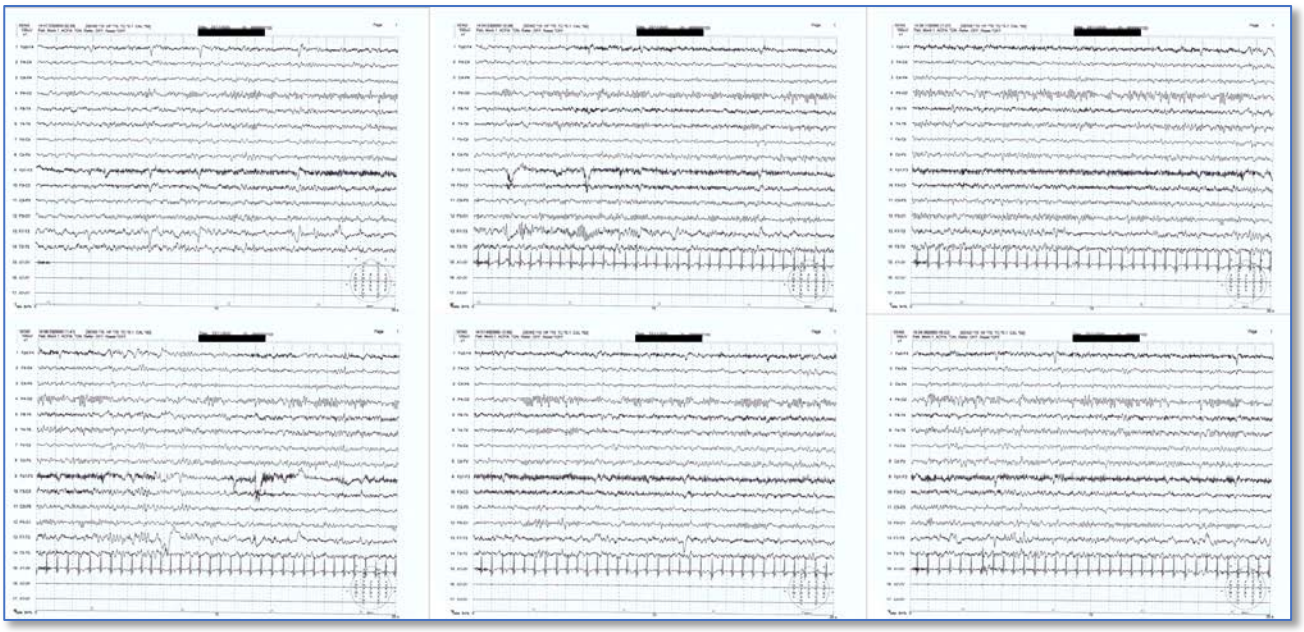

Figure 15: Pt-11 (part 4). Postoperative EEG.
Postoperative EEG demonstrates complete resolution of epileptiform activity in these six pages of traces.

Pt-12 (Figure 16) is a 22-year-old woman with drug-resistant focal epilepsy associated with a type Ia FCD, histologically confirmed, located in the posterior segment of the left superior frontal sulcus. Surgery was undertaken primarily on the basis of neurophysiological data obtained during long-term Video-SEEG monitoring, and she has been seizure-free for >1 year. Structural MRI was noninformative, while ^{18}F-FDG-PET scan demonstrated a regional hypometabolism.

The topographic pattern of cortical FLAIR hyperintensity appears to mirror the effective connectivity between the regions where epileptiform figures were recorded. Note: The temporal lobe was not sampled with SEEG electrodes because it was not included in the hypotheses on the epileptogenic zone formulated on the basis of noninvasive anatomo-electro-clinical evaluation.

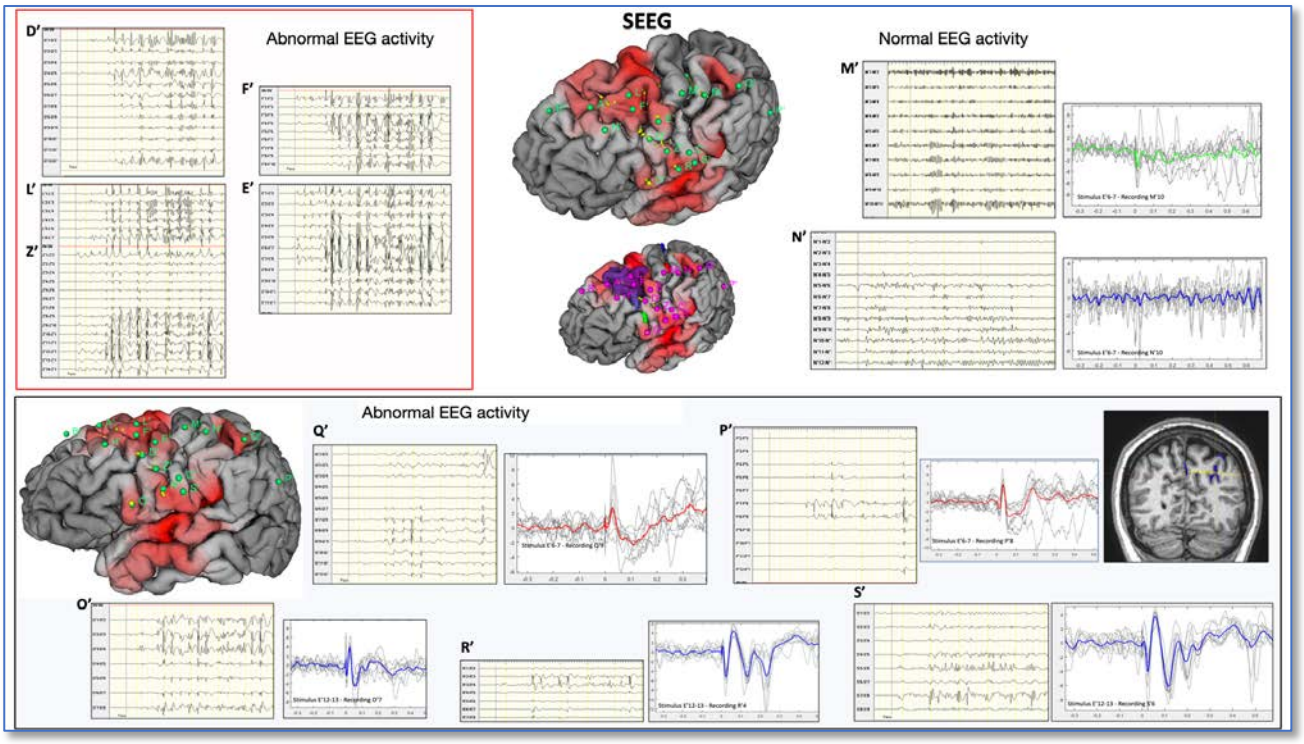

Figure 16: Pt-12. Interictal EEG, evoked potentials and SUPR-FLAIR-sa.
Interictal epileptiform EEG anomalies, cortico-cortical evoked potentials (CCEPs) and SUPR-FLAIR-sa pattern. The blue area in the 3D rendering is the most significant cluster of SUPR-PET-sa.
In the red inset, SEEG traces from intra-/perilesional contacts (electrodes D', L', Z', F', E') show subcontinuous high-voltage fast spikes and polyspikes in the absence of a background rhythm. Low-frequency (1 Hz) bipolar stimulation of two contacts within the dysplasia (E' 6–7) elicited CCEPs with N1 < 20 ms, recorded predominantly by electrodes implanted over cortical territories that exhibit relative cortical FLAIR hyperintensity on the 3D surface rendering (warm colors), namely the superior parietal and opercular fronto-centro-parietal regions (electrodes Q', O', R', S').
These neurophysiological findings indicate effective connectivity between the dysplasia and these areas. Moreover, electrodes in these same regions, despite a preserved background rhythm, record interictal spikes and polyspikes with morphology similar to that observed within the dysplasia, suggesting spread of interictal epileptiform activity to these territories. By contrast, the primary sensorimotor areas sampled by electrodes M' and N', although topographically close to the dysplasia, show no electrophysiological connectivity (no CCEPs) and no SUPR-FLAIR hyperintensity, and they do not exhibit interictal epileptiform activity.

Limitations of the study of chapter I

The major limitation is that this is a pilot study, presented primarily to illustrate the method, with results that are anecdotal rather than definitive. We did not include examples of method failures, which can occur for various technical reasons, for instance, imperfect segmentation of tissue classes. Moreover, from a clinico-pathological perspective, we focused solely on increases in cortical intensity and made no systematic attempt to analyze reductions in cortical FLAIR signal.

A further critical limitation of SUPR-FLAIR-sa is its dependence on scanner specificity. Inter-scanner variability makes robust analysis impractical when patients and controls are not imaged on the same hardware, likely due to substantial differences in B0/B1 homogeneity and sequence implementation.

Even when the scanner is identical, major acquisition–software updates can introduce image differences that are not recoverable with statistical harmonization alone (Figure 17).

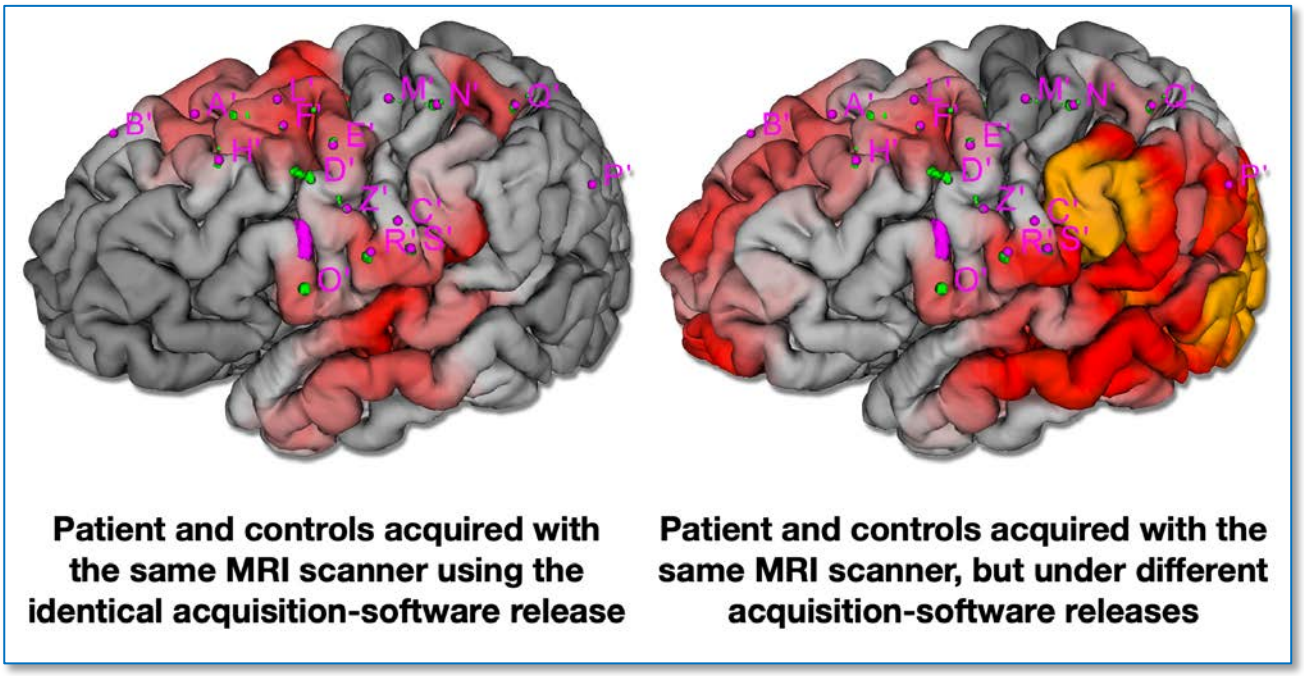

Figure 17: Importance of inter-scanner variability.
Left panel: Left-hemisphere SUPR-FLAIR-sa for Pt-12, rendered with the same parameters as Figure 16.
Right panel: Reanalysis using a different control cohort acquired several years earlier on the same MRI system but under a different acquisition–software release. Note the systematic offset in surface values and the apparent emergence of a posterior hyperintense cluster, likely reflecting software-version effects rather than underlying biology.

Conclusion of chapter I

The SUPR-FLAIR method is useful for presurgical planning in epilepsy surgery, both for SEEG electrode implantation and for resective or disconnective procedures. It enables the seamless, largely automated (via custom scripts) inclusion of FLAIR-hyperintense cortical lesions, those already appreciable on routine MRI inspection, within multimodal 3D planning scenes.

Further along this line, its statistical extension, SUPR-FLAIR-sa, appears helpful in uncovering subtly hyperintense cortical lesions that are difficult to detect on visual MRI review because of their very low contrast. A first systematic study aimed at estimating its diagnostic performance is presented in the next chapter.

In addition, this statistic approach reveals FLAIR-hyperintense cortical regions outside the strictly defined EZ, suggesting that the FLAIR signal is not determined solely by fixed structural properties of the tissue.

CHAPTER II: DIAGNOSTIC PERFORMANCE OF SUPR-FLAIR-SA IN DRUG-RESISTANT, MRI-NEGATIVE, SUSPECTED TEMPORAL LOBE EPILEPSY

This chapter presents entirely new data[3] and is based on a study conceived and carried out during the doctoral period.

Objective

To assess the diagnostic performance of SUPR-FLAIR-sa in MRI-negative patients undergoing temporal lobe surgery and to explore its relationship to surgical outcome and to SUPR-PET-sa.

Study Design

Retrospective single-center cohort study.

Patients and methods

Study design, population, clinical characterization and MRI acquisition

We retrospectively reviewed a consecutive, single-center cohort of MRI-negative patients with presumed temporal lobe epilepsy who underwent temporal lobe surgery between July 2013 and July 2021; all had at least 24 months of postoperative follow-up.

Semiology was categorized as mesial or lateral. ^{18}F-FDG-PET and SEEG were reviewed when performed. Histopathology and Engel outcome (Engel et al., 1993) at last follow-up were recorded.

The MRI data was acquired using the same scanner and parameters as described in Chapter I.

[3] The Chapter II dataset derives from the neurosurgery specialization thesis "Chirurgia dell'epilessia del lobo temporale. Work-up pre-chirurgico e risultati post-operatori in una serie retrospettiva di pazienti con risonanza magnetica negativa" (University of Pavia, 2022; candidate: Dr. Gianluca Mezzini; supervisor: Prof. Lorenzo Magrassi; co-supervisor: Dr. Francesco Cardinale).

Performance analysis: reference standard and case definitions

To estimate diagnostic performance (sensitivity and specificity), we assembled a retrospective sample comprising 21 surgical patients and an independent control cohort of 30 healthy participants. Each individual was analyzed with SUPR-FLAIR-sa on a single-subject basis, as illustrated in the preceding chapter.

For both patients and controls, the test was deemed:

- Positive when there was at least one significant cluster (vertex-wise $P < 0.05$).
- Negative when no significant cluster was identified.

From these rules, we derived standard performance categories:

- True positive (TP): seizure-free patients with the peak significant cluster (vertex-wise $P<0.05$) falling in the RZ[4]
- False negative (FN): patients with no significant cluster
- True negative (TN): healthy controls with no significant cluster
- False positive (FP):
    - (i) healthy controls with significant clusters
    - (ii) patients whose SUPR-FLAIR-sa localized inside the RZ but who were not seizure-free
    - (iii) seizure-free patients whose peak localized outside the RZ.

We excluded from performance computations eight non–seizure-free patients whose peak lay outside the RZ, because the ground truth regarding the unresected EZ was indeterminate (i.e., incomplete resection vs. incorrect localization could not be resolved).

[4] We treated the resection zone as a pragmatic surrogate for the epileptogenic zone. In patients who became seizure-free postoperatively, we infer that the EZ was encompassed, at least in its crucial extent, by the RZ, while recognizing that strict identity between RZ and EZ cannot be guaranteed.

Results

Clinical results

Symptoms were suggestive of Mesial Temporal Lobe Epilepsy (MTLE) in 10/29 patients, while the remaining 19 presented with ictal semiology likely related to a temporal lateral symptomatogenic zone.

^{18}F-FDG-PET was obtained in 24/29 patients. In 22 of them it revealed temporal hypometabolism at visual inspection of images, while it was not informative in the remaining two.

SEEG was performed in 17/29 patients (2 bilateral investigations).

Outcome on seizures was satisfactory in the majority of the cases:

- Engel I: 18/29 (62%)
- Engel II: 7/29 (24%)
- Engel III: 4/29 (14%)

A definite epileptogenic substrate was uncommon at histological examination. Most specimens showed no specific lesional pathology, with findings as follows:

- Nonspecific gliosis 22/29 (76%)
- Malformation of cortical development 5/29 (17%)
- Hippocampal sclerosis 2/29 (7%)

SUPR-FLAIR-sa diagnostic performance

Performance analysis subset included 21 patients and 30 healthy controls, as follows:

- True Positive (TP): 7
    - 7 seizure free patients with SUPR-FLAIR-sa significant peak cluster inside the RZ
- True Negative (TN): 17
    - 17 healthy controls without any significant SUPR-FLAIR-sa clusters
- False Positive (FP): 21
    - 13 healthy controls with at least one significant SUPR-FLAIR-sa cluster
    - 5 seizure free patients with significant SUPR-FLAIR-sa peak cluster outside the RZ
    - 3 not seizure free patients with significant SUPR-FLAIR-sa peak cluster inside the RZ
- False Negative (FN): 6

- 6 patients without any significant SUPR-FLAIR-sa peak cluster (P<0.05)

Diagnostic performance was computed as usual:

- Sensitivity= TP / (TP+FN) —> 7 / (7+6) = 53.8%
- Specificity= TN / (TN+FP) —> 17 / (17+21) = 44.7%
- Positive Predictive Value (PPV)[5] ≈ 25%
- Negative Predictive Value (NPV)[6] ≈ 73.9%

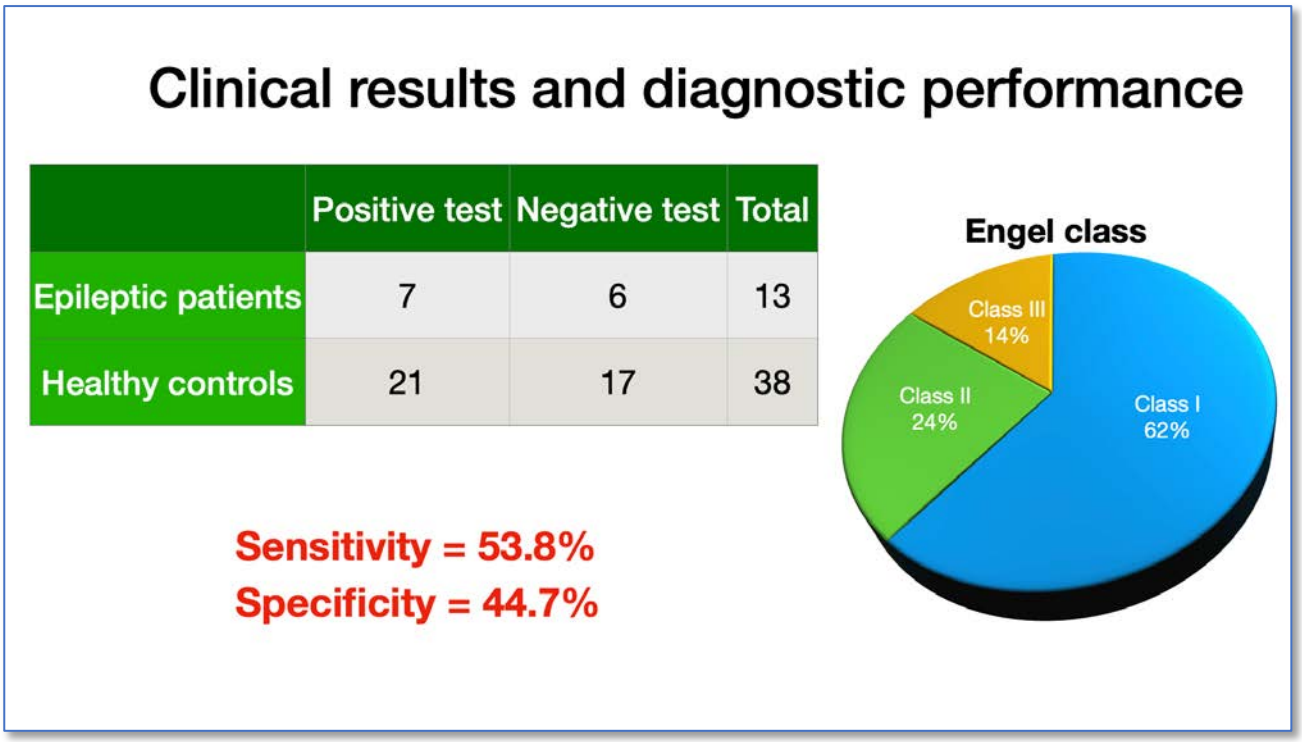

Figure 18: Summary of key findings from the SUPR-FLAIR-sa diagnostic performance study.

Secondary analyses

We can provide also the results of some auxiliary analyses.

Results of SUPR-FLAIR-sa with respect to epileptological outcome:

- 70% patients are seizure free when the significant cortical hyperintensity peak is included in the resection zone.

[5] Positive predictive value (PPV) is the probability that a person with a positive test result actually has the disease or condition being tested for. PPV = TP / TP + FP.
[6] Negative predictive value (NPV) is the probability that a person with a negative test result truly does not have the disease. NPV = TN / TN + FN.

- 38% patients are seizure free when the significant cortical hyperintensity peak is outside the resection zone.

The following table reports the results of SUPR-PET-sa with respect to epileptological outcome (P= 0.37):

Peak location (SUPR-PET-sa)	Seizure free (Engel I)	Not seizure free	Total
Peak inside RZ	11 (73%)	4 (27%)	15 (100%)
Peak outside RZ	5 (56%)	4 (44%)	9 (100%)

Concordance between SUPR-FLAIR-sa and SUPR-PET-sa:

- Patients with both peaks inside RZ: n = 9; 8/9 (89%) seizure-free.
- Patients with SUPR-FLAIR peak inside only: n = 2; 2/2 (100%) seizure-free.
- Patients with SUPR-PET peak inside only: n = 6; 3/6 (50%) seizure-free.
- Both peaks outside RZ: n = 7; 3/7 (43%) seizure-free.

These patterns suggest additive value when modalities are concordant and colocalize with the resection.

Limitations of the study of chapter II

The principal limitation of this study is the exclusion of patients with MRI-visible lesions; consequently, estimates of diagnostic performance apply only to the MRI-negative population. This is clinically compelling, because it addresses the most challenging candidates for surgery and informs selection and planning, but our sensitivity and specificity figures are not strictly valid, chiefly because false negatives were likely undercounted.

A second limitation is the modest sample size.

Conclusion of chapter II

SUPR-FLAIR-sa offers actionable, albeit imperfect, localization support in MRI-negative presumed TLE. When the surface-based statistical peak colocalizes with the resection zone, and especially when concordant with SUPR-PET-sa, postoperative seizure freedom is more likely. Prospective, adequately powered studies with standardized acquisition and appropriate control cohorts are needed to refine thresholds, validate performance, and define best practices for integrating SUPR-FLAIR-sa into surgical planning.

CHAPTER III: TRANSLATIONAL POTENTIAL FOR BASIC NEUROSCIENCE RESEARCH

Can FLAIR signal reflect physiological organization?

This chapter presents entirely new and previously unpublished findings. MRI data were acquired beforehand, but the further development of the statistical analysis methods and their application were carried out during the doctoral period.

Building on prior observations that modest cortical FLAIR hyperintensities may occur without an overt structural substrate, consistent with state-dependent patho-physiology related to epilepsy, we asked whether, in healthy individuals, inter-individual traits such as language lateralization and manual dominance/dexterity are associated with distinct SUPR-FLAIR patterns. In parallel, we tested whether SUPR-FLAIR-sa can detect hyperacute, task- or state-locked modulations of cortical FLAIR.
To address these questions, we performed some "between-subjects" analyses fitting surface-based GLMs to test associations between cortical FLAIR intensity and (i) language lateralization and (ii) handedness/dexterity. We also performed some "within-subject" paired analyses, conceptually analogous to model-based task f-MRI, to probe transient, task- or state-locked fluctuations in normalized cortical FLAIR signal.

Experiment A: association between SUPR-FLAIR and language lateralization and manual dexterity. A "between-subjects" analysis.

Subjects

The cohort comprised 95 healthy volunteers (50 female, 45 male). Mean age ± SD was 35.65 ± 13.53 years (range 11–59). Seventy-six participants were right-handed and 19 were left-handed (R and L, respectively). Among the left-handers, we distinguished 5 individuals with right-hemisphere language dominance, particularly in anterior language areas, from 14 with left-hemisphere dominance (hereafter rh_langdom and lh_langdom, respectively). Language lateralization was determined with task-based f-MRI comprising three paradigms: phonemic/semantic fluency, name association, and sentence comprehension (Figure 19 and Figure 21).

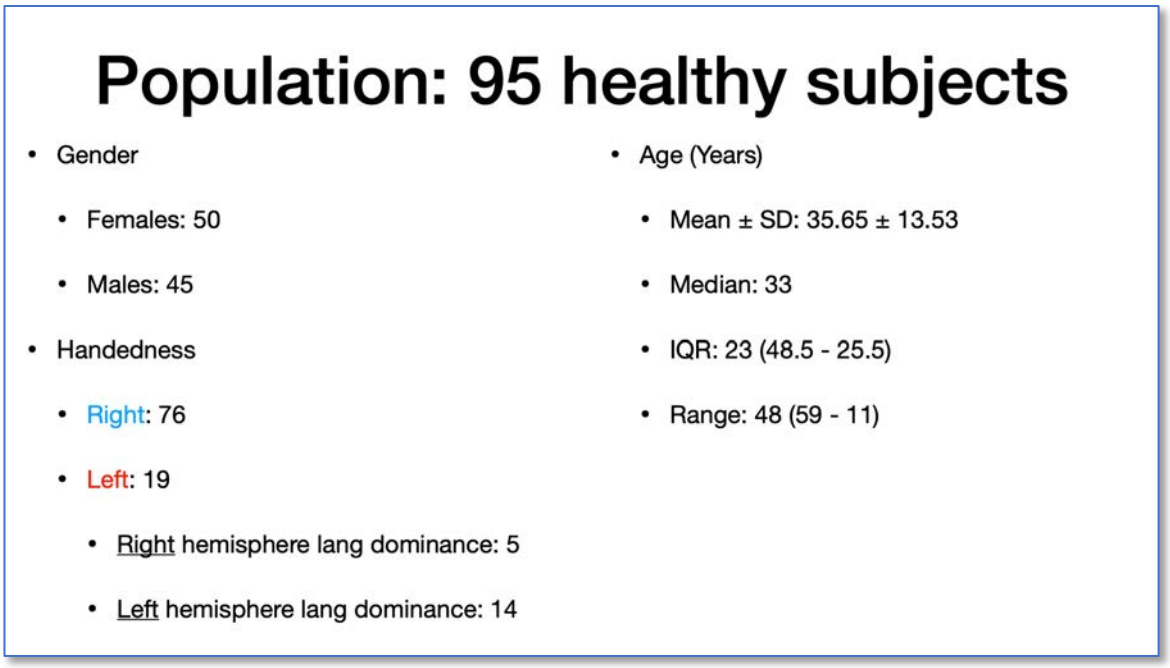

Figure 19: Demographic and functional characteristics of the enrolled healthy-subject cohort

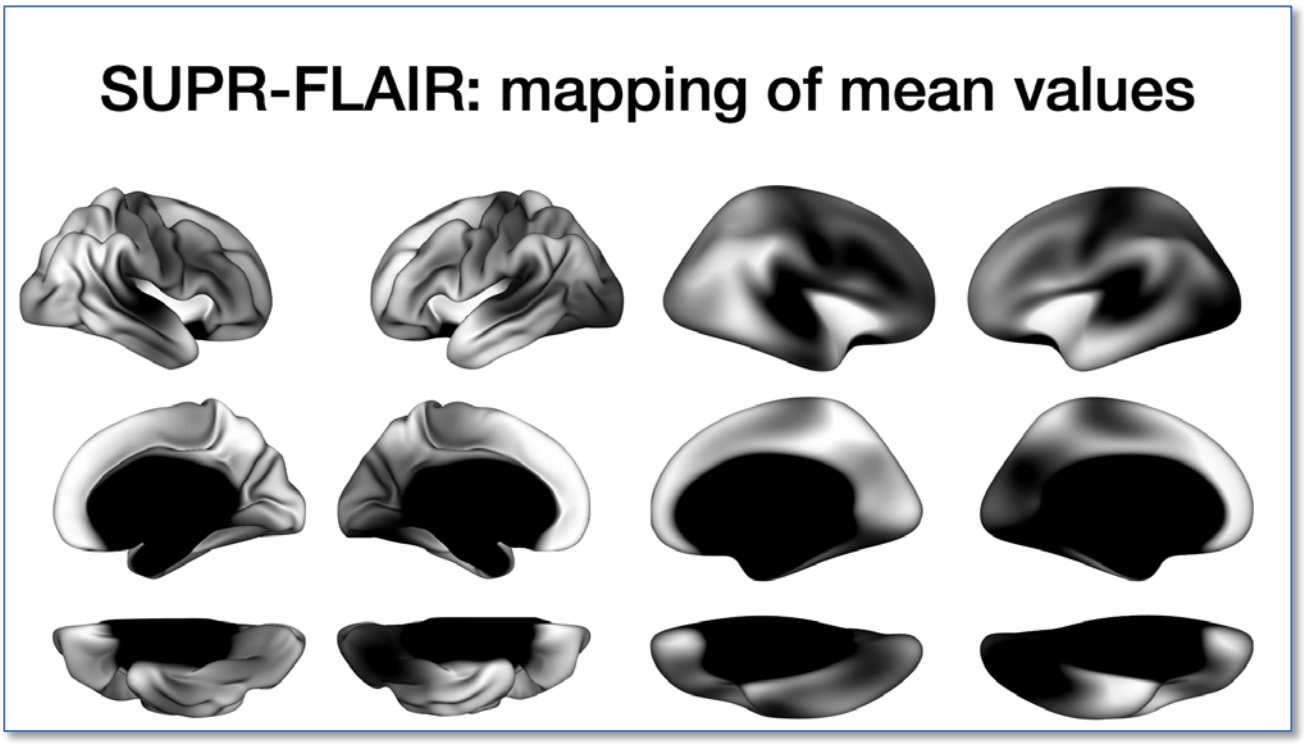

Figure 20: Group-mean SUPR-FLAIR maps from all 95 participants were projected onto the semi-inflated pial surface (left) and the inflated surface (right) of the FreeSurfer fsaverage template. Clear spatial heterogeneity is evident: the sensorimotor and auditory cortices appear relatively hypointense, whereas the left temporal pole and right inferior parietal lobule are relatively hyperintense. The left occipital lobe also appears hypointense, likely due to B0 field inhomogeneity[7].

[7] We conducted analogous analyses in additional healthy cohorts scanned on different MRI systems. The only feature that did not replicate was the left occipital hypointensity, which is likely artifactual. This did not affect our experiments, as all images in the present study were acquired on the same scanner.

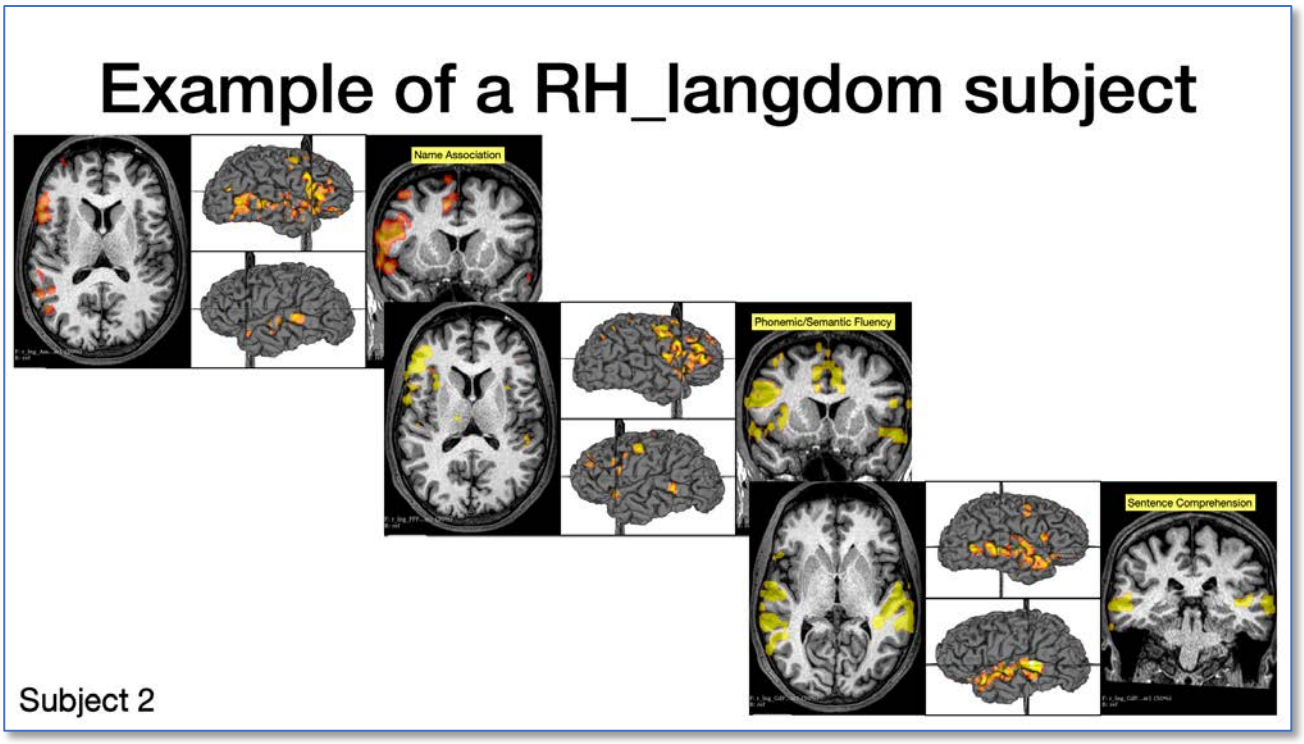

Figure 21: Task-based f-MRI from one of the five participants (Subject 2) classified as rh_langdom (right-hemisphere language dominance).

MRI acquisition

MRI acquisition parameters were identical to those detailed in Chapter I.

Subgroups, analyses and results

We conducted four analyses: the first included all 95 participants; the remaining three excluded, respectively, left-handers with left-hemisphere language dominance, right-handers, and left-handers with right-hemisphere language dominance. The first three analyses were designed to compare SUPR-FLAIR maps between right- versus left-hemisphere language lateralization, whereas the fourth aimed to examine differences between right- and left-handers while holding language lateralization constant.

Analysis A1

This first analysis examines differences in SUPR-FLAIR mapping between left-handers with right-hemisphere language dominance (rh_langdom) and all other participants (left- or right-handers) with left-hemisphere language dominance (lh_langdom). We fit a vertex-wise GLM with SUPR-FLAIR as the dependent variable and language lateralization as the independent variable, adjusting (as covariates) for age, gender, handedness, and cortical thickness (included as a Per-Vertex

Regressor - PVR). In other words, this was a multivariate "between-subjects" analysis testing the contrast rh_langdom – lh_langdom.

In the figures for this section (and the parallel figures that follow), which show Freeview (FreeSurfer's viewer) screenshots, the t-test significance values for the rh_langdom – lh_langdom contrast are mapped as signed –log10(P), after surface-based smoothing with a 15 or 25 mm kernel radius. We use a heat colormap: warm colors (positive sign; significance increasing from red to yellow) mark vertices where cortical FLAIR intensity is higher in rh_langdom, whereas cool colors (negative sign; significance increasing from blue to cyan) mark vertices where FLAIR intensity is higher in lh_langdom. The balance of positive and negative values is visible both on the surface maps and in the accompanying histograms. Statistical thresholds are reported beneath the histograms in the "Min" field. Because the plotted values (Val) are –log10(P), recall that $P = 10^{(-Val)}$; thus 1, 1.3, 2, 3 … correspond to P = 0.1, 0.05, 0.01, 0.001, etc.

Main findings appreciable in Figure 22 are:

- Global pattern: most cortical regions show higher SUPR-FLAIR intensity in participants with lh_langdom.
- Language-related areas (rh_langdom > lh_langdom): participants with rh_langdom exhibit focal hyperintensity in language-critical territories, with a left-lateralized emphasis in anterior and posterior language regions (including the planum temporale, and especially primary auditory cortex), as well as the opercular sensorimotor area. Posterior language cortex is also hyperintense on the right, albeit less markedly.
- Posterior networks: even stronger effects appear posteriorly, particularly inferiorly encompassing the occipital pole and extending along the ventral and dorsal visual streams, ventrally approaching the putative visual word-form area, and dorsally reaching the superior sensorimotor cortex from the hand knob to the paracentral lobule. The pattern is bilateral, more evident on the left at the occipital pole and on the right in the sensorimotor cortex and along the intraparietal sulcus.

Figure 23, which displays results after smaller-kernel surface smoothing (15 mm), thus higher sensitivity but lower Signal-to-Noise Ratio (SNR), also reveals that:

- Language areas are bilateral, though consistently more significant on the left; additional clusters emerge in right Broca's region and operculum.

- The posterior occipito-basal hyperintensity extends further anteriorly, especially on the left, forming a “tongue” that approaches the visual word-form area even more closely.
- Intraparietal sulcus hyperintensity is bilateral.
- Additional clusters appear in the cingulate gyrus, bilaterally in the retro-splenial/isthmus part.

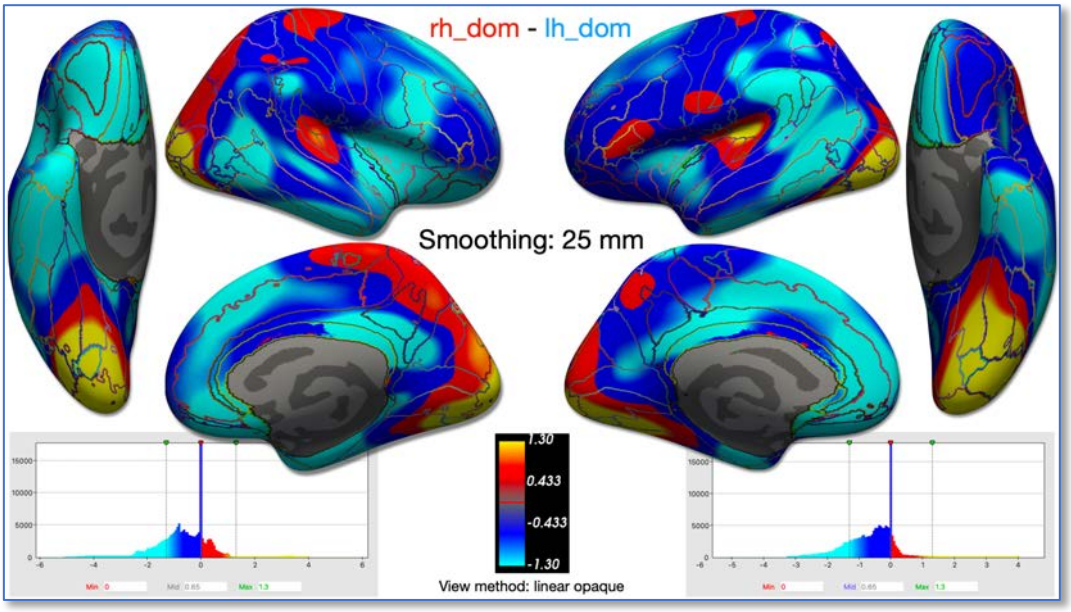

Figure 22: Contrast rh_langdom – lh_langdom, adjusted for age, gender, handedness, and cortical thickness. All output values (Min = 0) are mapped onto the inflated surface of the FreeSurfer fsaverage template.

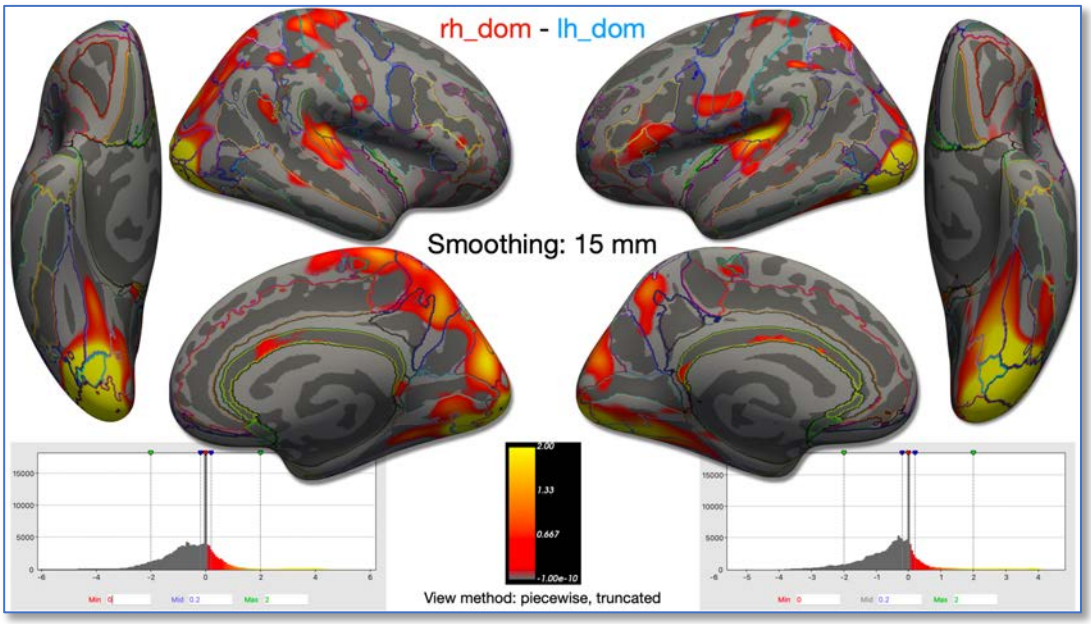

Figure 23: Same analysis as in Figure 5 but after smoothing with a smaller kernel radius (15 mm). Negative-signed values have been masked (truncated color scale) to better highlight cortical regions with higher FLAIR intensity in rh_langdom. In addition, the color rendering uses a piecewise scheme rather than linear opaque. All output values (Min = 0) are mapped onto the inflated surface of the FreeSurfer fsaverage template.

Analysis A2

Same design as Analysis A1, but excluding left-handers with left-hemisphere language dominance, to further isolate the effect of language lateralization. In practice, we stratified the sample by removing participants who were left-handed yet left-dominant for language. This yielded a "between-subjects" multivariate vertex-wise GLM with the primary contrast rh_langdom (all left-handers) – lh_langdom (all right-handers) (5 L vs. 76 R), adjusting for age, gender, handedness, and cortical thickness.

Key findings evident in Figure 24 are:

- The balance between warm and cool colors shifts to roughly 50/50 (as seen in both the maps and histograms), indicating that, relative to Analysis 1, the total area showing higher cortical FLAIR intensity in right-dominant language speakers is substantially larger.
- Evidence of bilateral hyperintensity in language territories is reinforced. Involvement of the superior temporal sulcus (Brodmann area 22) accompanies that of the Heschl gyri. On the left, additional foci appear in the temporal pole and posterior orbitofrontal cortex.
- Posterior occipito-basal hyperintensity is again bilateral, extending toward the visual word-form region.
- Sensorimotor hyperintensity is bilateral, with a markedly stronger effect at the right hand-knob. Bilateral (right-predominant) hyperintensity along the intraparietal sulcus is confirmed, and bilateral SMA involvement is more apparent.
- Cingulate gyrus clusters are again present, particularly on the right, with a bilateral spot at the isthmus, as already seen in Analysis A1.

Figure 25 corroborates these findings and additionally reveals small hyperintense spots at the temporal poles.

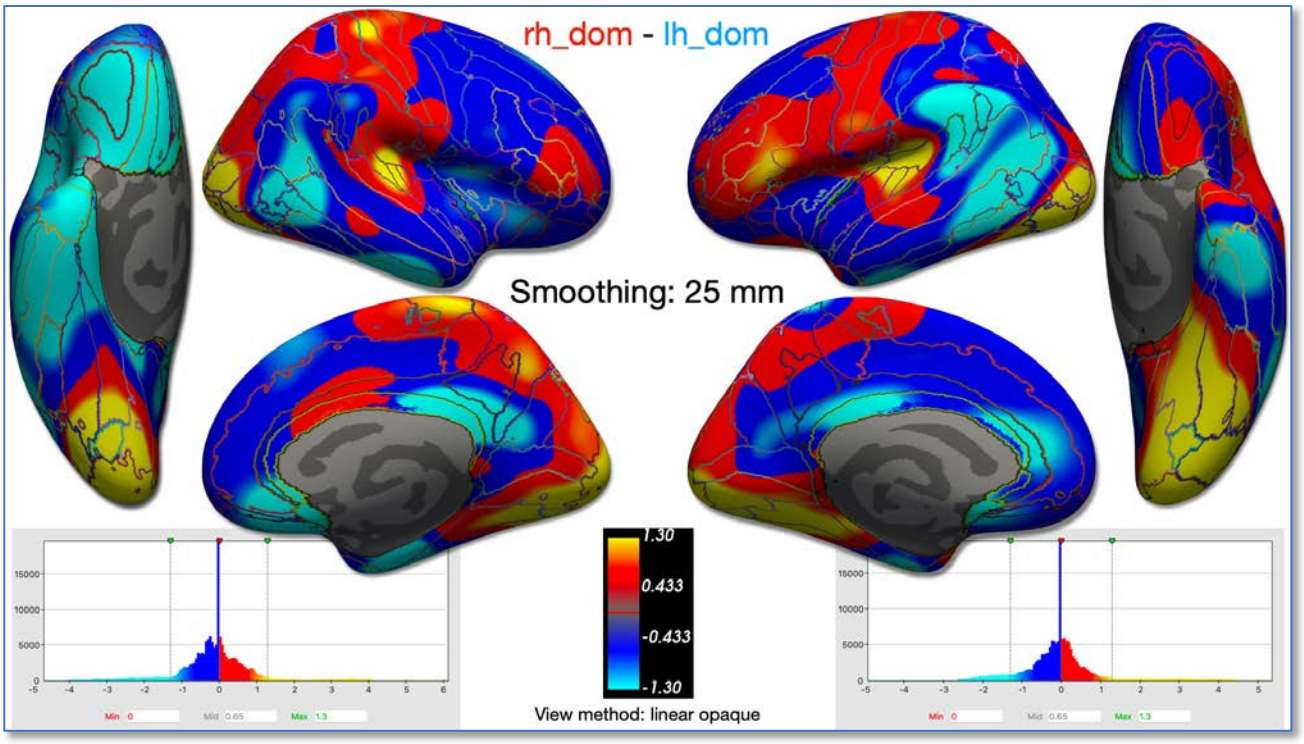

Figure 24: Contrast rh_langdom – lh_langdom, adjusted for age, gender, handedness, and cortical thickness, after excluding left-handers with left-hemisphere language dominance.
All output values (Min = 0) are mapped onto the inflated surface of the FreeSurfer fsaverage template.

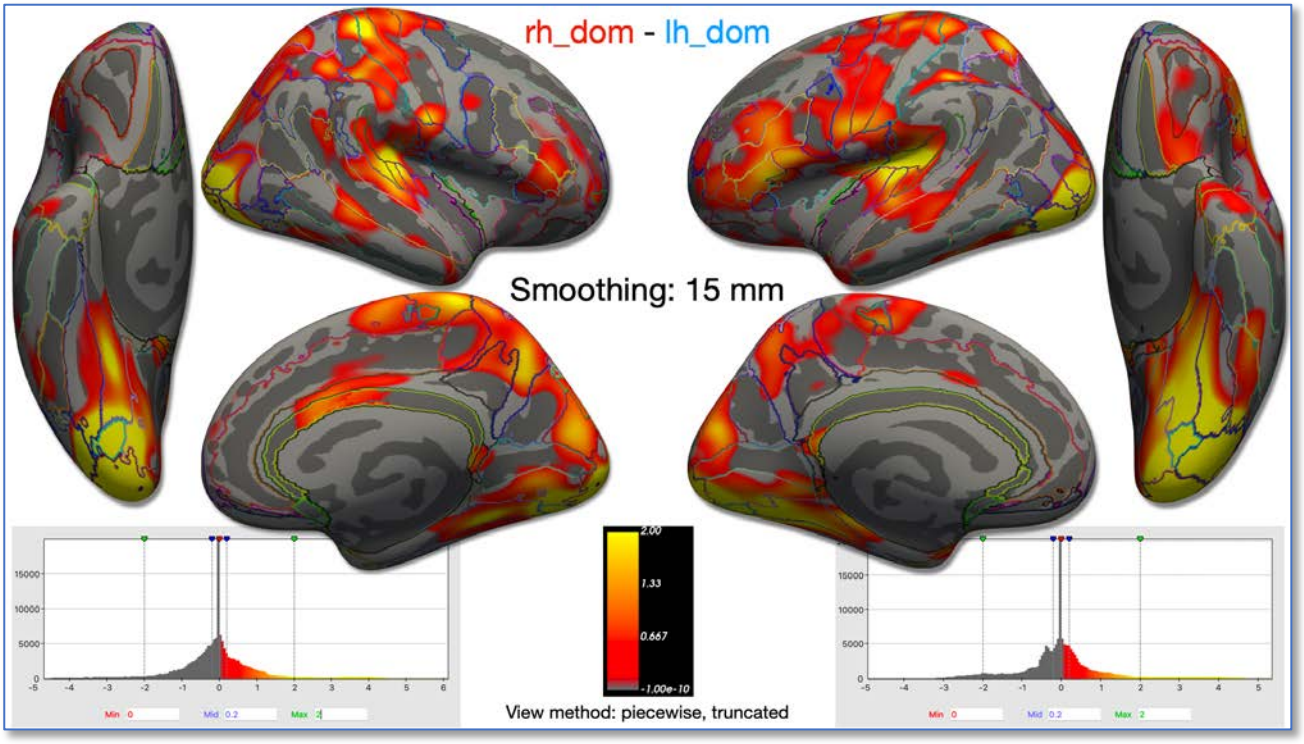

Figure 25: Same analysis as in Figure 24 but after smoothing with a smaller kernel radius (15 mm).
All output values (Min = 0) are mapped onto the inflated surface of the FreeSurfer fsaverage template.

Analysis A3

Here we excluded all right-handed participants, stratifying the sample to isolate the pure effect of language lateralization. This produced another "between-subjects" multivariate vertex-wise GLM with the primary contrast rh_langdom (all left-handers) – lh_langdom (all left-handers) (5 L vs. 14 L), adjusting for age, gender, and cortical thickness. This design isolates the effect of language lateralization independent of handedness.

Key findings in Figure 26 are:

- Bilateral hyperintensity in primary auditory cortex is confirmed, now more significant on the right. The Broca's area focus persists, but only on the left.
- Posterior occipito-basal hyperintensity is again present, markedly stronger on the right. A right-lateralized dorsal-stream hyperintensity is also evident, though it does not extend to the sensorimotor cortex.

Figure 27 (smaller surface-smoothing kernel) further shows:

- Persistent hyperintense spots in the left subcentral lobule.
- Bilateral foci along the intraparietal sulcus.
- A left-lateralized spot near the visual word-form area.

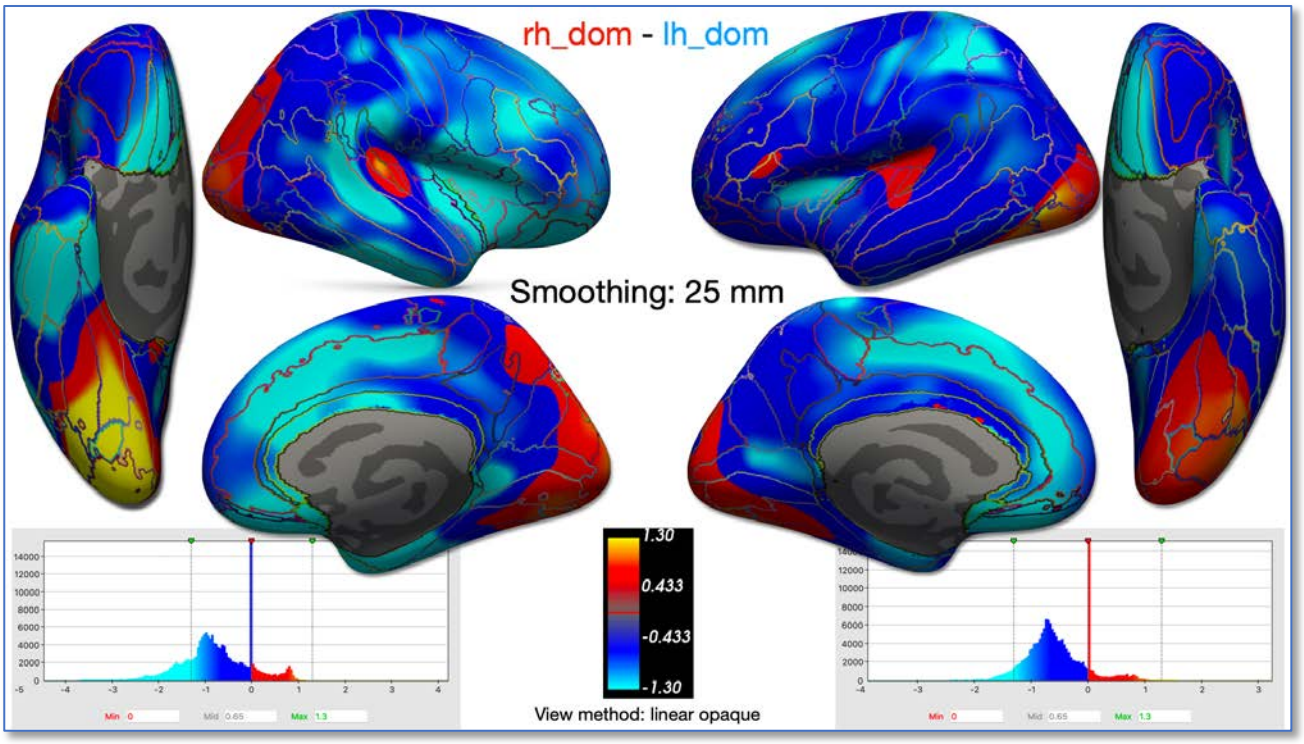

Figure 26: Contrast rh_langdom – lh_langdom, adjusted for age, gender, handedness, and cortical thickness, after excluding right-handers.
All output values (Min = 0) are mapped onto the inflated surface of the FreeSurfer fsaverage template.

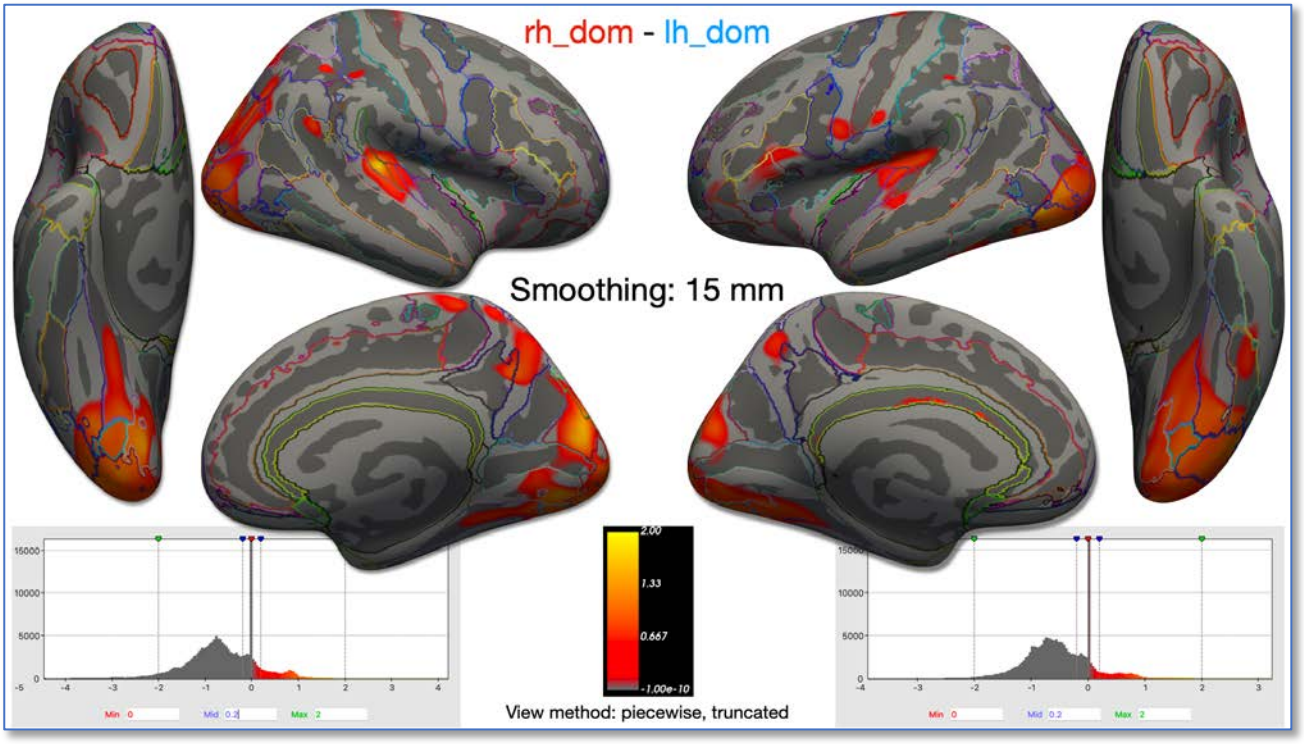

Figure 27: Same analysis as in Figure 26 but after smoothing with a smaller kernel radius (15 mm).
All output values (Min = 0) are mapped onto the inflated surface of the FreeSurfer fsaverage template.

Figure 28 provides additional detail for this analysis. Using a Bayesian cluster-wise analysis, clusters from the significance maps were ranked in descending order of significance (table not shown here; further examples appear later). For each cluster, a label was generated (not displayed in this figure and not perfectly coincident with the corresponding colored spot owing to differing thresholding criteria). A green sphere marks the peak (minimum-P) vertex within each cluster. The box-and-whisker plot summarizes SUPR-FLAIR values from the 19 observations, grouped by language lateralization, and also reports group means.

The vertex highlighted in the left hemisphere is the most significant within a cluster located in the posterior language region, specifically at the posterior segment of the left Sylvian fissure according to the Destrieux atlas (Lat_Fissure-post_sgt). At this site, normalized cortical FLAIR intensity is higher in participants with right-hemisphere language dominance. The mean SUPR-FLAIR increase is +0.042, approximately 4% of the control group mean. The average difference across the entire cluster is +0.046, essentially identical.

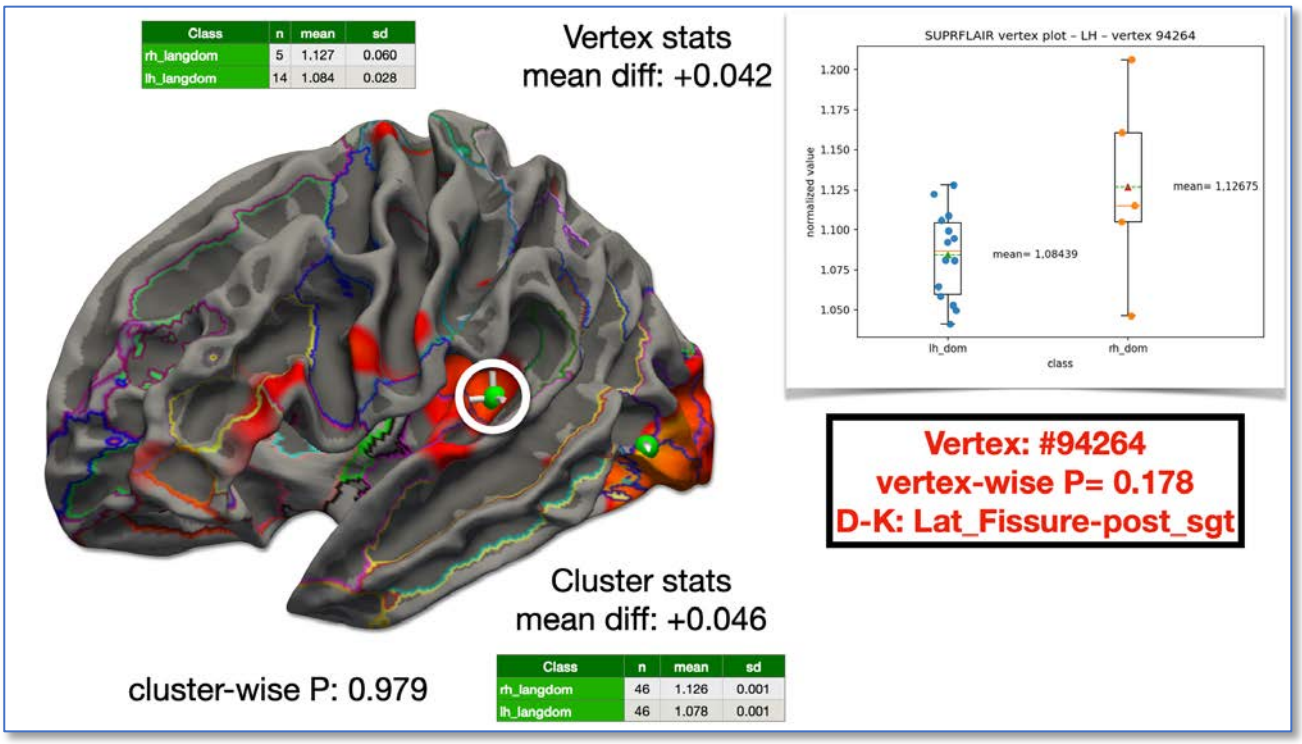

Figure 28: Same analysis as in Figure 27 but with all output values (Min = 0) mapped onto the white matter surface (GWMI) of the FreeSurfer fsaverage template.
Green dots mark the peak (minimum-P) vertex of each cluster identified by the cluster-wise analysis. The white circle highlights the vertex indicated by the 3D cross; the box plot and vertex statistics in the figure refer to this vertex.

Analysis A4

In this analysis, we excluded left-handers with right-hemisphere language dominance, stratifying the sample to isolate the pure effect of handedness (all included participants had left-hemisphere language dominance). We then fit a "between-subjects", vertex-wise multivariate GLM with the primary contrast left-handers - right-handers (14 - 76), adjusting for age, gender, and cortical thickness.

Main findings in Figure 29 are:

- Nearly the entire cortex, excluding the most posterior territories and an area in the left gyrus cinguli, shows higher intensity in left-handers.
- Left-handers exhibit bilateral hyperintensity in language areas; among posterior regions, Brodmann area 22 is particularly prominent.
- In primary sensorimotor cortex, hyperintensity is bilateral in left-handers, especially in the inferior third of the pre- and postcentral gyri, the suprasylvian opercular cortex proper, and the insula.
- Left-handers also show greater hyperintensity in the anterior segment of the right intraparietal sulcus.
- Much of the frontal cortex, including the orbitofrontal region, is bilaterally more hyperintense in left-handers.
- Additional hyperintensity is evident in the cingulate gyrus of left-handers, right-sided, posterior to the genu of the corpus callosum.
- Finally, left-handers display bilaterally greater hyperintensity at the temporal poles, extending along the parahippocampal gyrus and the inferior temporal gyrus.

Figure 30, which presents the results of the same analysis after 15-mm smoothing, consolidates most of the findings observed in the previous figure.

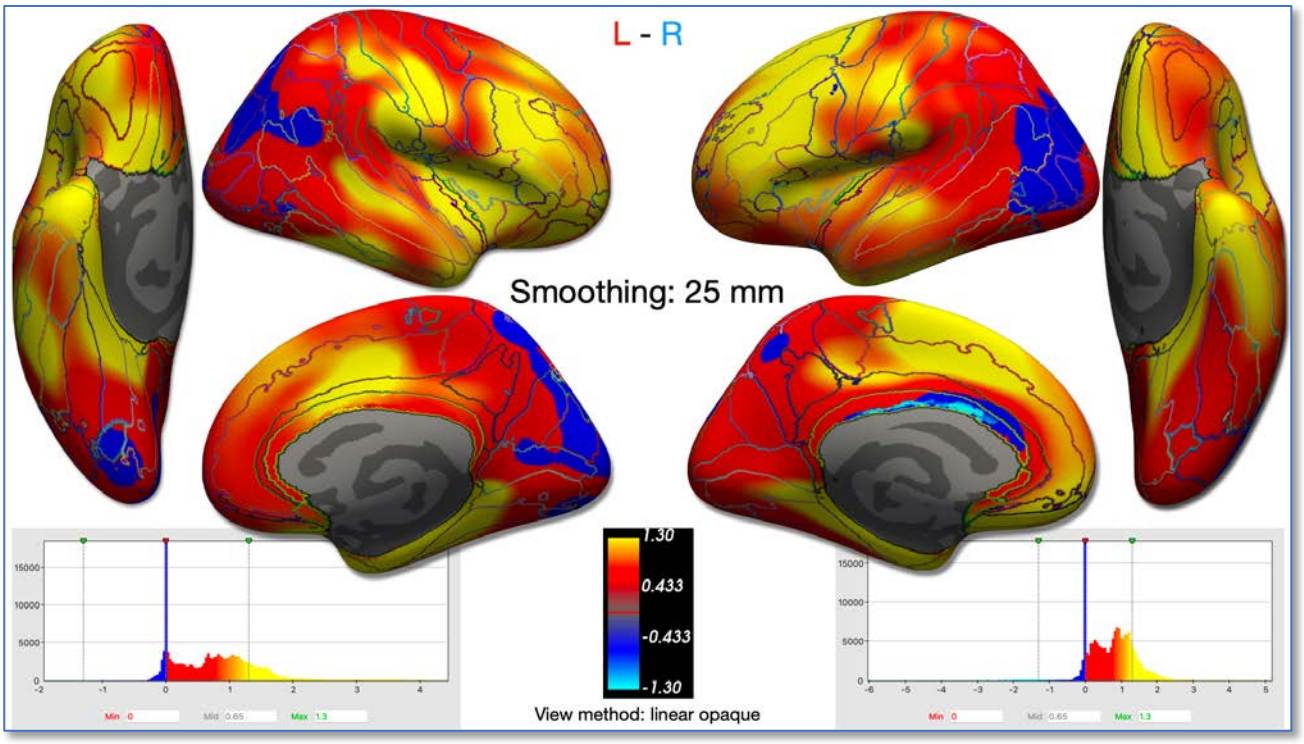

Figure 29: Contrast left-handers – right-handers, adjusted for age, gender and cortical thickness, after excluding left-handers with right language lateralization.
All output values (Min = 0) are mapped onto the inflated surface of the FreeSurfer fsaverage template.

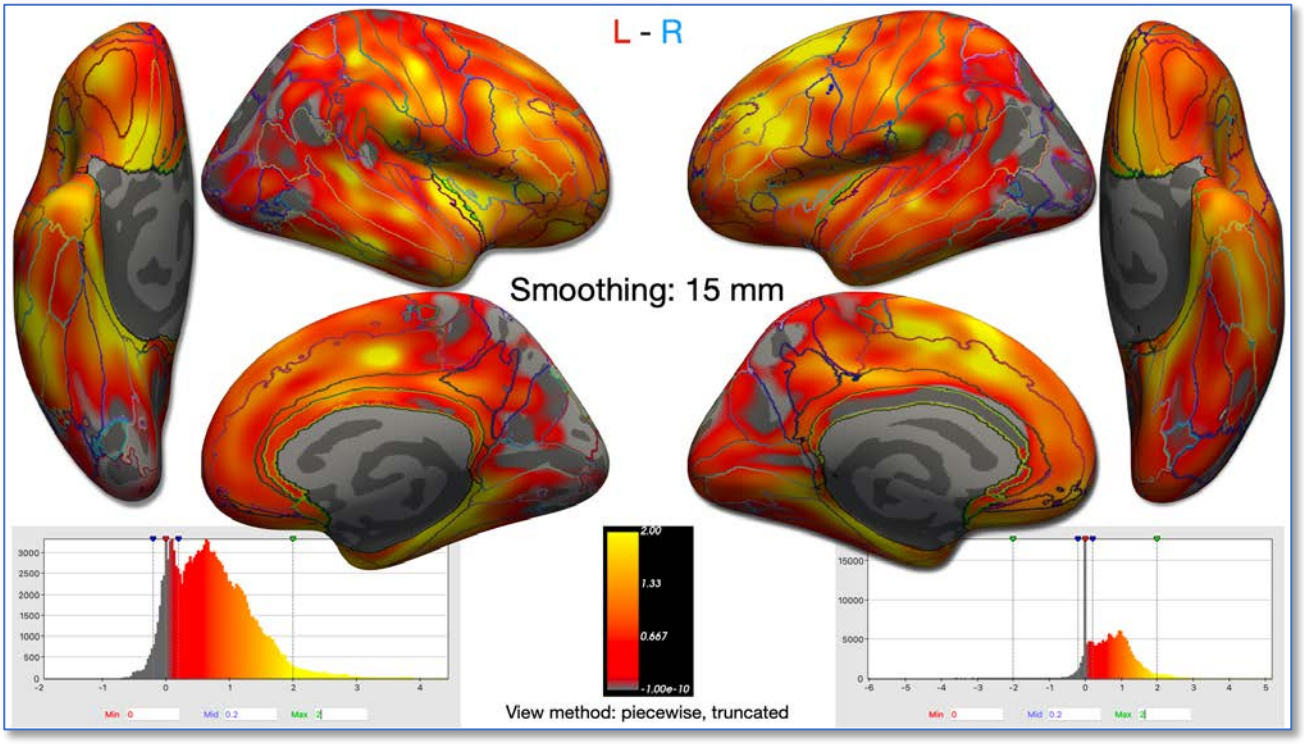

Figure 30: Same analysis as in Figure 29 but after smoothing with a smaller kernel radius (15 mm).
All output values (Min = 0) are mapped onto the inflated surface of the FreeSurfer fsaverage template.

Integrated summary of all analyses from Experiment A

Figure 31 re-displays, for ease of comparison, the lateral and medial views of the fsaverage inflated surface for the four analyses just presented. The main takeaways are:

- Language areas appear more FLAIR-intense in participants with right-hemisphere language lateralization documented by f-MRI. However, despite the marked f-MRI lateralization, the FLAIR effect is bilateral and remains more significant on the left than on the right.
- In the same right-lateralized group, cortical FLAIR hyperintensity is especially evident in posterior territories, notably at the occipital pole and along the ventral visual stream.
- Left-handers show diffusely higher bilateral FLAIR intensity across most of the cortex, except in the most posterior regions.
- The combination of right-hemisphere language dominance and left-handedness accentuates relative FLAIR hyperintensity in the sensorimotor cortex and intraparietal sulcus, bilaterally, once the sample is stratified by excluding left-handers with left-hemisphere language dominance.
- Multivariate modeling (covariate-adjusted GLMs) improves estimation but does not, by itself, fully isolate the effects of interest (hemispheric language dominance and handedness); sample stratification is also necessary.

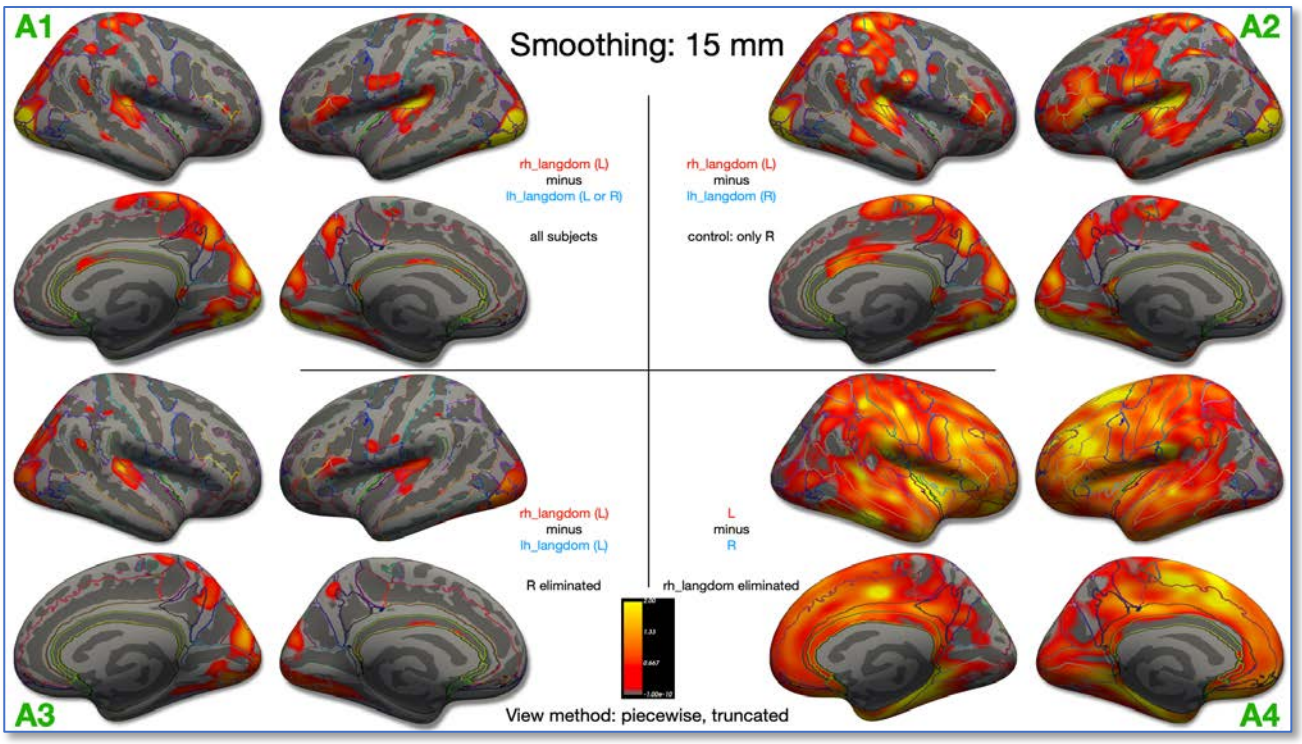

Figure 31: main images from previous figures for side-to-side comparison.

In Figure 32 results are shown for each left-handed participant with right-hemisphere language dominance, contrasted against the right-handed cohort. Subject 2 is the participant whose f-MRI appeared in Figure 21. Key findings are:

- Broca's region: focal hyperintensity in Subject 2 (bilateral) and Subject 3 (right).
- Heschl/Wernicke region: focal hyperintensity in Subject 1 (right) and in Subjects 2 and 4 (left).
- Posterior cortex: hyperintensity in all subjects, bilateral in Subjects 1, 3, and 4; right-lateralized in Subjects 2 and 5.

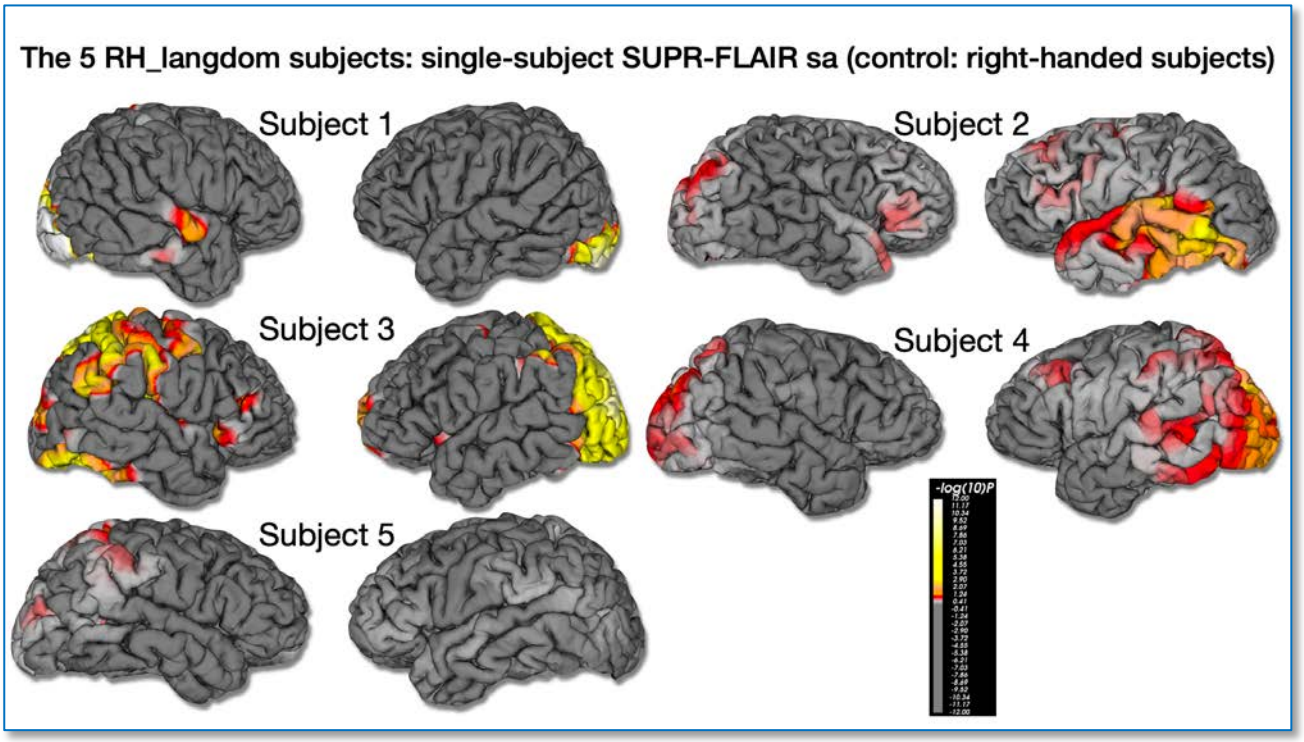

Figure 32: Single-subject SUPR-FLAIR-sa.
For each left-handed participant with right-hemisphere language dominance (rh_langdom), the figure shows vertex-wise results contrasted against the right-handed cohort.

Experiment B: association between SUPR-FLAIR and finger-tapping paradigm. A "within-subject" analysis with repeated task–rest runs

Subjects

Three healthy right-handed male volunteers underwent the experiment.

MRI acquisition, paradigm and analysis

High-resolution 3D T1w and axial 2D FLAIR sequences were acquired on the same scanner and with the same parameters described in Chapter I. Within a single session, six or four consecutive FLAIR

runs (~5 min each) were obtained, as detailed in Figure 33. A within-subject, vertex-wise paired t-test (task − rest) was performed, with run pairings chosen to preserve temporal adjacency, for example, for Subject 1: 4–1, 5–2, 6–3.

Given the focus on sensorimotor activation, eye state (eyes closed vs. open) was included only as a covariate for statistical adjustment.

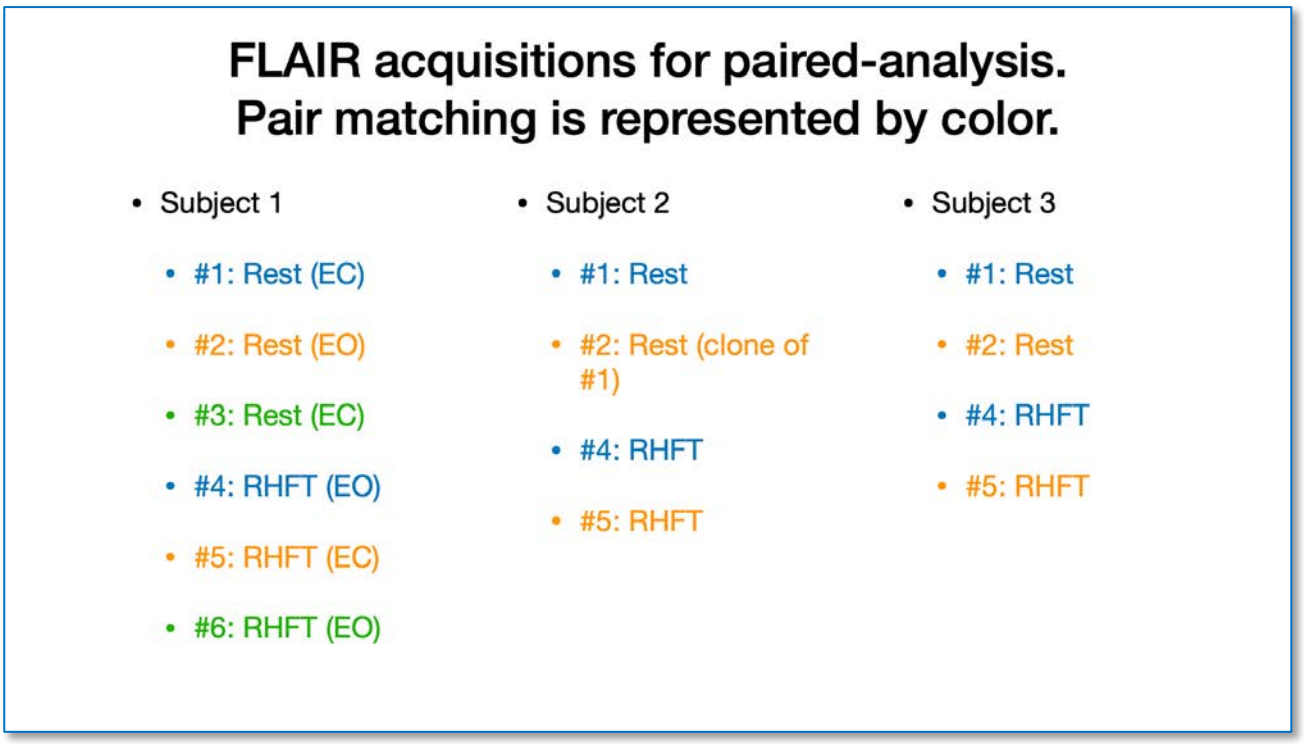

Figure 33: List of FLAIR acquisitions for the three subjects.
For all three participants, scans at rest were acquired first, followed by an equal number during task execution. Only Subject 1 included an alternation of eyes-closed/eyes-open states. Because Subject 2's second rest scan was unusable due to file corruption, we duplicated the first rest run. Colors indicate the pairings used for analysis, chosen to maintain the same temporal spacing between rest and task. Abbreviations: EC = Eyes Closed; EO = Eyes Open; RHFT = Right-Hand Finger Tapping.

Results

Results are shown in Figure 34 and Figure 35.

Within the sensorimotor network, two positive clusters are evident: (i) a prominent focus at the left hand-knob in primary sensorimotor cortex, maximal over the postcentral gyral crown and the posterior bank of the central sulcus but extending also to the precentral gyrus; and (ii) a second cluster in the left posterior medial frontal gyrus encompassing SMA/pre-SMA. Both clusters are strongly lateralized to the left hemisphere, in clear concordance with the right-hand finger-tapping task.

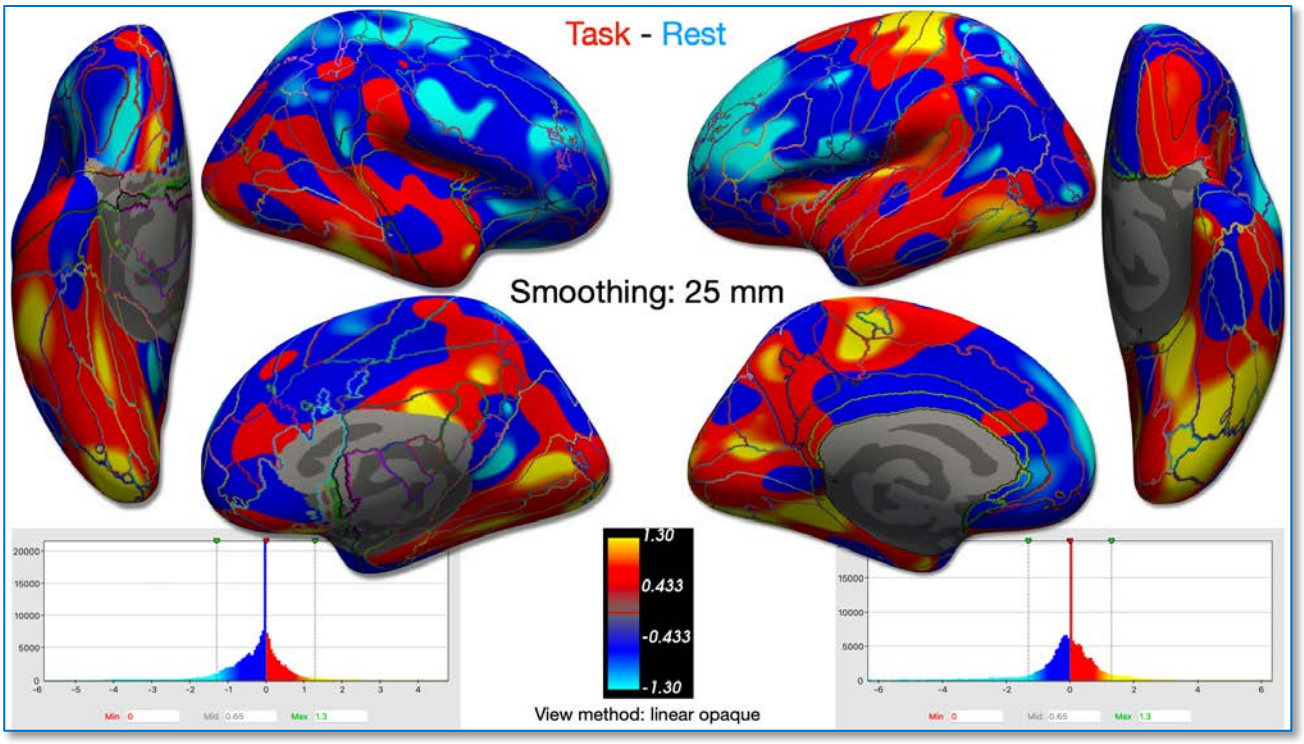

Figure 34: Contrast task – rest, adjusted for eyes condition (eyes closed/open).
All output values (Min = 0) are mapped onto the inflated surface of the FreeSurfer fsaverage template.

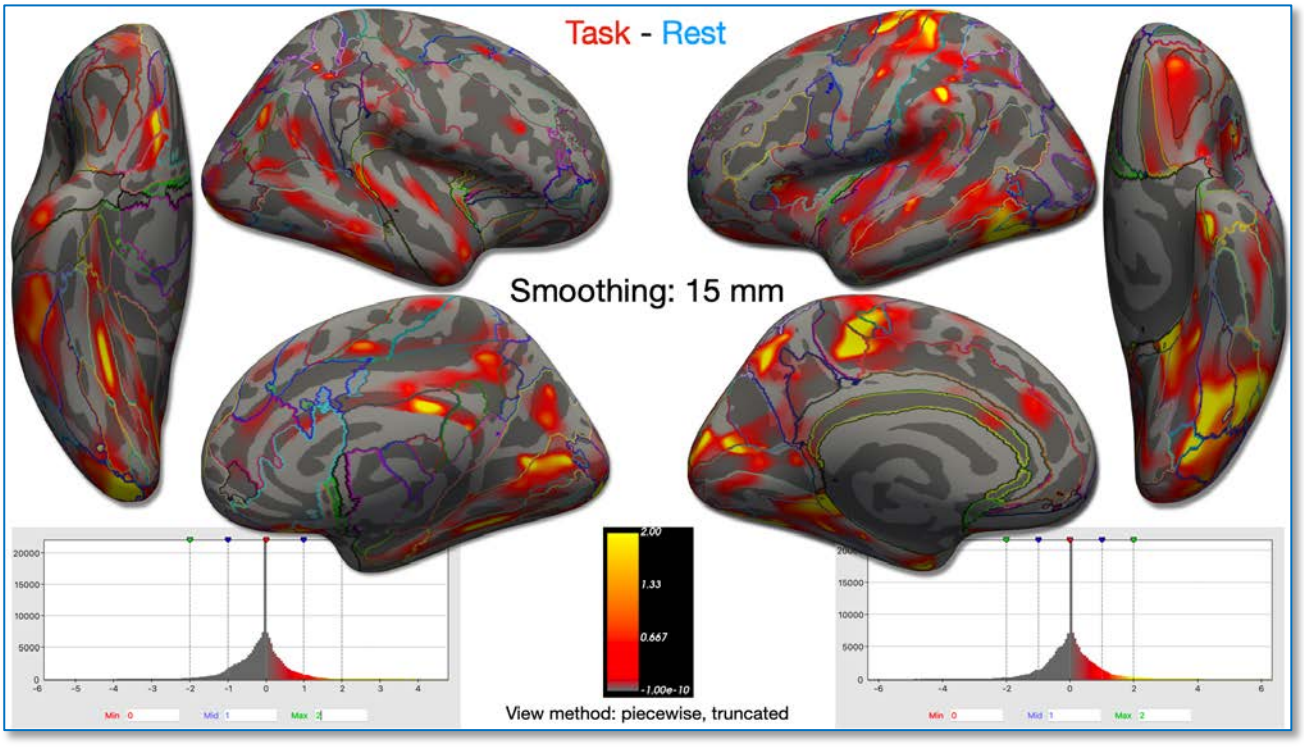

Figure 35: Same analysis as in Figure 34 but after smoothing with a smaller kernel radius (15 mm).
All output values (Min = 0) are mapped onto the inflated surface of the FreeSurfer fsaverage template.

Additional details are provided in Figure 36 and Figure 37. At the peak (minimum-P) vertex of the hand-knob cluster, the box plot shows a mean increase of 0.015 in normalized cortical FLAIR during task versus rest. The paired “spaghetti” plot demonstrates that all seven vertex pairs exhibit higher task values. The pairwise differences are of similar magnitude, suggesting no consistent temporal trend (e.g., summation or adaptation) over the acquisition interval.

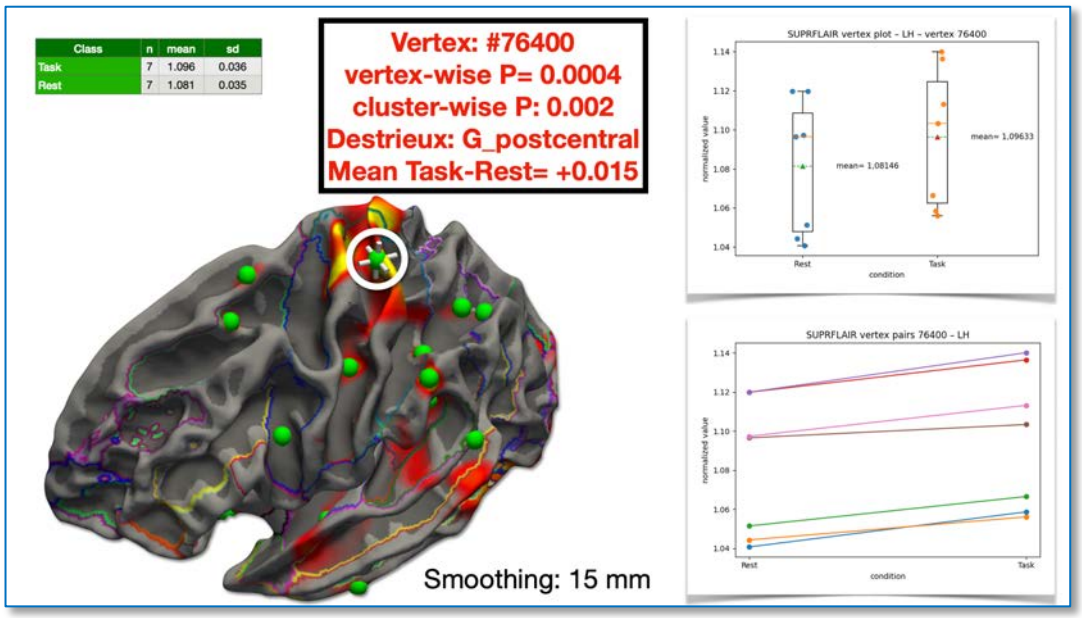

Figure 36: Vertex-wise statistics at the peak (minimum-P) vertex of the positive cluster in the hand-knob region.

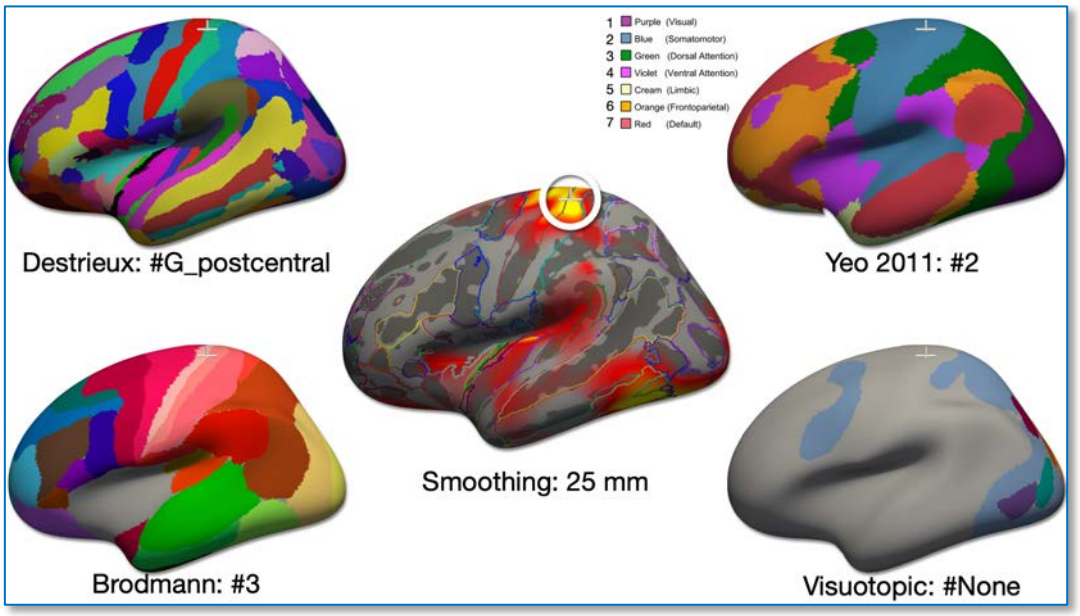

Figure 37: Cross-atlas localization of the hand-knob cluster peak (minimum-P vertex): Destrieux (Fischl et al., 2004), Yeo 2011 (Yeo et al., 2011), Brodmann, and visuotopic parcellations (Van Essen 2012).

Experiment C: association between SUPR-FLAIR and Eyes Moving Task - Eyes Open Rest paradigm. A "within-subjects" analysis with single task - rest runs

Subjects

Two healthy right-handed male volunteers underwent the experiment.

MRI acquisition, paradigm and analysis

High-resolution 3D T1w and axial 2D FLAIR sequences were acquired on the same scanner and with the same parameters described in Chapter I. Within a single session, two FLAIR runs (~5 min each) were obtained, as detailed in Figure 38. A "within-subject", vertex-wise paired t-test (task – rest) was performed.

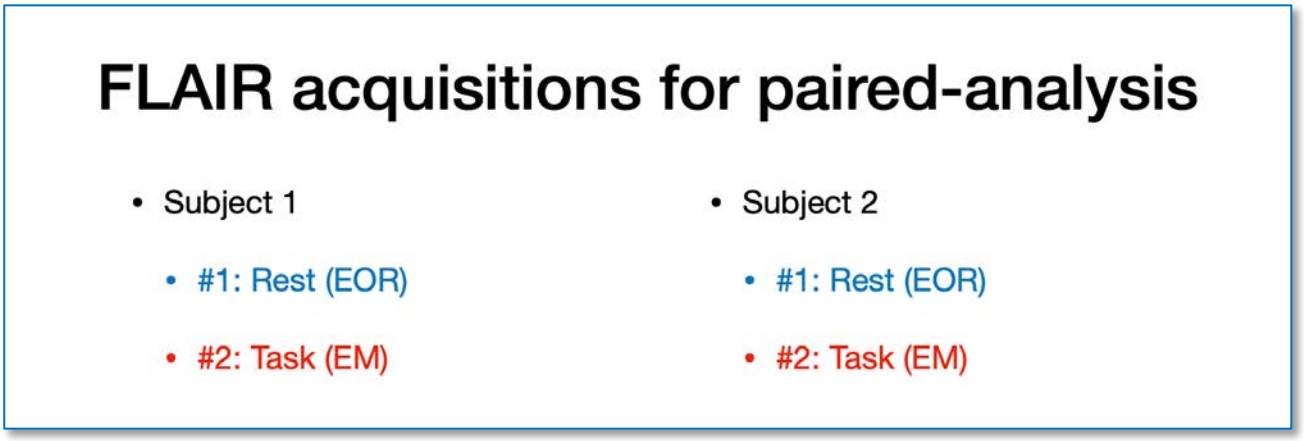

Figure 38: List of FLAIR acquisitions for the two subjects.
For both the participants, scans at rest were acquired first, followed by one run during task execution.
Abbreviations: EO = Eyes Open Rest; EM = Eyes Moving.

Results

Results are shown in Figure 39 and Figure 40.

Despite abundant eye–movement–related artifacts, a cluster of interest can be identified in the posterior segment of the right superior frontal sulcus, corresponding to the Frontal Eye Field (FEF).

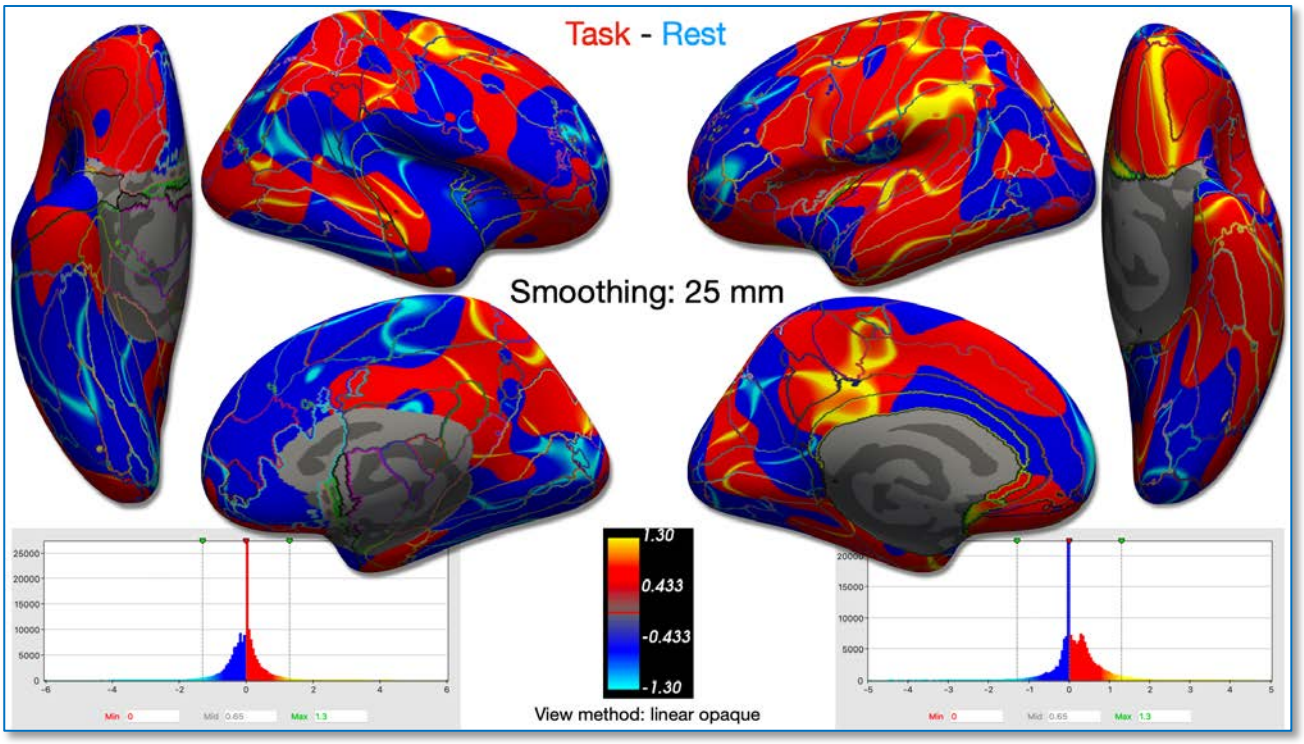

Figure 39: Contrast task – rest.
All output values (Min = 0) are mapped onto the inflated surface of the FreeSurfer fsaverage template.
Motion artifacts, likely related to task performance, produce spurious, curvilinear bands of "significance" that do not respect anatomical boundaries and cut across both positive and negative clusters.

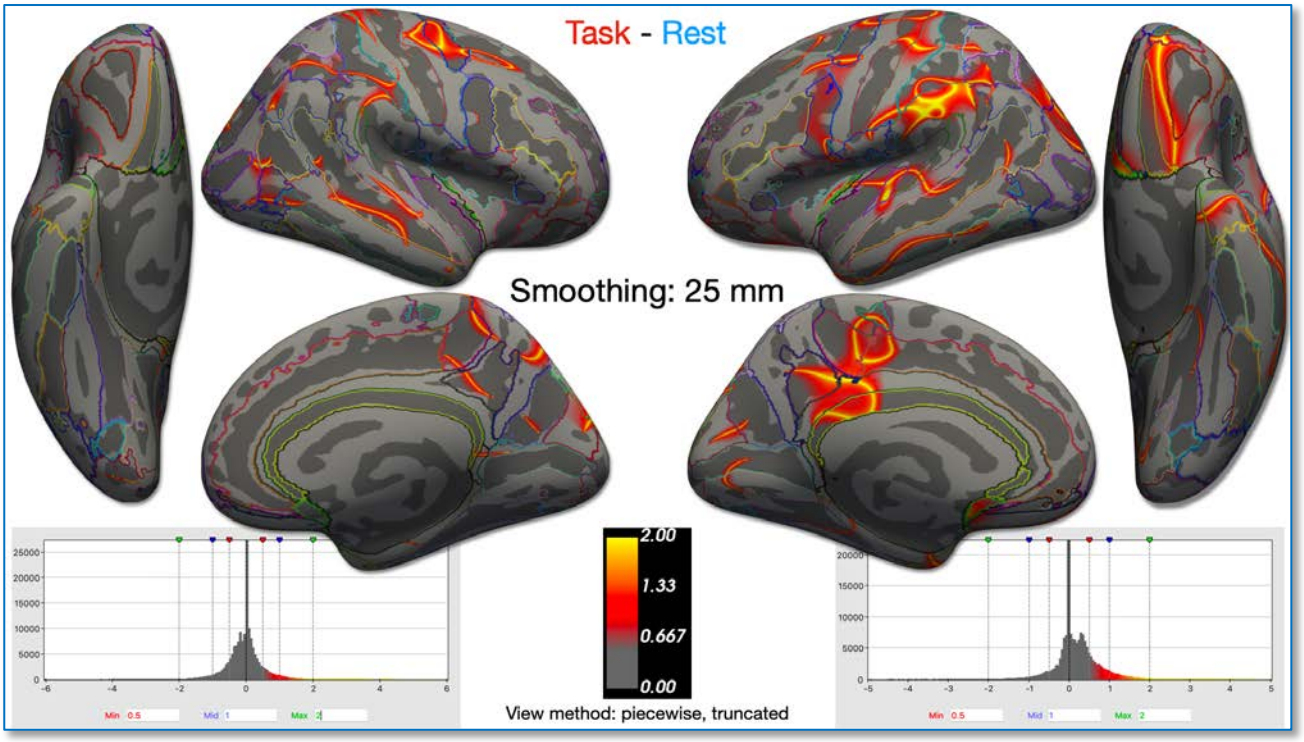

Figure 40: Same analysis as in Figure 39 but after smoothing with a smaller kernel radius (15 mm).
All output values (Min = 0) are mapped onto the inflated surface of the FreeSurfer fsaverage template.

Additional details are provided in Figure 41 and Figure 42.

At the peak (minimum-P) vertex of the FEF cluster, the box plot shows a mean increase of 0.004 in normalized cortical FLAIR during task versus rest. The paired “spaghetti” plot demonstrates that both vertex pairs exhibit higher task values.

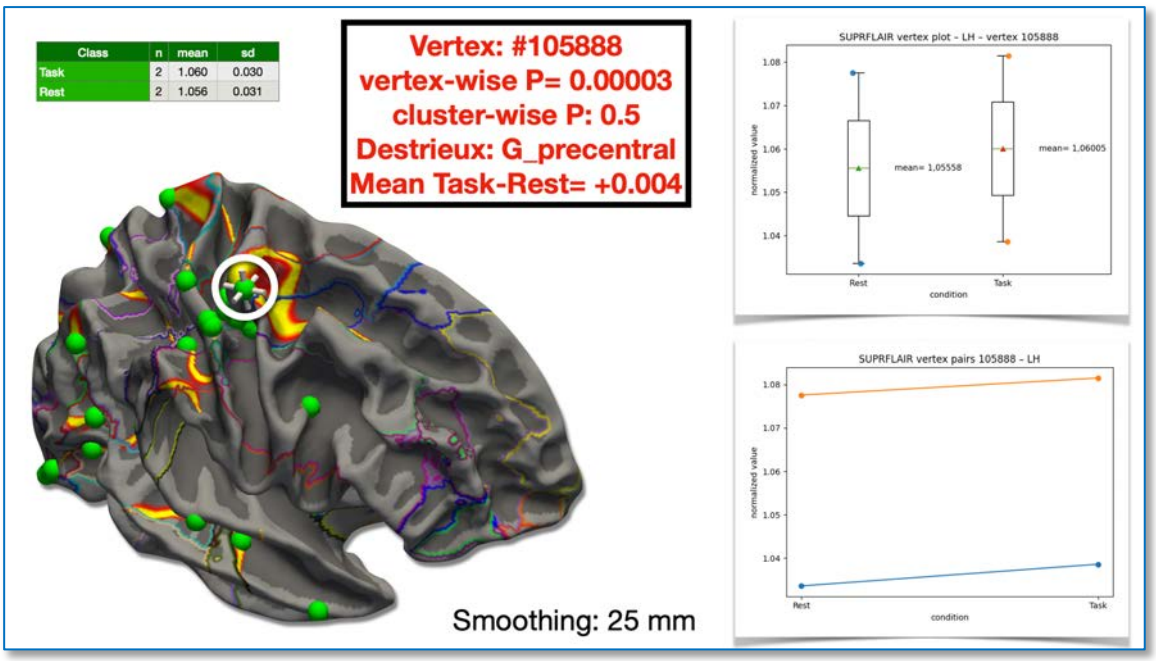

Figure 41: Vertex-wise statistics at the peak (minimum-P) vertex of the positive cluster in the FEF region.

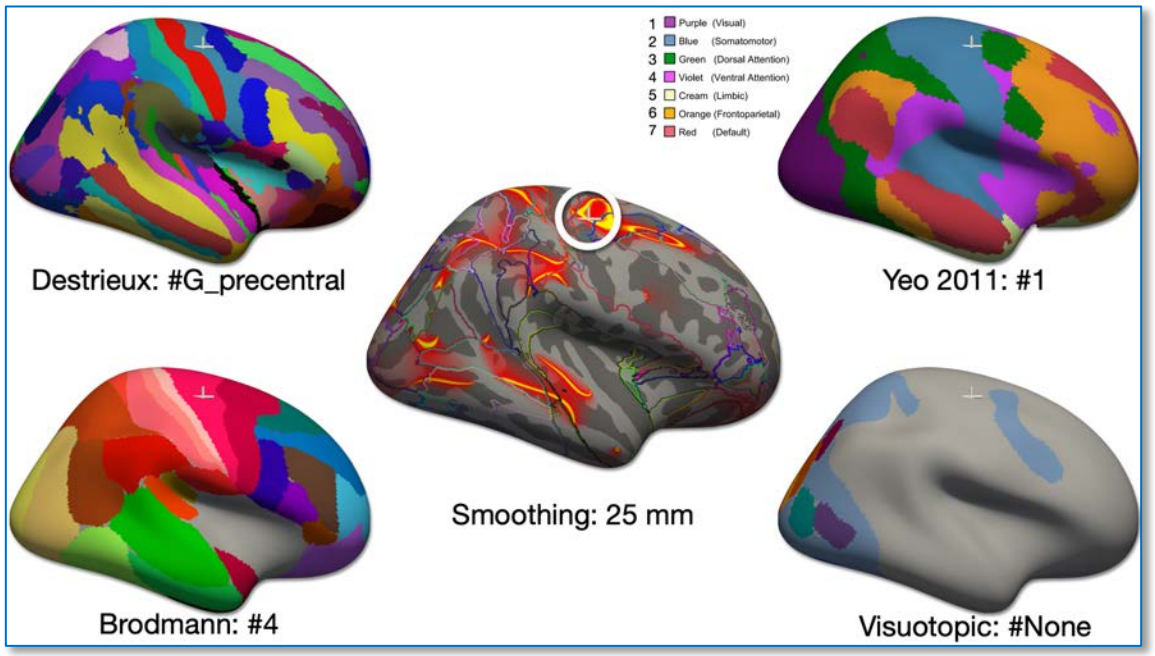

Figure 42: Cross-atlas localization of the FEF cluster peak (minimum-P vertex): Destrieux (Fischl et al., 2004), Yeo 2011 (Yeo et al., 2011), Brodmann, and visuotopic parcellations (Van Essen 2005, 2012).

Experiment D: association between SUPR-FLAIR and two different rest conditions (Eyes Open Rest - Eyes Closed Rest). A "within-subjects" analysis with single "task - rest" runs

Subjects

Forty-four healthy male volunteers underwent the experiment. As visible in Figure 43, this subgroup of the 95 subjects included 35 right-handers and 9 left-handers (none of them with right lateralization of the language).

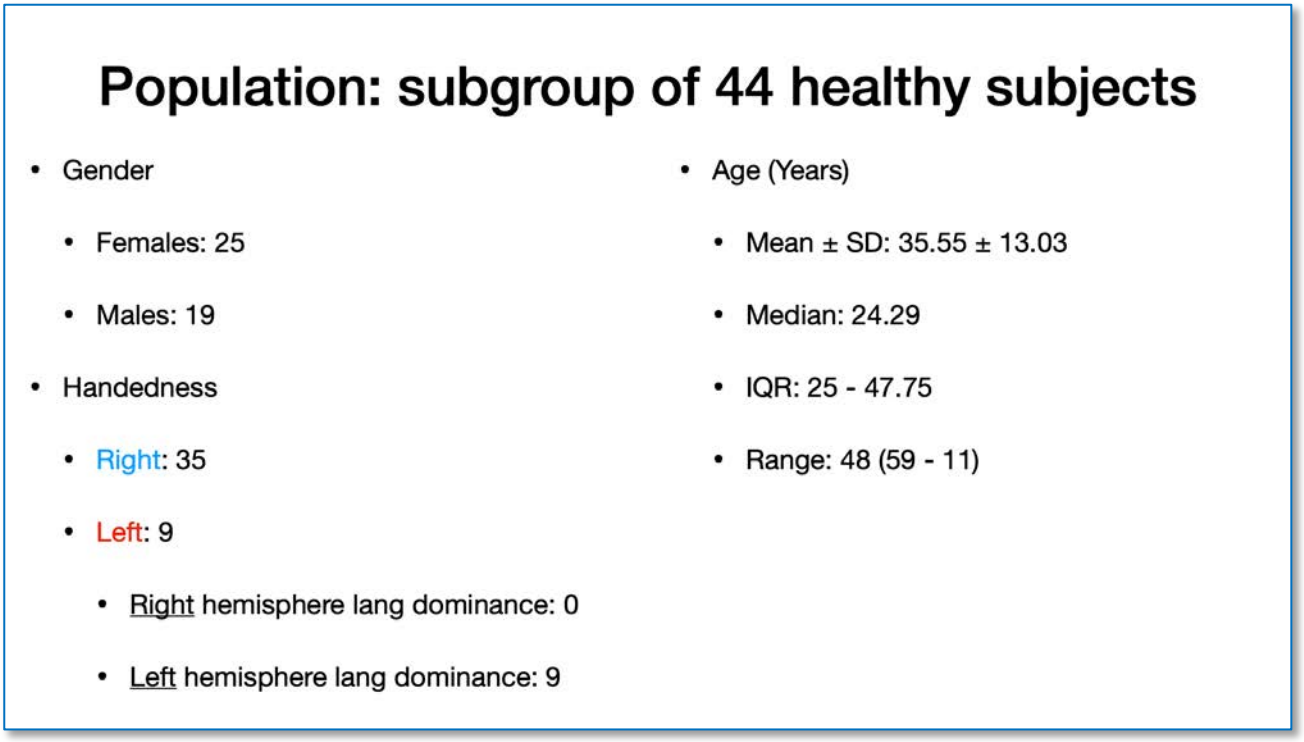

Figure 43: Demographic and functional characteristics of the studied subgroup of subjects.

MRI acquisition, paradigm and analysis

High-resolution 3D T1w and axial 2D FLAIR sequences were acquired on the same scanner and with the same parameters described in Chapter I. Within a single session, two FLAIR runs (~5 min each) were obtained, as detailed in Figure 44. A "within-subject", vertex-wise paired t-test (EOR state - ECR state)[8] was performed.

[8] EOR= Eyes Open Rest. ECR= Eyes Closed Rest.

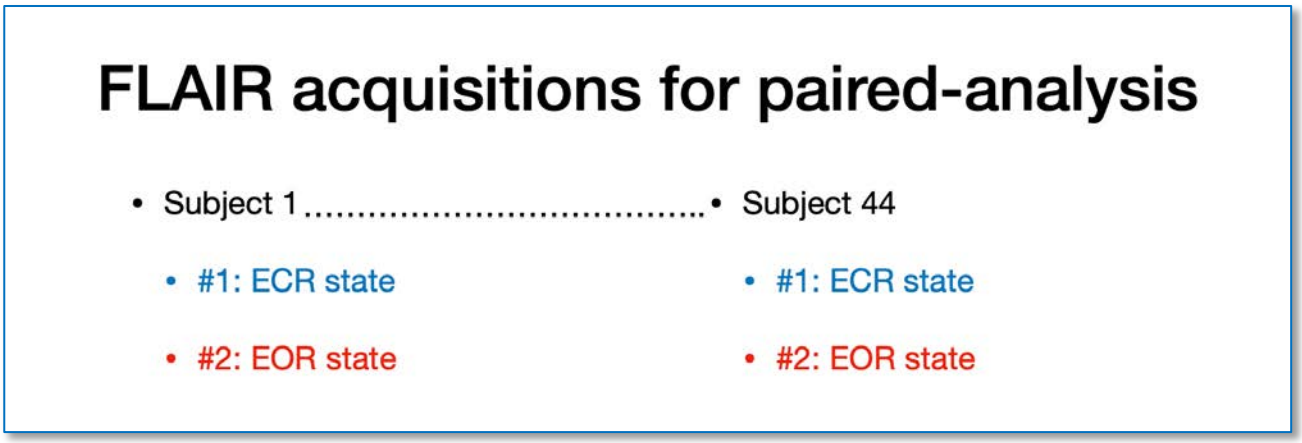

Figure 44: List of FLAIR acquisitions for all subjects.
Scan in EC state was acquired first, followed by scan during EO state.
Abbreviations: ECR = Eyes Closed Rest; EOR = Eyes Open Rest.

Results

Results are shown in Figure 45 and Figure 46.

Overall, as evident from both the surface maps (showing the paired-analysis scalars) and the histograms, relative FLAIR hyperintensity predominates in the right hemisphere.

Numerous positive clusters indicate regions where cortical FLAIR intensity is higher during Eyes Open Rest (EOR) than Eyes Closed Rest (ECR). Salient effects are present in primary and associative visual cortices, with a left-sided predominance. Additional foci of relative hyperintensity are evident along the ventral and dorsal visual streams; in sensorimotor cortex and the frontal eye fields (especially on the right); in the right precuneus; in posterior language cortex; and in left S2. Finally, the most significant cluster overall appears bilaterally in orbitofrontal cortex, although, anticipating the interpretive notes, this likely reflects eye–movement artifacts.

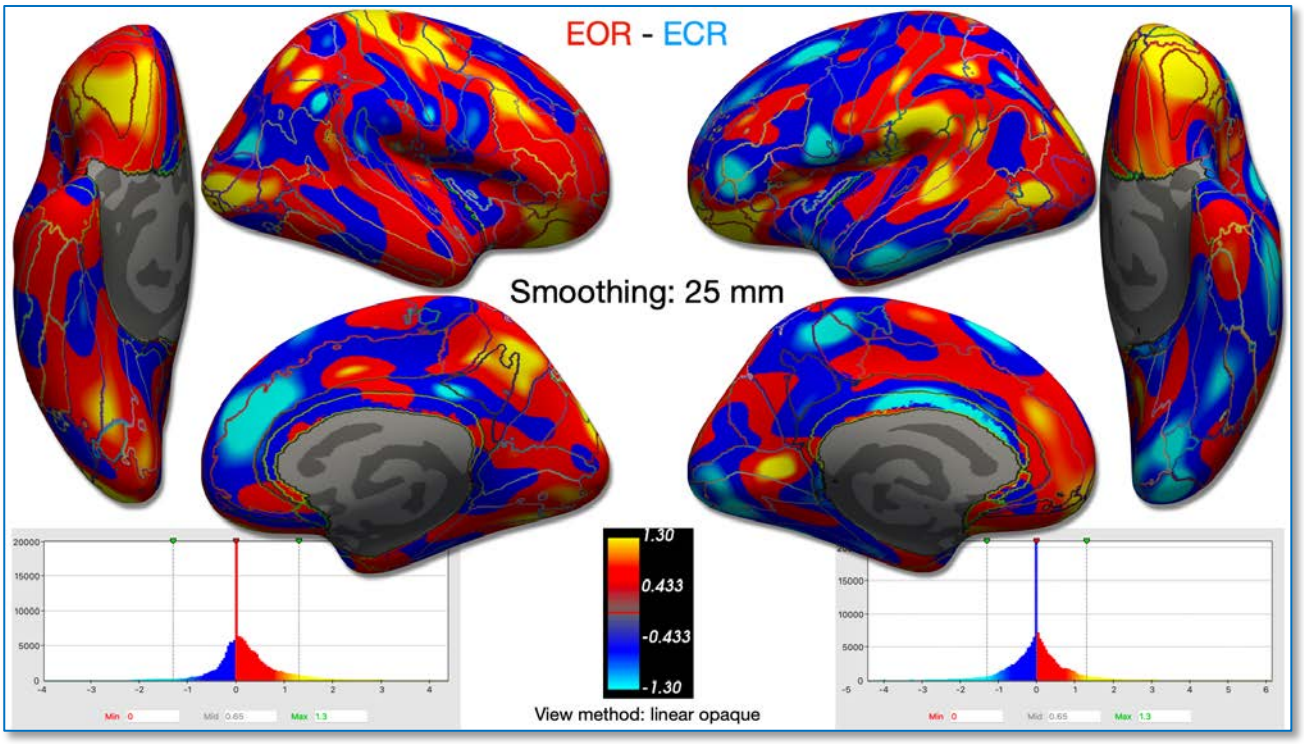

Figure 45: Contrast EOR - ECR.
All output values (Min = 0) are mapped onto the inflated surface of the FreeSurfer fsaverage template.

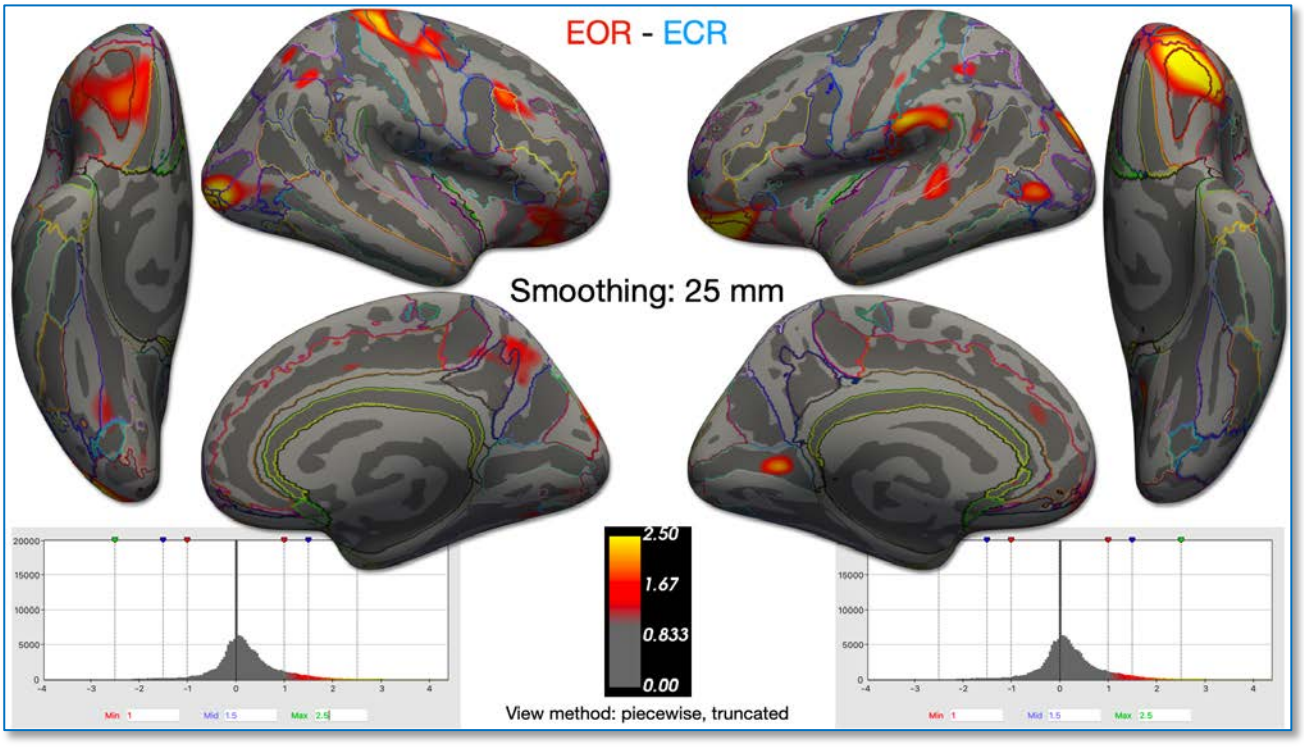

Figure 46: Same analysis as in Figure 45 but after significance thresholding (P<0.1).
All output values (Min = 1) are mapped onto the inflated surface of the FreeSurfer fsaverage template.

Additional details are provided in Figure 47, Figure 48, Figure 49, Figure 50 and Figure 51.

A positive cluster of primary interest is located in the calcarine cortex, where the box plot shows a mean increase of 0.001 in normalized cortical FLAIR during EOR relative to ECR. The paired "spaghetti" plot indicates that not all vertex pairs exhibit higher EOR values (Figure 48).

Some other positive clusters localize to associative visual areas (Figure 50 and Figure 51).

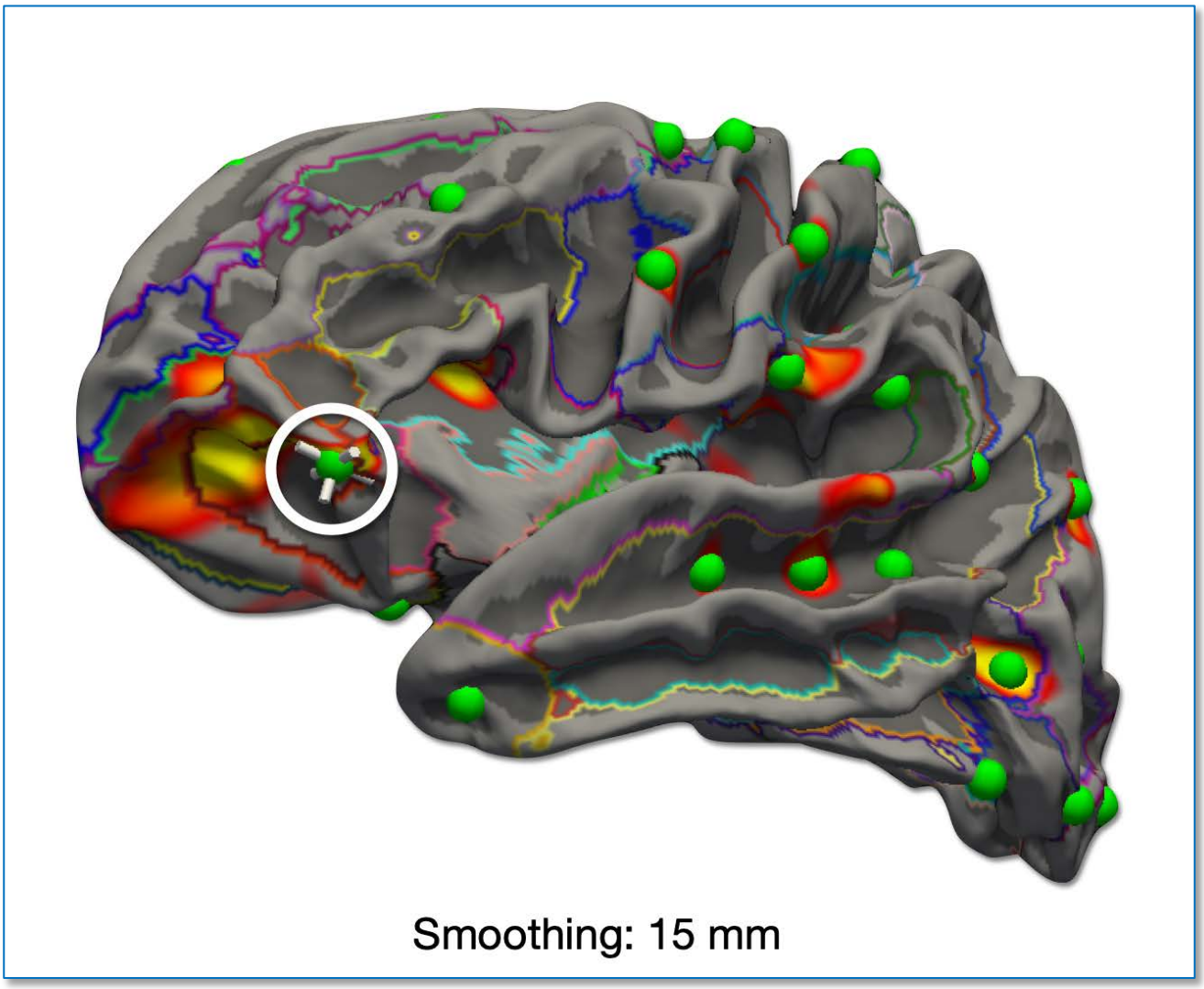

Figure 47: The most significant cluster is orbitofrontal, but the FLAIR hyperintensity at this site is likely attributable to eye-movement artifacts. Indeed, exploratory eye movements are greater during Eyes Open Rest (EOR) than during Eyes Closed Rest (ECR).

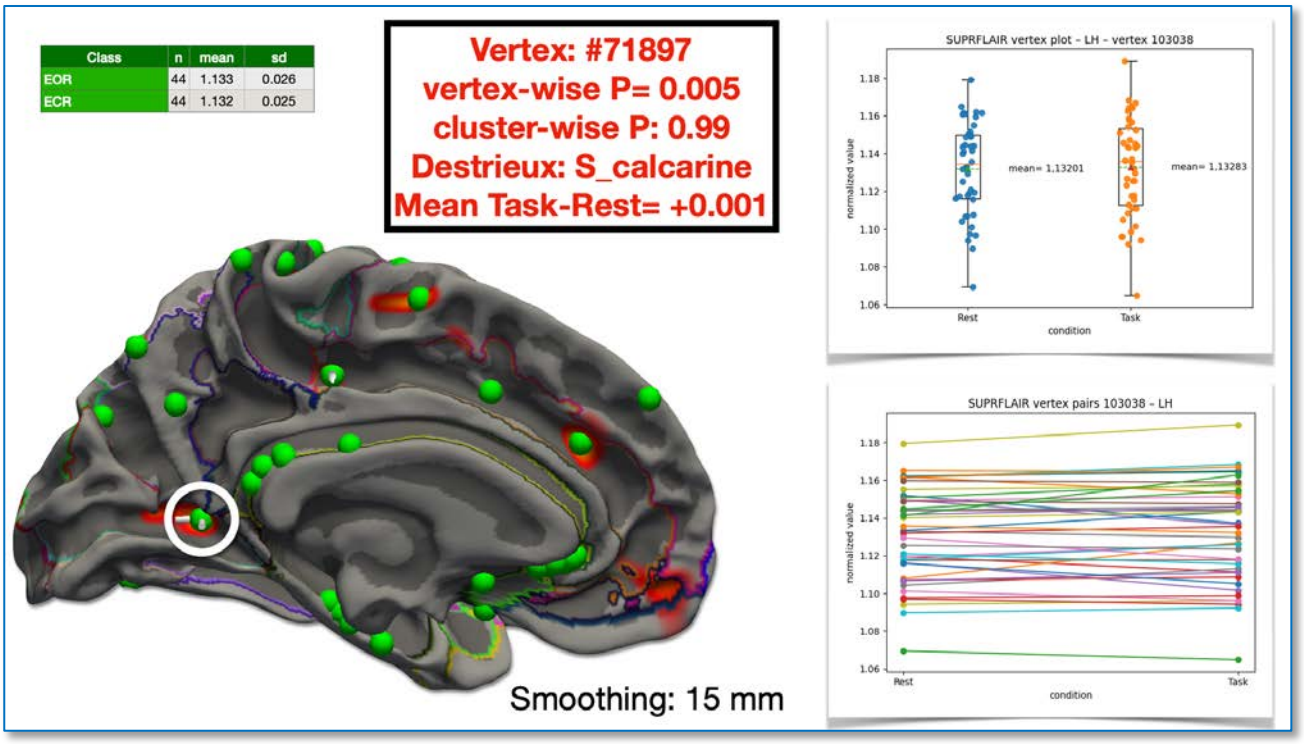

Figure 48: Vertex-wise statistics at the peak (minimum-P) vertex of the positive cluster in the primary visual cortex.

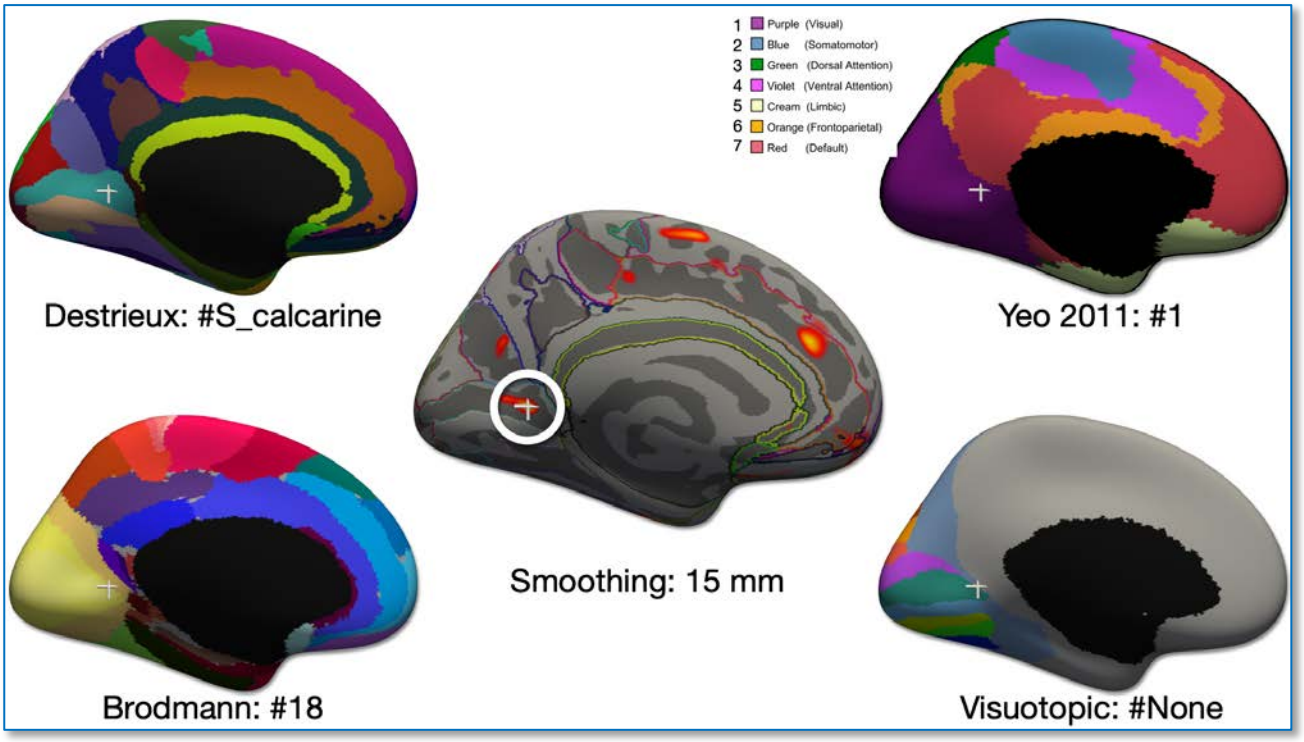

Figure 49: Cross-atlas localization of the calcarine cluster peak (minimum-P vertex): Destrieux, Yeo 2011, Brodmann, and visuotopic parcellations. In the Visuotopic atlas, the vertex is assigned to an unlabeled ("None") parcel but lies immediately adjacent to ventral V1 (V1v).

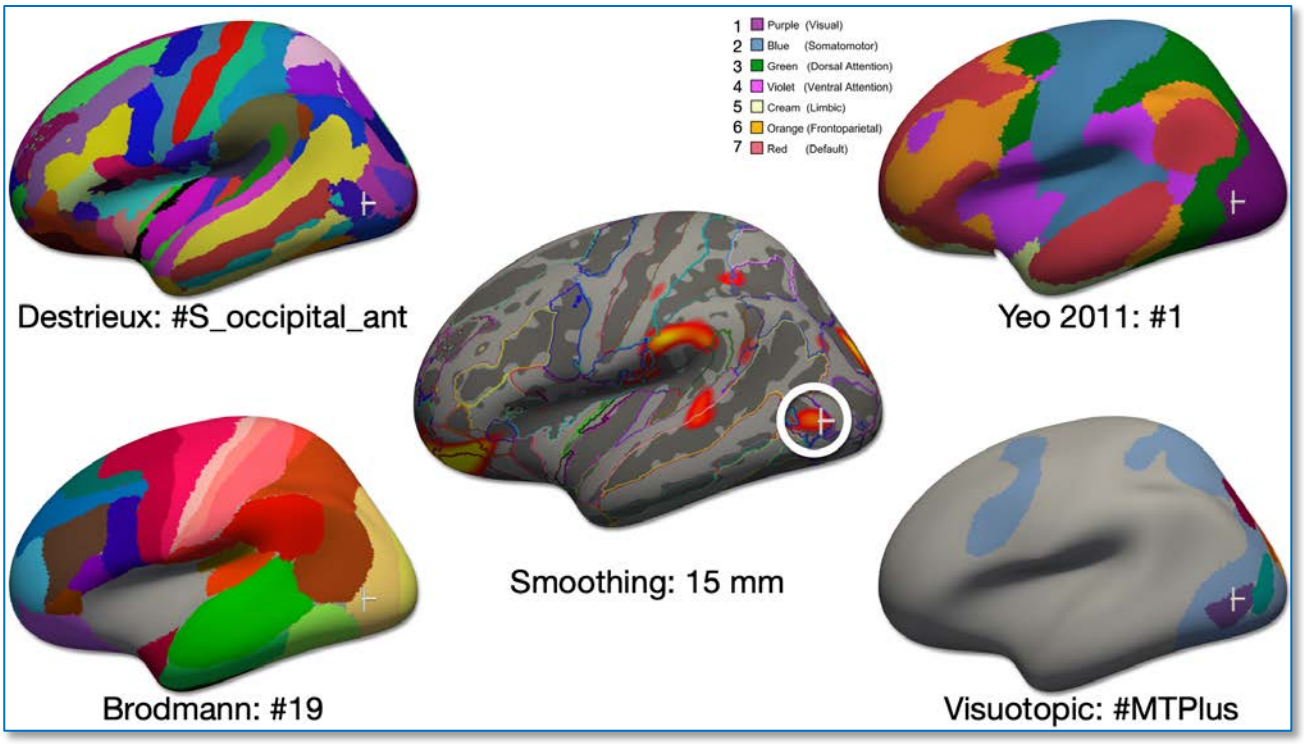

Figure 50: Cross-atlas localization of the lateral occipital cluster peak (minimum-P vertex): Destrieux, Yeo 2011, Brodmann, and visuotopic parcellations.

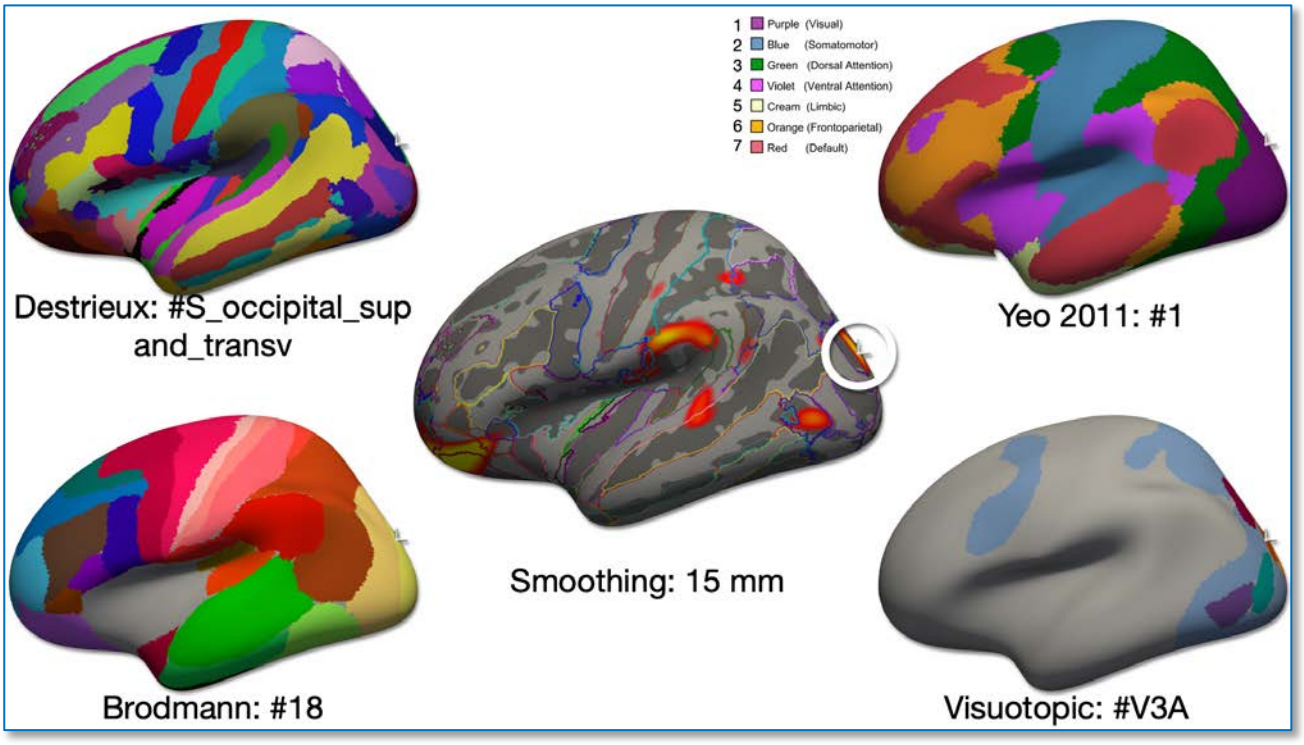

Figure 51: Cross-atlas localization of the posterior occipital cluster peak (minimum-P vertex): Destrieux, Yeo 2011, Brodmann, and visuotopic parcellations.

Limitations of the study of chapter III

The principal limitation of the experiments reported in Chapter III is the small sample size, across all experiments and especially in B and C. The combination of limited n and very small effect sizes substantially reduces statistical power, most notably for cluster-wise analyses.

Conclusion of chapter III

The central takeaway is that the FLAIR signal is not purely structural, and certainly not driven solely by structural abnormalities. The between-subjects analyses in Experiment A suggest distinct patterns of cortical FLAIR intensity as a function of hemispheric language dominance and hand dominance. Moreover, the findings from Experiments B and C indicate that acute (short–timescale) changes in cortical FLAIR intensity can be detected under model-based f-MRI–like conditions, i.e., task–rest contrasts (finger tapping and eye movements). Similarly, Experiment D suggests that cortical FLAIR intensity can be modulated acutely by state transitions such as Eyes Open Rest (EOR) versus Eyes Closed Rest (ECR).

CHAPTER IV: DISCUSSION

Discussion of general aspects

This work had two overarching aims: (i) to assess the clinical utility of SUPR-FLAIR—and its vertex-wise statistical extension, SUPR-FLAIR-sa—for advanced diagnostics and presurgical planning in epilepsy; and (ii) to explore its translational potential as a putative sensor of cortical functional organization capable of capturing short-timescale state modulations.

Our pipeline combines T1–FLAIR coregistration, voxel-wise normalization of FLAIR to the white-matter median, and surface sampling along the cortical normal to generate vertex-wise maps of normalized signal (SUPR-FLAIR). These maps are then interrogated with surface-based GLMs, with optional covariate adjustment. The workflow yields a consistent representation of the FLAIR signal across the cortical mantle and exposes reproducible spatial heterogeneity that aligns with known cytoarchitectonic patterns (e.g., relatively lower values in central and occipital regions), a useful premise for both “within-subject” and “between-subject” comparisons.

Discussion of clinical application (chapters I and II)

Utility for surgical planning and topographic definition

In presurgical planning, SUPR-FLAIR projects cortical FLAIR signal onto the brain surface and incorporates it into multimodal 3D planning scenes for SEEG and resection (via 3D Slicer with angiographic/structural overlays), streamlining hypothesis generation and trajectory design. As outlined in Chapter I, the initial impetus was pragmatic: in MRI-visible lesions, surface projection replaces laborious slice-by-slice contouring, allowing the lesion’s margins to be appreciated directly on the cortical surface with minimal operator input (patients Pt-01-03;Figure 4, Figure 5 and Figure 6). The concept is simple but impactful in contemporary surgical workflows, where 3D multimodal imaging is increasingly standard and demonstrably useful (Vollmar et al., 2008; Cardinale et al., 2013, 2015; Nowell et al., 2015; Duncan et al., 2016; Bunyaratavej and Siwanuwatn, 2017; Chen et al., 2017; Minkin et al., 2017; Sparks et al., 2017; Tringali et al., 2018; Scorza et al., 2021; Zhao et al., 2021; d’Orio et al., 2024).

Utility for detecting lesions that are inconspicuous on conventional inspection

Simply projecting cortical FLAIR intensity onto the brain surface can, by itself, facilitate recognition of epileptogenic lesions as focal hyperintense areas. For example, in Pt-04, Figure 7 panel B makes the FCD along the superior temporal gyrus more apparent than standard review of 2D slices. However, purely visual detection of subtly hyperintense superficial areas is often hampered by the nonuniform distribution of FLAIR signal across the cortical mantle (Figure 1 panel D). In a study of 112 neurologically normal adults published by Karaarslan and Arslan, 95% showed lower FLAIR signal intensity in the Peri-Rolandic Cortex (PRC) compared to the superior frontal cortex, with only 5% having isointense signal (Karaarslan and Arslan, 2003), and this was probably the first note on this evidence. We were the first, to our knowledge, to highlight this point specifically for surface-based FLAIR usage, consistent with prior reports from T2*-weighted mapping (Cohen-Adad, 2014; Van Essen, 2014; Wasserthal et al., 2014).

The statistical extension of the method, SUPR-FLAIR-sa, can accentuate subtle cortical hyperintensities that often escape routine visual review, thereby refining the topographic hypothesis and informing downstream decisions: targeted second reads of MRI/PET, SEEG electrode placement, Radio-Frequency Thermo-Coagulation (RFTC) planning, and resection/disconnection strategies, even in MRI-negative cases (Pts 02-03 for validation of the method —Figure 5 and Figure 6; Pts 04-05 as examples of helpfulness in MRI-negative cases —Figure 7, Figure 8 and Figure 9).

These directions align with, and extend, prior work on post-processing for MRI-negative epilepsy and FCD (e.g., VBM and SBA methods). With a specific focus on detecting MRI-inconspicuous FCD, Focke and colleagues developed voxel-based methods to enhance the visualization of subtle FLAIR hyperintensities (Focke et al., 2008, 2009). More recently, within the voxel-based family, the FlaT1 method, implemented in the SWANe (Standardized Workflow for Advanced Neuroimaging in Epilepsy — SWANe) software platform, has been proposed; it leverages the FLAIR-to–T1w ratio to improve lesion conspicuity (Genovese et al., 2024).

In contrast to voxel-based approaches, we first developed a surface-based method to analyze cortical FLAIR signal intensity (Cardinale et al., 2015). As in voxel-based pipelines, intensities are normalized by division by the white-matter median. The resulting normalized values are then compared with a healthy-control cohort using a vertex-wise GLM, with FLAIR intensity as the

outcome and group (patient vs. control) as the main explanatory factor. Nuisance covariates can be included to adjust for confounders and improve model robustness.

The first attempt to use surface-based MRI analysis tools for clinical purposes, comparing a single patient with a group of healthy controls, was probably that of Thesen and colleagues, who presented the results of a method based on the construction of a vertex-wise model to analyze several morphometric features as predictors of the presence of an FCD. Using optimized parameters and a combined measure of cortical thickness and gray–white matter contrast, their method detected 92% of cortical lesions (sensitivity) while maintaining a low false-positive rate (96% specificity), correctly distinguishing patients from controls in 94% of cases (Thesen et al., 2011).

Following our pilot study, other groups investigated surface-based analysis of cortical FLAIR signal for advanced diagnostics and presurgical planning in epilepsy. Sophie Adler and colleagues developed a classifier using surface-derived features to identify focal abnormalities of cortical development in a pediatric cohort, including FLAIR signal intensity among measures such as cortical thickness, gray-white blurring, sulcal depth and curvature, local cortical deformation, and per-vertex interhemispheric asymmetry (Adler et al., 2017). The same group subsequently evaluated a similar multimodal surface-feature classifier, again incorporating cortical FLAIR intensity, for automated FCD detection to inform SEEG planning (Wagstyl et al., 2020).

Of particular interest, the MELD (Multi-centre Epilepsy Lesion Detection) project includes cortical FLAIR intensity sampled at 25%, 50%, and 75% of cortical thickness, and at 0.5 and 1 mm below the gray/white interface, within a rich feature set for lesion detection (Cohen et al., 2022; Spitzer et al., 2022; Wagstyl et al., 2022; Ripart et al., 2025).

We can therefore state that the method we developed has garnered interest within the image-processing community focused on increasing diagnostic sensitivity, particularly for FCD, in the context of epilepsy surgery.

It is important to emphasize that, although SUPR-FLAIR-sa can help flag epileptogenic lesions that are difficult to visualize, particularly FCD, it cannot, like any statistics-based post-processing method, provide precise lesion boundary delineation. Two considerations drive this limitation: (i) the surface smoothing required to improve SNR inevitably blurs edges; and (ii) there is no absolute, pre-definable significance threshold, especially in frameworks where one comparison group consists of a single patient. Accordingly, in MRI-negative cases SUPR-FLAIR-sa should be regarded as a

locator/screening tool, not a contouring tool. Indeed, varying the significance threshold, more or less liberally, is central to dynamically interrogating the statistical output. This inevitably produces different silhouettes of the highest-significance cluster, which therefore cannot be treated as a reliable surrogate for lesion segmentation. The illustrative Pt-04 case (Figure 7) exemplifies this: adopting more permissive thresholds visibly expands the cluster boundaries to encompass regions beyond the temporal lobe, such as the orbitofrontal cortex.

Ability to reveal subtle extra-lesional hyperintensities

Dynamic interrogation of the statistical output can uncover relative cortical FLAIR hyperintensities that lie outside the boundaries of overt structural change. A paradigmatic example is the group with HS presented in Chapter I (Pts 06–10; Figure 10 and Figure 11). In these patients, surface-based statistics typically highlight increased signal in the parahippocampal gyrus, uncus, and temporal pole, with the most significant cluster often in the mesial temporal pole, a pattern first reported in our pilot study (Cardinale et al., 2015). While the association between HS and temporo-polar abnormalities (atrophy and gray-white blurring) was well established (Garbelli et al., 2012), the FLAIR hyperintensity itself had not been emphasized. This observation aligns with SEEG data from Chabardès and colleagues showing that, in 23/40 mesial temporal epilepsy cases, the temporal pole was involved at seizure onset, sometimes simultaneously with, or even preceding, the hippocampus (Chabardès et al., 2005).

At the temporal pole, one might still invoke a structural substrate to explain the FLAIR increase in some patients; however, histology in our five HS cases, consistent with hundreds of surgical cases at our center, showed no anatomo-pathological abnormalities in the uncus or parahippocampal cortex. Moreover, as illustrated in Figure 11, relaxing the vertex-wise threshold reveals additional foci, most notably within the cingulate gyrus, a region with well-known connectivity to mesial temporal structures.

The existence of extra-temporal neocortical FLAIR hyperintensities was later confirmed in a pediatric HS cohort, encompassing not only the limbic system but also frontal and parieto–occipital territories (Adler et al., 2018a). In an expanded analysis from the same group, increased FLAIR intensity was demonstrated across bilateral limbic and paralimbic cortices (hippocampus, parahippocampus, cingulate, temporopolar, insular, orbitofrontal), with the largest effect sizes in periallocortical limbic and insular classes as defined by the von Economo–Koskinas taxonomy. In healthy controls,

systematic covariance analysis showed that limbic-like similarity patterns, especially those characteristic of the hippocampus, predicted the topography of FLAIR “hypersignal” in patients; these effects were robust to correction for morphometric confounds (Adler et al., 2018b).

The presence of relative FLAIR hyperintensity outside the boundaries of the epileptogenic lesion is observed not only in patients with HS but also in those with other lesion types, as originally illustrated in our 2015 pilot study (Cardinale et al., 2015). In Chapter I, we presented additional exemplars: a patient with FCD type IIb (Pt-05, Figure 8 and Figure 9), one with FCD type Ia (Pt-12, Figure 16) and a patient with a temporal polar tumor (PLNTY) (Pt-11, Figure 12, Figure 13, Figure 14 and Figure 15).

The Pt-05 case (Figure 8 e Figure 9) illustrates not only how SUPR-FLAIR-sa can function as a lesion-detection tool in an MRI-negative case, but it also shows that the pattern of relative FLAIR hyperintensity can reconfigure over time: following resection of the lesion/epileptogenic zone from the right temporal lobe, new hyperintense areas appeared, predominantly in the ipsilateral frontal lobe, whereas preexisting contralateral posterior clusters disappeared, suggesting shifts in cortico-cortical connectivity. In a related report on this same patient, we showed that epileptiform activity in the superior temporal gyrus interfered with the function of the contralateral homologous cortex and its associated network, and that this connectivity changed substantially after RF-TCs performed prior to the resective surgery (Abarrategui et al., 2023).

At this point, it is instructive to consider Pt-11 (Figure 12, Figure 13, Figure 14 and Figure 15). This case shows that FLAIR hyperintensities, sometimes diffuse and bilateral, can occur not only with FCD or HS, but also in tumor-related epilepsy (here, a PLNTY). This supports the view that extra-lesional hyperintensity is not substrate-specific; rather, it may reflect bioelectric phenomena (and their effects) driven by epilepsy itself. In interpreting similar findings (at least in HS), Adler et al. argued that by highlighting periallocortical transition zones and limbic cortices, FLAIR intensity mapping and covariance patterns support a susceptibility model of TLE gray-matter pathology grounded in cytoarchitecture; they further suggested that limbic/paralimbic cortices may be preferentially vulnerable, with chronic FLAIR changes potentially secondary to chronic glial activation (Adler et al., 2018b). Based on our illustrative cases, representative of a broader clinical experience, we add that extra-lesional relative FLAIR hyperintensity can be reversible, and new hyperintense areas may

emerge after surgery. Because routine postoperative imaging is typically obtained ~6 months after resection, we cannot determine the temporal dynamics of these changes and thus whether they are acute, subacute, or chronic.

Pt-12 further informs the discussion by demonstrating effective cortico-cortical connectivity between regions showing extra-lesional FLAIR hyperintensity. We obviously lack histological specimens from these territories and therefore cannot exclude microstructural alterations, reversible or otherwise, such as those associated with inflammatory processes within the epileptic network. Nonetheless, the evidence favors a functional rather than purely structural basis for these signals, especially in light of the Chapter III experiments.

Overall, what mechanism could underlie extra-lesional FLAIR hyperintensity, particularly given its apparent reversibility? A contributory role of neuroinflammation is biologically plausible, as inflammatory cascades can perturb glial water homeostasis and modulate microvascular/Blood–Brain Barrier (BBB) permeability, thereby increasing interstitial water content and prolonging T2/FLAIR signal. That said, FLAIR abnormalities are not specific for inflammation and should be interpreted in conjunction with multimodal biomarkers and the broader clinical–electrophysiological context (see discussion of Chapter III for additional considerations).

Diagnostic performance in MRI-negative TLE

SUPR-FLAIR-sa has been part of the Claudio Munari Center's workflow from the outset as an adjunct to diagnostic evaluation and surgical planning. However, we had never formally quantified its performance. A first preliminary effort in this direction is presented in Chapter II.

In the retrospective MRI-negative cohort, sensitivity was ~54% and specificity ~45% under the prespecified case definitions. Although, to our knowledge, no study uses identical ground-truth definitions (TP, TN, FP, FN) for a head-to-head comparison, these figures are broadly consistent with the MELD consortium report (sensitivity 59%, specificity 44% — Spitzer et al., 2022). Notably, because our series comprised only MRI-negative cases, a sensitivity of 54% represents a meaningful improvement over conventional visual MRI review.

Going back to the results of our study we can underline that patients were more often seizure-free when the significant peak ($P<0.05$) lay within the RZ (70% vs 38% when the peak lay outside). Concordance between SUPR-FLAIR-sa and SUPR-PET-sa peaks inside the RZ further improved outcome associations (e.g., 8/9 seizure-free). These data support SUPR-FLAIR-sa as supportive localization in difficult MRI-negative patients, especially when triangulated with PET and SEEG.

Discussion of translational potential for basic neuroscience research (chapter III)

FLAIR MRI is sensitive to water content and myelination, and is mainly used to detect lesions. Interestingly, even in healthy individuals, FLAIR reveals characteristic cortical signal patterns. As we have already mentioned, a notable finding is that the peri-Rolandic cortex, encompassing the precentral and postcentral gyri around the central sulcus, appears hypointense relative to other cortical areas on FLAIR images (Karaarslan and Arslan, 2003). The researchers reported that 95% of 112 neurologically normal adults showed lower FLAIR signal intensity in the PRC compared to the superior frontal cortex, with only 5% having isointense signal. The low FLAIR signal in motor cortex was observed bilaterally, there was no significant left-right difference in the visual grading of PRC intensity in healthy subjects. These observations suggest that the FLAIR hypointensity of the motor cortex is a normal anatomic marker (likely reflecting high myelin or iron content in motor cortical layers) rather than an effect of handedness or usage. In fact, this symmetric cortical FLAIR pattern has even been proposed as a helpful landmark for identifying the central sulcus during MRI interpretation. Overall, while cortical FLAIR signal variability in healthy people has not been deeply analyzed for functional correlations, the existing data indicate a consistent pattern in primary sensorimotor areas. Notably, we found no studies explicitly linking normal inter-individual FLAIR signal differences to language dominance or handedness. Most research on brain lateralization uses structural measures like volume or thickness rather than raw FLAIR intensity.

Handedness, manual dexterity and cortical morphology

Handedness is one of the most obvious human functional asymmetries, and many studies have asked whether it corresponds to anatomical asymmetries in the brain. Surface-based MRI analyses

and other structural approaches have indeed found subtle differences associated with handedness, especially in motor and language-related cortices. One foundational study (Amunts et al., 1996) used high-resolution MRI to measure the anatomy of the central sulcus in left- and right-handers. They discovered that the depth of the central sulcus is correlated with handedness: in right-handed individuals, the left central sulcus was significantly deeper than the right, whereas in left-handers the pattern was reversed. In other words, each person's dominant-hemisphere motor cortex tended to have a greater intrasulcal surface area, consistent with greater development of neural connections controlling the preferred hand. This was a crucial early demonstration of a structure–function correlation in cortical anatomy. Subsequent MRI morphometry studies reinforced this idea. For example, Foundas and coworkers (Foundas et al., 1998) reported that right-handers have a larger precentral gyrus on the left (asymmetry favoring the dominant side), whereas left-handers showed no consistent asymmetry: left-handers had a more symmetric motor cortex structure. Such findings align with functional MRI results indicating left-handers do not have as strongly lateralized motor representations (Dassonville et al., 1997; Singh et al., 1998; Solodkin et al., 2001; Klöppel et al., 2007; Grabowska et al., 2012). Additionally, Hervé and coworkers (Hervé et al., 2005) found that gray matter volume in the central sulcus correlates with hand motor skill, but in a manner that differed by handedness, suggesting that how structural variation relates to dexterity might depend on whether one is left- or right-handed. Concordantly, another study noted that the asymmetry in the size of the hand representation area in primary motor cortex correlates with asymmetry in actual hand performance on motor tasks, linking anatomical and functional lateralization of manual dexterity (Volkmann et al., 1998).

Despite these observations, identifying robust and widespread anatomical markers of handedness has been challenging. Many early VBM studies failed to find large structural differences between left- and right-handers. For instance, a VBM analysis of 465 individuals (67 left-handed) by reported no significant gray matter volume differences related to handedness anywhere in the brain (Good et al., 2001; Guadalupe et al., 2014). This suggests that any morphological differences due to handedness are quite subtle and easily masked by inter-individual variability. Indeed, later studies indicated that handedness effects may only emerge in very large samples or in specific measures (such as cortical shape or regional asymmetries rather than absolute volumes). Powell and coworkers examined sulcal geometry in dozens of subjects and noted differences in the shape of Broca's area sulci (pars orbitalis and triangularis) between left- and right-handers, including a difference in volumetric asymmetry of the pars orbitalis (Powell et al., 2012). Similarly, a 2007 study

analyzed cortical thickness asymmetries and suggested that certain asymmetries in frontal and occipital regions might vary with handedness (as well as sex), although findings were complex (Hamilton et al., 2007). Overall, these studies hinted that while gross anatomical measures (total volumes) show minimal handedness effect, more refined metrics (sulcal depth, regional cortical thickness, or surface area asymmetry) do reflect the motor dominance of one hemisphere.

Modern large-cohort studies using SBA have provided the clearest picture by leveraging big data. The largest of these, mapped subtle cortical asymmetries associated with left-handedness in ~32,000 individuals (Sha et al., 2021). They found that left-handed people tend to have a slightly reduced leftward asymmetry (or a greater rightward bias) in specific cortical regions. Notably, regions in the frontal and temporal lobes showed this effect, for example, parts of the precentral gyrus, anterior insula, and fusiform gyrus were somewhat more symmetric or even right-biased in left-handers compared to right-handers. These areas are involved in language and motor functions, aligning with the idea that left-handers have a more bilaterally distributed neural architecture for tasks that are typically left-hemisphere dominant in right-handers (Giovagnoli et al., 2024). Indeed, Sha et al. reported a general shift of neural resources toward the right hemisphere in left-handers, consistent with their higher likelihood of right-hemisphere language or ambidextrous motor control. Intriguingly, they also identified specific links between handedness and asymmetries in classical language regions: for example, the surface area asymmetry of the pars triangularis and the adjacent anterior insula showed differences in left-handers. These regions normally exhibit leftward asymmetry in right-handers (and are strongly activated in the left hemisphere during language tasks); in left-handers, the asymmetry was less pronounced. This finding bridges hand preference with language networks anatomically. Furthermore, genetic analyses indicate that some of the same genetic factors influence both handedness and brain asymmetry, e.g. a polygenic score for left-handedness is associated with reduced leftward asymmetry in certain areas (like the insula and fusiform cortex). In summary, the latest evidence from tens of thousands of subjects confirms there are structural brain correlates of handedness, but they are distributed and subtle, involving slight asymmetries in motor and language-related cortex, rather than gross anatomical differences.

Beyond the cortex, other MRI-derived structural biomarkers have been linked to handedness as well. For example, the corpus callosum, the major interhemispheric fiber tract, has long been studied for potential differences. Some early work by Witelson reported that left-handers had a larger corpus callosum cross-sectional area on average, presumably due to greater interhemispheric connectivity (Witelson SF, 1985). However, this wasn’t consistently replicated by all studies. A more nuanced

analysis in 2010 suggested that it's not simply "left- vs right-handed" that matters, but the degree of handedness: individuals with weaker hand preference (more ambidextrous) had thicker callosal midbody regions than strongly lateralized individuals, regardless of being left or right hand dominant (Lüders et al., 2010). In other words, a more bilateral use of hands corresponds to a larger callosum, supporting the idea that callosal size reflects the extent of interhemispheric integration of motor functions rather than handedness per se. Additionally, subcortical structures involved in motor control show handedness associations. A recent study found that non-right-handers had significantly larger basal ganglia volumes (specifically, a larger right putamen and left globus pallidus) compared to right-handers (Jang H et al., 2017). They also reported a negative correlation between a person's handedness laterality score and the volume of these nuclei, suggesting that left-handers (and those who are more ambidextrous) have hypertrophy in motor coordination hubs. These differences might reflect adaptive or developmental factors conferring left-handers with slightly enhanced subcortical motor resources. Overall, while the primary motor cortex and associated pathways are largely symmetric in structure, handedness does leave subtle anatomical fingerprints across the brain, detectable with sensitive morphometric analyses in large samples.

Language lateralization and structural MRI biomarkers

Just as handedness relates to motor cortex anatomy, language lateralization has been studied in relation to cortical structure. Historically, one anatomical feature stood out, the planum temporale (PT). Since the sixties it was noted that the left hemisphere often appears larger in the posterior superior temporal region. A seminal post-mortem study quantified this: the left planum temporale was larger than the right in ~65% of brains, whereas right > left was seen in only ~11% (Geschwind and Levitsky, 1968). This pronounced leftward asymmetry of the PT was presumed to be an anatomical correlate of left-hemisphere language specialization in most people, detectable in vivo by means of carotid arteriography and demonstration of concordant asymmetry of vascular pattern (LeMay and Culebras, 1972). For decades, the PT asymmetry was essentially considered an anatomic marker of language dominance (Tzourio-Mazoyer et al., 2018). With the advent of in vivo MRI, these asymmetries were confirmed in large samples: for example, population studies show on average ~20–30% larger volume or surface area in the left PT than right, in both males and females (Karlsson and Ocklenburg, 2025). However, a critical question is: does the degree or direction of an individual's PT asymmetry predict their functional language lateralization? Modern studies combining structural

MRI with language f-MRI or the Wada test have examined this, and the answer is more complex than initially assumed.

Large-sample studies have found that handedness alone does not strongly affect PT asymmetry at the group level. For instance, surface-based analyses in over 2,000 people reported a robust leftward PT asymmetry on average, but no significant difference between left- and right-handers in that asymmetry (Ocklenburg et al., 2025). Even with over 100 left-handers included, no reliable shift in PT size asymmetry emerged for handedness. Thus, being left-handed does not necessarily mean one's left planum temporale is smaller or more symmetric. Many left-handers still show a typical left > right PT, and many right-handers also have that asymmetry. This underscores that anatomical asymmetry of PT is not simply a proxy for handedness. More pertinent is the relationship between PT structure and language hemisphere dominance. A recent study addressed this directly by measuring PT surface area asymmetry and performing language f-MRI in 287 healthy adults. It was found that PT asymmetry was not a valid marker of an individual's hemispheric language dominance (Tzourio-Mazoyer et al., 2018). In other words, knowing someone's anatomical PT asymmetry alone could not reliably tell you which hemisphere was dominant for language. This result revises the earlier hypothesis of PT as a one-to-one "anatomical signature" of language lateralization.

Interestingly, while gross PT asymmetry didn't predict hemisphere dominance, it did correlate with the degree of language lateralization in certain regions. The same 2017 study noted that individuals with a strongly leftward PT tended to show more left-lateralized activation in the auditory cortex and surrounding temporal areas during a word listening task. Conversely, those with a more symmetric or rightward PT had more bilateral activation in these auditory-language regions. This was driven by an association with the right hemisphere: effectively, a larger right PT was linked to less leftward functional lateralization (more involvement of the right auditory regions). The authors concluded that while PT surface asymmetry does not determine which hemisphere is dominant overall, the size of the right planum temporale in particular might act as a marker of how much the right hemisphere participates in speech processing. One interpretation is that a larger right PT could indicate a brain that is anatomically and functionally more bilateral for language. These nuanced findings highlight that structure–function relationships in language lateralization are not all-or-none. An extreme leftward PT is neither necessary nor sufficient for left-hemisphere language, but anatomical symmetry can reflect more distributed processing.

Beyond macro-structure, researchers have begun to “look deeper” into the cortex for clues about language dominance, examining microstructural properties using advanced MRI contrasts. Recent studies suggest that microstructural asymmetries in language cortex may be more tightly linked to functional lateralization than macro volumetric asymmetries (Qin P et al., 2024). For example, the planum temporale exhibits not only a size asymmetry, but also differences in histological architecture between hemispheres. Post-mortem studies have shown the left PT has a higher density of cortical columns and neuropil, and more large pyramidal neurons, compared to the right (Karlsson and Ocklenburg, 2025). Modern in vivo methods like Neurite Orientation Dispersion and Density Imaging (NODDI) have confirmed a higher neurite density and dendritic complexity in left auditory cortex relative to right in healthy individuals (Ocklenburg et al., 2018) found a significant leftward asymmetry in NODDI metrics within the PT, indicating more abundant and more widely dispersed neural fibers in left auditory cortex. These microstructural differences likely underpin the processing power of the dominant auditory-language hemisphere. Crucially, a very recent multimodal study (Qin et al., 2024) demonstrated that such microstructural asymmetries predict language function lateralization. In 907 healthy right-handed participants, the researchers measured each person’s functional language lateralization (using f-MRI during auditory-language tasks) and correlated it with various structural metrics of the PT. The results showed that individuals with greater leftward asymmetry in PT microstructure, such as higher left-versus-right differences in intracortical myelin content, neurite density, or even subtle cortical surface area, tended to have more left-lateralized auditory language activation. They found significant associations between the functional laterality index and asymmetries in surface area, myelin, and neurite architecture in the PT. Interestingly, these structure-function correlations were highly specific to the planum temporale region itself (they did not simply reflect a whole-brain effect). This indicates that the local structural asymmetry of a cortical region underlies its own functional lateralization.

In summary, cutting-edge evidence highlights that while traditional MRI measures of gross anatomy (like bulk volume) provide incomplete insight into language lateralization, more fine-grained features, cortical layering, myelination, and connectivity, show a tighter coupling with which hemisphere dominates language processing.

Studies Directly Examining FLAIR Signal Variability

Although we identified many studies on structural asymmetries and lateralization, very few have directly examined cortical FLAIR signal variations in relation to handedness or language dominance in healthy people. FLAIR is primarily used to detect lesions, and some clinical studies have used FLAIR asymmetries to lateralize pathology, for instance, analyzing hippocampal FLAIR signal to lateralize temporal lobe epilepsy (Huppertz et al., 2011). However, in the context of healthy individuals, FLAIR signal intensity has not been a common proxy for functional lateralization. No research to date (to our knowledge) has reported that subtle differences in FLAIR cortical intensities predict whether a person is left- or right-handed, or whether their language is left- or right-dominant. In our extensive search, we did not find studies that measure, say, if the dominant hemisphere's cortex has measurably different FLAIR signal (perhaps via texture or intensity analysis) in healthy volunteers.

Building on our prior observations that modest cortical FLAIR hyperintensities can arise without an overt structural substrate, we asked whether, in healthy individuals, inter-individual traits such as language lateralization and handedness/dexterity are associated with distinct SUPR-FLAIR patterns. To address this question, we conducted "between-subjects" analyses, fitting surface-based GLMs to test associations between cortical FLAIR intensity and (i) language lateralization and (ii) handedness/dexterity.

Inter-individual heterogeneity investigated by means of "between-subjects" analyses (Experiment A)

Our "between-subject" analyses suggest that cortical FLAIR intensity patterns vary with stable functional traits: hemispheric language dominance and handedness/dexterity. Group maps reveal bilateral, but often asymmetric, differences across anterior and posterior language territories, ventral/dorsal occipito-temporal streams, and, in stratified subsets, sensorimotor circuits and the intraparietal sulcus. While not "functional markers" per se, these distributions are compatible with subtle tissue microenvironment and/or architectural features that covary with functional organization.

In our study, consistent with most of the predominantly morphometric work mentioned above, right-hemisphere language lateralization (as defined by language f-MRI in the 5 rh_langdom subjects)

did not correspond to a purely right-sided pattern of relative FLAIR hyperintensity. Instead, we observed a bilateral pattern involving both anterior and posterior language areas. This can be interpreted on both technical and neurobiological grounds.

From a technical standpoint, it is important to recall that the 5 left-handed subjects classified as right-lateralized for language were labeled rh_langdom on the basis of a quantitative f-MRI assessment of language, exactly as the other 14 left-handers were classified as lh_langdom. Unfortunately, language f-MRI data were not available for the right-handed participants (for whom we arbitrarily assumed conventional left-hemisphere language dominance). As a consequence, we were unable to use the f-MRI output itself as a PVR, which would have allowed us to adjust our analyses more appropriately, rather than forcing what is in reality a bilateral distribution of language functions into a binary rh_langdom/lh_langdom classification.

Along the same interpretative line, we can make more neurobiological considerations. As already suggested, structure–function relationships in language lateralization are not all-or-none. On the one hand, the vast majority of right-handed individuals typically show strongly left-lateralized activation patterns on language f-MRI. On the other hand, morphometric studies and our own SUPR-FLAIR-based analyses suggest that left-handers exhibit a variable degree of "redistribution" of certain biomarkers toward the right hemisphere, up to an essentially symmetric configuration in those individuals who nonetheless show right-hemisphere language dominance on f-MRI. This pattern is consistent with a more distributed processing of language functions.

From a clinical perspective, SUPR-FLAIR-sa comparing left-handed patients to right-handed healthy controls could help estimate language lateralization in individuals who are unable to perform reliable language f-MRI paradigms, such as pediatric patients. In this respect, our observation that the most significant FLAIR intensity differences emerge at the level of the occipital poles may be particularly relevant. This phenomenon might be considered a red flag suggestive of a more bilateral distribution of language functions. Such an indicator could become an important element in planning surgical strategies, for example, in defining the topographic distribution of SEEG electrode implantation.

With regard to the comparison between left-handers and right-handers, focused on hand preference and manual dexterity irrespective (as far as possible) of language lateralization, similar considerations apply. The most salient finding is that left-handers exhibit bilaterally higher FLAIR intensity than right-handers, involving almost the entire hemispheric surface with the sole exception

of the most posterior regions. This result is well aligned with the morphometric studies discussed above, both at the cortical and subcortical level (basal ganglia, corpus callosum), and again supports the view that left-handedness reflects a condition of more widely distributed processing, rather than a simple mirror image of right-handedness.

Short-timescale state/task modulations (Experiments B–D)

Recent studies have demonstrated that even structural MRI signals (traditionally used for anatomy, e.g. T1w or FLAIR sequences) can exhibit rapid, transient changes during short-term tasks or state changes. These findings challenge the classical assumption that structural MRI measures change only over long periods. Three reports of task-induced changes in motor cortex structure have been published.

A recent study explicitly examined rapid structural MRI changes during a simple motor task (Olivo et al., 2022). The authors acquired multiple repeated T1w scans from 51 participants alternating between a finger-tapping task (2-minute blocks) and rest, over a 30–60 minute session. The structural images were analyzed for Gray Matter Volume (GMV) changes, and concurrent BOLD (Blood Oxygen Level Dependent) f-MRI was recorded for comparison. During the finger-tapping blocks, estimated GMV in the primary motor regions decreased relative to rest. The location of these GMV reductions did not correspond directly to the f-MRI activation maps, and the BOLD fluctuations did not explain the structural signal changes. In other words, the task-induced changes in the T1w images were real and not simply a bleed-through of the BOLD signal. This suggests that transient physiological changes (possibly related to blood volume or hydration) during activity can alter tissue contrast in structural MRI. The authors note these rapid GMV changes pose challenges for test–retest structural studies and might reflect underlying physiology (e.g. transient blood-flow or fluid shifts).

In an earlier study on motor learning, Taubert and colleagues provided evidence for within-session plasticity in motor cortex (Taubert et al., 2010). They had adults practice a balance task for 1 hour and took high-resolution MRI scans to measure cortical morphology pre- and post-training. They reported localized increases in cortical thickness of M1 (primary motor cortex) after just 1 hour of practice, specifically in the leg/trunk areas responsible for balance. The change in thickness appeared linear over the training session and was spatially specific to the task-related subregions. Importantly, they controlled for potential confounds: the rapid thickness increase was not

attributable to global blood-flow changes (resting CBF was monitored) and was not seen with mere repetitive limb movements without the balance challenge. This study, along with a replication they conducted, demonstrates functional task-specific structural MRI changes on the timescale of tens of minutes.

The third study combined EEG-neurofeedback training with MRI to probe fast structural changes (Nierhaus et al., 2021). Two groups of BCI-naïve subjects underwent 1 hour of Brain-Computer Interface (BCI) training, either via motor imagery or a visual P300-based neurofeedback task. T1 structural scans (and f-MRI) were taken before and after the 1-hour training. The authors found significant increases in T1w signal (gray-matter intensity/volume) in the specific cortical regions engaged by the task. For example, occipital and parietal areas showed increased signal after the visual BCI task, and sensorimotor cortex showed increases after the motor-imagery. These structural changes coincided with enhanced functional connectivity and BOLD activity in the same regions. The study suggests that even purely mental training for 60 minutes can rapidly alter structural MRI metrics in a region-specific manner. This was taken as evidence of fast "brain plasticity" measurable by structural MRI, with potential implications for neurorehabilitation (since changes were spatially targeted to functional areas).

Furthermore, two other studies demonstrated rapid structural changes with visual stimulation.

In a "within-subject" experiment (Månsson et al., 2020), 47 healthy adults were scanned with two high-resolution T1w MRI acquisitions (~4.4 minutes each), one during passive viewing of natural images and one during viewing of a neutral fixation cross. VBM and cortical thickness analyses revealed significant increases in grey-matter volume and cortical thickness in the visual cortex when participants viewed pictures compared to a blank fixation. Notably, these morphology changes were observed within a single scan (~263 seconds). The effect was bilateral in occipital cortex and statistically robust, suggesting that the current mental state or visual input can alter structural MRI metrics on the order of minutes. The authors framed this as evidence of extremely dynamic "neuroplasticity"[9] (or at least changes in MRI-derived morphology measures) and cautioned that a subject's brain state can confound structural measures.

[9] In this case, the authors are referring to so-called functional neuroplasticity. It is not our intention here to discuss in detail the distinction between structural and functional neuroplasticity; instead, we simply quote a few lines from Shadlen and Kandel: "There is now considerable evidence for functional plasticity at chemical synapses. These synapses often have a remarkable capacity for short-term physiological changes (lasting seconds to hours) that increase or

Another group independently replicated and extended Månsson et al.'s finding (Zaretskaya et al., 2023). In their study, also using high-resolution T1w scans during visual stimulation vs. control, they confirmed that visual stimulation induces a rapid, localized enlargement of gray-matter measures in visual cortex. Their analysis emphasized that the changes are functionally specific (only in visual regions during visual input) and occur on a fast timescale (within a single scanning session). These results strengthen the evidence that eyes-open conditions with rich visual stimuli can transiently increase cortical GM volume/thickness estimates.

Another recent study reported state-dependent structural changes (Uhlig et al., 2023). Beyond task execution, researchers have investigated whether transient physiological or psychological states modulate structural MRI signals. They examined acute psychosocial stress using the Trier Stress Test versus a control condition in a randomized experiment (67 subjects). Structural MRI (including quantitative T1 mapping and volumetric analysis) was performed twice: ~45 minutes before stress induction and ~90 minutes after onset. The findings were striking: subjects who underwent the stress showed increases in gray-matter volume in several cortical regions (anterior/mid cingulate, bilateral insula), whereas the control group (no stress) showed slight GMV decreases in those regions over the same timeframe. A significant group x time interaction in cerebral blood flow was also observed, and T1-relaxation values changed over time (interpreted as global physiology changes). Moreover, the magnitude of GMV change correlated with stress biomarkers (anxiety levels, heart rate variability). The authors suggest that acute stress can counteract or reverse normal moment-to-moment brain volume fluctuations, perhaps via neurovascular or metabolic mechanisms. This implies the "resting" structural brain isn't static, even psychological state shifts can rapidly influence MRI-derived morphology measures.

It is worth noting that most of the experiments discussed above used T1w MRI or related quantitative sequences to detect changes in volume or thickness. We identified only one study that explicitly employed a FLAIR sequence to capture task- or state-dependent cortical signal changes. Hajnal and colleagues, in one of the earliest applications of FLAIR (when the technique was still relatively new), used a gradient-echo FLAIR sequence to detect an approximately 3% signal change in the occipital cortex during visual stimulation (Hajnal et al., 1993). In practice, that implementation

decrease synaptic effectiveness. Long-term physiological changes (lasting days or longer) can give rise to anatomical alterations, including pruning of synapses and even growth of new ones." (Shadlen and Kandel, 2021)

of FLAIR was conceptually similar to echo-planar imaging as used in functional MRI, providing blood-oxygen-level–dependent contrast. Since that pioneering report, to the best of our knowledge, conventional FLAIR sequences have not been adopted in published task-dependent MRI studies.

Therefore, our "between-subjects" analyses are truly original. We examined whether SUPR-FLAIR-sa can detect hyperacute, task- or state-locked modulations of cortical FLAIR. To this end, we performed paired "within-subject" analyses, conceptually analogous to model-driven task f-MRI, to probe transient fluctuations in normalized cortical FLAIR associated with specific tasks or states. These analyses (finger tapping; eye-movement conditions; Eyes-Open-Rest vs Eyes-Closed-Rest) indicate that SUPR-FLAIR-sa can detect small, short-timescale differences in expected territories (sensory-motor hand-knob and SMA for finger tapping; calcarine and associative visual cortex for eyes-open), albeit with effects that are modest and susceptible to artifacts (e.g., orbito-frontal clusters likely driven by eye movements). This supports the view that a fraction of cortical FLAIR is state-dependent. How can we explain this?

What mechanisms might underlie task- or state-dependent modulations of cortical FLAIR signal intensity?

Fluid-Attenuated Inversion Recovery (FLAIR) MRI is highly sensitive to water content and distribution in brain tissues. FLAIR hyperintensities often reflect regions of increased interstitial or extravascular water. For example, age-related white matter hyperintensities can arise from a higher concentration of interstitial water due to minor BBB leakage, even when structural damage (e.g. demyelination) is mild (Haller et al., 2013). In essence, any process that shifts water into the cortical interstitium or cells, even subtly, can alter T2/FLAIR signal intensity. This sets the stage for understanding why cortical FLAIR signal might fluctuate with functional brain states.

Transient "functional edema" during neural activation

Intense or prolonged neuronal firing is known to cause transient, reversible MRI changes consistent with edema. As already mentioned, a striking example comes from epilepsy: during status epilepticus or severe seizures, patients often show acute cortical T2/FLAIR hyperintensities that resolve after the activity subsides. These transient FLAIR abnormalities are attributed to focal vasogenic cerebral edema induced by the intense neural activity (Repanshek et al., 2007). Although typical cognitive tasks are far less extreme, they represent a milder form of neural activation that

likely also induces micro-scale edema or water shifts. The observed task-locked FLAIR modulations in expected cortical areas (motor cortex during finger tapping, visual cortex with eyes open) suggest that even normal functional activation causes a small, localized increase in tissue water or T2 prolongation, essentially a "functional edema" on a much smaller scale. This could reflect a brief increase in water content (or altered water distribution) in the active cortex, analogous to the edema seen in seizures but to a far lesser degree.

Microvascular dynamics and BBB water exchange

Neurovascular coupling (functional hyperemia) may play a role in these FLAIR changes. When a brain region becomes active, arterioles dilate and cerebral blood flow increases. This surge in perfusion raises capillary hydrostatic pressure and could transiently enhance fluid exchange across the BBB, even if the BBB remains intact. Functional hyperemia can drive fluid movement in perivascular spaces: simulations and two-photon imaging in mice have shown that increased arteriolar pulsation during neural activity promotes Cerebro-Spinal Fluid (CSF) exchange in the paravascular space (Kedarasetti et al., 2020). In a human context, this means that heightened blood flow might push a bit of water from vessels into surrounding tissue (a form of vasogenic component). The BBB in healthy subjects doesn't suddenly "leak" in a gross sense, but subtle changes in water exchange rates or filtration could occur on the order of seconds. Indeed, minor, transient increases in extracellular water would lengthen T2 locally and thus brighten the FLAIR signal. Notably, the FLAIR sequence nulls free fluid like CSF, but interstitial water within cortex is not fully suppressed and would register as increased signal if its volume fraction rises.

Astrocyte swelling and glial water regulation

A significant portion of brain water is regulated by glial cells (especially astrocytes). During neural activity, astrocytes rapidly take up K^+ ions and glutamate from the synaptic space, triggering osmotic water influx into these cells. Astrocyte volume fluctuation is a normal part of neural circuit activation (Walch and Fiacco, 2022). In other words, when neurons fire, nearby astrocytes transiently swell as they absorb excess neurotransmitters and ions. This has two effects on water distribution: it reduces extracellular space (astrocytes physically enlarge, compressing the interstitial volume) and increases intracellular water within glia. The biophysical drivers have been studied in detail. Elevated extracellular K^+ during activity activates the astrocytic Na^+/K^+ ATPase pump (NKA) and other

transporters, leading to uptake of K^+ in exchange for Na^+ and triggering metabolic processes that produce osmolytes (e.g. lactate, bicarbonate). This combination, pump-driven ion shifts and metabolic osmolyte production, creates an intracellular osmotic gradient that draws water into astrocytes. Essentially, active astrocytes accumulate K^+, retain Na^+, and produce new anions; chloride efflux is reduced, all of which increase intracellular osmolarity. Water follows, causing the cells to swell. Notably, experiments show that blocking the Na^+/K^+ pump greatly reduces activity-induced astrocyte swelling, underscoring NKA's role in water uptake. The net result during a task stimulus is a slight cytotoxic edema, i.e. cell swelling, in the active cortex.

From an MRI standpoint, astrocyte swelling could influence FLAIR in two opposing ways. First, by drawing water into cells from the interstitial space, it could shorten T2 of some water (intracellular water often has shorter T2 than free water). This might diminish signal if considered alone. However, in practice astrocytes do not swell without source, they likely pull in additional water from capillaries to maintain osmotic balance. So, although extracellular space shrinks, the total tissue water might actually increase slightly (a combination of cytotoxic and vasogenic water influx). Even a few percent increase in tissue water content can measurably increase T2 signal. It's plausible that the FLAIR signal gains we see in active regions are dominated by the net increase in water content and a more uniform water distribution, overcoming any T2-shortening from compartmental shift. In support of this, severe astrocyte swelling in pathology (e.g. acute hyperammonemia or seizures) presents as bright FLAIR signal (due to edema) rather than loss of signal. Thus, normal physiological astrocyte swelling, much smaller in magnitude, likely contributes positively to FLAIR signal in active states by increasing the tissue water fraction (albeit modestly).

Evidence from human MRI studies of water dynamics

Beyond theoretical mechanisms, there is direct evidence that neuronal activity alters water distribution in the human brain on short timescales. Diffusion-weighted f-MRI studies have observed transient changes in water diffusion during stimulation. In a landmark human study, Le Bihan et al. reported a small but significant decrease in the Apparent Diffusion Coefficient (ADC) in visual cortex during visual stimulation, suggesting water was shifting into more restricted environments (Le Bihan et al., 2006). More specifically, they found that a "slowly diffusing" water pool expands by ~1–2% in active cortex at the expense of the faster-diffusing extracellular pool (i.e. water moving into cells or microspaces) during visual tasks. This aligns perfectly with the idea of astrocytic (and possibly neuronal) swelling reducing extracellular free water. Such water shifts occur within seconds,

indicating a truly neurophysiological effect rather than a slow vascular change. Subsequent research has reinforced this concept: MRI techniques capable of measuring trans-membrane water exchange have shown that active transcytolemmal water cycling increases with neuronal firing (Bai et al., 2019). For example, using an MRI approach with a contrast agent, researchers demonstrated that neural activity (modulated by K^+ levels or synaptic blockers) correlates with changes in steady-state water exchange rates across cell membranes. They conclude that water cycling is tightly coupled to neuronal activity, largely driven by the Na^+/K^+-ATPase pump. In essence, when neurons and glia are active, they "pump" water in and out at a higher rate as part of normal function. This provides a plausible biophysical basis for the state-dependent component of the FLAIR signal: a portion of the cortical FLAIR intensity arises from water that is actively cycled and redistributed in response to brain activity.

Summary of plausible biophysical explanations

In summary, a plausible explanation for the observed SUPR-FLAIR task modulations is that a fraction of the cortical FLAIR signal is indeed activity-dependent, reflecting dynamic water redistribution in the cortex. During brief tasks or state changes, neurons and glia in the "activated" region cause: (1) rapid astrocyte swelling (with water influx), (2) mild interstitial fluid changes (from both cellular uptake and vascular sources), and (3) possibly slight increases in local blood volume/fluid exchange. These mechanisms lead to small T2/FLAIR signal differences in functionally relevant cortical areas (Figure 52).

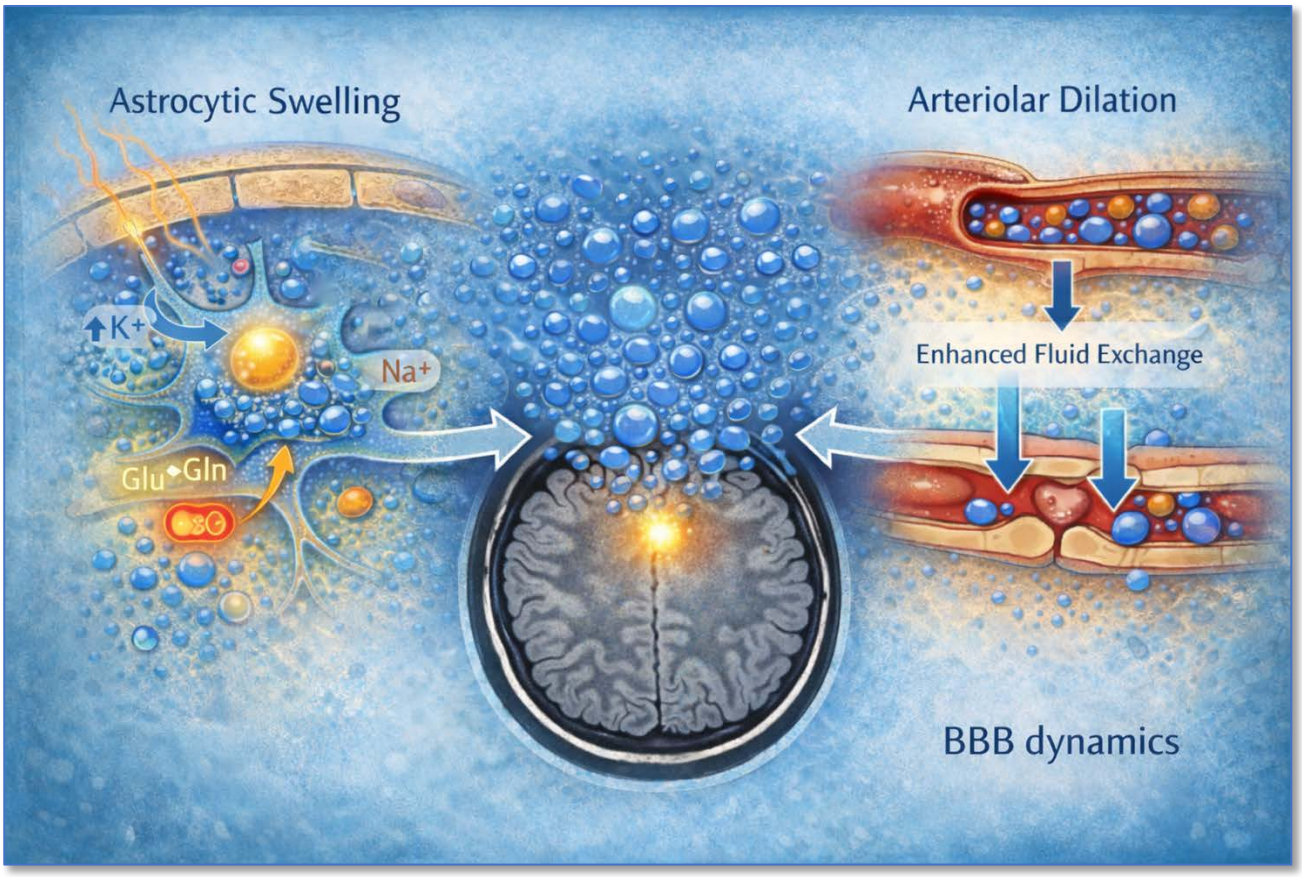

Figure 52: Schematic representation of the biophysical phenomena leading to an "acute" increase in cortical FLAIR signal.

This interpretation is strongly supported by human studies of transient diffusion changes and by the known biophysical coupling between ion transport, metabolism, and water movement in the brain. In essence, part of the brain's functional response includes a state-dependent water content change that FLAIR MRI, when processed appropriately (as in surface-projected analyses), is sensitive enough to detect.

Limitations and future directions

With regard to the clinical application of the SUPR-FLAIR-sa method, the most important limitation is its extreme scanner specificity. The statistical analysis is a "between-subjects" comparison based on a leave-one-out strategy; that is, it contrasts two groups, one consisting of the single patient and the other of multiple healthy controls. Because the effect size of interest is small, scanner-related differences would dominate and mask the cortical FLAIR hyperintensities associated with the pathological condition. Although the data are normalized, this is not sufficient to compensate for magnetic field inhomogeneities, which differ substantially between scanners. As a consequence, it is not possible to analyze a patient's data using controls acquired on a different scanner. This problem

could probably be mitigated in the future by developing calibration phantoms to be acquired before each examination, in both controls and patients.

Another technical limitation is the crucial importance of segmentation quality: inaccurate estimation of cortical surfaces irreversibly compromises the analyses. Although this is not discussed in the main text, it is worth noting that we acquired additional datasets on a 3T scanner; however, due to lower image quality and less reliable FreeSurfer segmentations, we were unable to use them in a robust way, either for clinical applications or for the more neurophysiological studies.

Beyond image quality, the method cannot be applied in patients who have already undergone previous surgery, nor in those with a severely distorted gray-white interface, either globally or in specific regions of the hemispheres.

The dependence on segmentation quality also makes it difficult to apply the method in very young children, in whom white-matter myelination is still largely incomplete and the gray–white interface is poorly defined. In addition, for the youngest patients it is practically impossible to obtain a sufficient number of healthy controls of comparable age.

A further limitation in the clinical domain is that FreeSurfer excludes the hippocampus and amygdala from the surface-based analysis, even though these structures are crucial in many patients with epilepsy.

As already emphasized, the major limitation of the study presented in Chapter II is that patients with clearly defined radiological lesions were not included; consequently, the reported sensitivity does not reflect the true value. In the future, the retrospective analysis will be extended to include these missing patients, together with a corresponding number of additional healthy controls.

With regard to the studies presented in Chapter III, the main limitation is the small sample size in each experiment. Given the very small effect sizes under investigation, it is not realistically possible to apply multiple-comparison correction procedures and thus to estimate Cluster-Wise Probability (CWP) in a reliable way. Nevertheless, the results are highly encouraging and motivate the design of

future studies with more rigorous task- or condition-based paradigms and adequately powered samples.

Potential clinical advantages, with downstream translational implications, may derive from the higher spatial resolution of the sequences used, from the possibility of investigating pathophysiological networks in a manner akin to resting-state MRI, and from the potential to identify markers relevant for language lateralization, particularly in challenging patients. Given the nature of the data, the application of machine-learning or deep-learning techniques would likely be advantageous.

Finally, it should be emphasized that, up to this point, we have essentially ignored the significance of cortical FLAIR hypointensities. This aspect also deserves extensive investigation in future work.

OVERALL CONCLUSION

The SUPR-FLAIR framework provides a practical and conceptually coherent way to “bring FLAIR onto the cortex,” enabling intuitive visualization of FLAIR-hyperintense cortical lesions within multimodal 3D scenes that incorporate FreeSurfer-derived surfaces. By improving the topographic definition of lesions relative to sulcal–gyral anatomy, vasculature, and SEEG electrodes, this approach supports more precise and informed surgical planning.

Its statistical extension, SUPR-FLAIR-sa, further enhances diagnostic yield by revealing lesions that are only subtly hyperintense on FLAIR and thus frequently missed on conventional slice-by-slice visual inspection. In MRI-negative epilepsy, arguably the most challenging clinical scenario, SUPR-FLAIR-sa can provide actionable, albeit imperfect, localization information, and its concordance with complementary surface-projected modalities such as SUPR-PET-sa appears to strengthen prognostic value.

Beyond lesion detection, SUPR-FLAIR-sa consistently highlights extra-lesional regions of relative cortical hyperintensity that map onto known or plausible epileptic/physiological networks in patients, as well as physiologically meaningful territories in healthy individuals. The patterns observed in relation to language lateralization and manual dominance, together with the short-timescale task- and state-dependent modulations detected in within-subject experiments, converge on the notion that cortical FLAIR signal is not purely structural. Rather, at least a fraction of the signal appears sensitive to state- and trait-dependent properties of the cortical microenvironment.

Overall, this work positions SUPR-FLAIR and SUPR-FLAIR-sa as a bridge between structural and functional imaging: a surface-based framework capable of augmenting presurgical evaluation in epilepsy while opening a window onto subtle aspects of cortical organization and dynamics. Further technical refinements, larger and more diverse cohorts, and integration with advanced analytic approaches (including machine learning and multimodal fusion) will be crucial to fully realize the clinical and neuroscientific potential of this method.

ACKNOWLEDGMENTS AND DISCLOSURE

Acknowledgments

This work is dedicated to the memory of our mentor and close friend, Claudio Munari.

First and foremost, I am deeply indebted to prof. Luca Bonini and prof. Pietro Avanzini for their invaluable support in analyzing the experimental data and in interpreting and discussing the results, but above all for their constant encouragement and motivation.
I am sincerely grateful to Luciana Gennari, without whom this research would not have been possible, and to Gianluca Mezzini for his collaboration on the study presented in Chapter II. I would also like to thank Nadia Colombo, Alberto Citterio, Silvia Squarza, Mariangela Piano, Marco Felisi, Luca Berta, Paola Colombo and Alberto Torresin for their essential and highly valued assistance. Furthermore, I am very grateful to Giorgio Lo Russo, Laura Castana, Piergiorgio d'Orio, Martina Revay and Ivana Sartori for their steady support and enthusiasm in the day-to-day use of the tools we developed.

Above all, I wish to thank all the volunteers who underwent MRI to establish the normative dataset.

Disclosures

I have recently signed a consulting agreement as a member of the Medical Advisory Committee (MAC) with Dixi Medical, the manufacturer of the SEEG electrodes at our center.

APPENDIX I – HOW TO

Basic commands (bash[10] or zsh[11]) for SUPR-FLAIR-sa

The main commands used for SUPR-FLAIR-sa pipeline are:

- FSL
    - *FSLeyes* (pronounced fossilise) is the FSL image viewer, part of FSL since FSL 5.0.10.
    - *FLIRT* (FMRIB's Linear Image Registration Tool) is a fully automated robust and accurate tool for linear (affine) intra- and inter-modal brain image registration.
    - *fslstats* is a general tool for calculating various values/statistics from the image intensities.
    - *fslmaths* is a very general image calculator and can be used to perform a great variety of manipulations of images.
- Freesurfer
    - *Freeview* is a visualization tool similar in functionality to tkmedit, tksurfer, and scuba.
    - *recon-all* performs all, or any part of, the FreeSurfer cortical reconstruction process.
    - *mris_preproc* is a script to prepare surface-based data for high-level analysis by resampling surface or volume source data to a common subject (usually an average subject) and then concatenating them into one file which can then be used by a number of programs (e.g., mri_glmfit).
    - *mri_surf2surf* resamples one Cortical Surface onto another.
    - *mri_concat* concatenates input data sets.
    - *mri_glmfit* performs general linear model (GLM) analysis in the volume or the surface. Options include simulation for correction for multiple comparisons, weighted LMS, variance smoothing, PCA/SVD analysis of residuals, per-voxel design matrices, and 'self' regressors. This program performs both the estimation and inference.

[10] BASH (Bourne Again SHell) is a shell very popular in Unix/Linux systems, included Apple Mac computers.
[11] zsh is the Z shell of Apple Mac computers.

Commands and scripts used for the analyses reported in chapter III

zsh commands

Commands used for analyses of Experiment A data

```
suprpath=~/Desktop/suprflair_big
flairseries=flair_ax
flairmeasure=r_${flairseries}_wm-norm-median

####################################
1) ANALISI SUPRFLAIR STATICA CONTRASTANDO RH_DOM VS LH_DOM, AGGIUSTANDO per handedness, age, sex e thickness_PVR
####################################
# Prepariamo i file mgh con gli scalari della thickness a differenti livelli di smoothing:
hemis=(lh rh)
smooth=(5 15 25)
for h in $hemis; do
 for sm in $smooth; do
mris_preproc \
 --fsgd $suprpath/langdom_handagesex.fsgd \
 --cache-in thickness.fwhm$sm.fsaverage \
 --target fsaverage \
 --hemi $h \
 --out $suprpath/$h.thickness.sm${sm}.mgh
 done
done

# Prepariamo i file mgh con gli scalari della suprflair smoothando a diversi livelli in parallelo:
hemis=(lh rh)
for h in $hemis; do
 mris_preproc \
  --fsgd "$suprpath/langdom_handagesex.fsgd" \
  --meas "${flairmeasure}.mgh" \
  --target fsaverage \
  --hemi "$h" \
  --out  "$suprpath/${h}.${flairmeasure}.mgh"
done

hemis=(lh rh)
smooth=(5 15 25)
for h in $hemis; do
 for sm in $smooth; do
  mri_surf2surf \
   --s fsaverage \
   --hemi "$h" \
   --fwhm "$sm" \
   --sval "$suprpath/${h}.${flairmeasure}.mgh" \
   --tval "$suprpath/${h}.${flairmeasure}.sm${sm}.mgh" &
 done
done
wait

# Prepariamo i file mgh con gli scalari della suprflair dei soli destrimani smoothando a diversi livelli in parallelo:
hemis=(lh rh)
for h in $hemis; do
 mris_preproc \
  --fsgd "$suprpath/onlyR.fsgd" \
  --meas "${flairmeasure}.mgh" \
  --target fsaverage \
  --hemi "$h" \
  --out  "$suprpath/${h}.${flairmeasure}_onlyR.mgh"
done

hemis=(lh rh)
smooth=(5 15 25)
for h in $hemis; do
 for sm in $smooth; do
  mri_surf2surf \
   --s fsaverage \
   --hemi "$h" \
   --fwhm "$sm" \
   --sval "$suprpath/${h}.${flairmeasure}_onlyR.mgh" \
   --tval "$suprpath/${h}.${flairmeasure}_onlyR.sm${sm}.mgh" &
 done
done
wait

# calcoliamo anche il valore medio di tutti i soggetti della suprflair dei destrimani per ragioni iconografiche
hemis=(lh rh)
smooth=(5 15 25)
for h in $hemis; do
 for sm in $smooth; do
  mri_concat \
   --i "$suprpath/$h.${flairmeasure}_onlyR.sm${sm}.mgh" \
   --o "$suprpath/$h.${flairmeasure}_onlyR.sm${sm}.mean.fsaverage.mgh" \
   --mean
 done
done

# Analizziamo la differenza media di FLAIR corticale tra i due gruppi di dominanza emisferica per il linguaggio (rh_dom, lh_dom), aggiustando per dominanza manuale (0=R, 1=L), età e sesso (0=F, 1=M), nonché per thickness a livello di vertice (PVR= Per Vertex Regressor)
hemis=(lh rh)
smooth=(5 15 25)
for h in $hemis; do
 for sm in $smooth; do
mri_glmfit \
 --glmdir $suprpath/$h.langdom-RHDOMminusLHDOM_handagesex-adjusted_sm${sm}_doss \
 --y $suprpath/$h.$flairmeasure.sm${sm}.mgh \
 --fsgd $suprpath/langdom_handagesex.fsgd doss \
 --pvr $suprpath/$h.thickness.sm${sm}.mgh \
 --C $suprpath/langdom-RHDOMminusLHDOM_handagesex-adjusted_doss.mtx \
 --surf fsaverage $h \
 --cortex \
 --eres-save
 done
done

# Copiamo tutti i file sig.mgh in 0_sig con nomi esplicativi
hemis=(lh rh)
smooth=(5 15 25)
for h in $hemis; do
 for sm in $smooth; do
  cp $suprpath/$h.langdom-RHDOMminusLHDOM_handagesex-adjusted_sm${sm}_doss/langdom-RHDOMminusLHDOM_handagesex-adjusted_doss/sig.mgh $suprpath/0_sig/$h.langdom-RHDOMminusLHDOM_handagesex-adjusted_sm${sm}_doss_sig.mgh
 done
done

# Guardiamo i risultati con freeview
freeview \
-colorscale -orthographic -viewport 3d -view left -hide-3d-slices -hide-3d-frames -nocursor -viewsize 500 500 \
-v /Applications/freesurfer/subjects/fsaverage/mri/brain.mgz:visible=0 \
-f /Applications/freesurfer/subjects/fsaverage/surf/lh.white\
:visible=0\
:curvature_method=binary\
:annot=/Applications/freesurfer/subjects/fsaverage/label/lh.aparc.a2005s.annot:annot_outline=1\
:annot=/Applications/freesurfer/subjects/fsaverage/label/lh.aparc.a2009s.annot:annot_outline=1\
:annot=/Applications/freesurfer/subjects/fsaverage/label/lh.PALS_B12_Brodmann.annot:annot_outline=0\
:annot=/Applications/freesurfer/subjects/fsaverage/label/lh.PALS_B12_Visuotopic.annot:annot_outline=0\
:annot=/Applications/freesurfer/subjects/fsaverage/label/lh.Yeo2011_7Networks_N1000.annot:annot_outline=0\
:annot=/Applications/freesurfer/subjects/fsaverage/label/lh.Yeo2011_17Networks_N1000.annot:annot_outline=0\
:overlay=$suprpath/0_sig/lh.langdom-RHDOMminusLHDOM_handagesex-adjusted_sm5_doss_sig.mgh:overlay_threshold=0,1.3:overlay_mask=/Applications/freesurfer/subjects/fsaverage/label/lh.cortex.label\
:overlay=$suprpath/0_sig/lh.langdom-RHDOMminusLHDOM_handagesex-adjusted_sm15_doss_sig.mgh:overlay_threshold=0,1.3:overlay_mask=/Applications/freesurfer/subjects/fsaverage/label/lh.cortex.label\
:overlay=$suprpath/0_sig/lh.langdom-RHDOMminusLHDOM_handagesex-adjusted_sm25_doss_sig.mgh:overlay_threshold=0,1.3:overlay_mask=/Applications/freesurfer/subjects/fsaverage/label/lh.cortex.label \
-f /Applications/freesurfer/subjects/fsaverage/surf/lh.pial_semi_inflated\
:visible=0\
:curvature_method=binary\
:annot=/Applications/freesurfer/subjects/fsaverage/label/lh.aparc.a2005s.annot:annot_outline=1\
:annot=/Applications/freesurfer/subjects/fsaverage/label/lh.aparc.a2009s.annot:annot_outline=1\
:annot=/Applications/freesurfer/subjects/fsaverage/label/lh.PALS_B12_Brodmann.annot:annot_outline=0\
:annot=/Applications/freesurfer/subjects/fsaverage/label/lh.PALS_B12_Visuotopic.annot:annot_outline=0\
:annot=/Applications/freesurfer/subjects/fsaverage/label/lh.Yeo2011_7Networks_N1000.annot:annot_outline=0\
:annot=/Applications/freesurfer/subjects/fsaverage/label/lh.Yeo2011_17Networks_N1000.annot:annot_outline=0\
:overlay=$suprpath/0_sig/lh.langdom-RHDOMminusLHDOM_handagesex-adjusted_sm5_doss_sig.mgh:overlay_threshold=0,1.3:overlay_mask=/Applications/freesurfer/subjects/fsaverage/label/lh.cortex.label\
:overlay=$suprpath/0_sig/lh.langdom-RHDOMminusLHDOM_handagesex-adjusted_sm15_doss_sig.mgh:overlay_threshold=0,1.3:overlay_mask=/Applications/freesurfer/subjects/fsaverage/label/lh.cortex.label\
:overlay=$suprpath/0_sig/lh.langdom-RHDOMminusLHDOM_handagesex-adjusted_sm25_doss_sig.mgh:overlay_threshold=0,1.3:overlay_mask=/Applications/freesurfer/subjects/fsaverage/label/lh.cortex.label \
-f /Applications/freesurfer/subjects/fsaverage/surf/lh.inflated\
:visible=1\
:curvature_method=binary\
:annot=/Applications/freesurfer/subjects/fsaverage/label/lh.aparc.a2005s.annot:annot_outline=1\
:annot=/Applications/freesurfer/subjects/fsaverage/label/lh.aparc.a2009s.annot:annot_outline=1\
:annot=/Applications/freesurfer/subjects/fsaverage/label/lh.PALS_B12_Brodmann.annot:annot_outline=0\
:annot=/Applications/freesurfer/subjects/fsaverage/label/lh.PALS_B12_Visuotopic.annot:annot_outline=0\
:annot=/Applications/freesurfer/subjects/fsaverage/label/lh.Yeo2011_7Networks_N1000.annot:annot_outline=0\
:annot=/Applications/freesurfer/subjects/fsaverage/label/lh.Yeo2011_17Networks_N1000.annot:annot_outline=0\
:overlay=$suprpath/0_sig/lh.langdom-RHDOMminusLHDOM_handagesex-adjusted_sm5_doss_sig.mgh:overlay_threshold=0,1.3:overlay_mask=/Applications/freesurfer/subjects/fsaverage/label/lh.cortex.label\
:overlay=$suprpath/0_sig/lh.langdom-RHDOMminusLHDOM_handagesex-adjusted_sm15_doss_sig.mgh:overlay_threshold=0,1.3:overlay_mask=/Applications/freesurfer/subjects/fsaverage/label/lh.cortex.label\
:overlay=$suprpath/0_sig/lh.langdom-RHDOMminusLHDOM_handagesex-adjusted_sm25_doss_sig.mgh:overlay_threshold=0,1.3:overlay_mask=/Applications/freesurfer/subjects/fsaverage/label/lh.cortex.label &

freeview \
-colorscale -orthographic -viewport 3d -view right -hide-3d-slices -hide-3d-frames -nocursor -viewsize 500 500 \
-v /Applications/freesurfer/subjects/fsaverage/mri/brain.mgz:visible=0 \
-f /Applications/freesurfer/subjects/fsaverage/surf/rh.white\
:visible=0\
:curvature_method=binary\
:annot=/Applications/freesurfer/subjects/fsaverage/label/rh.aparc.a2005s.annot:annot_outline=1\
:annot=/Applications/freesurfer/subjects/fsaverage/label/rh.aparc.a2009s.annot:annot_outline=1\
```

```
:annot=/Applications/freesurfer/subjects/fsaverage/label/rh.PALS_B12_Brodmann.annot:annot_outline=0\
:annot=/Applications/freesurfer/subjects/fsaverage/label/rh.PALS_B12_Visuotopic.annot:annot_outline=0\
:annot=/Applications/freesurfer/subjects/fsaverage/label/rh.Yeo2011_7Networks_N1000.annot:annot_outlin
e=0\
:annot=/Applications/freesurfer/subjects/fsaverage/label/rh.Yeo2011_17Networks_N1000.annot:annot_outli
ne=0\
:overlay=$suprpath/0_sig/rh.langdom-RHDOMminusLHDOM_handagesex-
adjusted_sm5_doss_sig.mgh:overlay_threshold=0,1.3:overlay_mask=/Applications/freesurfer/subjects/fsaver
age/label/rh.cortex.label\
:overlay=$suprpath/0_sig/rh.langdom-RHDOMminusLHDOM_handagesex-
adjusted_sm15_doss_sig.mgh:overlay_threshold=0,1.3:overlay_mask=/Applications/freesurfer/subjects/fsave
rage/label/rh.cortex.label\
:overlay=$suprpath/0_sig/rh.langdom-RHDOMminusLHDOM_handagesex-
adjusted_sm25_doss_sig.mgh:overlay_threshold=0,1.3:overlay_mask=/Applications/freesurfer/subjects/fsave
rage/label/rh.cortex.label \
-f /Applications/freesurfer/subjects/fsaverage/surf/rh.pial_semi_inflated\
:visible=0\
:curvature_method=binary\
:annot=/Applications/freesurfer/subjects/fsaverage/label/rh.aparc.a2005s.annot:annot_outline=1\
:annot=/Applications/freesurfer/subjects/fsaverage/label/rh.aparc.a2009s.annot:annot_outline=1\
:annot=/Applications/freesurfer/subjects/fsaverage/label/rh.PALS_B12_Brodmann.annot:annot_outline=0\
:annot=/Applications/freesurfer/subjects/fsaverage/label/rh.PALS_B12_Visuotopic.annot:annot_outline=0\
:annot=/Applications/freesurfer/subjects/fsaverage/label/rh.Yeo2011_7Networks_N1000.annot:annot_outlin
e=0\
:annot=/Applications/freesurfer/subjects/fsaverage/label/rh.Yeo2011_17Networks_N1000.annot:annot_outli
ne=0\
:overlay=$suprpath/0_sig/rh.langdom-RHDOMminusLHDOM_handagesex-
adjusted_sm5_doss_sig.mgh:overlay_threshold=0,1.3:overlay_mask=/Applications/freesurfer/subjects/fsaver
age/label/rh.cortex.label\
:overlay=$suprpath/0_sig/rh.langdom-RHDOMminusLHDOM_handagesex-
adjusted_sm15_doss_sig.mgh:overlay_threshold=0,1.3:overlay_mask=/Applications/freesurfer/subjects/fsave
rage/label/rh.cortex.label\
:overlay=$suprpath/0_sig/rh.langdom-RHDOMminusLHDOM_handagesex-
adjusted_sm25_doss_sig.mgh:overlay_threshold=0,1.3:overlay_mask=/Applications/freesurfer/subjects/fsave
rage/label/rh.cortex.label \
-f /Applications/freesurfer/subjects/fsaverage/surf/rh.inflated\
:visible=1\
:curvature_method=binary\
:annot=/Applications/freesurfer/subjects/fsaverage/label/rh.aparc.a2005s.annot:annot_outline=1\
:annot=/Applications/freesurfer/subjects/fsaverage/label/rh.aparc.a2009s.annot:annot_outline=1\
:annot=/Applications/freesurfer/subjects/fsaverage/label/rh.PALS_B12_Brodmann.annot:annot_outline=0\
:annot=/Applications/freesurfer/subjects/fsaverage/label/rh.PALS_B12_Visuotopic.annot:annot_outline=0\
:annot=/Applications/freesurfer/subjects/fsaverage/label/rh.Yeo2011_7Networks_N1000.annot:annot_outlin
e=0\
:annot=/Applications/freesurfer/subjects/fsaverage/label/rh.Yeo2011_17Networks_N1000.annot:annot_outli
ne=0\
:overlay=$suprpath/0_sig/rh.langdom-RHDOMminusLHDOM_handagesex-
adjusted_sm5_doss_sig.mgh:overlay_threshold=0,1.3:overlay_mask=/Applications/freesurfer/subjects/fsaver
age/label/rh.cortex.label\
:overlay=$suprpath/0_sig/rh.langdom-RHDOMminusLHDOM_handagesex-
adjusted_sm15_doss_sig.mgh:overlay_threshold=0,1.3:overlay_mask=/Applications/freesurfer/subjects/fsave
rage/label/rh.cortex.label\
:overlay=$suprpath/0_sig/rh.langdom-RHDOMminusLHDOM_handagesex-
adjusted_sm25_doss_sig.mgh:overlay_threshold=0,1.3:overlay_mask=/Applications/freesurfer/subjects/fsave
rage/label/rh.cortex.label

# Facciamo la cluster-wise analysis
hemis=(lh rh)
smooth=(5 15 25)
signes=(pos neg)
for h in $hemis; do
  for sm in $smooth; do
    for sign in $signes; do
    mri_glmfit-sim \
      --glmdir $suprpath/$h.langdom-RHDOMminusLHDOM_handagesex-adjusted_sm${sm}_doss \
      --perm 5000 1 $sign \
      --cwp 0.999 \
      --2spaces \
      --bg 8 \
      --overwrite
    done
  done
done

hemis=(lh rh)
smooth=(5 15 25)
signes=(pos neg)
surfaces=(white pial inflated)
for h in $hemis; do
  for sm in $smooth; do
    for sign in $signes; do
      mri_surfcluster \
        --in        $suprpath/$h.langdom-RHDOMminusLHDOM_handagesex-adjusted_sm${sm}_doss/langdom-
RHDOMminusLHDOM_handagesex-adjusted_doss/sig.mgh \
        --csd                                        $suprpath/$h.langdom-RHDOMminusLHDOM_handagesex-
adjusted_sm${sm}_doss/csd/all.perm.th10.${sign}-langdom-RHDOMminusLHDOM_handagesex-
adjusted_doss.csd \
        --subject fsaverage \
        --hemi $h \
        --surf white \
        --thmin 1 \
        --sign $sign \
        --annot aparc.a2005s \
        --olab      $suprpath/$h.langdom-RHDOMminusLHDOM_handagesex-adjusted_sm${sm}_doss/langdom-
RHDOMminusLHDOM_handagesex-adjusted_doss/$h.cluster_perm5000_cft1_${sign}_cwp0999_sm${sm} \
        --sum       $suprpath/$h.langdom-RHDOMminusLHDOM_handagesex-adjusted_sm${sm}_doss/langdom-
RHDOMminusLHDOM_handagesex-
adjusted_doss/$h.cluster_perm5000_cft1_${sign}_cwp0999_sm${sm}_summary.txt
    done
  done
done

for h in $hemis; do
  for sm in $smooth; do
    for sign in $signes; do
      python3 $suprpath/scripts/make_wpts_from_clusters_space.py \
        --summary                                    "$suprpath/$h.langdom-RHDOMminusLHDOM_handagesex-
adjusted_sm${sm}_doss/langdom-RHDOMminusLHDOM_handagesex-
adjusted_doss/$h.cluster_perm5000_cft1_${sign}_cwp0999_sm${sm}_summary.txt" \
        --hemi $h --subject fsaverage --surf white \
        --subjects-dir "$SUBJECTS_DIR" \
        --space scanner \
        --out-wpts                                   "$suprpath/$h.langdom-RHDOMminusLHDOM_handagesex-
adjusted_sm${sm}_doss/langdom-RHDOMminusLHDOM_handagesex-
adjusted_doss/$h.cluster_perm5000_cft1_${sign}_cwp0999_sm${sm}_summary.wpts"
    done
  done
done

# Plottiamo i dati a livello di un vertice
python $suprpath/scripts/plot_vertex_boxplot.py \
  --overlay "$suprpath/lh.r_flair_ax_wm-norm-median.sm15.mgh" \
  --fsgd "$suprpath/langdom_handagesex.fsgd" \
  --vertices 115718 \
  --prefix  "box" \
  --title-base "SUPRFLAIR vertex plot" \
  --xlabel "class" \
  --ylabel "normalized value" \
  --show-points --meanline --stats \
  --meanline --mean-both \
  --annotate-means --annotate-pos inline --mean-digits 6 --annotate-xoffset 0.25 \
  --stats-csv "$suprpath/graphs/vertex_lh_v115718.csv" \
  --csv-sep ";" --decimal "," \
  --outdir  "$suprpath/graphs"

python $suprpath/scripts/plot_vertex_boxplot.py \
  --overlay "$suprpath/lh.r_flair_ax_wm-norm-median.sm15.mgh" \
  --fsgd "$suprpath/langdom_handagesex.fsgd" \
  --vertices 115718 \
  --prefix  "box" \
  --title-base "SUPRFLAIR vertex plot" \
  --xlabel "class" \
  --ylabel "normalized value" \
  --show-points --meanline --stats \
  --meanline --mean-both \
  --annotate-means --annotate-pos inline --mean-digits 6 --annotate-xoffset 0.25 \
  --stats-csv "$suprpath/graphs/vertex_lh_v115718.csv" \
  --csv-sep ";" --decimal "," \
  --outdir  "$suprpath/graphs"

# plottiamo i dati di una label
python $suprpath/scripts/label_to_csv_groups.py \
  --label                $suprpath/lh.langdom-RHDOMminusLHDOM_handagesex-adjusted_sm15_doss/langdom-
RHDOMminusLHDOM_handagesex-adjusted_doss/lh.cluster_perm5000_cft1_pos_cwp0999_sm15-0001.label
\
  --mgh   $suprpath/lh.$flairmeasure.sm15.mgh \
  --fsgd  $suprpath/langdom_handagesex.fsgd \
  --out   $suprpath/graphs/lh.cluster_perm5000_cft1_pos_cwp0999_sm15-0001_roi_values.csv \
  --stats-out $suprpath/graphs/lh.cluster_perm5000_cft1_pos_cwp0999_sm15-0001_roi_stats.csv \
  --class-a rh_dom --class-b lh_dom

python $suprpath/scripts/label_to_csv_groups.py \
  --label                $suprpath/lh.langdom-RHDOMminusLHDOM_handagesex-adjusted_sm15_doss/langdom-
RHDOMminusLHDOM_handagesex-adjusted_doss/lh.cluster_perm5000_cft1_pos_cwp0999_sm15-0002.label
\
  --mgh   $suprpath/lh.$flairmeasure.sm15.mgh \
  --fsgd  $suprpath/langdom_handagesex.fsgd \
  --out   $suprpath/graphs/lh.cluster_perm5000_cft1_pos_cwp0999_sm15-0002_roi_values.csv \
  --stats-out $suprpath/graphs/lh.cluster_perm5000_cft1_pos_cwp0999_sm15-0002_roi_stats.csv \
  --class-a rh_dom --class-b lh_dom

####################################
2) ANALISI SUPRFLAIR STATICA CONTRASTANDO RH_DOM VS LH_DOM, AGGIUSTANDO per handedness, age,
sex e thickness_PVR, dopo aver eliminato i mancini LH_DOM
####################################

# Prepariamo i file mgh con gli scalari della thickness a differenti livelli di smoothing:
hemis=(lh rh)
smooth=(5 15 25)
for h in $hemis; do
  for sm in $smooth; do
mris_preproc \
  --fsgd $suprpath/langdom_handagesex_noLHDOM_Lhand.fsgd \
  --cache-in thickness.fwhm$sm.fsaverage \
  --target fsaverage \
  --hemi $h \
  --out $suprpath/$h.thickness_noLHDOM_Lhand.sm${sm}.mgh
  done
done

# Prepariamo i file mgh con gli scalari della suprflair smoothando a diversi livelli in parallelo:
hemis=(lh rh)
for h in $hemis; do
  mris_preproc \
    --fsgd "$suprpath/langdom_handagesex_noLHDOM_Lhand.fsgd" \
    --meas "${flairmeasure}.mgh" \
    --target fsaverage \
    --hemi "$h" \
    --out  "$suprpath/${h}.${flairmeasure}_noLHDOM_Lhand.mgh"
done

hemis=(lh rh)
smooth=(5 15 25)
for h in $hemis; do
  for sm in $smooth; do
    mri_surf2surf \
      --s fsaverage \
      --hemi "$h" \
      --fwhm "$sm" \
      --sval "$suprpath/${h}.${flairmeasure}_noLHDOM_Lhand.mgh" \
      --tval "$suprpath/${h}.${flairmeasure}_noLHDOM_Lhand.sm${sm}.mgh" &
  done
done
wait

# Analizziamo la differenza media di FLAIR corticale tra i due gruppi di dominanza emisferica per il linguaggio
(rh_dom, lh_dom), aggiustando per dominanza manuale (0=R, 1=L), età e sesso (0=F, 1=M), nonché per
thickness a livello di vertice (PVR= Per Vertex Regressor)

hemis=(lh rh)
smooth=(5 15 25)
for h in $hemis; do
  for sm in $smooth; do
mri_glmfit \
  --glmdir                                   $suprpath/$h.langdom-RHDOMminusLHDOM_handagesex-
adjusted_noLHDOM_Lhand_sm${sm}_doss \
```

```
 --y $suprpath/$h.${flairmeasure}_noLHDOM_Lhand.sm${sm}.mgh \
 --fsgd $suprpath/langdom_handagesex_noLHDOM_Lhand.fsgd doss \
 --pvr $suprpath/$h.thickness_noLHDOM_Lhand.sm${sm}.mgh \
 --C $suprpath/langdom-RHDOMminusLHDOM_handagesex-adjusted_doss_noLHDOM_Lhand.mtx \
 --surf fsaverage $h \
 --cortex \
 --eres-save
 done
done

# Copiamo tutti i file sig.mgh in 0_sig con nomi esplicativi
hemis=(lh rh)
smooth=(5 15 25)
for h in $hemis; do
 for sm in $smooth; do
cp                                                    $suprpath/$h.langdom-RHDOMminusLHDOM_handagesex-
adjusted_noLHDOM_Lhand_sm${sm}_doss/langdom-RHDOMminusLHDOM_handagesex-
adjusted_doss_noLHDOM_Lhand/sig.mgh    $suprpath/0_sig/$h.langdom-RHDOMminusLHDOM_handagesex-
adjusted_noLHDOM_Lhand_sm${sm}_doss_sig.mgh
 done
done

# Guardiamo i risultati con freeview
freeview \
-colorscale -orthographic -viewport 3d -view left -hide-3d-slices -hide-3d-frames -nocursor -viewsize 500 500 \
-v /Applications/freesurfer/subjects/fsaverage/mri/brain.mgz:visible=0 \
-f /Applications/freesurfer/subjects/fsaverage/surf/lh.white\
:visible=0\
:curvature_method=binary\
:annot=/Applications/freesurfer/subjects/fsaverage/label/lh.aparc.a2005s.annot:annot_outline=1\
:annot=/Applications/freesurfer/subjects/fsaverage/label/lh.aparc.a2009s.annot:annot_outline=1\
:annot=/Applications/freesurfer/subjects/fsaverage/label/lh.PALS_B12_Brodmann.annot:annot_outline=0\
:annot=/Applications/freesurfer/subjects/fsaverage/label/lh.PALS_B12_Visuotopic.annot:annot_outline=0\
:annot=/Applications/freesurfer/subjects/fsaverage/label/lh.Yeo2011_7Networks_N1000.annot:annot_outlin
e=0\
:annot=/Applications/freesurfer/subjects/fsaverage/label/lh.Yeo2011_17Networks_N1000.annot:annot_outli
ne=0\
:overlay=$suprpath/0_sig/lh.langdom-RHDOMminusLHDOM_handagesex-
adjusted_noLHDOM_Lhand_sm5_doss_sig.mgh:overlay_threshold=0,1.3:overlay_mask=/Applications/freesur
fer/subjects/fsaverage/label/lh.cortex.label\
:overlay=$suprpath/0_sig/lh.langdom-RHDOMminusLHDOM_handagesex-
adjusted_noLHDOM_Lhand_sm15_doss_sig.mgh:overlay_threshold=0,1.3:overlay_mask=/Applications/freesu
rfer/subjects/fsaverage/label/lh.cortex.label\
:overlay=$suprpath/0_sig/lh.langdom-RHDOMminusLHDOM_handagesex-
adjusted_noLHDOM_Lhand_sm25_doss_sig.mgh:overlay_threshold=0,1.3:overlay_mask=/Applications/freesu
rfer/subjects/fsaverage/label/lh.cortex.label \
-f /Applications/freesurfer/subjects/fsaverage/surf/lh.pial_semi_inflated\
:visible=0\
:curvature_method=binary\
:annot=/Applications/freesurfer/subjects/fsaverage/label/lh.aparc.a2005s.annot:annot_outline=1\
:annot=/Applications/freesurfer/subjects/fsaverage/label/lh.aparc.a2009s.annot:annot_outline=1\
:annot=/Applications/freesurfer/subjects/fsaverage/label/lh.PALS_B12_Brodmann.annot:annot_outline=0\
:annot=/Applications/freesurfer/subjects/fsaverage/label/lh.PALS_B12_Visuotopic.annot:annot_outline=0\
:annot=/Applications/freesurfer/subjects/fsaverage/label/lh.Yeo2011_7Networks_N1000.annot:annot_outlin
e=0\
:annot=/Applications/freesurfer/subjects/fsaverage/label/lh.Yeo2011_17Networks_N1000.annot:annot_outli
ne=0\
:overlay=$suprpath/0_sig/lh.langdom-RHDOMminusLHDOM_handagesex-
adjusted_noLHDOM_Lhand_sm5_doss_sig.mgh:overlay_threshold=0,1.3:overlay_mask=/Applications/freesur
fer/subjects/fsaverage/label/lh.cortex.label\
:overlay=$suprpath/0_sig/lh.langdom-RHDOMminusLHDOM_handagesex-
adjusted_noLHDOM_Lhand_sm15_doss_sig.mgh:overlay_threshold=0,1.3:overlay_mask=/Applications/freesu
rfer/subjects/fsaverage/label/lh.cortex.label\
:overlay=$suprpath/0_sig/lh.langdom-RHDOMminusLHDOM_handagesex-
adjusted_noLHDOM_Lhand_sm25_doss_sig.mgh:overlay_threshold=0,1.3:overlay_mask=/Applications/freesu
rfer/subjects/fsaverage/label/lh.cortex.label \
-f /Applications/freesurfer/subjects/fsaverage/surf/lh.inflated\
:visible=1\
:curvature_method=binary\
:annot=/Applications/freesurfer/subjects/fsaverage/label/lh.aparc.a2005s.annot:annot_outline=1\
:annot=/Applications/freesurfer/subjects/fsaverage/label/lh.aparc.a2009s.annot:annot_outline=1\
:annot=/Applications/freesurfer/subjects/fsaverage/label/lh.PALS_B12_Brodmann.annot:annot_outline=0\
:annot=/Applications/freesurfer/subjects/fsaverage/label/lh.PALS_B12_Visuotopic.annot:annot_outline=0\
:annot=/Applications/freesurfer/subjects/fsaverage/label/lh.Yeo2011_7Networks_N1000.annot:annot_outlin
e=0\
:annot=/Applications/freesurfer/subjects/fsaverage/label/lh.Yeo2011_17Networks_N1000.annot:annot_outli
ne=0\
:overlay=$suprpath/0_sig/lh.langdom-RHDOMminusLHDOM_handagesex-
adjusted_noLHDOM_Lhand_sm5_doss_sig.mgh:overlay_threshold=0,1.3:overlay_mask=/Applications/freesur
fer/subjects/fsaverage/label/lh.cortex.label\
:overlay=$suprpath/0_sig/lh.langdom-RHDOMminusLHDOM_handagesex-
adjusted_noLHDOM_Lhand_sm15_doss_sig.mgh:overlay_threshold=0,1.3:overlay_mask=/Applications/freesu
rfer/subjects/fsaverage/label/lh.cortex.label\
:overlay=$suprpath/0_sig/lh.langdom-RHDOMminusLHDOM_handagesex-
adjusted_noLHDOM_Lhand_sm25_doss_sig.mgh:overlay_threshold=0,1.3:overlay_mask=/Applications/freesu
rfer/subjects/fsaverage/label/lh.cortex.label &

freeview \
-colorscale -orthographic -viewport 3d -view right -hide-3d-slices -hide-3d-frames -nocursor -viewsize 500 500
\
-v /Applications/freesurfer/subjects/fsaverage/mri/brain.mgz:visible=0 \
-f /Applications/freesurfer/subjects/fsaverage/surf/rh.white\
:visible=0\
:curvature_method=binary\
:annot=/Applications/freesurfer/subjects/fsaverage/label/rh.aparc.a2005s.annot:annot_outline=1\
:annot=/Applications/freesurfer/subjects/fsaverage/label/rh.aparc.a2009s.annot:annot_outline=1\
:annot=/Applications/freesurfer/subjects/fsaverage/label/rh.PALS_B12_Brodmann.annot:annot_outline=0\
:annot=/Applications/freesurfer/subjects/fsaverage/label/rh.PALS_B12_Visuotopic.annot:annot_outline=0\
:annot=/Applications/freesurfer/subjects/fsaverage/label/rh.Yeo2011_7Networks_N1000.annot:annot_outlin
e=0\
:annot=/Applications/freesurfer/subjects/fsaverage/label/rh.Yeo2011_17Networks_N1000.annot:annot_outli
ne=0\
:overlay=$suprpath/0_sig/rh.langdom-RHDOMminusLHDOM_handagesex-
adjusted_noLHDOM_Lhand_sm5_doss_sig.mgh:overlay_threshold=0,1.3:overlay_mask=/Applications/freesur
fer/subjects/fsaverage/label/rh.cortex.label\
:overlay=$suprpath/0_sig/rh.langdom-RHDOMminusLHDOM_handagesex-
adjusted_noLHDOM_Lhand_sm15_doss_sig.mgh:overlay_threshold=0,1.3:overlay_mask=/Applications/freesu
rfer/subjects/fsaverage/label/rh.cortex.label\
:overlay=$suprpath/0_sig/rh.langdom-RHDOMminusLHDOM_handagesex-
adjusted_noLHDOM_Lhand_sm25_doss_sig.mgh:overlay_threshold=0,1.3:overlay_mask=/Applications/freesu
rfer/subjects/fsaverage/label/rh.cortex.label \
-f /Applications/freesurfer/subjects/fsaverage/surf/rh.pial_semi_inflated\
:visible=0\
:curvature_method=binary\
:annot=/Applications/freesurfer/subjects/fsaverage/label/rh.aparc.a2005s.annot:annot_outline=1\
:annot=/Applications/freesurfer/subjects/fsaverage/label/rh.aparc.a2009s.annot:annot_outline=1\
:annot=/Applications/freesurfer/subjects/fsaverage/label/rh.PALS_B12_Brodmann.annot:annot_outline=0\
:annot=/Applications/freesurfer/subjects/fsaverage/label/rh.PALS_B12_Visuotopic.annot:annot_outline=0\
:annot=/Applications/freesurfer/subjects/fsaverage/label/rh.Yeo2011_7Networks_N1000.annot:annot_outlin
e=0\
:annot=/Applications/freesurfer/subjects/fsaverage/label/rh.Yeo2011_17Networks_N1000.annot:annot_outli
ne=0\
:overlay=$suprpath/0_sig/rh.langdom-RHDOMminusLHDOM_handagesex-
adjusted_noLHDOM_Lhand_sm5_doss_sig.mgh:overlay_threshold=0,1.3:overlay_mask=/Applications/freesur
fer/subjects/fsaverage/label/rh.cortex.label\
:overlay=$suprpath/0_sig/rh.langdom-RHDOMminusLHDOM_handagesex-
adjusted_noLHDOM_Lhand_sm15_doss_sig.mgh:overlay_threshold=0,1.3:overlay_mask=/Applications/freesu
rfer/subjects/fsaverage/label/rh.cortex.label\
:overlay=$suprpath/0_sig/rh.langdom-RHDOMminusLHDOM_handagesex-
adjusted_noLHDOM_Lhand_sm25_doss_sig.mgh:overlay_threshold=0,1.3:overlay_mask=/Applications/freesu
rfer/subjects/fsaverage/label/rh.cortex.label

# Facciamo la cluster-wise analysis
hemis=(lh rh)
smooth=(5 15 25)
signes=(pos neg)
for h in $hemis; do
 for sm in $smooth; do
  for sign in $signes; do
  mri_glmfit-sim \
    --glmdir                                          $suprpath/$h.langdom-RHDOMminusLHDOM_handagesex-
adjusted_noLHDOM_Lhand_sm${sm}_doss \
    --perm 5000 1 $sign \
    --cwp 0.999 \
    --2spaces \
    --bg 8 \
    --overwrite
  done
 done
done

hemis=(lh rh)
smooth=(5 15 25)
signes=(pos neg)
surfaces=(white pial inflated)
for h in $hemis; do
 for sm in $smooth; do
  for sign in $signes; do
   mri_surfcluster \
    --in                                              $suprpath/$h.langdom-RHDOMminusLHDOM_handagesex-
adjusted_noLHDOM_Lhand_sm${sm}_doss/langdom-RHDOMminusLHDOM_handagesex-
adjusted_doss_noLHDOM_Lhand/sig.mgh \
    --csd                                             $suprpath/$h.langdom-RHDOMminusLHDOM_handagesex-
adjusted_noLHDOM_Lhand_sm${sm}_doss/csd/all.perm.th10.${sign}-langdom-
RHDOMminusLHDOM_handagesex-adjusted_doss_noLHDOM_Lhand.csd \
    --subject fsaverage \
    --hemi $h \
    --surf white \
    --thmin 1 \
    --sign $sign \
    --annot aparc.a2005s \
    --olab                                            $suprpath/$h.langdom-RHDOMminusLHDOM_handagesex-
adjusted_noLHDOM_Lhand_sm${sm}_doss/langdom-RHDOMminusLHDOM_handagesex-
adjusted_doss_noLHDOM_Lhand/$h.cluster_perm5000_cft1_${sign}_cwp0999_sm${sm} \
    --sum                                             $suprpath/$h.langdom-RHDOMminusLHDOM_handagesex-
adjusted_noLHDOM_Lhand_sm${sm}_doss/langdom-RHDOMminusLHDOM_handagesex-
adjusted_doss_noLHDOM_Lhand/$h.cluster_perm5000_cft1_${sign}_cwp0999_sm${sm}_summary.txt
  done
 done
done


for h in $hemis; do
 for sm in $smooth; do
  for sign in $signes; do
   python3 $suprpath/scripts/make_wpts_from_clusters_space.py \
    --summary                                         "$suprpath/$h.langdom-RHDOMminusLHDOM_handagesex-
adjusted_noLHDOM_Lhand_sm${sm}_doss/langdom-RHDOMminusLHDOM_handagesex-
adjusted_doss_noLHDOM_Lhand/$h.cluster_perm5000_cft1_${sign}_cwp0999_sm${sm}_summary.txt" \
    --hemi $h --subject fsaverage --surf white \
    --subjects-dir "$SUBJECTS_DIR" \
    --space scanner \
    --out-wpts                                        "$suprpath/$h.langdom-RHDOMminusLHDOM_handagesex-
adjusted_noLHDOM_Lhand_sm${sm}_doss/langdom-RHDOMminusLHDOM_handagesex-
adjusted_doss_noLHDOM_Lhand/$h.cluster_perm5000_cft1_${sign}_cwp0999_sm${sm}_summary.wpts"
  done
 done
done

####################################
3) ANALISI SUPRFLAIR STATICA CONTRASTANDO RHDOM_L - LHDOM_L, AGGIUSTANDO per age, sex e
thickness_PVR, dopo aver eliminato i destrimani
####################################

# Prepariamo i file mgh con gli scalari della thickness a differenti livelli di smoothing:
hemis=(lh rh)
smooth=(5 15 25)
for h in $hemis; do
```

```
 for sm in $smooth; do
mris_preproc \
 --fsgd $suprpath/langdom_handagesex_noRhand.fsgd \
 --cache-in thickness.fwhm$sm.fsaverage \
 --target fsaverage \
 --hemi $h \
 --out $suprpath/$h.thickness_noRhand.sm${sm}.mgh
 done
done

# Prepariamo i file mgh con gli scalari della suprflair smoothando a diversi livelli in parallelo:
hemis=(lh rh)
for h in $hemis; do
 mris_preproc \
  --fsgd "$suprpath/noRhand.fsgd" \
  --meas "${flairmeasure}.mgh" \
  --target fsaverage \
  --hemi "$h" \
  --out  "$suprpath/${h}.${flairmeasure}_noRhand.mgh"
done

hemis=(lh rh)
smooth=(5 15 25)
for h in $hemis; do
 for sm in $smooth; do
  mri_surf2surf \
   --s fsaverage \
   --hemi "$h" \
   --fwhm "$sm" \
   --sval "$suprpath/${h}.${flairmeasure}_noRhand.mgh" \
   --tval "$suprpath/${h}.${flairmeasure}_noRhand.sm${sm}.mgh" &
 done
done
wait

# Analizziamo la differenza media di FLAIR corticale tra i due gruppi di dominanza emisferica per il linguaggio (lh_dom, rh_dom), aggiustando per età e sesso (0=F, 1=M), nonché per thickness a livello di vertice (PVR= Per Vertex Regressor)
hemis=(lh rh)
smooth=(5 15 25)
for h in $hemis; do
 for sm in $smooth; do
mri_glmfit \
 --glmdir $suprpath/$h.langdom-RHDOMminusLHDOM_handagesex-adjusted_noRhand_sm${sm}_doss \
 --y $suprpath/$h.${flairmeasure}_noRhand.sm${sm}.mgh \
 --fsgd $suprpath/langdom_handagesex_noRhand.fsgd doss \
 --pvr $suprpath/$h.thickness_noRhand.sm${sm}.mgh \
 --C $suprpath/langdom-RHDOMminusLHDOM_handagesex-adjusted_doss_noRhand.mtx \
 --surf fsaverage $h \
 --cortex \
 --eres-save
 done
done

# Copiamo tutti i file sig.mgh in 0_sig con nomi esplicativi
hemis=(lh rh)
smooth=(5 15 25)
for h in $hemis; do
 for sm in $smooth; do
cp    $suprpath/$h.langdom-RHDOMminusLHDOM_handagesex-adjusted_noRhand_sm${sm}_doss/langdom-RHDOMminusLHDOM_handagesex-adjusted_doss_noRhand/sig.mgh          $suprpath/0_sig/$h.langdom-RHDOMminusLHDOM_handagesex-adjusted_noRhand_sm${sm}_doss_sig.mgh
 done
done

# Guardiamo i risultati con freeview
freeview \
-colorscale -orthographic -viewport 3d -view left -hide-3d-slices -hide-3d-frames -nocursor -viewsize 500 500 \
-v /Applications/freesurfer/subjects/fsaverage/mri/brain.mgz:visible=0 \
-f /Applications/freesurfer/subjects/fsaverage/surf/lh.white\
:visible=0\
:curvature_method=binary\
:annot=/Applications/freesurfer/subjects/fsaverage/label/lh.aparc.a2005s.annot:annot_outline=1\
:annot=/Applications/freesurfer/subjects/fsaverage/label/lh.aparc.a2009s.annot:annot_outline=1\
:annot=/Applications/freesurfer/subjects/fsaverage/label/lh.PALS_B12_Brodmann.annot:annot_outline=0\
:annot=/Applications/freesurfer/subjects/fsaverage/label/lh.PALS_B12_Visuotopic.annot:annot_outline=0\
:annot=/Applications/freesurfer/subjects/fsaverage/label/lh.Yeo2011_7Networks_N1000.annot:annot_outline=0\
:annot=/Applications/freesurfer/subjects/fsaverage/label/lh.Yeo2011_17Networks_N1000.annot:annot_outline=0\
:overlay=$suprpath/0_sig/lh.langdom-RHDOMminusLHDOM_handagesex-adjusted_noRhand_sm5_doss_sig.mgh:overlay_threshold=0,1.3:overlay_mask=/Applications/freesurfer/subjects/fsaverage/label/lh.cortex.label\
:overlay=$suprpath/0_sig/lh.langdom-RHDOMminusLHDOM_handagesex-adjusted_noRhand_sm15_doss_sig.mgh:overlay_threshold=0,1.3:overlay_mask=/Applications/freesurfer/subjects/fsaverage/label/lh.cortex.label\
:overlay=$suprpath/0_sig/lh.langdom-RHDOMminusLHDOM_handagesex-adjusted_noRhand_sm25_doss_sig.mgh:overlay_threshold=0,1.3:overlay_mask=/Applications/freesurfer/subjects/fsaverage/label/lh.cortex.label \
-f /Applications/freesurfer/subjects/fsaverage/surf/lh.pial_semi_inflated\
:visible=0\
:curvature_method=binary\
:annot=/Applications/freesurfer/subjects/fsaverage/label/lh.aparc.a2005s.annot:annot_outline=1\
:annot=/Applications/freesurfer/subjects/fsaverage/label/lh.aparc.a2009s.annot:annot_outline=1\
:annot=/Applications/freesurfer/subjects/fsaverage/label/lh.PALS_B12_Brodmann.annot:annot_outline=0\
:annot=/Applications/freesurfer/subjects/fsaverage/label/lh.PALS_B12_Visuotopic.annot:annot_outline=0\
:annot=/Applications/freesurfer/subjects/fsaverage/label/lh.Yeo2011_7Networks_N1000.annot:annot_outline=0\
:annot=/Applications/freesurfer/subjects/fsaverage/label/lh.Yeo2011_17Networks_N1000.annot:annot_outline=0\
:overlay=$suprpath/0_sig/lh.langdom-RHDOMminusLHDOM_handagesex-adjusted_noRhand_sm5_doss_sig.mgh:overlay_threshold=0,1.3:overlay_mask=/Applications/freesurfer/subjects/fsaverage/label/lh.cortex.label\
:overlay=$suprpath/0_sig/lh.langdom-RHDOMminusLHDOM_handagesex-adjusted_noRhand_sm15_doss_sig.mgh:overlay_threshold=0,1.3:overlay_mask=/Applications/freesurfer/subjects/fsaverage/label/lh.cortex.label\
:overlay=$suprpath/0_sig/lh.langdom-RHDOMminusLHDOM_handagesex-adjusted_noRhand_sm25_doss_sig.mgh:overlay_threshold=0,1.3:overlay_mask=/Applications/freesurfer/subjects/fsaverage/label/lh.cortex.label \
-f /Applications/freesurfer/subjects/fsaverage/surf/lh.inflated\
:visible=1\
:curvature_method=binary\
:annot=/Applications/freesurfer/subjects/fsaverage/label/lh.aparc.a2005s.annot:annot_outline=1\
:annot=/Applications/freesurfer/subjects/fsaverage/label/lh.aparc.a2009s.annot:annot_outline=1\
:annot=/Applications/freesurfer/subjects/fsaverage/label/lh.PALS_B12_Brodmann.annot:annot_outline=0\
:annot=/Applications/freesurfer/subjects/fsaverage/label/lh.PALS_B12_Visuotopic.annot:annot_outline=0\
:annot=/Applications/freesurfer/subjects/fsaverage/label/lh.Yeo2011_7Networks_N1000.annot:annot_outline=0\
:annot=/Applications/freesurfer/subjects/fsaverage/label/lh.Yeo2011_17Networks_N1000.annot:annot_outline=0\
:overlay=$suprpath/0_sig/lh.langdom-RHDOMminusLHDOM_handagesex-adjusted_noRhand_sm5_doss_sig.mgh:overlay_threshold=0,1.3:overlay_mask=/Applications/freesurfer/subjects/fsaverage/label/lh.cortex.label\
:overlay=$suprpath/0_sig/lh.langdom-RHDOMminusLHDOM_handagesex-adjusted_noRhand_sm15_doss_sig.mgh:overlay_threshold=0,1.3:overlay_mask=/Applications/freesurfer/subjects/fsaverage/label/lh.cortex.label\
:overlay=$suprpath/0_sig/lh.langdom-RHDOMminusLHDOM_handagesex-adjusted_noRhand_sm25_doss_sig.mgh:overlay_threshold=0,1.3:overlay_mask=/Applications/freesurfer/subjects/fsaverage/label/lh.cortex.label \
-f /Applications/freesurfer/subjects/fsaverage/surf/lh.inflated\
:visible=1\
:curvature_method=binary\
:annot=/Applications/freesurfer/subjects/fsaverage/label/lh.aparc.a2005s.annot:annot_outline=1\
:annot=/Applications/freesurfer/subjects/fsaverage/label/lh.aparc.a2009s.annot:annot_outline=1\
:annot=/Applications/freesurfer/subjects/fsaverage/label/lh.PALS_B12_Brodmann.annot:annot_outline=0\
:annot=/Applications/freesurfer/subjects/fsaverage/label/lh.PALS_B12_Visuotopic.annot:annot_outline=0\
:annot=/Applications/freesurfer/subjects/fsaverage/label/lh.Yeo2011_7Networks_N1000.annot:annot_outline=0\
:annot=/Applications/freesurfer/subjects/fsaverage/label/lh.Yeo2011_17Networks_N1000.annot:annot_outline=0\
:overlay=$suprpath/0_sig/lh.langdom-RHDOMminusLHDOM_handagesex-adjusted_noRhand_sm5_doss_sig.mgh:overlay_threshold=0,1.3:overlay_mask=/Applications/freesurfer/subjects/fsaverage/label/lh.cortex.label\
:overlay=$suprpath/0_sig/lh.langdom-RHDOMminusLHDOM_handagesex-adjusted_noRhand_sm15_doss_sig.mgh:overlay_threshold=0,1.3:overlay_mask=/Applications/freesurfer/subjects/fsaverage/label/lh.cortex.label\
:overlay=$suprpath/0_sig/lh.langdom-RHDOMminusLHDOM_handagesex-adjusted_noRhand_sm25_doss_sig.mgh:overlay_threshold=0,1.3:overlay_mask=/Applications/freesurfer/subjects/fsaverage/label/lh.cortex.label &

freeview \
-colorscale -orthographic -viewport 3d -view right -hide-3d-slices -hide-3d-frames -nocursor -viewsize 500 500 \
-v /Applications/freesurfer/subjects/fsaverage/mri/brain.mgz:visible=0 \
-f /Applications/freesurfer/subjects/fsaverage/surf/rh.white\
:visible=0\
:curvature_method=binary\
:annot=/Applications/freesurfer/subjects/fsaverage/label/rh.aparc.a2005s.annot:annot_outline=1\
:annot=/Applications/freesurfer/subjects/fsaverage/label/rh.aparc.a2009s.annot:annot_outline=1\
:annot=/Applications/freesurfer/subjects/fsaverage/label/rh.PALS_B12_Brodmann.annot:annot_outline=0\
:annot=/Applications/freesurfer/subjects/fsaverage/label/rh.PALS_B12_Visuotopic.annot:annot_outline=0\
:annot=/Applications/freesurfer/subjects/fsaverage/label/rh.Yeo2011_7Networks_N1000.annot:annot_outline=0\
:annot=/Applications/freesurfer/subjects/fsaverage/label/rh.Yeo2011_17Networks_N1000.annot:annot_outline=0\
:overlay=$suprpath/0_sig/rh.langdom-RHDOMminusLHDOM_handagesex-adjusted_noRhand_sm5_doss_sig.mgh:overlay_threshold=0,1.3:overlay_mask=/Applications/freesurfer/subjects/fsaverage/label/rh.cortex.label\
:overlay=$suprpath/0_sig/rh.langdom-RHDOMminusLHDOM_handagesex-adjusted_noRhand_sm15_doss_sig.mgh:overlay_threshold=0,1.3:overlay_mask=/Applications/freesurfer/subjects/fsaverage/label/rh.cortex.label\
:overlay=$suprpath/0_sig/rh.langdom-RHDOMminusLHDOM_handagesex-adjusted_noRhand_sm25_doss_sig.mgh:overlay_threshold=0,1.3:overlay_mask=/Applications/freesurfer/subjects/fsaverage/label/rh.cortex.label \
-f /Applications/freesurfer/subjects/fsaverage/surf/rh.pial_semi_inflated\
:visible=0\
:curvature_method=binary\
:annot=/Applications/freesurfer/subjects/fsaverage/label/rh.aparc.a2005s.annot:annot_outline=1\
:annot=/Applications/freesurfer/subjects/fsaverage/label/rh.aparc.a2009s.annot:annot_outline=1\
:annot=/Applications/freesurfer/subjects/fsaverage/label/rh.PALS_B12_Brodmann.annot:annot_outline=0\
:annot=/Applications/freesurfer/subjects/fsaverage/label/rh.PALS_B12_Visuotopic.annot:annot_outline=0\
:annot=/Applications/freesurfer/subjects/fsaverage/label/rh.Yeo2011_7Networks_N1000.annot:annot_outline=0\
:annot=/Applications/freesurfer/subjects/fsaverage/label/rh.Yeo2011_17Networks_N1000.annot:annot_outline=0\
:overlay=$suprpath/0_sig/rh.langdom-RHDOMminusLHDOM_handagesex-adjusted_noRhand_sm5_doss_sig.mgh:overlay_threshold=0,1.3:overlay_mask=/Applications/freesurfer/subjects/fsaverage/label/rh.cortex.label\
:overlay=$suprpath/0_sig/rh.langdom-RHDOMminusLHDOM_handagesex-adjusted_noRhand_sm15_doss_sig.mgh:overlay_threshold=0,1.3:overlay_mask=/Applications/freesurfer/subjects/fsaverage/label/rh.cortex.label\
:overlay=$suprpath/0_sig/rh.langdom-RHDOMminusLHDOM_handagesex-adjusted_noRhand_sm25_doss_sig.mgh:overlay_threshold=0,1.3:overlay_mask=/Applications/freesurfer/subjects/fsaverage/label/rh.cortex.label \
-f /Applications/freesurfer/subjects/fsaverage/surf/rh.inflated\
:visible=1\
:curvature_method=binary\
:annot=/Applications/freesurfer/subjects/fsaverage/label/rh.aparc.a2005s.annot:annot_outline=1\
:annot=/Applications/freesurfer/subjects/fsaverage/label/rh.aparc.a2009s.annot:annot_outline=1\
:annot=/Applications/freesurfer/subjects/fsaverage/label/rh.PALS_B12_Brodmann.annot:annot_outline=0\
:annot=/Applications/freesurfer/subjects/fsaverage/label/rh.PALS_B12_Visuotopic.annot:annot_outline=0\
:annot=/Applications/freesurfer/subjects/fsaverage/label/rh.Yeo2011_7Networks_N1000.annot:annot_outline=0\
:annot=/Applications/freesurfer/subjects/fsaverage/label/rh.Yeo2011_17Networks_N1000.annot:annot_outline=0\
:overlay=$suprpath/0_sig/rh.langdom-RHDOMminusLHDOM_handagesex-adjusted_noRhand_sm5_doss_sig.mgh:overlay_threshold=0,1.3:overlay_mask=/Applications/freesurfer/subjects/fsaverage/label/rh.cortex.label\
:overlay=$suprpath/0_sig/rh.langdom-RHDOMminusLHDOM_handagesex-adjusted_noRhand_sm15_doss_sig.mgh:overlay_threshold=0,1.3:overlay_mask=/Applications/freesurfer/subjects/fsaverage/label/rh.cortex.label\
:overlay=$suprpath/0_sig/rh.langdom-RHDOMminusLHDOM_handagesex-adjusted_noRhand_sm25_doss_sig.mgh:overlay_threshold=0,1.3:overlay_mask=/Applications/freesurfer/subjects/fsaverage/label/rh.cortex.label

# Facciamo la cluster-wise analysis
hemis=(lh rh)
smooth=(5 15 25)
signes=(pos neg)
for h in $hemis; do
 for sm in $smooth; do
  for sign in $signes; do
  mri_glmfit-sim \
   --glmdir $suprpath/$h.langdom-RHDOMminusLHDOM_handagesex-adjusted_noRhand_sm${sm}_doss \
   --perm 5000 1 $sign \
   --cwp 0.999 \
   --2spaces \
   --bg 8 \
   --overwrite
  done
 done
done

hemis=(lh rh)
smooth=(5 15 25)
signes=(pos neg)
surfaces=(white pial inflated)
for h in $hemis; do
 for sm in $smooth; do
  for sign in $signes; do
    mri_surfcluster \
     --in                                $suprpath/$h.langdom-RHDOMminusLHDOM_handagesex-adjusted_noRhand_sm${sm}_doss/langdom-RHDOMminusLHDOM_handagesex-adjusted_doss_noRhand/sig.mgh \
     --csd                               $suprpath/$h.langdom-RHDOMminusLHDOM_handagesex-adjusted_noRhand_sm${sm}_doss/csd/all.perm.th10.${sign}-langdom-RHDOMminusLHDOM_handagesex-adjusted_doss_noRhand.csd \
      --subject fsaverage \
```

```
      --hemi $h \
      --surf white \
      --thmin 1 \
      --sign $sign \
      --annot aparc.a2005s \
      --olab                                    $suprpath/$h.langdom-RHDOMminusLHDOM_handagesex-
adjusted_noRhand_sm${sm}_doss/langdom-RHDOMminusLHDOM_handagesex-
adjusted_doss_noRhand/$h.cluster_perm5000_cft1_${sign}_cwp0999_sm${sm} \
      --sum                                     $suprpath/$h.langdom-RHDOMminusLHDOM_handagesex-
adjusted_noRhand_sm${sm}_doss/langdom-RHDOMminusLHDOM_handagesex-
adjusted_doss_noRhand/$h.cluster_perm5000_cft1_${sign}_cwp0999_sm${sm}_summary.txt
   done
  done
done

for h in $hemis; do
 for sm in $smooth; do
  for sign in $signes; do
   python3 $suprpath/scripts/make_wpts_from_clusters_space.py \
    --summary                                 "$suprpath/$h.langdom-RHDOMminusLHDOM_handagesex-
adjusted_noRhand_sm${sm}_doss/langdom-RHDOMminusLHDOM_handagesex-
adjusted_doss_noRhand/$h.cluster_perm5000_cft1_${sign}_cwp0999_sm${sm}_summary.txt" \
    --hemi $h --subject fsaverage --surf white \
    --subjects-dir "$SUBJECTS_DIR" \
    --space scanner \
    --out-wpts                                "$suprpath/$h.langdom-RHDOMminusLHDOM_handagesex-
adjusted_noRhand_sm${sm}_doss/langdom-RHDOMminusLHDOM_handagesex-
adjusted_doss_noRhand/$h.cluster_perm5000_cft1_${sign}_cwp0999_sm${sm}_summary.wpts"
   done
  done
done

# Plottiamo i dati a livello di un vertice
python $suprpath/scripts/plot_vertex_boxplot.py \
 --overlay "$suprpath/lh.r_flair_ax_wm-norm-median_noRhand.sm15.mgh" \
 --fsgd "$suprpath/langdom_handagesex_noRhand.fsgd" \
 --vertices 69974 \
 --prefix  "box" \
 --title-base "SUPRFLAIR vertex plot" \
 --xlabel "class" \
 --ylabel "normalized value" \
 --show-points --meanline --stats \
 --meanline --mean-both \
 --annotate-means --annotate-pos inline --mean-digits 6 --annotate-xoffset 0.25 \
 --stats-csv "$suprpath/graphs/vertex_lh_v69974.csv" \
 --csv-sep ";" --decimal "," \
 --outdir  "$suprpath/graphs"

python $suprpath/scripts/plot_vertex_boxplot.py \
 --overlay "$suprpath/lh.r_flair_ax_wm-norm-median_noRhand.sm15.mgh" \
 --fsgd "$suprpath/langdom_handagesex_noRhand.fsgd" \
 --vertices 94264 \
 --prefix  "box" \
 --title-base "SUPRFLAIR vertex plot" \
 --xlabel "class" \
 --ylabel "normalized value" \
 --show-points --meanline --stats \
 --meanline --mean-both \
 --annotate-means --annotate-pos inline --mean-digits 6 --annotate-xoffset 0.25 \
 --stats-csv "$suprpath/graphs/vertex_lh_v94264.csv" \
 --csv-sep ";" --decimal "," \
 --outdir  "$suprpath/graphs"

# plottiamo i dati di una label
python $suprpath/scripts/label_to_csv_groups.py \
 --label   $suprpath/lh.langdom-RHDOMminusLHDOM_handagesex-adjusted_noRhand_sm15_doss/langdom-
RHDOMminusLHDOM_handagesex-adjusted_doss_noRhand/lh.cluster_perm5000_cft1_pos_cwp0999_sm15-
0001.label \
 --mgh   $suprpath/lh.r_flair_ax_wm-norm-median_noRhand.sm15.mgh \
 --fsgd  $suprpath/noRhand.fsgd \
 --out   $suprpath/graphs/lh.cluster_perm5000_cft1_pos_cwp0999_sm15-0001_roi_values.csv \
 --stats-out $suprpath/graphs/lh.cluster_perm5000_cft1_pos_cwp0999_sm15-0001_roi_stats.csv \
 --class-a rh_dom --class-b lh_dom

python $suprpath/scripts/label_to_csv_groups.py \
 --label   $suprpath/lh.langdom-RHDOMminusLHDOM_handagesex-adjusted_noRhand_sm15_doss/langdom-
RHDOMminusLHDOM_handagesex-adjusted_doss_noRhand/lh.cluster_perm5000_cft1_pos_cwp0999_sm15-
0006.label \
 --mgh   $suprpath/lh.$flairmeasure.sm15.mgh \
 --fsgd  $suprpath/langdom_handagesex.fsgd \
 --out   $suprpath/graphs/lh.cluster_perm5000_cft1_pos_cwp0999_sm15-0006_roi_values.csv \
 --stats-out $suprpath/graphs/lh.cluster_perm5000_cft1_pos_cwp0999_sm15-0006_roi_stats.csv \
 --class-a rh_dom --class-b lh_dom

#####################################
4) ANALISI SUPRFLAIR STATICA CONTRASTANDO L VS R, AGGIUSTANDO per age, sex e thickness_PVR, dopo aver
eliminato i mancini RH_DOM
#####################################

# Prepariamo i file mgh con gli scalari della thickness a differenti livelli di smoothing:

hemis=(lh rh)
smooth=(5 15 25)
for h in $hemis; do
 for sm in $smooth; do
mris_preproc \
 --fsgd $suprpath/handedness_agesex_noRHDOM_Lhand.fsgd \
 --cache-in thickness.fwhm$sm.fsaverage \
 --target fsaverage \
 --hemi $h \
 --out $suprpath/$h.thickness_noRHDOM_Lhand.sm${sm}.mgh
 done
done

# Prepariamo i file mgh con gli scalari della suprflair smoothando a diversi livelli in parallelo:
hemis=(lh rh)
for h in $hemis; do
 mris_preproc \
  --fsgd "$suprpath/handedness_agesex_noRHDOM_Lhand.fsgd" \
  --meas "${flairmeasure}.mgh" \
  --target fsaverage \
  --hemi "$h" \
  --out  "$suprpath/${h}.${flairmeasure}_noRHDOM_Lhand.mgh"
done

hemis=(lh rh)
smooth=(5 15 25)
for h in $hemis; do
 for sm in $smooth; do
  mri_surf2surf \
   --s fsaverage \
   --hemi "$h" \
   --fwhm "$sm" \
   --sval "$suprpath/${h}.${flairmeasure}_noRHDOM_Lhand.mgh" \
   --tval "$suprpath/${h}.${flairmeasure}_noRHDOM_Lhand.sm${sm}.mgh" &
 done
done
wait

# Analizziamo la differenza media di FLAIR corticale tra i due gruppi di dominanza manuale (L, R), aggiustando
per età e sesso (0=F, 1=M), nonché per thickness a livello di vertice (PVR= Per Vertex Regressor)

hemis=(lh rh)
smooth=(5 15 25)
for h in $hemis; do
 for sm in $smooth; do
mri_glmfit \
 --glmdir $suprpath/$h.handedness-LminusR_agesex-adjusted_noRHDOM_Lhand_sm${sm}_doss \
 --y $suprpath/$h.${flairmeasure}_noRHDOM_Lhand.sm${sm}.mgh \
 --fsgd $suprpath/handedness_agesex_noRHDOM_Lhand.fsgd doss \
 --pvr $suprpath/$h.thickness_noRHDOM_Lhand.sm${sm}.mgh \
 --C $suprpath/handedness-LminusR_agesex-adjusted_doss_noRHDOM_Lhand.mtx \
 --surf fsaverage $h \
 --cortex \
 --eres-save
 done
done

# Copiamo tutti i file sig.mgh in 0_sig con nomi esplicativi
hemis=(lh rh)
smooth=(5 15 25)
for h in $hemis; do
 for sm in $smooth; do
cp        $suprpath/$h.handedness-LminusR_agesex-adjusted_noRHDOM_Lhand_sm${sm}_doss/handedness-
LminusR_agesex-adjusted_doss_noRHDOM_Lhand/sig.mgh                $suprpath/0_sig/$h.handedness-
LminusR_agesex-adjusted_noRHDOM_Lhand_sm${sm}_doss_sig.mgh
 done
done

# Guardiamo i risultati con freeview
freeview \
-colorscale -orthographic -viewport 3d -view left -hide-3d-slices -hide-3d-frames -nocursor -viewsize 500 500 \
-v /Applications/freesurfer/subjects/fsaverage/mri/brain.mgz:visible=0 \
-f /Applications/freesurfer/subjects/fsaverage/surf/lh.white\
:visible=0\
:curvature_method=binary\
:annot=/Applications/freesurfer/subjects/fsaverage/label/lh.aparc.a2005s.annot:annot_outline=1\
:annot=/Applications/freesurfer/subjects/fsaverage/label/lh.aparc.a2009s.annot:annot_outline=1\
:annot=/Applications/freesurfer/subjects/fsaverage/label/lh.PALS_B12_Brodmann.annot:annot_outline=0\
:annot=/Applications/freesurfer/subjects/fsaverage/label/lh.PALS_B12_Visuotopic.annot:annot_outline=0\
:annot=/Applications/freesurfer/subjects/fsaverage/label/lh.Yeo2011_7Networks_N1000.annot:annot_outlin
e=0\
:annot=/Applications/freesurfer/subjects/fsaverage/label/lh.Yeo2011_17Networks_N1000.annot:annot_outli
ne=0\
:overlay=$suprpath/0_sig/lh.handedness-LminusR_agesex-
adjusted_noRHDOM_Lhand_sm5_doss_sig.mgh:overlay_threshold=0,1.3:overlay_mask=/Applications/freesur
fer/subjects/fsaverage/label/lh.cortex.label\
:overlay=$suprpath/0_sig/lh.handedness-LminusR_agesex-
adjusted_noRHDOM_Lhand_sm15_doss_sig.mgh:overlay_threshold=0,1.3:overlay_mask=/Applications/frees
urfer/subjects/fsaverage/label/lh.cortex.label\
:overlay=$suprpath/0_sig/lh.handedness-LminusR_agesex-
adjusted_noRHDOM_Lhand_sm25_doss_sig.mgh:overlay_threshold=0,1.3:overlay_mask=/Applications/frees
urfer/subjects/fsaverage/label/lh.cortex.label \
-f /Applications/freesurfer/subjects/fsaverage/surf/lh.pial_semi_inflated\
:visible=0\
:curvature_method=binary\
:annot=/Applications/freesurfer/subjects/fsaverage/label/lh.aparc.a2005s.annot:annot_outline=1\
:annot=/Applications/freesurfer/subjects/fsaverage/label/lh.aparc.a2009s.annot:annot_outline=1\
:annot=/Applications/freesurfer/subjects/fsaverage/label/lh.PALS_B12_Brodmann.annot:annot_outline=0\
:annot=/Applications/freesurfer/subjects/fsaverage/label/lh.PALS_B12_Visuotopic.annot:annot_outline=0\
:annot=/Applications/freesurfer/subjects/fsaverage/label/lh.Yeo2011_7Networks_N1000.annot:annot_outlin
e=0\
:annot=/Applications/freesurfer/subjects/fsaverage/label/lh.Yeo2011_17Networks_N1000.annot:annot_outli
ne=0\
:overlay=$suprpath/0_sig/lh.handedness-LminusR_agesex-
adjusted_noRHDOM_Lhand_sm5_doss_sig.mgh:overlay_threshold=0,1.3:overlay_mask=/Applications/freesur
fer/subjects/fsaverage/label/lh.cortex.label\
:overlay=$suprpath/0_sig/lh.handedness-LminusR_agesex-
adjusted_noRHDOM_Lhand_sm15_doss_sig.mgh:overlay_threshold=0,1.3:overlay_mask=/Applications/frees
urfer/subjects/fsaverage/label/lh.cortex.label\
:overlay=$suprpath/0_sig/lh.handedness-LminusR_agesex-
adjusted_noRHDOM_Lhand_sm25_doss_sig.mgh:overlay_threshold=0,1.3:overlay_mask=/Applications/frees
urfer/subjects/fsaverage/label/lh.cortex.label \
-f /Applications/freesurfer/subjects/fsaverage/surf/lh.inflated\
:visible=1\
:curvature_method=binary\
:annot=/Applications/freesurfer/subjects/fsaverage/label/lh.aparc.a2005s.annot:annot_outline=1\
:annot=/Applications/freesurfer/subjects/fsaverage/label/lh.aparc.a2009s.annot:annot_outline=1\
:annot=/Applications/freesurfer/subjects/fsaverage/label/lh.PALS_B12_Brodmann.annot:annot_outline=0\
:annot=/Applications/freesurfer/subjects/fsaverage/label/lh.PALS_B12_Visuotopic.annot:annot_outline=0\
:annot=/Applications/freesurfer/subjects/fsaverage/label/lh.Yeo2011_7Networks_N1000.annot:annot_outlin
e=0\
:annot=/Applications/freesurfer/subjects/fsaverage/label/lh.Yeo2011_17Networks_N1000.annot:annot_outli
ne=0\
:overlay=$suprpath/0_sig/lh.handedness-LminusR_agesex-
adjusted_noRHDOM_Lhand_sm5_doss_sig.mgh:overlay_threshold=0,1.3:overlay_mask=/Applications/freesur
fer/subjects/fsaverage/label/lh.cortex.label\
:overlay=$suprpath/0_sig/lh.handedness-LminusR_agesex-
adjusted_noRHDOM_Lhand_sm15_doss_sig.mgh:overlay_threshold=0,1.3:overlay_mask=/Applications/frees
urfer/subjects/fsaverage/label/lh.cortex.label\
:overlay=$suprpath/0_sig/lh.handedness-LminusR_agesex-
adjusted_noRHDOM_Lhand_sm25_doss_sig.mgh:overlay_threshold=0,1.3:overlay_mask=/Applications/frees
urfer/subjects/fsaverage/label/lh.cortex.label &

freeview \
-colorscale -orthographic -viewport 3d -view right -hide-3d-slices -hide-3d-frames -nocursor -viewsize 500 500
\
-v /Applications/freesurfer/subjects/fsaverage/mri/brain.mgz:visible=0 \
```

```
-f /Applications/freesurfer/subjects/fsaverage/surf/rh.white\
:visible=0\
:curvature_method=binary\
:annot=/Applications/freesurfer/subjects/fsaverage/label/rh.aparc.a2005s.annot:annot_outline=1\
:annot=/Applications/freesurfer/subjects/fsaverage/label/rh.aparc.a2009s.annot:annot_outline=1\
:annot=/Applications/freesurfer/subjects/fsaverage/label/rh.PALS_B12_Brodmann.annot:annot_outline=0\
:annot=/Applications/freesurfer/subjects/fsaverage/label/rh.PALS_B12_Visuotopic.annot:annot_outline=0\
:annot=/Applications/freesurfer/subjects/fsaverage/label/rh.Yeo2011_7Networks_N1000.annot:annot_outlin
e=0\
:annot=/Applications/freesurfer/subjects/fsaverage/label/rh.Yeo2011_17Networks_N1000.annot:annot_outli
ne=0\
:overlay=$suprpath/0_sig/rh.handedness-LminusR_agesex-
adjusted_noRHDOM_Lhand_sm5_doss_sig.mgh:overlay_threshold=0,1.3:overlay_mask=/Applications/freesur
fer/subjects/fsaverage/label/rh.cortex.label\
:overlay=$suprpath/0_sig/rh.handedness-LminusR_agesex-
adjusted_noRHDOM_Lhand_sm15_doss_sig.mgh:overlay_threshold=0,1.3:overlay_mask=/Applications/frees
urfer/subjects/fsaverage/label/rh.cortex.label\
:overlay=$suprpath/0_sig/rh.handedness-LminusR_agesex-
adjusted_noRHDOM_Lhand_sm25_doss_sig.mgh:overlay_threshold=0,1.3:overlay_mask=/Applications/frees
urfer/subjects/fsaverage/label/rh.cortex.label \
-f /Applications/freesurfer/subjects/fsaverage/surf/rh.pial_semi_inflated\
:visible=0\
:curvature_method=binary\
:annot=/Applications/freesurfer/subjects/fsaverage/label/rh.aparc.a2005s.annot:annot_outline=1\
:annot=/Applications/freesurfer/subjects/fsaverage/label/rh.aparc.a2009s.annot:annot_outline=1\
:annot=/Applications/freesurfer/subjects/fsaverage/label/rh.PALS_B12_Brodmann.annot:annot_outline=0\
:annot=/Applications/freesurfer/subjects/fsaverage/label/rh.PALS_B12_Visuotopic.annot:annot_outline=0\
:annot=/Applications/freesurfer/subjects/fsaverage/label/rh.Yeo2011_7Networks_N1000.annot:annot_outlin
e=0\
:annot=/Applications/freesurfer/subjects/fsaverage/label/rh.Yeo2011_17Networks_N1000.annot:annot_outli
ne=0\
:overlay=$suprpath/0_sig/rh.handedness-LminusR_agesex-
adjusted_noRHDOM_Lhand_sm5_doss_sig.mgh:overlay_threshold=0,1.3:overlay_mask=/Applications/freesur
fer/subjects/fsaverage/label/rh.cortex.label\
:overlay=$suprpath/0_sig/rh.handedness-LminusR_agesex-
adjusted_noRHDOM_Lhand_sm15_doss_sig.mgh:overlay_threshold=0,1.3:overlay_mask=/Applications/frees
urfer/subjects/fsaverage/label/rh.cortex.label\
:overlay=$suprpath/0_sig/rh.handedness-LminusR_agesex-
adjusted_noRHDOM_Lhand_sm25_doss_sig.mgh:overlay_threshold=0,1.3:overlay_mask=/Applications/frees
urfer/subjects/fsaverage/label/rh.cortex.label \
-f /Applications/freesurfer/subjects/fsaverage/surf/rh.inflated\
:visible=1\
:curvature_method=binary\
:annot=/Applications/freesurfer/subjects/fsaverage/label/rh.aparc.a2005s.annot:annot_outline=1\
:annot=/Applications/freesurfer/subjects/fsaverage/label/rh.aparc.a2009s.annot:annot_outline=1\
:annot=/Applications/freesurfer/subjects/fsaverage/label/rh.PALS_B12_Brodmann.annot:annot_outline=0\
:annot=/Applications/freesurfer/subjects/fsaverage/label/rh.PALS_B12_Visuotopic.annot:annot_outline=0\
:annot=/Applications/freesurfer/subjects/fsaverage/label/rh.Yeo2011_7Networks_N1000.annot:annot_outlin
e=0\
:annot=/Applications/freesurfer/subjects/fsaverage/label/rh.Yeo2011_17Networks_N1000.annot:annot_outli
ne=0\
:overlay=$suprpath/0_sig/rh.handedness-LminusR_agesex-
adjusted_noRHDOM_Lhand_sm5_doss_sig.mgh:overlay_threshold=0,1.3:overlay_mask=/Applications/freesur
fer/subjects/fsaverage/label/rh.cortex.label\
:overlay=$suprpath/0_sig/rh.handedness-LminusR_agesex-
adjusted_noRHDOM_Lhand_sm15_doss_sig.mgh:overlay_threshold=0,1.3:overlay_mask=/Applications/frees
urfer/subjects/fsaverage/label/rh.cortex.label\
:overlay=$suprpath/0_sig/rh.handedness-LminusR_agesex-
adjusted_noRHDOM_Lhand_sm25_doss_sig.mgh:overlay_threshold=0,1.3:overlay_mask=/Applications/frees
urfer/subjects/fsaverage/label/rh.cortex.label

# Facciamo la cluster-wise analysis
hemis=(lh rh)
smooth=(5 15 25)
signes=(pos neg)
for h in $hemis; do
 for sm in $smooth; do
  for sign in $signes; do
   mri_glmfit-sim \
    --glmdir $suprpath/$h.handedness-LminusR_agesex-adjusted_noRHDOM_Lhand_sm${sm}_doss \
    --perm 5000 1 $sign \
    --cwp 0.999 \
    --2spaces \
    --bg 8 \
    --overwrite
  done
 done
done

hemis=(lh rh)
smooth=(5 15 25)
signes=(pos neg)
surfaces=(white pial inflated)
for h in $hemis; do
 for sm in $smooth; do
  for sign in $signes; do
   mri_surfcluster \
    --in                    $suprpath/$h.handedness-LminusR_agesex-
adjusted_noRHDOM_Lhand_sm${sm}_doss/handedness-LminusR_agesex-
adjusted_doss_noRHDOM_Lhand/sig.mgh \
    --csd                   $suprpath/$h.handedness-LminusR_agesex-
adjusted_noRHDOM_Lhand_sm${sm}_doss/csd/all.perm.th10.${sign}-handedness-LminusR_agesex-
adjusted_doss_noRHDOM_Lhand.csd \
    --subject fsaverage \
    --hemi $h \
    --surf white \
    --thmin 1 \
    --sign $sign \
    --annot aparc.a2005s \
    --olab                  $suprpath/$h.handedness-LminusR_agesex-
adjusted_noRHDOM_Lhand_sm${sm}_doss/handedness-LminusR_agesex-
adjusted_doss_noRHDOM_Lhand/$h.cluster_perm5000_cft1_${sign}_cwp0999_sm${sm} \
    --sum                   $suprpath/$h.handedness-LminusR_agesex-
adjusted_noRHDOM_Lhand_sm${sm}_doss/handedness-LminusR_agesex-
adjusted_doss_noRHDOM_Lhand/$h.cluster_perm5000_cft1_${sign}_cwp0999_sm${sm}_summary.txt
  done
 done
done

for h in $hemis; do
 for sm in $smooth; do
  for sign in $signes; do
   python3 $suprpath/scripts/make_wpts_from_clusters_space.py \
    --summary               "$suprpath/$h.handedness-LminusR_agesex-
adjusted_noRHDOM_Lhand_sm${sm}_doss/handedness-LminusR_agesex-
adjusted_doss_noRHDOM_Lhand/$h.cluster_perm5000_cft1_${sign}_cwp0999_sm${sm}_summary.txt" \
    --hemi $h --subject fsaverage --surf white \
    --subjects-dir "$SUBJECTS_DIR" \
    --space scanner \
    --out-wpts              "$suprpath/$h.handedness-LminusR_agesex-
adjusted_noRHDOM_Lhand_sm${sm}_doss/handedness-LminusR_agesex-
adjusted_doss_noRHDOM_Lhand/$h.cluster_perm5000_cft1_${sign}_cwp0999_sm${sm}_summary.wpts"
  done
 done
done
```

Commands used for analyses of Experiment B (and Experiment C, very similar) data

```
suprpath=~/Desktop/suprflair_FT_Cico_Lauretta_Silvia
flairseries=flair_ax
flairmeasure=r_${flairseries}_wm-norm-median

# Prepariamo i file mgh con gli scalari della thickness a differenti livelli di smoothing:
hemis=(lh rh)
smooth=(5 15 25)
for h in $hemis; do
 for sm in $smooth; do
mris_preproc \
 --fsgd $suprpath/pairs.fsgd \
 --cache-in thickness.fwhm$sm.fsaverage \
 --target fsaverage \
 --hemi $h \
 --out $suprpath/$h.thickness.sm${sm}.mgh
 done
done

# Prepariamo i file mgh con gli scalari della suprflair smoothando a diversi livelli in parallelo:
hemis=(lh rh)
for h in $hemis; do
 mris_preproc \
  --fsgd "$suprpath/pairs.fsgd" \
  --meas "${flairmeasure}.mgh" \
  --target fsaverage \
  --hemi "$h" \
  --out  "$suprpath/${h}.${flairmeasure}.mgh"
done

hemis=(lh rh)
smooth=(5 15 25)

for h in $hemis; do
 for sm in $smooth; do
  mri_surf2surf \
   --s fsaverage \
   --hemi "$h" \
   --fwhm "$sm" \
   --sval "$suprpath/${h}.${flairmeasure}.mgh" \
   --tval "$suprpath/${h}.${flairmeasure}.sm${sm}.mgh" &
 done
done
wait

# Per preparare i file mgh con le differenze degli scalari (?h.paired-diff.flair_ax.mgh):
hemis=(lh rh)
for h in $hemis; do
 mris_preproc \
  --fsgd "$suprpath/pairs.fsgd" \
  --meas "${flairmeasure}.mgh" \
  --target fsaverage \
  --hemi "$h" \
  --paired-diff \
  --out "$suprpath/${h}.paired-diff.${flairmeasure}.mgh"
done

hemis=(lh rh)
smooth=(5 15 25)
for h in $hemis; do
 for sm in $smooth; do
  mri_surf2surf \
   --s fsaverage \
   --hemi "$h" \
   --fwhm "$sm" \
   --sval "$suprpath/${h}.paired-diff.${flairmeasure}.mgh" \
   --tval "$suprpath/${h}.paired-diff.${flairmeasure}.sm${sm}.mgh" &
 done
done
wait

# Facciamo l'analisi (aggiustando per apertura occhi)
hemis=(lh rh)
smooth=(5 15 25)
for h in $hemis; do
 for sm in $smooth; do
mri_glmfit \
 --glmdir $suprpath/$h.glm-paired-diff_eyescov_sm${sm}_doss \
 --y $suprpath/$h.paired-diff.$flairmeasure.sm${sm}.mgh \
 --fsgd $suprpath/paired-diff_eyescov.fsgd doss \
 --C $suprpath/all_mean_eyescov.mtx \
 --surf fsaverage $h \
 --cortex \
 --eres-save
 done
```

```
done

# Facciamo l'analisi anche senza aggiustare, per poi plottare

# Copiamo tutti i file sig.mgh in 0_sig con nomi esplicativi
hemis=(lh rh)
smooth=(5 15 25)
for h in $hemis; do
  for sm in $smooth; do
cp $suprpath/$h.glm-paired-diff_eyescov_sm${sm}_doss/all_mean_eyescov/sig.mgh \
$suprpath/0_sig/$h.Task-Rest-mean_eyescov_sm${sm}_doss_sig.mgh
  done
done

# guardiamo con Freeview:
freeview \
-colorscale -orthographic -viewport 3d -view left -hide-3d-slices -hide-3d-frames -nocursor -viewsize 500 500 \
-v /Applications/freesurfer/subjects/fsaverage/mri/brain.mgz:visible=0 \
-f /Applications/freesurfer/subjects/fsaverage/surf/lh.white\
:visible=0\
:curvature_method=binary\
:annot=/Applications/freesurfer/subjects/fsaverage/label/lh.aparc.a2005s.annot:annot_outline=1\
:annot=/Applications/freesurfer/subjects/fsaverage/label/lh.aparc.a2009s.annot:annot_outline=1\
:annot=/Applications/freesurfer/subjects/fsaverage/label/lh.PALS_B12_Brodmann.annot:annot_outline=0\
:annot=/Applications/freesurfer/subjects/fsaverage/label/lh.PALS_B12_Visuotopic.annot:annot_outline=0\
:annot=/Applications/freesurfer/subjects/fsaverage/label/lh.Yeo2011_7Networks_N1000.annot:annot_outlin
e=0\
:annot=/Applications/freesurfer/subjects/fsaverage/label/lh.Yeo2011_17Networks_N1000.annot:annot_outli
ne=0\
:overlay=$suprpath/0_sig/lh.Task-Rest-
mean_eyescov_sm5_doss_sig.mgh:overlay_threshold=0,1.3:overlay_mask=/Applications/freesurfer/subjects/
fsaverage/label/lh.cortex.label\
:overlay=$suprpath/0_sig/lh.Task-Rest-
mean_eyescov_sm15_doss_sig.mgh:overlay_threshold=0,1.3:overlay_mask=/Applications/freesurfer/subjects
/fsaverage/label/lh.cortex.label\
:overlay=$suprpath/0_sig/lh.Task-Rest-
mean_eyescov_sm25_doss_sig.mgh:overlay_threshold=0,1.3:overlay_mask=/Applications/freesurfer/subjects
/fsaverage/label/lh.cortex.label \
-f /Applications/freesurfer/subjects/fsaverage/surf/lh.pial_semi_inflated\
:visible=0\
:curvature_method=binary\
:annot=/Applications/freesurfer/subjects/fsaverage/label/lh.aparc.a2005s.annot:annot_outline=1\
:annot=/Applications/freesurfer/subjects/fsaverage/label/lh.aparc.a2009s.annot:annot_outline=1\
:annot=/Applications/freesurfer/subjects/fsaverage/label/lh.PALS_B12_Brodmann.annot:annot_outline=0\
:annot=/Applications/freesurfer/subjects/fsaverage/label/lh.PALS_B12_Visuotopic.annot:annot_outline=0\
:annot=/Applications/freesurfer/subjects/fsaverage/label/lh.Yeo2011_7Networks_N1000.annot:annot_outlin
e=0\
:annot=/Applications/freesurfer/subjects/fsaverage/label/lh.Yeo2011_17Networks_N1000.annot:annot_outli
ne=0\
:overlay=$suprpath/0_sig/lh.Task-Rest-
mean_eyescov_sm5_doss_sig.mgh:overlay_threshold=0,1.3:overlay_mask=/Applications/freesurfer/subjects/
fsaverage/label/lh.cortex.label\
:overlay=$suprpath/0_sig/lh.Task-Rest-
mean_eyescov_sm15_doss_sig.mgh:overlay_threshold=0,1.3:overlay_mask=/Applications/freesurfer/subjects
/fsaverage/label/lh.cortex.label\
:overlay=$suprpath/0_sig/lh.Task-Rest-
mean_eyescov_sm25_doss_sig.mgh:overlay_threshold=0,1.3:overlay_mask=/Applications/freesurfer/subjects
/fsaverage/label/lh.cortex.label \
-f /Applications/freesurfer/subjects/fsaverage/surf/lh.inflated\
:visible=1\
:curvature_method=binary\
:annot=/Applications/freesurfer/subjects/fsaverage/label/lh.aparc.a2005s.annot:annot_outline=1\
:annot=/Applications/freesurfer/subjects/fsaverage/label/lh.aparc.a2009s.annot:annot_outline=1\
:annot=/Applications/freesurfer/subjects/fsaverage/label/lh.PALS_B12_Brodmann.annot:annot_outline=0\
:annot=/Applications/freesurfer/subjects/fsaverage/label/lh.PALS_B12_Visuotopic.annot:annot_outline=0\
:annot=/Applications/freesurfer/subjects/fsaverage/label/lh.Yeo2011_7Networks_N1000.annot:annot_outlin
e=0\
:annot=/Applications/freesurfer/subjects/fsaverage/label/lh.Yeo2011_17Networks_N1000.annot:annot_outli
ne=0\
:overlay=$suprpath/0_sig/lh.Task-Rest-
mean_eyescov_sm5_doss_sig.mgh:overlay_threshold=0,1.3:overlay_mask=/Applications/freesurfer/subjects/
fsaverage/label/lh.cortex.label\
:overlay=$suprpath/0_sig/lh.Task-Rest-
mean_eyescov_sm15_doss_sig.mgh:overlay_threshold=0,1.3:overlay_mask=/Applications/freesurfer/subjects
/fsaverage/label/lh.cortex.label\
:overlay=$suprpath/0_sig/lh.Task-Rest-
mean_eyescov_sm25_doss_sig.mgh:overlay_threshold=0,1.3:overlay_mask=/Applications/freesurfer/subjects
/fsaverage/label/lh.cortex.label &


freeview \
-colorscale -orthographic -viewport 3d -view right -hide-3d-slices -hide-3d-frames -nocursor -viewsize 500 500
\
-v /Applications/freesurfer/subjects/fsaverage/mri/brain.mgz:visible=0 \
-f /Applications/freesurfer/subjects/fsaverage/surf/rh.white\
:visible=0\
:curvature_method=binary\
:annot=/Applications/freesurfer/subjects/fsaverage/label/rh.aparc.a2005s.annot:annot_outline=1\
:annot=/Applications/freesurfer/subjects/fsaverage/label/rh.aparc.a2009s.annot:annot_outline=1\
:annot=/Applications/freesurfer/subjects/fsaverage/label/rh.PALS_B12_Brodmann.annot:annot_outline=0\
:annot=/Applications/freesurfer/subjects/fsaverage/label/rh.PALS_B12_Visuotopic.annot:annot_outline=0\
:annot=/Applications/freesurfer/subjects/fsaverage/label/rh.Yeo2011_7Networks_N1000.annot:annot_outlin
e=0\
:annot=/Applications/freesurfer/subjects/fsaverage/label/rh.Yeo2011_17Networks_N1000.annot:annot_outli
ne=0\
:overlay=$suprpath/0_sig/rh.Task-Rest-
mean_eyescov_sm5_doss_sig.mgh:overlay_threshold=0,1.3:overlay_mask=/Applications/freesurfer/subjects/
fsaverage/label/rh.cortex.label\
:overlay=$suprpath/0_sig/rh.Task-Rest-
mean_eyescov_sm15_doss_sig.mgh:overlay_threshold=0,1.3:overlay_mask=/Applications/freesurfer/subjects
/fsaverage/label/rh.cortex.label\
:overlay=$suprpath/0_sig/rh.Task-Rest-
mean_eyescov_sm25_doss_sig.mgh:overlay_threshold=0,1.3:overlay_mask=/Applications/freesurfer/subjects
/fsaverage/label/rh.cortex.label \
-f /Applications/freesurfer/subjects/fsaverage/surf/rh.pial_semi_inflated\
:visible=0\
:curvature_method=binary\
:annot=/Applications/freesurfer/subjects/fsaverage/label/rh.aparc.a2005s.annot:annot_outline=1\
:annot=/Applications/freesurfer/subjects/fsaverage/label/rh.aparc.a2009s.annot:annot_outline=1\
:annot=/Applications/freesurfer/subjects/fsaverage/label/rh.PALS_B12_Brodmann.annot:annot_outline=0\
:annot=/Applications/freesurfer/subjects/fsaverage/label/rh.PALS_B12_Visuotopic.annot:annot_outline=0\
:annot=/Applications/freesurfer/subjects/fsaverage/label/rh.Yeo2011_7Networks_N1000.annot:annot_outlin
e=0\
:annot=/Applications/freesurfer/subjects/fsaverage/label/rh.Yeo2011_17Networks_N1000.annot:annot_outli
ne=0\
:overlay=$suprpath/0_sig/rh.Task-Rest-
mean_eyescov_sm5_doss_sig.mgh:overlay_threshold=0,1.3:overlay_mask=/Applications/freesurfer/subjects/
fsaverage/label/rh.cortex.label\
:overlay=$suprpath/0_sig/rh.Task-Rest-
mean_eyescov_sm15_doss_sig.mgh:overlay_threshold=0,1.3:overlay_mask=/Applications/freesurfer/subjects
/fsaverage/label/rh.cortex.label\
:overlay=$suprpath/0_sig/rh.Task-Rest-
mean_eyescov_sm25_doss_sig.mgh:overlay_threshold=0,1.3:overlay_mask=/Applications/freesurfer/subjects
/fsaverage/label/rh.cortex.label

# Facciamo la cluster-wise analysis
hemis=(lh rh)
smooth=(5 15 25)
signes=(pos neg)
for h in $hemis; do
  for sm in $smooth; do
    for sign in $signes; do
    mri_glmfit-sim \
      --glmdir $suprpath/$h.glm-paired-diff_eyescov_sm${sm}_doss \
      --perm 5000 1 $sign \
      --cwp 0.999 \
      --2spaces \
      --bg 8 \
      --overwrite
    done
  done
done

hemis=(lh rh)
smooth=(5 15 25)
signes=(pos neg)
surfaces=(white pial inflated)
for h in $hemis; do
  for sm in $smooth; do
    for sign in $signes; do
      mri_surfcluster \
        --in $suprpath/$h.glm-paired-diff_eyescov_sm${sm}_doss/all_mean_eyescov/sig.mgh \
        --csd                $suprpath/$h.glm-paired-diff_eyescov_sm${sm}_doss/csd/all.perm.th10.${sign}-
all_mean_eyescov.csd \
        --subject fsaverage \
        --hemi $h \
        --surf white \
        --thmin 1 \
        --sign $sign \
        --annot aparc.a2005s \
        --olab                                                                    $suprpath/$h.glm-paired-
diff_eyescov_sm${sm}_doss/all_mean_eyescov/$h.cluster_perm5000_cft1_${sign}_cwp0999_sm${sm} \
        --sum                                                                     $suprpath/$h.glm-paired-
diff_eyescov_sm${sm}_doss/all_mean_eyescov/$h.cluster_perm5000_cft1_${sign}_cwp0999_sm${sm}_sum
mary.txt
    done
  done
done

for h in $hemis; do
  for sm in $smooth; do
    for sign in $signes; do
      python3 $suprpath/scripts/make_wpts_from_clusters_space.py \
        --summary                                                                 "$suprpath/$h.glm-paired-
diff_eyescov_sm${sm}_doss/all_mean_eyescov/$h.cluster_perm5000_cft1_${sign}_cwp0999_sm${sm}_sum
mary.txt" \
        --hemi $h --subject fsaverage --surf white \
        --subjects-dir "$SUBJECTS_DIR" \
        --space scanner \
        --out-wpts                                                                "$suprpath/$h.glm-paired-
diff_eyescov_sm${sm}_doss/all_mean_eyescov/$h.cluster_perm5000_cft1_${sign}_cwp0999_sm${sm}_sum
mary.wpts"
    done
  done
done

# plottiamo
python $suprpath/scripts/label_to_csv_rest_task.py \
  --label                                                                         $suprpath/lh.glm-paired-
diff_eyescov_sm15_doss/all_mean_eyescov/lh.cluster_perm5000_cft1_pos_cwp0999_sm15-0002.label \
  --mgh   $suprpath/lh.r_flair_ax_wm-norm-median.sm15.mgh \
  --fsgd  $suprpath/pairs.fsgd \
  --out   $suprpath/graphs/lh.cluster_perm5000_cft1_pos_cwp0999_sm15-0002_roi_values_rest_task.csv \
  --stats-out $suprpath/graphs/lh.cluster_perm5000_cft1_pos_cwp0999_sm15-0002_roi_stats_rest_task.csv

# Per plottare i dati a livello di un dato vertice
python $suprpath/scripts/plot_vertex_boxplot.py \
  --overlay "$suprpath/lh.r_flair_ax_wm-norm-median.sm15.mgh" \
  --fsgd "$suprpath/pairs.fsgd" \
  --vertices 76400 \
  --prefix  "box" \
  --title-base "SUPRFLAIR vertex plot" \
  --xlabel "condition" \
  --ylabel "normalized value" \
  --x-order "Rest,Task" \
  --show-points --meanline --mean-both \
  --annotate-means --annotate-pos inline --mean-digits 6 --annotate-xoffset 0.25 \
```

```
 --stats --stats-csv "$suprpath/graphs/stats_lh_v76400.csv" \
 --csv-sep ";" \
 --decimal "," \
 --outdir  "$suprpath/graphs"

# per plottare i dati di un vertice a coppie con linee
python $suprpath/scripts/plot_lines.py \
 --overlay $suprpath/lh.r_flair_ax_wm-norm-median.sm15.mgh \
 --fsgd $suprpath/pairs.fsgd \
 --check-vertex 76400 \
 --check-out $suprpath/graphs/report_pairs_v76400.csv \
 --vertices 76400 \
 --title-base "SUPRFLAIR vertex pairs" \
 --xlabel "condition" \
 --ylabel "normalized value" \
 --x-order "Rest,Task" \
 --pair-by auto \
 --check-pairs \
 --csv-sep ";" \
 --csv-dec ","
```

Commands used for analyses of Experiment D data

```
suprpath=~/Desktop/suprflair_EYES
flairseries=flair_ax
flairmeasure=r_${flairseries}_wm-norm-median

# Prepariamo i file mgh con gli scalari della thickness a differenti livelli di smoothing:
hemis=(lh rh)
smooth=(5 15 25)
for h in $hemis; do
 for sm in $smooth; do
mris_preproc \
 --fsgd $suprpath/handedness.fsgd \
 --cache-in thickness.fwhm$sm.fsaverage \
 --target fsaverage \
 --hemi $h \
 --out $suprpath/$h.thickness.sm${sm}.mgh
 done
done

# Prepariamo i file mgh con gli scalari della suprflair smoothando a diversi livelli in parallelo:
hemis=(lh rh)
for h in $hemis; do
 mris_preproc \
  --fsgd "$suprpath/pairs.fsgd" \
  --meas "${flairmeasure}.mgh" \
  --target fsaverage \
  --hemi "$h" \
  --out  "$suprpath/${h}.${flairmeasure}.mgh"
done

hemis=(lh rh)
smooth=(5 15 25)
for h in $hemis; do
 for sm in $smooth; do
  mri_surf2surf \
   --s fsaverage \
   --hemi "$h" \
   --fwhm "$sm" \
   --sval "$suprpath/${h}.${flairmeasure}.mgh" \
   --tval "$suprpath/${h}.${flairmeasure}.sm${sm}.mgh" &
 done
done
wait

# Prepariamo i file mgh con le differenze degli scalari (?h.paired-diff.${flairseries}.mgh):
hemis=(lh rh)
for h in $hemis; do
 mris_preproc \
  --fsgd "$suprpath/pairs.fsgd" \
  --meas "${flairmeasure}.mgh" \
  --target fsaverage \
  --hemi "$h" \
  --paired-diff \
  --out "$suprpath/${h}.paired-diff.${flairmeasure}.mgh"
done

hemis=(lh rh)
smooth=(5 15 25)
for h in $hemis; do
 for sm in $smooth; do
  mri_surf2surf \
   --s fsaverage \
   --hemi "$h" \
   --fwhm "$sm" \
   --sval "$suprpath/${h}.paired-diff.${flairmeasure}.mgh" \
   --tval "$suprpath/${h}.paired-diff.${flairmeasure}.sm${sm}.mgh" &
 done
done
wait

# facciamo l'analisi multivariata:
hemis=(lh rh)
smooth=(5 15 25)
for h in $hemis; do
 for sm in $smooth; do
mri_glmfit \
 --glmdir $suprpath/$h.glm-paired-diff_handagesexcov_thicknesspvr_sm${sm}_doss \
 --y $suprpath/$h.paired-diff.$flairmeasure.sm${sm}.mgh \
 --fsgd $suprpath/paired-diff_handagesexcov.fsgd doss \
 --pvr $suprpath/$h.thickness.sm${sm}.mgh \
 --C $suprpath/taskrestmean_handagesexcov.mtx \
 --surf fsaverage $h \
 --cortex \
 --eres-save
 done
done

# Copiamo tutti i file sig.mgh in 0_sig con nomi esplicativi
hemis=(lh rh)
smooth=(5 15 25)
for h in $hemis; do
 for sm in $smooth; do
cp                                                                    $suprpath/$h.glm-paired-
diff_handagesexcov_thicknesspvr_sm${sm}_doss/taskrestmean_handagesexcov/sig.mgh \
$suprpath/0_sig/$h.Task-Rest-mean_handagesexcov_thicknesspvr_sm${sm}_doss_sig.mgh
 done
done

# Per guardare i risultati con freeview
freeview \
-colorscale -orthographic -viewport 3d -view left -hide-3d-slices -hide-3d-frames -nocursor -viewsize 500 500 \
-v /Applications/freesurfer/subjects/fsaverage/mri/brain.mgz:visible=0 \
-f /Applications/freesurfer/subjects/fsaverage/surf/lh.white\
:visible=0\
:curvature_method=binary\
:annot=/Applications/freesurfer/subjects/fsaverage/label/lh.aparc.a2005s.annot:annot_outline=1\
:annot=/Applications/freesurfer/subjects/fsaverage/label/lh.aparc.a2009s.annot:annot_outline=1\
:annot=/Applications/freesurfer/subjects/fsaverage/label/lh.PALS_B12_Brodmann.annot:annot_outline=0\
:annot=/Applications/freesurfer/subjects/fsaverage/label/lh.PALS_B12_Visuotopic.annot:annot_outline=0\
:annot=/Applications/freesurfer/subjects/fsaverage/label/lh.Yeo2011_7Networks_N1000.annot:annot_outlin
e=0\
:annot=/Applications/freesurfer/subjects/fsaverage/label/lh.Yeo2011_17Networks_N1000.annot:annot_outli
ne=0\
:overlay=$suprpath/0_sig/lh.Task-Rest-
mean_handagesexcov_thicknesspvr_sm5_doss_sig.mgh:overlay_threshold=0,1.3:overlay_mask=/Applications
/freesurfer/subjects/fsaverage/label/lh.cortex.label\
:overlay=$suprpath/0_sig/lh.Task-Rest-
mean_handagesexcov_thicknesspvr_sm15_doss_sig.mgh:overlay_threshold=0,1.3:overlay_mask=/Application
s/freesurfer/subjects/fsaverage/label/lh.cortex.label\
:overlay=$suprpath/0_sig/lh.Task-Rest-
mean_handagesexcov_thicknesspvr_sm25_doss_sig.mgh:overlay_threshold=0,1.3:overlay_mask=/Application
s/freesurfer/subjects/fsaverage/label/lh.cortex.label \
-f /Applications/freesurfer/subjects/fsaverage/surf/lh.pial_semi_inflated\
:visible=0\
:curvature_method=binary\
:annot=/Applications/freesurfer/subjects/fsaverage/label/lh.aparc.a2005s.annot:annot_outline=1\
:annot=/Applications/freesurfer/subjects/fsaverage/label/lh.aparc.a2009s.annot:annot_outline=1\
:annot=/Applications/freesurfer/subjects/fsaverage/label/lh.PALS_B12_Brodmann.annot:annot_outline=0\
:annot=/Applications/freesurfer/subjects/fsaverage/label/lh.PALS_B12_Visuotopic.annot:annot_outline=0\
:annot=/Applications/freesurfer/subjects/fsaverage/label/lh.Yeo2011_7Networks_N1000.annot:annot_outlin
e=0\
:annot=/Applications/freesurfer/subjects/fsaverage/label/lh.Yeo2011_17Networks_N1000.annot:annot_outli
ne=0\
:overlay=$suprpath/0_sig/lh.Task-Rest-
mean_handagesexcov_thicknesspvr_sm5_doss_sig.mgh:overlay_threshold=0,1.3:overlay_mask=/Applications
/freesurfer/subjects/fsaverage/label/lh.cortex.label\
:overlay=$suprpath/0_sig/lh.Task-Rest-
mean_handagesexcov_thicknesspvr_sm15_doss_sig.mgh:overlay_threshold=0,1.3:overlay_mask=/Application
s/freesurfer/subjects/fsaverage/label/lh.cortex.label\
:overlay=$suprpath/0_sig/lh.Task-Rest-
mean_handagesexcov_thicknesspvr_sm25_doss_sig.mgh:overlay_threshold=0,1.3:overlay_mask=/Application
s/freesurfer/subjects/fsaverage/label/lh.cortex.label \
-f /Applications/freesurfer/subjects/fsaverage/surf/lh.inflated\
:visible=1\
:curvature_method=binary\
:annot=/Applications/freesurfer/subjects/fsaverage/label/lh.aparc.a2005s.annot:annot_outline=1\
:annot=/Applications/freesurfer/subjects/fsaverage/label/lh.aparc.a2009s.annot:annot_outline=1\
:annot=/Applications/freesurfer/subjects/fsaverage/label/lh.PALS_B12_Brodmann.annot:annot_outline=0\
:annot=/Applications/freesurfer/subjects/fsaverage/label/lh.PALS_B12_Visuotopic.annot:annot_outline=0\
:annot=/Applications/freesurfer/subjects/fsaverage/label/lh.Yeo2011_7Networks_N1000.annot:annot_outlin
e=0\
:annot=/Applications/freesurfer/subjects/fsaverage/label/lh.Yeo2011_17Networks_N1000.annot:annot_outli
ne=0\
:overlay=$suprpath/0_sig/lh.Task-Rest-
mean_handagesexcov_thicknesspvr_sm5_doss_sig.mgh:overlay_threshold=0,1.3:overlay_mask=/Applications
/freesurfer/subjects/fsaverage/label/lh.cortex.label\
:overlay=$suprpath/0_sig/lh.Task-Rest-
mean_handagesexcov_thicknesspvr_sm15_doss_sig.mgh:overlay_threshold=0,1.3:overlay_mask=/Application
s/freesurfer/subjects/fsaverage/label/lh.cortex.label\
:overlay=$suprpath/0_sig/lh.Task-Rest-
mean_handagesexcov_thicknesspvr_sm25_doss_sig.mgh:overlay_threshold=0,1.3:overlay_mask=/Application
s/freesurfer/subjects/fsaverage/label/lh.cortex.label &

freeview \
-colorscale -orthographic -viewport 3d -view right -hide-3d-slices -hide-3d-frames -nocursor -viewsize 500 500
\
-v /Applications/freesurfer/subjects/fsaverage/mri/brain.mgz:visible=0 \
-f /Applications/freesurfer/subjects/fsaverage/surf/rh.white\
:visible=0\
:curvature_method=binary\
:annot=/Applications/freesurfer/subjects/fsaverage/label/rh.aparc.a2005s.annot:annot_outline=1\
:annot=/Applications/freesurfer/subjects/fsaverage/label/rh.aparc.a2009s.annot:annot_outline=1\
:annot=/Applications/freesurfer/subjects/fsaverage/label/rh.PALS_B12_Brodmann.annot:annot_outline=0\
:annot=/Applications/freesurfer/subjects/fsaverage/label/rh.PALS_B12_Visuotopic.annot:annot_outline=0\
:annot=/Applications/freesurfer/subjects/fsaverage/label/rh.Yeo2011_7Networks_N1000.annot:annot_outlin
e=0\
:annot=/Applications/freesurfer/subjects/fsaverage/label/rh.Yeo2011_17Networks_N1000.annot:annot_outli
ne=0\
:overlay=$suprpath/0_sig/rh.Task-Rest-
mean_handagesexcov_thicknesspvr_sm5_doss_sig.mgh:overlay_threshold=0,1.3:overlay_mask=/Applications
/freesurfer/subjects/fsaverage/label/rh.cortex.label\
:overlay=$suprpath/0_sig/rh.Task-Rest-
mean_handagesexcov_thicknesspvr_sm15_doss_sig.mgh:overlay_threshold=0,1.3:overlay_mask=/Application
s/freesurfer/subjects/fsaverage/label/rh.cortex.label\
:overlay=$suprpath/0_sig/rh.Task-Rest-
mean_handagesexcov_thicknesspvr_sm25_doss_sig.mgh:overlay_threshold=0,1.3:overlay_mask=/Application
s/freesurfer/subjects/fsaverage/label/rh.cortex.label \
-f /Applications/freesurfer/subjects/fsaverage/surf/rh.pial_semi_inflated\
```

```
:visible=0\
:curvature_method=binary\
:annot=/Applications/freesurfer/subjects/fsaverage/label/rh.aparc.a2005s.annot:annot_outline=1\
:annot=/Applications/freesurfer/subjects/fsaverage/label/rh.aparc.a2009s.annot:annot_outline=1\
:annot=/Applications/freesurfer/subjects/fsaverage/label/rh.PALS_B12_Brodmann.annot:annot_outline=0\
:annot=/Applications/freesurfer/subjects/fsaverage/label/rh.PALS_B12_Visuotopic.annot:annot_outline=0\
:annot=/Applications/freesurfer/subjects/fsaverage/label/rh.Yeo2011_7Networks_N1000.annot:annot_outlin
e=0\
:annot=/Applications/freesurfer/subjects/fsaverage/label/rh.Yeo2011_17Networks_N1000.annot:annot_outli
ne=0\
:overlay=$suprpath/0_sig/rh.Task-Rest-
mean_handagesexcov_thicknesspvr_sm5_doss_sig.mgh:overlay_threshold=0,1.3:overlay_mask=/Applications
/freesurfer/subjects/fsaverage/label/rh.cortex.label\
:overlay=$suprpath/0_sig/rh.Task-Rest-
mean_handagesexcov_thicknesspvr_sm15_doss_sig.mgh:overlay_threshold=0,1.3:overlay_mask=/Application
s/freesurfer/subjects/fsaverage/label/rh.cortex.label\
:overlay=$suprpath/0_sig/rh.Task-Rest-
mean_handagesexcov_thicknesspvr_sm25_doss_sig.mgh:overlay_threshold=0,1.3:overlay_mask=/Application
s/freesurfer/subjects/fsaverage/label/rh.cortex.label \
-f /Applications/freesurfer/subjects/fsaverage/surf/rh.inflated\
:visible=1\
:curvature_method=binary\
:annot=/Applications/freesurfer/subjects/fsaverage/label/rh.aparc.a2005s.annot:annot_outline=1\
:annot=/Applications/freesurfer/subjects/fsaverage/label/rh.aparc.a2009s.annot:annot_outline=1\
:annot=/Applications/freesurfer/subjects/fsaverage/label/rh.PALS_B12_Brodmann.annot:annot_outline=0\
:annot=/Applications/freesurfer/subjects/fsaverage/label/rh.PALS_B12_Visuotopic.annot:annot_outline=0\
:annot=/Applications/freesurfer/subjects/fsaverage/label/rh.Yeo2011_7Networks_N1000.annot:annot_outlin
e=0\
:annot=/Applications/freesurfer/subjects/fsaverage/label/rh.Yeo2011_17Networks_N1000.annot:annot_outli
ne=0\
:overlay=$suprpath/0_sig/rh.Task-Rest-
mean_handagesexcov_thicknesspvr_sm5_doss_sig.mgh:overlay_threshold=0,1.3:overlay_mask=/Applications
/freesurfer/subjects/fsaverage/label/rh.cortex.label\
:overlay=$suprpath/0_sig/rh.Task-Rest-
mean_handagesexcov_thicknesspvr_sm15_doss_sig.mgh:overlay_threshold=0,1.3:overlay_mask=/Application
s/freesurfer/subjects/fsaverage/label/rh.cortex.label\
:overlay=$suprpath/0_sig/rh.Task-Rest-
mean_handagesexcov_thicknesspvr_sm25_doss_sig.mgh:overlay_threshold=0,1.3:overlay_mask=/Application
s/freesurfer/subjects/fsaverage/label/rh.cortex.label

# Facciamo la cluster-wise analysis
hemis=(lh rh)
smooth=(5 15 25)
signes=(pos neg)
for h in $hemis; do
 for sm in $smooth; do
  for sign in $signes; do
  mri_glmfit-sim \
   --glmdir $suprpath/$h.glm-paired-diff_handagesexcov_thicknesspvr_sm${sm}_doss \
   --perm 5000 1 $sign \
   --cwp 0.999 \
   --2spaces \
   --bg 8 \
   --overwrite
  done
 done
done

hemis=(lh rh)
smooth=(5 15 25)
signes=(pos neg)
surfaces=(white pial inflated)
for h in $hemis; do
 for sm in $smooth; do
  for sign in $signes; do
    mri_surfcluster \
     --in                                                    $suprpath/$h.glm-paired-
diff_handagesexcov_thicknesspvr_sm${sm}_doss/taskrestmean_handagesexcov/sig.mgh \
     --csd                                                   $suprpath/$h.glm-paired-
diff_handagesexcov_thicknesspvr_sm${sm}_doss/csd/all.perm.th10.${sign}-taskrestmean_handagesexcov.csd
\
     --subject fsaverage \
     --hemi $h \
     --surf white \
     --thmin 1 \
     --sign $sign \
     --annot aparc.a2005s \
     --olab                                                  $suprpath/$h.glm-paired-
diff_handagesexcov_thicknesspvr_sm${sm}_doss/taskrestmean_handagesexcov/$h.cluster_perm5000_cft1_$
{sign}_cwp0999_sm${sm} \
     --sum                                                   $suprpath/$h.glm-paired-
diff_handagesexcov_thicknesspvr_sm${sm}_doss/taskrestmean_handagesexcov/$h.cluster_perm5000_cft1_$
{sign}_cwp0999_sm${sm}_summary.txt
  done
 done
done

for h in $hemis; do
 for sm in $smooth; do
  for sign in $signes; do
    python3 $suprpath/scripts/make_wpts_from_clusters_space.py \
     --summary                                               "$suprpath/$h.glm-paired-
diff_handagesexcov_thicknesspvr_sm${sm}_doss/taskrestmean_handagesexcov/$h.cluster_perm5000_cft1_$
{sign}_cwp0999_sm${sm}_summary.txt" \
     --hemi $h --subject fsaverage --surf white \
     --subjects-dir "$SUBJECTS_DIR" \
     --space scanner \
     --out-wpts                                              "$suprpath/$h.glm-paired-
diff_handagesexcov_thicknesspvr_sm${sm}_doss/taskrestmean_handagesexcov/$h.cluster_perm5000_cft1_$
{sign}_cwp0999_sm${sm}_summary.wpts"
  done
 done
done

# plottiamo
python $suprpath/scripts/label_to_csv_rest_task.py \
 --label                                                   $suprpath/lh.glm-paired-
diff_handagesexcov_thicknesspvr_sm25_doss/taskrestmean_handagesexcov/lh.cluster_perm5000_cft1_pos_
cwp0999_sm25-0006.label \
 --mgh   $suprpath/lh.r_flair_ax_wm-norm-median.sm25.mgh \
 --fsgd  $suprpath/pairs.fsgd \
 --out   $suprpath/graphs/lh.cluster_perm5000_cft1_pos_cwp0999_sm25-0006_roi_values_rest_task.csv \
 --stats-out $suprpath/graphs/lh.cluster_perm5000_cft1_pos_cwp0999_sm25-0006_roi_stats_rest_task.csv

python $suprpath/scripts/label_to_csv_rest_task.py \
 --label                                                   $suprpath/lh.glm-paired-
diff_handagesexcov_thicknesspvr_sm15_doss/taskrestmean_handagesexcov/lh.cluster_perm5000_cft1_pos_
cwp0999_sm15-0010.label \
 --mgh   $suprpath/lh.r_flair_ax_wm-norm-median.sm15.mgh \
 --fsgd  $suprpath/pairs.fsgd \
 --out   $suprpath/graphs/lh.cluster_perm5000_cft1_pos_cwp0999_sm15-0010_roi_values_rest_task.csv \
 --stats-out $suprpath/graphs/lh.cluster_perm5000_cft1_pos_cwp0999_sm15-0010_roi_stats_rest_task.csv

python $suprpath/scripts/label_to_csv_rest_task.py \
 --label                                                   $suprpath/lh.glm-paired-
diff_handagesexcov_thicknesspvr_sm15_doss/taskrestmean_handagesexcov/lh.cluster_perm5000_cft1_pos_
cwp0999_sm15-0001.label \
 --mgh   $suprpath/lh.r_flair_ax_wm-norm-median.sm15.mgh \
 --fsgd  $suprpath/pairs.fsgd \
 --out   $suprpath/graphs/lh.cluster_perm5000_cft1_pos_cwp0999_sm15-0001_roi_values_rest_task.csv \
 --stats-out $suprpath/graphs/lh.cluster_perm5000_cft1_pos_cwp0999_sm15-0001_roi_stats_rest_task.csv

# Per plottare i dati a livello di un dato vertice
# omettendo --outdir si ottiene l'apertura del grafico che poi può essere salvato

python $suprpath/scripts/plot_vertex_boxplot.py \
 --overlay "$suprpath/lh.r_flair_ax_wm-norm-median.sm25.mgh" \
 --fsgd "$suprpath/pairs.fsgd" \
 --vertices 71897 \
 --prefix  "box" \
 --title-base "SUPRFLAIR vertex plot" \
 --xlabel "condition" \
 --ylabel "normalized value" \
 --x-order "Rest,Task" \
 --show-points --meanline --mean-both \
 --annotate-means --annotate-pos inline --mean-digits 6 --annotate-xoffset 0.25 \
 --stats --stats-csv "$suprpath/graphs/stats_lh_v71897.csv" \
 --csv-sep ";" \
 --decimal "," \
 --outdir  "$suprpath/graphs"

python $suprpath/scripts/plot_vertex_boxplot.py \
 --overlay "$suprpath/lh.r_flair_ax_wm-norm-median.sm15.mgh" \
 --fsgd "$suprpath/pairs.fsgd" \
 --vertices 103038 \
 --prefix  "box" \
 --title-base "SUPRFLAIR vertex plot" \
 --xlabel "condition" \
 --ylabel "normalized value" \
 --x-order "Rest,Task" \
 --show-points --meanline --mean-both \
 --annotate-means --annotate-pos inline --mean-digits 6 --annotate-xoffset 0.25 \
 --stats --stats-csv "$suprpath/graphs/stats_lh_v103038.csv" \
 --csv-sep ";" \
 --decimal "," \
 --outdir  "$suprpath/graphs"

python $suprpath/scripts/plot_vertex_boxplot.py \
 --overlay "$suprpath/lh.r_flair_ax_wm-norm-median.sm15.mgh" \
 --fsgd "$suprpath/pairs.fsgd" \
 --vertices 16696 \
 --prefix  "box" \
 --title-base "SUPRFLAIR vertex plot" \
 --xlabel "condition" \
 --ylabel "normalized value" \
 --x-order "Rest,Task" \
 --show-points --meanline --mean-both \
 --annotate-means --annotate-pos inline --mean-digits 6 --annotate-xoffset 0.25 \
 --stats --stats-csv "$suprpath/graphs/stats_lh_v16696.csv" \
 --csv-sep ";" \
 --decimal "," \
 --outdir  "$suprpath/graphs"


# per plottare i dati di un vertice a coppie con linee

python $suprpath/scripts/plot_lines.py \
 --overlay $suprpath/lh.r_flair_ax_wm-norm-median.sm25.mgh \
 --fsgd $suprpath/pairs.fsgd \
 --check-vertex 71897 \
 --check-out $suprpath/graphs/report_pairs_v71897.csv \
 --vertices 71897 \
 --title-base "SUPRFLAIR vertex pairs" \
 --xlabel "condition" \
 --ylabel "normalized value" \
 --x-order "Rest,Task" \
 --pair-by auto \
 --check-pairs \
 --csv-sep ";" \
 --csv-dec ","

python $suprpath/scripts/plot_lines.py \
 --overlay $suprpath/lh.r_flair_ax_wm-norm-median.sm15.mgh \
 --fsgd $suprpath/pairs.fsgd \
 --check-vertex 103038 \
 --check-out $suprpath/graphs/report_pairs_v103038.csv \
 --vertices 103038 \
 --title-base "SUPRFLAIR vertex pairs" \
 --xlabel "condition" \
 --ylabel "normalized value" \
 --x-order "Rest,Task" \
 --pair-by auto \
 --check-pairs \
 --csv-sep ";" \
 --csv-dec ","

python $suprpath/scripts/plot_lines.py \
 --overlay $suprpath/lh.r_flair_ax_wm-norm-median.sm15.mgh \
 --fsgd $suprpath/pairs.fsgd \
 --check-vertex 16696 \
 --check-out $suprpath/graphs/report_pairs_v16696.csv \
 --vertices 16696 \
```

```
--title-base "SUPRFLAIR vertex pairs" \
--xlabel "condition" \
--ylabel "normalized value" \
--x-order "Rest,Task" \
--pair-by auto \
--check-pairs \
--csv-sep ";" \
--csv-dec ","
```

python scripts

We developed several Python scripts to facilitate the analyses reported in Chapter III:

- Script (1): fs_vertex_extract
    - Goal: FreeSurfer vertex-based extractor for specific regions (labels). Output: CSV with one record per vertex and columns for all requested scalar measures.
- Script (2): summarize_clusters.py
    - Goal: summarize FreeSurfer surface clusters
- Script (3): label_to_csv_groups
    - Goal: Create two CSV files from a multi-frame MGH/MGZ file and a two-group FSGD, including descriptive statistics
- Script (4): label_to_csv_rest_task
    - Goal: For each vertex of a label, extract: vertex ID; coordinates (x, y, z) from the label; mean value of the measure in Rest (average across Rest frames); mean value of the measure in Task (average across Task frames)
- Script (5): make_wpts_from_clusters_space
    - Goal: Create a point set (.wpts) from the VtxMax entries in the *mri_surfcluster* summary
- Script (6): plot_vertex_boxplot
    - Goal: Box plots for FreeSurfer single-vertex data, separated by class (FSGD)
- Script (7): plot_lines
    - Goal: Plot Rest→Task line charts per vertex, with pairing by *subject name* from the FSGD and explicit control of the order on the X-axis

In the following pages, the code for the aforementioned scripts is provided.

```python
#!/usr/bin/env python3
# -*- coding: utf-8 -*-
"""
SCRIPT: FS_VERTEX-EXTRACT

Estrattore vertex-based FreeSurfer per regioni (label) specifiche.
Output: CSV con un record per vertice e colonne per tutte le misure scalari richieste.

Caratteristiche chiave:
- Spazio di destinazione delle misure selezionabile: default **fsaverage** (non nativo).
- Spazio delle label selezionabile: **--label-space fsaverage|native** (default = stesso di --target-space).
- Colonne per versioni smussate (FWHM 5, 15, 25) per ogni misura (su spazio target).
- Colonne calcolate: simple_label, hemi_simple_label.
- Separatore campi e decimali configurabili da CLI.
- Opzionale: generazione automatica dei file su fsaverage e/o smoothing mancanti (mri_surf2surf).

Uso tipico (fsaverage, default):
  python fs_vertex_extract.py \
    --demographics /path/dati/demografia.csv \
    --measures thickness r_flair_ax_wm-norm-median r_flair3d_wm-norm-median \
    --labels BA1_exvivo BA2_exvivo BA3a_exvivo.thresh BA3b_exvivo.thresh \
    --output /path/out/vertex_data.csv

Per generare i file mappati su fsaverage e le versioni smoothed se mancanti:
  ... --compute-maps

Richiede: nibabel, pandas, numpy ; FreeSurfer installato; SUBJECTS_DIR definita (o --subjects-dir).
CSV anagrafica con separatore ';' e colonne: subject;sex;age;handedness
"""

import os
import sys
import argparse
import glob
import subprocess
from typing import List, Dict, Optional

import numpy as np
import pandas as pd
import nibabel as nib
from nibabel.freesurfer.io import read_morph_data, read_label

ALLOWED_EXTS = ("", ".curv", ".mgh", ".mgz")


def eprint(*args, **kwargs):
    print(*args, file=sys.stderr, **kwargs)


def find_subjects_dir(cli_subjects_dir: Optional[str]) -> str:
    sd = cli_subjects_dir or os.environ.get("SUBJECTS_DIR")
    if not sd or not os.path.isdir(sd):
        raise RuntimeError(
            "SUBJECTS_DIR non impostata o non valida. Passa --subjects-dir o esporta la variabile d'ambiente."
        )
    return os.path.abspath(sd)


def _glob_existing(paths: List[str]) -> List[str]:
    out = []
    for p in paths:
        if "*" in p or "?" in p:
            out.extend(glob.glob(p))
        elif os.path.isfile(p):
            out.append(p)
    return out


def find_measure_file_native(surf_dir: str, hemi: str, var: str) -> Optional[str]:
    """Cerca la misura nello spazio nativo del soggetto (cartella surf del soggetto)."""
    candidates = []
    bases = [var, var.replace("-", "_")]
    for base in bases:
        for ext in ALLOWED_EXTS:
            candidates.append(os.path.join(surf_dir, f"{hemi}.{base}{ext}"))
        candidates.append(os.path.join(surf_dir, f"{hemi}.{base}.*"))
    candidates = _glob_existing(candidates)
    if not candidates:
        return None
    def score(p):
        if p.endswith(".mgh") or p.endswith(".mgz"):
            return 0
        if p.endswith(".curv"):
            return 1
        base = os.path.basename(p)
        if base == f"{hemi}.{var}" or base == f"{hemi}.{var.replace('-','_')}":
            return -1
        return 2
    candidates.sort(key=lambda p: (score(p), len(p)))
    return candidates[0]
```

```python


def find_measure_file_fsavg(surf_dir: str, hemi: str, var: str) -> Optional[str]:
    """Cerca la misura già mappata su fsaverage nella cartella surf del soggetto."""
    bases = [
        f"{hemi}.{var}.fsaverage",
        f"{hemi}.{var.replace('-', '_')}.fsaverage",
        f"{hemi}.{var}.fsavg",
        f"{hemi}.{var.replace('-', '_')}.fsavg",
        f"{hemi}.{var}.*fsaverage*",
        f"{hemi}.{var.replace('-', '_')}.*fsaverage*",
    ]
    candidates = []
    for b in bases:
        candidates.append(os.path.join(surf_dir, b + ".mgh"))
        candidates.append(os.path.join(surf_dir, b + ".mgz"))
        if "*" in b:
            candidates.append(os.path.join(surf_dir, b))
    candidates = _glob_existing(candidates)
    if not candidates:
        return None
    def score(p):
        s = 0
        if ".fsaverage" in p or ".fsavg" in p:
            s -= 1
        if p.endswith(".mgh") or p.endswith(".mgz"):
            s -= 1
        return s, len(p)
    candidates.sort(key=lambda p: score(p))
    return candidates[0]


def find_smoothed_file_fsavg(surf_dir: str, hemi: str, var: str, fwhm: int) -> Optional[str]:
    """Cerca varianti smussate su fsaverage con pattern comuni."""
    bases = [
        f"{hemi}.{var}.fsaverage.fwhm{fwhm}",
        f"{hemi}.{var}.fwhm{fwhm}.fsaverage",
        f"{hemi}.{var}.fsaverage.sm{fwhm:02d}",
        f"{hemi}.{var}.sm{fwhm:02d}.fsaverage",
        f"{hemi}.{var.replace('-', '_')}.fsaverage.fwhm{fwhm}",
        f"{hemi}.{var.replace('-', '_')}.fwhm{fwhm}.fsaverage",
        f"{hemi}.{var.replace('-', '_')}.fsaverage.sm{fwhm:02d}",
        f"{hemi}.{var.replace('-', '_')}.sm{fwhm:02d}.fsaverage",
    ]
    candidates = []
    for b in bases:
        candidates.append(os.path.join(surf_dir, b + ".mgh"))
        candidates.append(os.path.join(surf_dir, b + ".mgz"))
        candidates.append(os.path.join(surf_dir, b))  # per glob vari
    candidates = _glob_existing(candidates)
    if not candidates:
        return None
    def score(p):
        s = 0
        if ".fsaverage" in p or ".fsavg" in p:
            s -= 1
        if p.endswith(".mgh") or p.endswith(".mgz"):
            s -= 1
        return s, len(p)
    candidates.sort(key=lambda p: score(p))
    return candidates[0]


def read_measure_values(path: str) -> np.ndarray:
    """Legge vettore per-vertex da file FreeSurfer."""
    if path.endswith((".mgh", ".mgz")):
        arr = np.asarray(nib.load(path).get_fdata()).squeeze()
    else:
        arr = read_morph_data(path)
    return arr.astype(float)


def ensure_fsavg_measure(
    subject: str,
    hemi: str,
    var: str,
    base_native_path: str,
    surf_dir: str,
    fsaverage: str,
    fwhm: Optional[int] = None,
) -> Optional[str]:
    """
    Genera (con mri_surf2surf) un file mappato su fsaverage (opzionalmente smussato).
    Scrive in: <surf_dir>/<hemi>.<var>.fsaverage[.fwhmK].mgh
    """
    out_name = f"{hemi}.{var.replace('-', '_')}.fsaverage"
    if fwhm is not None:
        out_name += f".fwhm{fwhm}"
    out_path = os.path.join(surf_dir, out_name + ".mgh")

```

```
    cmd = [
        "mri_surf2surf",
        "--s", subject,
        "--hemi", hemi,
        "--sval", base_native_path,
        "--tval", out_path,
        "--trgsubject", fsaverage,
    ]
    if fwhm is not None:
        cmd += ["--fwhm", str(fwhm)]
    eprint(f"[mri_surf2surf] Map {var} -> fsaverage (fwhm={fwhm}) per {subject} {hemi}")
    try:
        subprocess.run(cmd, check=True, stdout=subprocess.PIPE, stderr=subprocess.PIPE)
    except FileNotFoundError:
        eprint("[ATTENZIONE] mri_surf2surf non trovato nel PATH. Salto generazione fsaverage.")
        return None
    except subprocess.CalledProcessError as exc:
        eprint(exc.stderr.decode("utf-8", errors="ignore"))
        eprint(f"[ATTENZIONE] mri_surf2surf fallito per {subject} {hemi} {var} (fsaverage; fwhm={fwhm}).")
        return None

    if os.path.isfile(out_path):
        return out_path
    return None


def ensure_label_for_subject(
    subjects_dir: str,
    subject: str,
    hemi: str,
    label_name: str,
    fsaverage: str = "fsaverage",
) -> str:
    """
    Garantisce che <subject>/label/<hemi>.<label_name>.label esista (proiettando da fsaverage).
    """
    target = os.path.join(subjects_dir, subject, "label", f"{hemi}.{label_name}.label")
    if os.path.isfile(target):
        return target

    src = os.path.join(subjects_dir, fsaverage, "label", f"{hemi}.{label_name}.label")
    if not os.path.isfile(src):
        raise FileNotFoundError(f"Label sorgente non trovata: {src}")

    os.makedirs(os.path.dirname(target), exist_ok=True)

    cmd = [
        "mri_label2label",
        "--srclabel", src,
        "--srcsubject", fsaverage,
        "--trglabel", target,
        "--trgsubject", subject,
        "--hemi", hemi,
        "--regmethod", "surface",
    ]
    eprint(f"[mri_label2label] Proietto {label_name} ({hemi}) su {subject} (fsaverage→native) ...")
    try:
        subprocess.run(cmd, check=True, stdout=subprocess.PIPE, stderr=subprocess.PIPE)
    except subprocess.CalledProcessError as exc:
        eprint(exc.stderr.decode("utf-8", errors="ignore"))
        raise RuntimeError(f"mri_label2label fsaverage→native fallita per {subject} {hemi} {label_name}")

    if not os.path.isfile(target):
        raise RuntimeError(f"Generazione label fallita: atteso {target}")
    return target


def ensure_label_on_target(
    subjects_dir: str,
    src_subject: str,
    trg_subject: str,
    hemi: str,
    label_name: str,
) -> str:
    """
    Garantisce una versione della label di src_subject proiettata su trg_subject.
    Salva in: $SUBJECTS_DIR/<src_subject>/label/<hemi>.<label_name>.to-<trg_subject>.label
    """
    out_dir = os.path.join(subjects_dir, src_subject, "label")
    os.makedirs(out_dir, exist_ok=True)
    target = os.path.join(out_dir, f"{hemi}.{label_name}.to-{trg_subject}.label")
    if os.path.isfile(target):
        return target

    src = os.path.join(subjects_dir, src_subject, "label", f"{hemi}.{label_name}.label")
    if not os.path.isfile(src):
        raise FileNotFoundError(f"Label sorgente non trovata: {src}")

    cmd = [
        "mri_label2label",
```

```
        "--srclabel", src,
        "--srcsubject", src_subject,
        "--trglabel", target,
        "--trgsubject", trg_subject,
        "--hemi", hemi,
        "--regmethod", "surface",
    ]
    eprint(f"[mri_label2label] Proietto {label_name} ({hemi}) {src_subject}→{trg_subject} ...")
    try:
        subprocess.run(cmd, check=True, stdout=subprocess.PIPE, stderr=subprocess.PIPE)
    except subprocess.CalledProcessError as exc:
        eprint(exc.stderr.decode("utf-8", errors="ignore"))
        raise RuntimeError(f"mri_label2label {src_subject}→{trg_subject} fallita per {hemi} {label_name}")

    if not os.path.isfile(target):
        raise RuntimeError(f"Generazione label fallita: atteso {target}")
    return target


def compute_simple_label(label: str) -> str:
    """
    Unifica:
      - BA3a_exvivo(.thresh) e BA3b_exvivo(.thresh) -> BA3_exvivo(.thresh)
      - BA4a_exvivo(.thresh) e BA4p_exvivo(.thresh) -> BA4_exvivo(.thresh)
    Mantiene eventuale suffisso '.thresh' se presente.
    """
    lab = label.strip()
    suffix = ""
    if lab.endswith(".thresh"):
        base = lab[:-len(".thresh")]
        suffix = ".thresh"
    else:
        base = lab
    mapping = {
        "BA3a_exvivo": "BA3_exvivo",
        "BA3b_exvivo": "BA3_exvivo",
        "BA4a_exvivo": "BA4_exvivo",
        "BA4p_exvivo": "BA4_exvivo",
    }
    base_simple = mapping.get(base, base)
    return base_simple + suffix


def main():
    parser = argparse.ArgumentParser(
        description="Estrai valori vertex-based in label selezionate (FreeSurfer)."
    )
    parser.add_argument(
        "--demographics",
        required=True,
        help="CSV anagrafica con colonne subject;sex;age;handedness (sep=';').",
    )
    parser.add_argument(
        "--measures",
        nargs="+",
        required=True,
        help="Nomi delle misure (file in surf/, es. thickness r_flair_ax_wm-norm-median ...).",
    )
    parser.add_argument(
        "--labels",
        nargs="+",
        required=True,
        help="Nomi label (senza prefisso emisfero), es. BA1_exvivo BA2_exvivo BA3a_exvivo.thresh ...",
    )
    parser.add_argument(
        "--hemis",
        nargs="+",
        default=["lh", "rh"],
        choices=["lh", "rh"],
        help="Emisferi da includere (default: lh rh).",
    )
    parser.add_argument("--subjects-dir", help="Override di $SUBJECTS_DIR.")
    parser.add_argument("--output", default="vertex_data.csv", help="Percorso file CSV in output (default:
vertex_data.csv).")
    parser.add_argument(
        "--out-sep",
        default=";",
        help="Separatore CSV di output (default: ';').",
    )
    parser.add_argument(
        "--out-decimal",
        default=",",
        help="Separatore decimale nel CSV di output (default: ','). Usa '.' per il punto decimale.",
    )
    parser.add_argument(
        "--fsaverage",
        default="fsaverage",
        help="Nome soggetto fsaverage (default: fsaverage).",
    )
    parser.add_argument(
```

```
        "--target-space",
        choices=["fsaverage", "native"],
        default="fsaverage",
        help="Spazio delle misure/vertici: 'fsaverage' (default) o 'native' (soggetto).",
    )
    parser.add_argument(
        "--label-space",
        choices=["fsaverage", "native"],
        help="Spazio in cui sono definite le label: 'fsaverage' o 'native' (default = come --target-space).",
    )
    parser.add_argument(
        "--compute-maps",
        action="store_true",
        help="Se attivo, genera file mappati su fsaverage e/o smussati se mancanti (mri_surf2surf).",
    )
    parser.add_argument(
        "--project-labels-from-fsaverage",
        action="store_true",
        help="Se --label-space=native e manca una label, proiettala da fsaverage al soggetto.",
    )
    parser.add_argument(
        "--fwhm-levels",
        nargs="+",
        type=int,
        default=[5, 15, 25],
        help="Livelli FWHM per cui estrarre (o calcolare) le versioni smussate. Default: 5 15 25",
    )
    args = parser.parse_args()

    subjects_dir = find_subjects_dir(args.subjects_dir)
    label_space = args.label_space if args.label_space else args.target_space
    compute_maps = args.compute_maps

    # Leggi anagrafica (sep=';')
    demo = pd.read_csv(args.demographics, sep=";", dtype={"subject": str})
    required_cols = {"subject", "sex", "age", "handedness"}
    if not required_cols.issubset(set(demo.columns)):
        raise RuntimeError(f"Il file anagrafica deve contenere colonne: {required_cols}")

    demo["subject"] = demo["subject"].astype(str)
    demo["handedness"] = (
        demo["handedness"].astype(str)
        .str.strip()
        .str.upper()
        .replace({"RIGHT": "R", "LEFT": "L", "DX": "R", "SX": "L"})
    )
    try:
        demo["age"] = pd.to_numeric(demo["age"], errors="coerce")
    except Exception:
        pass

    out_rows: List[Dict] = []

    # Label base dir per fsaverage
    fsavg_label_dir = os.path.join(subjects_dir, args.fsaverage, "label")

    for _, row in demo.iterrows():
        subj = row["subject"]
        sex = row["sex"]
        age = row["age"]
        handedness = row["handedness"]

        subj_dir = os.path.join(subjects_dir, subj)
        surf_dir = os.path.join(subj_dir, "surf")

        if not os.path.isdir(surf_dir):
            eprint(f"[ATTENZIONE] Mancante surf/: {surf_dir}  (skip soggetto)")
            continue

        for hemi in args.hemis:
            measure_arrays: Dict[str, np.ndarray] = {}
            nverts_ref: Optional[int] = None

            # Carica misure nello spazio target richiesto
            for var in args.measures:
                base_native_path = None
                arr_base = None

                if args.target_space == "fsaverage":
                    fsavg_path = find_measure_file_fsavg(surf_dir, hemi, var)
                    if fsavg_path is None:
                        base_native_path = find_measure_file_native(surf_dir, hemi, var)
                        if base_native_path is not None and compute_maps:
                            fsavg_path = ensure_fsavg_measure(
                                subject=subj,
                                hemi=hemi,
                                var=var,
                                base_native_path=base_native_path,
                                surf_dir=surf_dir,
                                fsaverage=args.fsaverage,
```

```
                                fwhm=None,
                            )
                    if fsavg_path is not None:
                        try:
                            arr_base = read_measure_values(fsavg_path)
                        except Exception as exc:
                            eprint(f"[ERRORE] Lettura '{os.path.basename(fsavg_path)}' per {subj} {hemi}: {exc}")
                            arr_base = None
                else:
                    base_native_path = find_measure_file_native(surf_dir, hemi, var)
                    if base_native_path is not None:
                        try:
                            arr_base = read_measure_values(base_native_path)
                        except Exception as exc:
                            eprint(f"[ERRORE] Lettura misura '{var}' per {subj} {hemi}: {exc}")
                            arr_base = None

                if arr_base is not None:
                    measure_arrays[var] = arr_base
                    if nverts_ref is None:
                        nverts_ref = arr_base.shape[0]
                    elif arr_base.shape[0] != nverts_ref:
                        eprint(f"[ATTENZIONE] '{var}' ha nverts={arr_base.shape[0]} diverso da {nverts_ref} per {subj} {hemi}. Skip base.")
                        measure_arrays.pop(var, None)
                        arr_base = None

                # Smoothed livelli
                for fwhm in args.fwhm_levels:
                    key = f"{var}_fwhm{fwhm}"
                    arr_sm = None

                    if args.target_space == "fsaverage":
                        sm_path = find_smoothed_file_fsavg(surf_dir, hemi, var, fwhm)
                        if sm_path is None and compute_maps:
                            if base_native_path is None:
                                base_native_path = find_measure_file_native(surf_dir, hemi, var)
                            if base_native_path is not None:
                                sm_path = ensure_fsavg_measure(
                                    subject=subj,
                                    hemi=hemi,
                                    var=var,
                                    base_native_path=base_native_path,
                                    surf_dir=surf_dir,
                                    fsaverage=args.fsaverage,
                                    fwhm=fwhm,
                                )
                        if sm_path is not None:
                            try:
                                arr_sm = read_measure_values(sm_path)
                            except Exception as exc:
                                eprint(f"[ERRORE] Lettura smoothing fsavg '{key}' per {subj} {hemi}: {exc}")
                                arr_sm = None
                    else:
                        # in spazio nativo: accetta file smussati nativi (retro-compatibilità)
                        from glob import glob as _glob
                        sm_path = None
                        for p in _glob(os.path.join(surf_dir, f"{hemi}.{var}.fwhm{fwhm}*")) + \
                                 _glob(os.path.join(surf_dir, f"{hemi}.{var.replace('-', '_')}.fwhm{fwhm}*")) + \
                                 _glob(os.path.join(surf_dir, f"{hemi}.{var}.sm{fwhm:02d}*")) + \
                                 _glob(os.path.join(surf_dir, f"{hemi}.{var.replace('-', '_')}.sm{fwhm:02d}*")):
                            if os.path.isfile(p):
                                sm_path = p
                                break
                        if sm_path is not None:
                            try:
                                arr_sm = read_measure_values(sm_path)
                            except Exception as exc:
                                eprint(f"[ERRORE] Lettura smoothing native '{key}' per {subj} {hemi}: {exc}")
                                arr_sm = None

                    if arr_sm is not None:
                        if nverts_ref is None:
                            nverts_ref = arr_sm.shape[0]
                        if arr_sm.shape[0] != nverts_ref:
                            eprint(f"[ATTENZIONE] '{os.path.basename(sm_path)}' ha nverts={arr_sm.shape[0]} diverso da {nverts_ref} per {subj} {hemi}. Skip.")
                        else:
                            measure_arrays[key] = arr_sm

            if not measure_arrays:
                eprint(f"[INFO] Nessuna misura valida per {subj} {hemi}, salto alle label successive.")
                continue

            # per ciascuna label, estrai gli indici vertex in base allo spazio label richiesto
            for lab in args.labels:
                if label_space == "fsaverage":
                    lab_path = os.path.join(fsavg_label_dir, f"{hemi}.{lab}.label")
                    if not os.path.isfile(lab_path):
                        eprint(f"[ATTENZIONE] Label fsaverage mancante: {lab_path}.")
```

```
                        continue
                else:
                    # label native presenti sul soggetto?
                    lab_path_native = os.path.join(subj_dir, "label", f"{hemi}.{lab}.label")
                    if not os.path.isfile(lab_path_native):
                        if args.project_labels_from_fsaverage:
                            try:
                                lab_path_native = ensure_label_for_subject(
                                    subjects_dir, subj, hemi, lab, fsaverage=args.fsaverage
                                )
                            except Exception as exc:
                                eprint(f"[ATTENZIONE] Impossibile ottenere label native {lab} per {subj} {hemi}: {exc}.
Skip.")
                                continue
                        else:
                            eprint(f"[ATTENZIONE] Label nativa mancante: {lab_path_native}.")
                            continue

                    # se target-space è fsaverage, serve proiezione della label nativa su fsaverage
                    if args.target_space == "fsaverage":
                        try:
                            lab_path = ensure_label_on_target(
                                subjects_dir, src_subject=subj, trg_subject=args.fsaverage, hemi=hemi, label_name=lab
                            )
                        except Exception as exc:
                            eprint(f"[ATTENZIONE] Impossibile proiettare label {lab} {subj}→{args.fsaverage}: {exc}. Skip.")
                            continue
                    else:
                        lab_path = lab_path_native

                # ora lab_path è nello stesso spazio delle misure (grazie alle proiezioni, se necessarie)
                try:
                    verts = read_label(lab_path).astype(int).ravel()
                except Exception as exc:
                    eprint(f"[ERRORE] Lettura label {lab_path}: {exc}. Skip.")
                    continue

                if nverts_ref is not None:
                    verts = verts[(verts >= 0) & (verts < nverts_ref)]

                if verts.size == 0:
                    eprint(f"[INFO] Label vuota per {subj} {hemi} {lab}.")
                    continue

                # compila righe: una per vertex
                simple_lab = compute_simple_label(lab)
                hemi_label = f"{hemi}.{lab}"
                hemi_simple_label = f"{hemi}.{simple_lab}"
                for v in verts:
                    rec = {
                        "subject": subj,
                        "sex": sex,
                        "age": age,
                        "handedness": handedness,
                        "hemi": hemi,
                        "vertex": int(v),
                        "label": lab,
                        "simple_label": simple_lab,
                        "hemi_label": hemi_label,
                        "hemi_simple_label": hemi_simple_label,
                    }
                    for key, arr in measure_arrays.items():
                        try:
                            rec[key] = float(arr[v])
                        except Exception:
                            rec[key] = np.nan
                    out_rows.append(rec)

    if not out_rows:
        eprint("[ERRORE] Nessuna riga prodotta. Controlla percorsi, misure e label.")
        sys.exit(2)

    df = pd.DataFrame(out_rows)

    # Ordine colonne: anagrafica + struttura + misure
    base_cols = [
        "subject", "sex", "age", "handedness",
        "hemi", "vertex",
        "label", "simple_label",
        "hemi_label", "hemi_simple_label"
    ]
    measure_cols = [c for c in df.columns if c not in base_cols]
    df = df[base_cols + measure_cols]

    # Scrittura CSV con controllo del separatore decimale
    out_sep = args.out_sep
    out_dec = args.out_decimal

    if out_dec == ".":
        df.to_csv(args.output, index=False, sep=out_sep)
```

```
    else:
        df_to_write = df.copy()
        float_cols = df_to_write.select_dtypes(include=[np.floating]).columns.tolist()
        def fmt(x):
            if pd.isna(x):
                return ""
            return ("%.6g" % x).replace(".", out_dec)
        for col in float_cols:
            df_to_write[col] = df_to_write[col].map(fmt)
        df_to_write.to_csv(args.output, index=False, sep=out_sep, na_rep="")

    print(f"[OK] Scritto: {args.output}")
    print(f"[INFO] Righe: {len(df)}, colonne: {len(df.columns)}")
    print(f"[INFO] Colonne: {', '.join(df.columns)}")


if __name__ == "__main__":
    main()

```

```python
#!/usr/bin/env python3
"""
SCRIPT: SUMMARIZE_CLUSTERS

Summarize FreeSurfer surface CLUSTERS (LH/RH; POS/NEG) in order of significance.

The script scans one or more GLM directories (glmdir) for cluster summary files
typically produced by `mri_glmfit-sim` or `mri_surfcluster`, e.g.:
  cache.th30.pos.sig.cluster.summary
  cache.th30.neg.sig.cluster.summary
and extracts for each cluster:
  - hemisphere, sign, cluster number
  - VtxMax (vertex id at peak)
  - Max         (peak statistic or -log10(p), see note below)
  - Size(mm^2)
  - CWP         (clusterwise p-value, if present)
  - NVtxs

It then prints a clean, sorted table for each hemisphere and sign;
by default it sorts by CWP ascending when available, otherwise by |Max| desc.
You can also save a CSV.

USAGE EXAMPLES
--------------
python summarize_clusters.py \
  --glmdir "/Users/cico/Desktop/suprflair_FT/lh.glm-paired-diff_sm25" \
  --glmdir "/Users/cico/Desktop/suprflair_FT/rh.glm-paired-diff_sm25" \
  --out "/Users/cico/Desktop/suprflair_FT/cluster_summary.csv"

OPTIONS
-------
--glmdir  : repeatable; one or more GLM dirs (lh and/or rh)
--out     : optional CSV path
--limit   : limit output to top-N per hemi/sign (after sorting)
--prefer  : 'cwp' (default) or 'max' to choose sorting metric preference

NOTE
----
- With `mri_glmfit-sim` clusterwise correction, the cluster summary contains
  'CWP' (clusterwise p-value). In that case the script orders by CWP asc.
- Without CWP (uncorrected clusters), 'Max' is used for sorting (|Max| desc).
- The "representative vertex" is taken as VtxMax (the vertex id at peak).
"""

import argparse
import csv
import re
from dataclasses import dataclass
from pathlib import Path
from typing import List, Optional, Tuple

@dataclass
class Cluster:
    hemi: str
    sign: str
    cluster_no: int
    vtxmax: int
    maxval: float
    size_mm2: float
    cwp: Optional[float]
    nvtxs: Optional[int]
    srcfile: str

def find_summary_files(glmdir: Path):
    """
    Return list of (sign, path_to_summary) for this glmdir, detecting 'pos'/'neg' from filename.
    """
    files = list(glmdir.rglob("*.sig.cluster.summary"))
    out = []
    for f in files:
        name = f.name.lower()
        if ".pos." in name:
            out.append(("pos", f))
        elif ".neg." in name:
            out.append(("neg", f))
        else:
            out.append(("unknown", f))
    return out

def guess_hemi(glmdir: Path) -> str:
    name = glmdir.name.lower()
    if name.startswith("lh") or "lh." in name or "_lh" in name:
        return "lh"
    if name.startswith("rh") or "rh." in name or "_rh" in name:
        return "rh"
    for p in glmdir.parts:
        pl = p.lower()
        if pl == "lh":
            return "lh"
        if pl == "rh":
```

```
            return "rh"
    return "hemi"

def parse_summary_file(path: Path, hemi_hint: str, sign_hint: str) -> List[Cluster]:
    clusters: List[Cluster] = []
    hemi = hemi_hint
    sign = sign_hint
    header_cols = None
    with path.open("r", encoding="utf-8", errors="ignore") as f:
        for line in f:
            line = line.strip()
            if not line:
                continue
            if line.startswith("#"):
                if "hemi " in line and hemi == "hemi":
                    m = re.search(r"hemi\s+([lr]h)\b", line)
                    if m: hemi = m.group(1)
                if "Threshold Sign" in line and sign == "unknown":
                    m = re.search(r"Threshold Sign\s+(\w+)", line)
                    if m: sign = m.group(1).lower()
                if line.startswith("# ClusterNo"):
                    header_cols = re.sub(r"#\s*", "", line).split()
                continue

            cols = line.split()
            def get_col(name: str):
                if header_cols and name in header_cols:
                    return header_cols.index(name)
                return None

            try:
                idx_cluster = get_col("ClusterNo") or 0
                idx_max     = get_col("Max") or 1
                idx_vtxmax  = get_col("VtxMax") or 2

                idx_size = None
                if header_cols:
                    for i, h in enumerate(header_cols):
                        if h.startswith("Size"):
                            idx_size = i
                            break
                if idx_size is None:
                    idx_size = 3

                idx_cwp = get_col("CWP")
                idx_nv  = get_col("NVtxs")

                parts = cols
                cluster_no = int(float(parts[idx_cluster]))
                maxval     = float(parts[idx_max])
                vtxmax     = int(float(parts[idx_vtxmax]))
                size_mm2   = float(parts[idx_size])
                cwp        = float(parts[idx_cwp]) if (idx_cwp is not None and len(parts) > idx_cwp) else None
                nvtxs      = int(float(parts[idx_nv])) if (idx_nv is not None and len(parts) > idx_nv) else None

                clusters.append(Cluster(
                    hemi=hemi, sign=sign, cluster_no=cluster_no, vtxmax=vtxmax,
                    maxval=maxval, size_mm2=size_mm2, cwp=cwp, nvtxs=nvtxs, srcfile=str(path)))
            except Exception:
                continue
    return clusters

def sort_clusters(clusters: List[Cluster], prefer: str) -> List[Cluster]:
    if prefer == "max":
        return sorted(clusters, key=lambda c: abs(c.maxval), reverse=True)
    def key(c: Cluster):
        if c.cwp is not None:
            return (0, c.cwp)
        else:
            return (1, -abs(c.maxval))
    return sorted(clusters, key=key)

def print_table(clusters: List[Cluster], hemi: str, sign: str, limit: Optional[int] = None):
    rows = [c for c in clusters if c.hemi == hemi and c.sign.startswith(sign)]
    if limit:
        rows = rows[:limit]
    if not rows:
        print(f"\n[{hemi.upper()} – {sign.upper()}] Nessun cluster trovato.")
        return
    print(f"\n[{hemi.upper()} – {sign.upper()}] {len(rows)} cluster (ordinati per significatività)")
    print("Cluster  VtxMax   Max        Size(mm^2)    CWP        NVtxs   File")
    for c in rows:
        cwp = f"{c.cwp:.5f}" if c.cwp is not None else "–"
        nv  = f"{c.nvtxs}" if c.nvtxs is not None else "–"
        print(f"{c.cluster_no:>6}  {c.vtxmax:>7}  {c.maxval:>8.3f}  {c.size_mm2:>12.2f}  {cwp:>9}  {nv:>7}
{Path(c.srcfile).name}")

def save_csv(clusters: List[Cluster], out_csv: Path):
    out_csv.parent.mkdir(parents=True, exist_ok=True)
    import csv
```

```
    with out_csv.open("w", newline="", encoding="utf-8") as f:
        w = csv.writer(f)
        w.writerow(["hemi", "sign", "cluster_no", "vtxmax", "max", "size_mm2", "cwp", "nvtxs", "srcfile"])
        for c in clusters:
            w.writerow([c.hemi, c.sign, c.cluster_no, c.vtxmax, c.maxval, c.size_mm2, c.cwp if c.cwp is not None else "",
                        c.nvtxs if c.nvtxs is not None else "", c.srcfile])
    print(f"\n[OK] Salvato CSV: {out_csv}")

def main():
    ap = argparse.ArgumentParser(description="Elenca i cluster (pos/neg) per LH/RH in ordine di significatività, con VtxMax.")
    ap.add_argument("--glmdir", action="append", required=True,
                    help="Directory di output mri_glmfit (una o più; es. lh.glm-..., rh.glm-...)")
    ap.add_argument("--out", default=None, help="CSV di output (opzionale)")
    ap.add_argument("--limit", type=int, default=None, help="Top-N per emisfero e segno (opzionale)")
    ap.add_argument("--prefer", choices=["cwp", "max"], default="cwp",
                    help="Criterio di ordinamento: usa CWP se presente (default) o Max")
    args = ap.parse_args()

    all_clusters: List[Cluster] = []

    for gdir in args.glmdir:
        g = Path(gdir)
        hemi = guess_hemi(g)
        found = find_summary_files(g)
        if not found:
            print(f"[WARN] Nessun *.sig.cluster.summary trovato in {g}. Hai già eseguito mri_glmfit-sim?")
            continue
        for sign, f in found:
            clusters = parse_summary_file(f, hemi_hint=hemi, sign_hint=sign)
            all_clusters.extend(clusters)

    if not all_clusters:
        print("[ERR] Nessun cluster trovato. Verifica di aver lanciato mri_glmfit-sim e che i file *.sig.cluster.summary esistano.")
        return

    sorted_all = sort_clusters(all_clusters, prefer=args.prefer)

    for hemi in ("lh", "rh"):
        for sign in ("pos", "neg"):
            table = [c for c in sorted_all if c.hemi == hemi and c.sign.startswith(sign)]
            if args.limit is not None:
                table = table[:args.limit]
            print_table(table, hemi, sign, limit=None)

    if args.out:
        save_csv(sorted_all, Path(args.out))

if __name__ == "__main__":
    main()
```

```python
#!/usr/bin/env python3
# -*- coding: utf-8 -*-
"""
SCRIPT: LABEL_TO_CSV_GROUPS

Crea due CSV a partire da un file MGH/MGZ multi-frame e un FSGD a due gruppi:
1) CSV per-vertice con: vertex_id; x; y; z; value_<ClassA>; value_<ClassB>
2) (opzionale) CSV con statistiche descrittive separate per ClassA e ClassB
   (n, n_valid, mean, sd, median, min, max, p25, p75, IQR)

- Separatore di campo: ';'
- Separatore decimale: ','
- I valori per gruppo sono la media sui frame di quel gruppo.

Requisiti: nibabel, numpy
    pip install nibabel numpy

Uso tipico:
    python label_to_csv_groups.py \
        --label /path/lh.ROI_fsaverage.label \
        --mgh   /path/lh.allinputs.sm05.mgh \
        --fsgd  /path/groups.fsgd \
        --out   /path/roi_values_groups.csv \
        --stats-out /path/roi_stats_groups.csv \
        --class-a Pazienti --class-b Controlli

Se --class-a/--class-b non sono forniti, lo script prova a dedurre le prime due classi
dal file FSGD (prima dai "Class:", altrimenti dalle righe "Input").
"""
import argparse
import csv
import re
import sys
from typing import List, Tuple, Dict, Optional

import numpy as np

try:
    import nibabel as nib
except Exception as e:
    print("Errore: serve 'nibabel' (pip install nibabel).", file=sys.stderr)
    raise

def fmt(v: float, ndigits: int = 6) -> str:
    """Formatta numeri con virgola come separatore decimale; stringa vuota per NaN."""
    try:
        if v is None or (isinstance(v, float) and np.isnan(v)):
            return ''
        s = f"{float(v):.{ndigits}f}"
        return s.replace('.', ',')
    except Exception:
        # fallback: sostituisci comunque il punto
        return str(v).replace('.', ',')

def load_mgh_2d(mgh_path: str) -> np.ndarray:
    img = nib.load(mgh_path)
    data = img.get_fdata()
    # Atteso: (nvert, 1, 1, nframe) oppure (nvert, nframe) o (nvert, 1, nframe)
    if data.ndim == 4:
        nvert = data.shape[0]
        nframe = data.shape[-1]
        arr = np.reshape(data, (nvert, nframe))
    elif data.ndim == 3:
        nvert = data.shape[0]
        nframe = data.shape[-1]
        arr = np.reshape(data, (nvert, nframe))
    elif data.ndim == 2:
        arr = data
    elif data.ndim == 1:
        arr = data[:, None]
    else:
        raise ValueError(f"Dimensioni MGH inaspettate: {data.shape}")
    return arr

def parse_label(label_path: str):
    """
    Ritorna:
      - lista degli ID vertice presenti nella label
      - dizionario vtx -> (x,y,z) dalle coordinate nella label
    Formato label FS: prima riga commento, seconda riga nvert, poi righe: vno x y z stat
    """
    vtx_ids: List[int] = []
    coords: Dict[int, Tuple[float, float, float]] = {}
    with open(label_path, 'r') as f:
        _ = f.readline()  # commento
        _ = f.readline()  # nvert (potrebbe non essere utilizzabile)
        for line in f:
            line = line.strip()
            if not line:
                continue
```

```
            parts = line.split()
            if len(parts) < 5:
                continue
            v = int(parts[0])
            x, y, z = map(float, parts[1:4])
            vtx_ids.append(v)
            coords[v] = (x, y, z)
    if not vtx_ids:
        raise ValueError(f"Nessun vertice trovato nella label {label_path}")
    return vtx_ids, coords

def parse_fsgd_groups(fsgd_path: str,
                      class_a: Optional[str] = None,
                      class_b: Optional[str] = None) -> Tuple[List[int], List[int], str, str]:
    """
    Legge l'FSGD e restituisce:
      - indici di frame per class_a
      - indici di frame per class_b
      - nomi canonici class_a, class_b (eventualmente dedotti)
    """
    declared_classes: List[str] = []
    frames_by_class: Dict[str, List[int]] = {}

    # raccogli "Class:"
    with open(fsgd_path, 'r') as f:
        for line in f:
            s = line.strip()
            if s.lower().startswith('class'):
                tokens = re.sub(r':', '', s).split(maxsplit=1)
                if len(tokens) == 2:
                    cname = tokens[1].strip()
                    if cname and cname not in declared_classes:
                        declared_classes.append(cname)

    # mappa frame -> classe
    frame = 0
    with open(fsgd_path, 'r') as f:
        for line in f:
            s = line.strip()
            if not s or not s.lower().startswith('input'):
                continue
            tokens = re.sub(r':', '', s).split()
            if len(tokens) < 3:
                raise ValueError(f"Riga Input anomala nell'FSGD: {s}")
            cname = tokens[2]
            frames_by_class.setdefault(cname, []).append(frame)
            frame += 1

    # decide classi
    if class_a is None or class_b is None:
        candidates = declared_classes[:] if len(declared_classes) >= 2 else list(frames_by_class.keys())
        if len(candidates) < 2:
            raise ValueError("Impossibile dedurre due classi dal file FSGD; specifica --class-a e --class-b.")
        if class_a is None:
            class_a = candidates[0]
        if class_b is None:
            class_b = candidates[1]

    idx_a = frames_by_class.get(class_a, [])
    idx_b = frames_by_class.get(class_b, [])
    if not idx_a:
        print(f"Attenzione: nessun frame con classe '{class_a}'", file=sys.stderr)
    if not idx_b:
        print(f"Attenzione: nessun frame con classe '{class_b}'", file=sys.stderr)
    return idx_a, idx_b, class_a, class_b

def compute_stats(x_arr):
    """Calcola stats su array 1D (ignora NaN)."""
    x = np.array(x_arr, dtype=float)
    x = x[np.isfinite(x)]
    if x.size == 0:
        return dict(n=0, n_valid=0, mean=np.nan, sd=np.nan, median=np.nan,
                    min=np.nan, max=np.nan, p25=np.nan, p75=np.nan, iqr=np.nan)
    p25, p75 = np.percentile(x, [25, 75])
    return dict(
        n=int(x.size),
        n_valid=int(np.isfinite(x).sum()),
        mean=float(np.nanmean(x)),
        sd=float(np.nanstd(x, ddof=1)) if x.size>1 else float('nan'),
        median=float(np.nanmedian(x)),
        min=float(np.nanmin(x)),
        max=float(np.nanmax(x)),
        p25=float(p25),
        p75=float(p75),
        iqr=float(p75 - p25),
    )

def main():
    ap = argparse.ArgumentParser(description="CSV per-vertice e statistiche per due gruppi definiti da FSGD (';' e virgola
decimale).")
```

```
    ap.add_argument('--label', required=True, help='Percorso alla label (es. lh.ROI_fsaverage.label)')
    ap.add_argument('--mgh', required=True, help='File MGH/MGZ multi-frame (tutti i soggetti/input)')
    ap.add_argument('--fsgd', required=True, help='File FSGD con Class e Input')
    ap.add_argument('--class-a', default=None, help='Nome della prima classe (se assente, dedotta)')
    ap.add_argument('--class-b', default=None, help='Nome della seconda classe (se assente, dedotta)')
    ap.add_argument('--out', required=True, help='Percorso del CSV di output per-vertice')
    ap.add_argument('--stats-out', default=None, help='Percorso del CSV di output per statistiche (opzionale)')
    args = ap.parse_args()

    # Indici frame per ciascun gruppo
    idx_a, idx_b, class_a, class_b = parse_fsgd_groups(args.fsgd, args.class_a, args.class_b)

    # Carica MGH
    arr = load_mgh_2d(args.mgh)
    nvert, nframe = arr.shape
    idx_a = [i for i in idx_a if 0 <= i < nframe]
    idx_b = [i for i in idx_b if 0 <= i < nframe]

    # Medie per gruppo
    a_mean = np.full(nvert, np.nan, dtype=float)
    b_mean = np.full(nvert, np.nan, dtype=float)
    if idx_a:
        a_mean = np.nanmean(arr[:, idx_a], axis=1)
    if idx_b:
        b_mean = np.nanmean(arr[:, idx_b], axis=1)

    # Leggi label
    vtx_ids, coords = parse_label(args.label)

    # CSV per-vertice
    with open(args.out, 'w', newline='') as f:
        w = csv.writer(f, delimiter=';')
        w.writerow(['vertex_id', 'x', 'y', 'z', f'value_{class_a}', f'value_{class_b}'])
        for v in vtx_ids:
            if v >= nvert:
                continue
            x, y, z = coords.get(v, (np.nan, np.nan, np.nan))
            w.writerow([v, fmt(x), fmt(y), fmt(z), fmt(a_mean[v]), fmt(b_mean[v])])

    print(f"Fatto! Salvato CSV per-vertice in: {args.out}")

    # CSV statistiche (opzionale)
    if args.stats_out:
        a_vec = [] if np.all(np.isnan(a_mean)) else [a_mean[v] for v in vtx_ids if v < nvert]
        b_vec = [] if np.all(np.isnan(b_mean)) else [b_mean[v] for v in vtx_ids if v < nvert]
        s_a = compute_stats(a_vec)
        s_b = compute_stats(b_vec)
        with open(args.stats_out, 'w', newline='') as fs:
            w = csv.writer(fs, delimiter=';')
            w.writerow(['group','n','n_valid','mean','sd','median','min','max','p25','p75','IQR'])
            w.writerow([class_a, s_a['n'], s_a['n_valid'], fmt(s_a['mean']), fmt(s_a['sd']), fmt(s_a['median']),
                        fmt(s_a['min']), fmt(s_a['max']), fmt(s_a['p25']), fmt(s_a['p75']), fmt(s_a['iqr'])])
            w.writerow([class_b, s_b['n'], s_b['n_valid'], fmt(s_b['mean']), fmt(s_b['sd']), fmt(s_b['median']),
                        fmt(s_b['min']), fmt(s_b['max']), fmt(s_b['p25']), fmt(s_b['p75']), fmt(s_b['iqr'])])
        print(f"Statistiche salvate in: {args.stats_out}")

    print(f"Classi: {class_a} (nframe={len(idx_a)}), {class_b} (nframe={len(idx_b)}) | Vertici nella label: {len(vtx_ids)} |
nframe totali: {nframe}")

if __name__ == '__main__':
    main()
```

```python
#!/usr/bin/env python3
# -*- coding: utf-8 -*-
"""
SCRIPT: LABEL_TO_CSV_REST_TASK

Estrae per ogni vertice di una label:
- ID vertice
- coordinate (x, y, z) dalla label
- valore medio della misura in Rest (media sui frame Rest)
- valore medio della misura in Task (media sui frame Task)

In più (opzionale) crea un secondo CSV con statistiche descrittive
separate per Rest e Task (n, mean, sd, median, min, max, p25, p75, IQR).

Requisiti: nibabel, numpy
    pip install nibabel numpy

Uso:
    python label_to_csv_rest_task.py \
        --label /path/lh.ROI.label \
        --mgh /path/lh.allinputs.flair3d.sm05.mgh \
        --fsgd /path/all_grouped_by-task.fsgd \
        --out /path/roi_values_rest_task.csv \
        --stats-out /path/roi_stats_rest_task.csv \
        [--cond-rest Rest] [--cond-task Task]

Nota: si assume che le righe "Input" dell'FSGD siano nel formato
      "Input: <soggetto> <condizione> [covariate...]"
      e che l'ordine delle righe corrisponda ai frame del file MGH.
"""
import argparse
import csv
import re
import sys
from typing import List, Tuple, Dict

import numpy as np

try:
    import nibabel as nib
except Exception as e:
    print("Errore: serve 'nibabel' (pip install nibabel).", file=sys.stderr)
    raise

def fmt(v: float, ndigits: int = 6) -> str:
    """Formatta numeri con virgola come separatore decimale; stringa vuota per NaN."""
    try:
        if v is None or (isinstance(v, float) and np.isnan(v)):
            return ''
        s = f"{float(v):.{ndigits}f}"
        return s.replace('.', ',')
    except Exception:
        return str(v).replace('.', ',')

def parse_fsgd_frames(fsgd_path: str, rest_name: str, task_name: str) -> Tuple[List[int], List[int]]:
    rest_idx: List[int] = []
    task_idx: List[int] = []
    frame = 0
    with open(fsgd_path, 'r') as f:
        for line in f:
            line = line.strip()
            if not line or not line.lower().startswith('input'):
                continue
            # tokenizza: es. "Input: subjID Rest ..." -> cond sta in tokens[2]
            tokens = re.sub(r':', '', line).split()
            if len(tokens) < 3:
                raise ValueError(f"Riga Input anomala nell'FSGD: {line}")
            cond = tokens[2]
            if cond == rest_name:
                rest_idx.append(frame)
            elif cond == task_name:
                task_idx.append(frame)
            frame += 1
    if not rest_idx:
        print(f"Attenzione: nessun frame con condizione '{rest_name}' trovato in {fsgd_path}", file=sys.stderr)
    if not task_idx:
        print(f"Attenzione: nessun frame con condizione '{task_name}' trovato in {fsgd_path}", file=sys.stderr)
    return rest_idx, task_idx

def load_mgh_2d(mgh_path: str) -> np.ndarray:
    img = nib.load(mgh_path)
    data = img.get_fdata()
    # Atteso: (nvert, 1, 1, nframe) oppure (nvert, nframe)
    if data.ndim == 4:
        nvert = data.shape[0]
        nframe = data.shape[-1]
        arr = np.reshape(data, (nvert, nframe))
    elif data.ndim == 2:
        arr = data
    elif data.ndim == 3:
```

```
        nvert = data.shape[0]
        nframe = data.shape[-1]
        arr = np.reshape(data, (nvert, nframe))
    elif data.ndim == 1:
        arr = data[:, None]
    else:
        raise ValueError(f"Dimensioni MGH inaspettate: {data.shape}")
    return arr

def parse_label(label_path: str) -> Tuple[List[int], Dict[int, Tuple[float, float, float]]]:
    """
    Ritorna:
      - lista degli ID vertice presenti nella label
      - dizionario vtx -> (x,y,z) dalle coordinate memorizzate nella label
    Formato label FS: prima riga commento, seconda riga nvert, poi righe: vno x y z stat
    """
    vtx_ids: List[int] = []
    coords: Dict[int, Tuple[float, float, float]] = {}
    with open(label_path, 'r') as f:
        header = f.readline()
        n_line = f.readline()
        try:
            int(n_line.strip())
        except Exception:
            pass
        for line in f:
            line = line.strip()
            if not line:
                continue
            parts = line.split()
            if len(parts) < 5:
                continue
            v = int(parts[0])
            x, y, z = map(float, parts[1:4])
            vtx_ids.append(v)
            coords[v] = (x, y, z)
    if not vtx_ids:
        raise ValueError(f"Nessun vertice trovato nella label {label_path}")
    return vtx_ids, coords

def compute_stats(x_arr):
    """Calcola stats su array 1D (ignora NaN)."""
    x = np.array(x_arr, dtype=float)
    x = x[np.isfinite(x)]
    if x.size == 0:
        return dict(n=0, n_valid=0, mean=np.nan, sd=np.nan, median=np.nan,
                    min=np.nan, max=np.nan, p25=np.nan, p75=np.nan, iqr=np.nan)
    p25, p75 = np.percentile(x, [25, 75])
    return dict(
        n=int(x.size),
        n_valid=int(np.isfinite(x).sum()),
        mean=float(np.nanmean(x)),
        sd=float(np.nanstd(x, ddof=1)) if x.size>1 else float('nan'),
        median=float(np.nanmedian(x)),
        min=float(np.nanmin(x)),
        max=float(np.nanmax(x)),
        p25=float(p25),
        p75=float(p75),
        iqr=float(p75 - p25),
    )

def main():
    ap = argparse.ArgumentParser(description="Estrae valori Rest/Task per vertici di una label e salva CSV con ';'.
Opzionale: CSV con statistiche per Rest/Task.")
    ap.add_argument('--label', required=True, help='Percorso alla label (es. lh.MIAroi.label su fsaverage)')
    ap.add_argument('--mgh', required=True, help='File MGH/MGZ multi-frame (tutti i soggetti/input)')
    ap.add_argument('--fsgd', required=True, help='File FSGD usato per mris_preproc (con Rest/Task)')
    ap.add_argument('--cond-rest', default='Rest', help="Nome condizione 'Rest' nel file FSGD (default: Rest)")
    ap.add_argument('--cond-task', default='Task', help="Nome condizione 'Task' nel file FSGD (default: Task)")
    ap.add_argument('--out', required=True, help='Percorso del CSV di output (per-vertice)')
    ap.add_argument('--stats-out', default=None, help='Percorso CSV per esportare statistiche descrittive (opzionale)')
    args = ap.parse_args()

    # 1) frame per ciascuna condizione
    rest_idx, task_idx = parse_fsgd_frames(args.fsgd, args.cond_rest, args.cond_task)
    if not rest_idx and not task_idx:
        print("Errore: nessun frame Rest/Task trovato; controlla --cond-rest/--cond-task e l'FSGD.", file=sys.stderr)
        sys.exit(1)

    # 2) carica MGH (vertici x frames)
    arr = load_mgh_2d(args.mgh)
    nvert, nframe = arr.shape
    # Sanitizza indici fuori range
    rest_idx = [i for i in rest_idx if 0 <= i < nframe]
    task_idx = [i for i in task_idx if 0 <= i < nframe]

    # 3) medie per condizione (per vertice)
    rest_mean = np.full(nvert, np.nan, dtype=float)
    task_mean = np.full(nvert, np.nan, dtype=float)
    if rest_idx:
```

```
        rest_mean = np.nanmean(arr[:, rest_idx], axis=1)
    if task_idx:
        task_mean = np.nanmean(arr[:, task_idx], axis=1)

    # 4) leggi label (ID e coordinate)
    vtx_ids, coords = parse_label(args.label)

    # 5) CSV per-vertice con ';' e virgola decimale
    with open(args.out, 'w', newline='') as f:
        writer = csv.writer(f, delimiter=';')
        writer.writerow(['vertex_id', 'x', 'y', 'z', f'value_{args.cond_rest}', f'value_{args.cond_task}'])
        for v in vtx_ids:
            if v >= nvert:
                continue
            x, y, z = coords.get(v, (np.nan, np.nan, np.nan))
            writer.writerow([v, fmt(x), fmt(y), fmt(z), fmt(rest_mean[v]), fmt(task_mean[v])])

    print(f"Fatto! Salvato CSV in: {args.out}")

    # 6) CSV statistiche (se richiesto)
    if args.stats_out:
        rest_vec = [] if np.all(np.isnan(rest_mean)) else [rest_mean[v] for v in vtx_ids if v < nvert]
        task_vec = [] if np.all(np.isnan(task_mean)) else [task_mean[v] for v in vtx_ids if v < nvert]
        s_rest = compute_stats(rest_vec)
        s_task = compute_stats(task_vec)
        with open(args.stats_out, 'w', newline='') as fs:
            w = csv.writer(fs, delimiter=';')
            w.writerow(['condition','n','n_valid','mean','sd','median','min','max','p25','p75','IQR'])
            w.writerow(['Rest', s_rest['n'], s_rest['n_valid'], fmt(s_rest['mean']), fmt(s_rest['sd']),
fmt(s_rest['median']),
                        fmt(s_rest['min']), fmt(s_rest['max']), fmt(s_rest['p25']), fmt(s_rest['p75']), fmt(s_rest['iqr'])])
            w.writerow(['Task', s_task['n'], s_task['n_valid'], fmt(s_task['mean']), fmt(s_task['sd']),
fmt(s_task['median']),
                        fmt(s_task['min']), fmt(s_task['max']), fmt(s_task['p25']), fmt(s_task['p75']), fmt(s_task['iqr'])])
        print(f"Statistiche salvate in: {args.stats_out}")

    print(f"Vertici in label: {len(vtx_ids)} | nframe totali: {nframe} | Rest={len(rest_idx)} | Task={len(task_idx)}")

if __name__ == '__main__':
    main()
```

```python
#!/usr/bin/env python3
"""
SCRIPT: MAKE_WPTS_FROM_CLUSTERS_SPACE

make_wpts_from_clusters_space.py

Crea un point set (.wpts) dai VtxMax del summary di mri_surfcluster.

- Legge il file *_summary.txt (mri_surfcluster --sum)
- Estrae in modo robusto tutti i VtxMax e le rispettive Annot
- Usa la superficie indicata (white / inflated / ecc.) per i vertici
- Converte opzionalmente in Scanner RAS (per Freeview)

USO TIPICO (Freeview):
  python3 make_wpts_from_clusters_space.py \
    --summary "lh.*_summary.txt" \
    --hemi lh \
    --subject fsaverage \
    --surf inflated \
    --subjects-dir $SUBJECTS_DIR \
    --space scanner \
    --out-wpts lh_clusters_scanner.wpts
"""

import argparse
import os
import re
import sys
import glob
import pathlib
from typing import List, Tuple

import numpy as np

try:
    import nibabel as nib
except ImportError:
    print("ERROR: nibabel required (pip install nibabel)", file=sys.stderr)
    sys.exit(1)


# ------------------------------------------------------------
# Utils
# ------------------------------------------------------------

def resolve_summary(pattern: str) -> str:
    """Risolve un pattern (glob) in un file summary, scegliendo il più recente."""
    pattern = os.path.expanduser(os.path.expandvars(pattern))
    matches = sorted(glob.glob(pattern))
    if not matches:
        raise FileNotFoundError(f"Nessun file trovato per pattern: {pattern}")
    # prendi il più recente per mtime
    return max(matches, key=lambda p: os.path.getmtime(p))


def parse_summary(summary_path: str) -> Tuple[List[int], List[str]]:
    """
    Parsing robusto del file *_summary.txt di mri_surfcluster.

    Restituisce:
      - lista dei VtxMax (int)
      - lista delle label (Annot, str)
    """

    with open(summary_path, "r", encoding="utf-8", errors="ignore") as f:
        lines = f.readlines()

    # 1) trova l'header con la parola "VtxMax"
    header_line_idx = None
    raw_header_tokens = None
    for i, ln in enumerate(lines):
        if re.search(r"\bVtxMax\b", ln):
            header_line_idx = i
            raw_header_tokens = re.split(r"\s+", ln.strip())
            break

    if header_line_idx is None or raw_header_tokens is None:
        raise RuntimeError("Header con 'VtxMax' non trovato nel summary")

    # 2) rimuovi eventuale '#' iniziale dall'header
    if raw_header_tokens[0] == "#" or raw_header_tokens[0].startswith("#"):
        header_tokens = raw_header_tokens[1:]
    else:
        header_tokens = raw_header_tokens

    # 3) indice della colonna "VtxMax" nell'header pulito
    try:
        vtx_col = header_tokens.index("VtxMax")
```

```
    except ValueError:
        raise RuntimeError("Colonna 'VtxMax' non trovata nell'header")

    # 4) parse delle righe successive (la tabella vera)
    vtx_list: List[int] = []
    labels: List[str] = []

    for ln in lines[header_line_idx + 1:]:
        if not ln.strip():
            continue
        if ln.lstrip().startswith("#"):
            continue

        parts = re.split(r"\s+", ln.strip())
        # le colonne dei dati corrispondono a header_tokens (senza '#')
        if len(parts) <= vtx_col:
            continue

        vtx_txt = parts[vtx_col]
        if not vtx_txt.isdigit():
            # se qui non è un numero, probabilmente non è una riga di dati
            continue

        vtx = int(vtx_txt)
        annot = parts[-1]  # Annot è l'ultima colonna

        vtx_list.append(vtx)
        labels.append(annot)

    if not vtx_list:
        raise RuntimeError("Nessun cluster trovato: controlla il formato del summary")

    return vtx_list, labels


def load_surface_coords(subjects_dir: str, subject: str, hemi: str, surf: str):
    """Carica le coordinate dei vertici dalla superficie <hemi>.<surf>."""
    surf_path = os.path.join(subjects_dir, subject, "surf", f"{hemi}.{surf}")
    if not os.path.exists(surf_path):
        raise FileNotFoundError(f"Superficie non trovata: {surf_path}")
    coords, faces = nib.freesurfer.read_geometry(surf_path)
    return coords


def tkreg_to_scanner(subjects_dir: str, subject: str) -> np.ndarray:
    """
    Matrice 4x4 per convertire coordinate surface/tkReg RAS -> Scanner RAS.

    M = vox2ras * inv(tkrvox2ras)
    """
    orig = os.path.join(subjects_dir, subject, "mri", "orig.mgz")
    if not os.path.exists(orig):
        raise FileNotFoundError(f"Volume orig.mgz non trovato: {orig}")

    img = nib.load(orig)
    vox2ras = img.affine

    try:
        tkr = img.header.get_vox2ras_tkr()
    except Exception:
        # fallback vecchio stile
        _, _, hdr = nib.freesurfer.io.read_mgh(orig, return_header=True)
        tkr = hdr.get_vox2ras_tkr()

    M = vox2ras @ np.linalg.inv(tkr)
    return M


# ------------------------------------------------------------
# Main
# ------------------------------------------------------------

def main():
    ap = argparse.ArgumentParser(
        description="Crea .wpts dai VtxMax del summary (coordinate scanner/surface)."
    )
    ap.add_argument("--summary", required=True,
                    help="File summary o pattern glob (es. 'lh.*_summary.txt').")
    ap.add_argument("--hemi", required=True, choices=["lh", "rh"],
                    help="Emisfero (lh/rh).")
    ap.add_argument("--subject", default="fsaverage",
                    help="Soggetto Freesurfer (default: fsaverage).")
    ap.add_argument("--surf", default="white",
                    help="Superficie (white, inflated, pial, ecc.).")
    ap.add_argument("--subjects-dir", default=os.environ.get("SUBJECTS_DIR", ""),
                    help="SUBJECTS_DIR (default: variabile d'ambiente).")
    ap.add_argument("--out-wpts", default=None,
                    help="Output .wpts (default: <hemi>_clusters_<space>.wpts).")
```

```
    ap.add_argument("--space", choices=["scanner", "surface"], default="scanner",
                    help="Spazio delle coordinate: 'scanner' (Freeview) o 'surface' (tkReg).")
    args = ap.parse_args()

    if not args.subjects_dir:
        print("ERROR: specifica --subjects-dir o imposta SUBJECTS_DIR", file=sys.stderr)
        sys.exit(2)

    # 1) Risolvi il summary (glob -> file)
    summary = resolve_summary(args.summary)
    print(f"Using summary: {summary}")

    # 2) Estrai VtxMax e Annot
    vtx, labels = parse_summary(summary)
    print(f"Trovati {len(vtx)} cluster")

    # 3) Carica superficie
    coords = load_surface_coords(args.subjects_dir, args.subject, args.hemi, args.surf)

    # 4) Prepara nome output
    if args.out_wpts is None:
        args.out_wpts = f"{args.hemi}_clusters_{args.space}.wpts"
    out_path = pathlib.Path(args.out_wpts).resolve()

    # 5) Matrice conversione surface->scanner, se richiesta
    M = None
    if args.space == "scanner":
        M = tkreg_to_scanner(args.subjects_dir, args.subject)

    # 6) Scrivi .wpts
    skipped = 0
    with open(out_path, "w") as f:
        for i, (vid, lab) in enumerate(zip(vtx, labels), start=1):
            if vid < 0 or vid >= len(coords):
                print(f"WARNING: vertex {vid} fuori range per la mesh, salto", file=sys.stderr)
                skipped += 1
                continue

            x, y, z = coords[vid]

            if M is not None:
                v = np.array([x, y, z, 1.0])
                x, y, z, _ = (M @ v).tolist()

            tag = f"C{i:02d}_vtx{vid}_{lab[:40].replace(' ', '_')}"
            f.write(f"{x:.5f} {y:.5f} {z:.5f} {tag}\n")

    print("\nDONE:")
    print(f"  -> {out_path}")
    if skipped:
        print(f"  (cluster saltati per vertex out-of-range: {skipped})")

    print("\nEsempio Freeview:")
    if args.space == "scanner":
        print(f"  freeview -v $SUBJECTS_DIR/{args.subject}/mri/orig.mgz "
              f"-f $SUBJECTS_DIR/{args.subject}/surf/{args.hemi}.{args.surf} "
              f"-w {out_path}")
    else:
        print(f"  freeview -f $SUBJECTS_DIR/{args.subject}/surf/{args.hemi}.{args.surf} "
              f"-w {out_path}")


if __name__ == "__main__":
    main()
```

```python
#!/usr/bin/env python3
"""
SCRIPT: PLOT_VERTEX_BOXPLOT

Box plot per dati FreeSurfer al singolo vertice, separati per classe (FSGD).

Funzionalità chiave
- Multi-overlay (es. LH e RH), multi-vertice.
- Etichette assi personalizzabili (--xlabel/--ylabel) e titolo base (--title-base).
- Media come linea (--meanline) e triangolino media anche con la linea (--mean-both).
- Annotazioni della media: --annotate-means; posizione (--annotate-pos inline/above);
  offset x (--annotate-xoffset); cifre (--mean-digits).
- Ordine delle classi sull'asse X: --x-order "Rest,Task".
- Statistiche descrittive (--stats) e salvataggio CSV (--stats-csv).
- Separatore CSV configurabile (--csv-sep, default ';') e separatore decimale (--decimal, default ',').
- Risoluzione robusta dei path overlay (.mgh/.mgz, con/senza .smXX).

Requisiti: nibabel, numpy, matplotlib
"""
import argparse
import os
import re
from collections import defaultdict
from pathlib import Path

import nibabel as nib
import numpy as np
import matplotlib.pyplot as plt


def parse_args():
    ap = argparse.ArgumentParser(
        description="Box plot Rest vs Task (o altre Class) al singolo vertice da overlay 4D + FSGD"
    )
    ap.add_argument("--overlay", required=True, nargs="+",
                    help="Uno o più overlay 4D .mgh/.mgz (senza paired-diff). Puoi passare LH e RH.")
    ap.add_argument("--fsgd", required=True, help="File .fsgd con gli Input (ordine dei frame)")
    ap.add_argument("--vertices", required=True, nargs="+", type=int,
                    help="Uno o più indici di vertice (0-based)")
    ap.add_argument("--outdir", default=None,
                    help="Cartella output per i PNG (creata se non esiste). Se omessa, mostra i grafici a schermo.")
    ap.add_argument("--prefix", default="box",
                    help="Prefisso dei file PNG (default: box)")
    ap.add_argument("--title-base", default=None,
                    help="Prefisso titolo del grafico; verrà completato con emisfero e vertice")
    ap.add_argument("--xlabel", default="Classe (condizione)",
                    help='Etichetta asse X (default: "Classe (condizione)")')
    ap.add_argument("--ylabel", default="FLAIR cortical intensity (a.u.)",
                    help='Etichetta asse Y (default: "FLAIR cortical intensity (a.u.)")')
    ap.add_argument("--show-points", action="store_true",
                    help="Mostra anche i punti individuali (jitter) sopra le scatole")
    ap.add_argument("--meanline", action="store_true",
                    help="Disegna la MEDIA come linea invece del triangolo (showmeans)")
    ap.add_argument("--mean-both", action="store_true",
                    help="Disegna SIA la linea della media SIA il triangolino (richiede --meanline)")
    ap.add_argument("--annotate-means", action="store_true",
                    help="Scrive il valore della media per ciascuna classe")
    ap.add_argument("--annotate-pos", choices=["above","inline"], default="inline",
                    help="Posizione del testo delle medie: above=sopra; inline=affianco alla scatola alla quota della media
(default: inline)")
    ap.add_argument("--annotate-xoffset", type=float, default=0.25,
                    help="Offset orizzontale per l'annotazione inline (default: 0.25 a destra)")
    ap.add_argument("--mean-digits", type=int, default=3,
                    help="Numero di cifre per la media annotata (default: 3)")
    ap.add_argument("--stats", action="store_true",
                    help="Stampa statistiche descrittive per ogni classe (n, media, mediana, sd, IQR)")
    ap.add_argument("--stats-csv", default=None,
                    help="Percorso CSV o cartella per salvare le statistiche (opzionale)")
    ap.add_argument("--csv-sep", default=";",
                    help="Separatore dei campi nel CSV (default: ;)")
    ap.add_argument("--decimal", default=",",
                    help="Separatore decimale per numeri in CSV e in console (default: ,)")
    ap.add_argument("--x-order", default=None,
                    help="Ordine delle classi sull'asse X (lista separata da virgole, es: Rest,Task)")
    return ap.parse_args()


def resolve_overlay_path(path: str) -> str:
    p = Path(path)
    if p.exists():
        return str(p)

    candidates = []
    stem = p.name

    # Alterna .mgh <-> .mgz
    if stem.endswith(".mgh"):
        candidates.append(str(p.with_suffix(".mgz")))
    elif stem.endswith(".mgz"):
        candidates.append(str(p.with_suffix(".mgh")))
```

```
90
91      # Rimuovi eventuale .smNN prima dell'estensione
92      if ".sm" in stem:
93          base, ext = os.path.splitext(stem)
94          base_no_sm = re.sub(r"\.sm\d+$", "", base)
95          candidates.append(str(p.with_name(base_no_sm + ext)))
96          if ext == ".mgh":
97              candidates.append(str(p.with_name(base_no_sm + ".mgz")))
98          elif ext == ".mgz":
99              candidates.append(str(p.with_name(base_no_sm + ".mgh")))
100
101     # Variante lisciata se non lo era
102     if ".sm" not in stem:
103         base, ext = os.path.splitext(stem)
104         for sm in (5, 10, 15, 20, 25):
105             candidates.append(str(p.with_name(f"{base}.sm{sm}{ext}")))
106
107     for cand in candidates:
108         if Path(cand).exists():
109             return cand
110
111     raise FileNotFoundError(
112         f"Overlay non trovato: {path}\nTentativi: " + "\n  - ".join(candidates)
113     )
114
115
116 def load_overlay_4d(path):
117     real_path = resolve_overlay_path(path)
118     img = nib.load(real_path)
119     dataobj = np.asarray(img.dataobj)
120     if dataobj.ndim == 4:
121         nvert, _, _, nframes = dataobj.shape
122         data = dataobj.reshape(nvert, nframes)
123     elif dataobj.ndim == 2:
124         data = dataobj
125         nvert, nframes = data.shape
126     else:
127         raise ValueError(f"Overlay con shape inaspettato: {dataobj.shape}")
128     return data, real_path
129
130
131 def load_fsgd_inputs_classes(fsgd_path):
132     inputs, classes = [], []
133     with open(fsgd_path, "r") as f:
134         for line in f:
135             if line.startswith("Input"):
136                 parts = line.strip().split()
137                 if len(parts) < 3:
138                     raise ValueError(f"Riga Input non riconosciuta: {line.strip()}")
139                 inputs.append(parts[1])
140                 classes.append(parts[2])
141     if not inputs:
142         raise ValueError("Nessun 'Input' trovato nell'FSGD.")
143     return inputs, classes
144
145
146 def guess_hemi_from_name(path: str) -> str:
147     name = Path(path).name.lower()
148     if "lh." in name or "_lh" in name or name.startswith("lh"):
149         return "lh"
150     if "rh." in name or "_rh" in name or name.startswith("rh"):
151         return "rh"
152     parts = [p.lower() for p in Path(path).parts]
153     if "lh" in parts:
154         return "lh"
155     if "rh" in parts:
156         return "rh"
157     return "hemi"
158
159
160 def boxplot_by_class(values_per_frame, classes, *, title=None,
161                      xlabel="Classe (condizione)", ylabel="FLAIR cortical intensity (a.u.)",
162                      show_points=False, out_png=None,
163                      meanline=False, mean_both=False,
164                      annotate_means=False, annotate_pos="inline", annotate_xoffset=0.25, mean_digits=3,
165                      stats=False, stats_csv_path=None, csv_sep=";", decimal=",",
166                      x_order=None):
167     # Raggruppa per classe nell'ordine di apparizione
168     seen = []
169     class_to_vals = defaultdict(list)
170     for v, c in zip(values_per_frame, classes):
171         if c not in seen:
172             seen.append(c)
173         class_to_vals[c].append(float(v))
174
175     # Ordina le classi secondo x_order, se fornito
176     if x_order:
177         desired = [s.strip() for s in x_order.split(",") if s.strip()]
178         lower_map = {c.lower(): c for c in seen}
179         ordered = []
```

```
        used = set()
        for d in desired:
            ckey = d.lower()
            if ckey in lower_map:
                c = lower_map[ckey]
                if c not in used:
                    ordered.append(c); used.add(c)
        for c in seen:
            if c not in used:
                ordered.append(c)
        labels = ordered
    else:
        labels = list(seen)

    data = [class_to_vals[c] for c in labels]

    # Statistiche opzionali
    if stats:
        print("\n[STAT]", title if title else "Box plot")
        print("Classe,n,mean,median,sd,iqr,min,max")
        stats_rows = []
        def fmt(x):
            try:
                import math
                if x is None or (isinstance(x, float) and (math.isnan(x) or math.isinf(x))):
                    return ""
                s = f"{x:.6g}"
            except Exception:
                s = str(x)
            return s.replace(".", decimal)
        for c, arr in zip(labels, data):
            arr = np.asarray(arr, dtype=float)
            n = arr.size
            mean = float(np.mean(arr)) if n>0 else float('nan')
            med  = float(np.median(arr)) if n>0 else float('nan')
            sd   = float(np.std(arr, ddof=1)) if n>1 else float('nan')
            if n>0:
                q75, q25 = np.percentile(arr, [75, 25])
                iqr = float(q75 - q25)
                mn, mx = float(np.min(arr)), float(np.max(arr))
            else:
                iqr = mn = mx = float('nan')
            print(f"{c},{n},{fmt(mean)},{fmt(med)},{fmt(sd)},{fmt(iqr)},{fmt(mn)},{fmt(mx)}")
            stats_rows.append((c,n,mean,med,sd,iqr,mn,mx))
        if stats_csv_path:
            stats_csv_path = Path(stats_csv_path)
            stats_csv_path.parent.mkdir(parents=True, exist_ok=True)
            import csv
            with stats_csv_path.open("w", newline="", encoding="utf-8") as f:
                w = csv.writer(f, delimiter=csv_sep)
                w.writerow(["class","n","mean","median","sd","iqr","min","max"])
                for (c,n,mean,med,sd,iqr,mn,mx) in stats_rows:
                    w.writerow([c, n, fmt(mean), fmt(med), fmt(sd), fmt(iqr), fmt(mn), fmt(mx)])
            print(f"[OK] Salvato stats CSV: {stats_csv_path}")

    plt.figure()
    # showmeans True: se meanline True, matplotlib usa una linea; se vuoi anche il triangolo, lo disegnamo dopo.
    plt.boxplot(data, tick_labels=labels, showmeans=True, meanline=meanline)
    plt.xlabel(xlabel)
    plt.ylabel(ylabel)
    if title:
        plt.title(title)

    ax = plt.gca()

    # Punti individuali jitter (opzionale)
    if show_points:
        rng = np.random.default_rng(42)
        for i, arr in enumerate(data, start=1):
            x = np.full(len(arr), i, dtype=float)
            x += rng.normal(0, 0.04, size=len(arr))
            plt.plot(x, arr, "o", alpha=0.9)

    # Calcola medie per marker/annotazioni
    means = []
    for arr in data:
        arr = np.asarray(arr, dtype=float)
        means.append(float(np.mean(arr)) if arr.size else float("nan"))

    # Se meanline è attivo e vuoi anche il triangolino → disegna marker manuali
    if meanline and mean_both:
        for i, m in enumerate(means, start=1):
            if np.isfinite(m):
                ax.plot(i, m, marker="^")

    # Se inline, allarga xlim per mostrare il testo spostato
    if annotate_means and annotate_pos == "inline" and len(data) > 0:
        xmin, xmax = ax.get_xlim()
        ncat = len(data)
        right_needed = ncat + 0.5 + max(0.0, annotate_xoffset)
```

```
        left_needed = 0.5 - min(0.0, annotate_xoffset)
        xmin = min(xmin, left_needed)
        xmax = max(xmax, right_needed)
        ax.set_xlim(xmin, xmax)

    # Annotazioni delle medie
    if annotate_means:
        # offset verticale per 'above'
        all_vals = np.concatenate([np.asarray(arr, dtype=float) for arr in data]) if data else np.array([])
        if all_vals.size > 0:
            ymin, ymax = float(np.min(all_vals)), float(np.max(all_vals))
            vrange = ymax - ymin if ymax > ymin else (abs(ymax) + 1.0)
            yoffs = 0.02 * vrange
        else:
            yoffs = 0.0

        for i, m in enumerate(means, start=1):
            if not np.isfinite(m):
                continue
            mtxt = f"{m:.{mean_digits}g}".replace(".", decimal)
            if annotate_pos == "inline":
                ax.text(i + annotate_xoffset, m, f"mean= {mtxt}", ha="left", va="center")
            else:
                ax.text(i, m + yoffs, f"mean= {mtxt}", ha="center", va="bottom")

    plt.tight_layout()
    if out_png:
        Path(out_png).parent.mkdir(parents=True, exist_ok=True)
        plt.savefig(out_png, dpi=150)
        print(f"[OK] Salvato: {out_png}")
        plt.close()
    else:
        plt.show()


def main():
    args = parse_args()

    inputs, classes = load_fsgd_inputs_classes(args.fsgd)
    outdir = Path(args.outdir) if args.outdir else None
    if outdir:
        outdir.mkdir(parents=True, exist_ok=True)

    for overlay in args.overlay:
        data, real_path = load_overlay_4d(overlay)
        nvert, nframes = data.shape
        if nframes != len(classes):
            raise ValueError(
                f"Mismatch tra n° frame overlay ({nframes}) e n° righe Input/Class FSGD ({len(classes)}).\n"
                f"Overlay: {real_path}"
            )
        hemi = guess_hemi_from_name(real_path)
        base_title = args.title_base or Path(real_path).name

        for v in args.vertices:
            v = int(v)
            if not (0 <= v < nvert):
                raise ValueError(f"Vertex {v} fuori range [0, {nvert-1}] per overlay {real_path}")
            vals = data[v, :]
            title = f"{base_title} — {hemi.upper()} — vertex {v}"

            if outdir:
                png_name = f"{args.prefix}_{hemi}_v{v}.png"
                out_png = str(outdir / png_name)
            else:
                out_png = None

            boxplot_by_class(
                values_per_frame=vals,
                classes=classes,
                title=title,
                xlabel=args.xlabel, ylabel=args.ylabel,
                show_points=args.show_points, out_png=out_png,
                meanline=args.meanline, mean_both=args.mean_both,
                annotate_means=args.annotate_means, annotate_pos=args.annotate_pos,
                annotate_xoffset=args.annotate_xoffset, mean_digits=args.mean_digits,
                stats=args.stats, stats_csv_path=args.stats_csv,
                csv_sep=args.csv_sep if hasattr(args, "csv_sep") else args.csv_sep,  # safeguard
                decimal=args.decimal,
                x_order=args.x_order,
            )


if __name__ == "__main__":
    main()
```

```python
#!/usr/bin/env python3
# -*- coding: utf-8 -*-
"""
SCRIPT: PLOT_LINES

plot_lines.py — Plot Rest→Task line charts per vertex con pairing per *nome soggetto* dal FSGD
e controllo esplicito dell'ordine sull'asse X.

Novità:
- --x-order auto|Rest,Task|Task,Rest
  * auto: legge l'ordine delle righe 'Class' nel FSGD e posiziona i punti di conseguenza (sinistra=prima classe).
  * Rest,Task / Task,Rest: impone manualmente l'ordine da sinistra a destra.
- Le etichette dei tick X vengono riordinate per essere coerenti con l'ordine scelto.
- LOG: stampa l'ordine X risolto e quando le etichette --xticks vengono riordinate per rispettare --x-order.

FIX:
- Allineati CSV e stampe di controllo all'ordine sinistra/destra usato nel grafico e nei tooltip
  (prima colonna/valore = lato sinistro, seconda = lato destro, Δ = destro − sinistro).
"""
import os, re, argparse, warnings, sys, csv
import nibabel as nib
import numpy as np
import matplotlib.pyplot as plt

try:
    import mplcursors
    HAVE_MPLCURSORS = True
except Exception:
    HAVE_MPLCURSORS = False

# ------------------------- Utilità parsing/key -------------------------
def infer_hemisphere_from_path(p: str) -> str:
    name = os.path.basename(p).lower()
    if name.startswith("lh.") or re.search(r'(^|[^\w])lh([^\w]|$)', name):
        return "LH"
    if name.startswith("rh.") or re.search(r'(^|[^\w])rh([^\w]|$)', name):
        return "RH"
    return "HEMI"

def parse_vertices(spec: str):
    vs = set()
    for chunk in spec.split(","):
        chunk = chunk.strip()
        if not chunk:
            continue
        if "-" in chunk:
            a, b = chunk.split("-", 1)
            a, b = int(a), int(b)
            lo, hi = (a, b) if a <= b else (b, a)
            vs.update(range(lo, hi + 1))
        else:
            vs.add(int(chunk))
    return sorted(vs)

def load_fsgd(fsgd_path: str):
    """
    Ritorna:
      - inputs: lista di stringhe ID (in ordine di apparizione)
      - classes_per_input: lista parallela con la classe di ciascun input
      - class_declared_order: lista di nomi classe nell'ordine delle righe 'Class ...'
    """
    inputs, classes_per_input, class_declared_order = [], [], []
    with open(fsgd_path, "r", encoding="utf-8", errors="ignore") as fh:
        for line in fh:
            s = line.strip()
            if not s or s.startswith("#"):
                continue
            low = s.lower()
            if low.startswith("class "):
                parts = s.split()
                if len(parts) >= 2:
                    class_declared_order.append(parts[1])
            elif low.startswith("input "):
                parts = s.split()
                if len(parts) >= 3:
                    inputs.append(parts[1])
                    classes_per_input.append(parts[2])
    return inputs, classes_per_input, class_declared_order

def _key_auto(input_id: str) -> str:
    base = os.path.splitext(os.path.basename(input_id))[0]
    key = re.sub(r'([_\-])?(rest|task)(match)?$', '', base, flags=re.IGNORECASE)
    return key

def _key_exact(input_id: str) -> str:
    return input_id

def _key_regex(input_id: str, pattern: str) -> str:
    base = os.path.splitext(os.path.basename(input_id))[0]
    m = re.search(pattern, base)
```

```
    if not m:
        return base
    return m.group(1) if m.groups() else m.group(0)

# ------------------------- Pairing per soggetto -------------------------
def build_pairs(inputs, classes, pair_by="auto", key_regex=None, fail_on_duplicates=False):
    if pair_by not in {"auto", "exact", "regex"}:
        raise ValueError("pair_by deve essere uno tra: auto, exact, regex")

    def make_key(s: str) -> str:
        if pair_by == "auto":
            return _key_auto(s)
        elif pair_by == "exact":
            return _key_exact(s)
        else:
            if not key_regex:
                raise ValueError("Con --pair-by regex devi specificare --key-regex")
            return _key_regex(s, key_regex)

    rest_map, task_map = {}, {}
    for i, (inp, cls) in enumerate(zip(inputs, classes)):
        k = make_key(inp)
        cl = cls.lower()
        if cl == "rest":
            rest_map.setdefault(k, []).append(i)
        elif cl == "task":
            task_map.setdefault(k, []).append(i)

    common = [k for k in rest_map if k in task_map]
    common.sort(key=lambda k: rest_map[k][0])

    pairs = []
    for k in common:
        r_list, t_list = rest_map[k], task_map[k]
        if len(r_list) > 1 or len(t_list) > 1:
            msg = f"Chiave '{k}': multiple occorrenze (REST:{len(r_list)} TASK:{len(t_list)}). Uso la prima."
            if fail_on_duplicates:
                raise RuntimeError(msg)
            warnings.warn(msg)
        pairs.append((k, r_list[0], t_list[0]))

    missing_rest = [k for k in task_map if k not in rest_map]
    missing_task = [k for k in rest_map if k not in task_map]
    if missing_rest:
        warnings.warn(f"Mancano REST per: {', '.join(missing_rest)}")
    if missing_task:
        warnings.warn(f"Mancano TASK per: {', '.join(missing_task)}")
    return pairs

# ------------------------- Dati e reporting -------------------------
def extract_data_array(img):
    data = np.asarray(img.dataobj)
    if data.ndim == 4:
        return data.reshape(data.shape[0], data.shape[3])
    if data.ndim == 2:
        return data
    nv = data.shape[0]
    nf = int(np.prod(data.shape[1:]))
    return data.reshape(nv, nf)

def _fmt_num(x: float, dec: str, fmt: str = ".6g") -> str:
    s = format(x, fmt)
    if dec != ".":
        s = s.replace(".", dec)
    return s

def print_pairs_report(pairs, inputs, classes, data=None, vertex_id=None,
                       order=("rest","task"), xtick_labels=("Rest","Task")):
    """
    Report testuale coerente con l'ordine scelto:
    - Colonna 1 = valore lato sinistro; Colonna 2 = valore lato destro; Δ = destro − sinistro.
    """
    print("== COPPIE REST↔TASK PER SOGGETTO ==")
    print(f"Totale coppie: {len(pairs)}")
    header = ["#", "KEY", "REST[idx]", "TASK[idx]"]
    if vertex_id is not None and data is not None:
        header += [f"{xtick_labels[0]}(v{vertex_id})", f"{xtick_labels[1]}(v{vertex_id})", "Δ"]
    print("\t".join(header))

    left_is_task = (order[0] == "task")
    for n, (key, r_idx, t_idx) in enumerate(pairs, start=1):
        rest_id = inputs[r_idx]
        task_id = inputs[t_idx]
        row = [f"{n}", key, f"{rest_id}[{r_idx}]", f"{task_id}[{t_idx}]"]
        if vertex_id is not None and data is not None:
            r = float(data[vertex_id, r_idx])
            t = float(data[vertex_id, t_idx])
            left_val  = t if left_is_task else r
            right_val = r if left_is_task else t
            row += [f"{left_val:.6g}", f"{right_val:.6g}", f"{(right_val-left_val):+.6g}"]
```

```
        print("\t".join(row))

def write_pairs_csv(pairs, inputs, classes, out_path, data=None, vertex_id=None,
                    order=("rest","task"), xtick_labels=("Rest","Task"),
                    csv_sep=";", csv_dec=","):
    """
    CSV coerente con l'ordine scelto:
    - Colonna <xtick_labels[0]> = lato sinistro; <xtick_labels[1]> = lato destro; delta = destro - sinistro.
    """
    if not isinstance(csv_sep, str) or len(csv_sep) != 1:
        warnings.warn(f"Separatore CSV non valido '{csv_sep}', uso ';'")
        csv_sep = ";"

    out_dir = os.path.dirname(out_path)
    if out_dir:
        os.makedirs(out_dir, exist_ok=True)
    header = ["n", "key", "rest_id", "rest_idx", "task_id", "task_idx"]
    if vertex_id is not None and data is not None:
        header += [f"{xtick_labels[0]}_v{vertex_id}", f"{xtick_labels[1]}_v{vertex_id}", "delta"]
    with open(out_path, "w", newline="", encoding="utf-8") as fh:
        w = csv.writer(fh, delimiter=csv_sep)
        w.writerow(["COPPIE REST↔TASK PER SOGGETTO"])
        w.writerow([f"totale_coppie={len(pairs)}"])
        w.writerow([])
        w.writerow(header)

        left_is_task = (order[0] == "task")
        for n, (key, r_idx, t_idx) in enumerate(pairs, start=1):
            rest_id = inputs[r_idx]
            task_id = inputs[t_idx]
            row = [n, key, rest_id, r_idx, task_id, t_idx]
            if vertex_id is not None and data is not None:
                r = float(data[vertex_id, r_idx])
                t = float(data[vertex_id, t_idx])
                left_val  = t if left_is_task else r
                right_val = r if left_is_task else t
                d = right_val - left_val
                row += [
                    _fmt_num(left_val,  csv_dec),
                    _fmt_num(right_val, csv_dec),
                    _fmt_num(d,         csv_dec),
                ]
            w.writerow(row)

# ------------------------- Plot -------------------------
def plot_for_vertex(data2d, vertex_id, pairs, title_base, hemi, xlabel, ylabel,
                    order=("rest","task"), xtick_labels=("Rest","Task"), enable_hover=True):
    r_idx = [r for _, r, _ in pairs]
    t_idx = [t for _, _, t in pairs]
    rv = data2d[vertex_id, r_idx]
    tv = data2d[vertex_id, t_idx]
    subj_labels = [k for k, _, _ in pairs]

    # determina y-left, y-right secondo l'ordine richiesto
    left_is_task = (order[0] == "task")
    y_left  = tv if left_is_task else rv
    y_right = rv if left_is_task else tv

    plt.figure()
    lines = []
    for i, subj in enumerate(subj_labels):
        (line,) = plt.plot([0, 1], [y_left[i], y_right[i]], marker="o")
        line._subj = subj
        line._idx = i
        lines.append(line)

    plt.xticks([0, 1], list(xtick_labels))
    if xlabel:
        plt.xlabel(xlabel)
    if ylabel:
        plt.ylabel(ylabel)
    plt.title(f"{title_base} {vertex_id} — {hemi}")
    plt.tight_layout()

    if enable_hover and HAVE_MPLCURSORS:
        cursor = mplcursors.cursor(lines, hover=True)

        @cursor.connect("add")
        def on_add(sel):
            i = getattr(sel.artist, "_idx", None)
            subj = getattr(sel.artist, "_subj", "Soggetto")
            if i is None:
                sel.annotation.set_text(subj); return
            left_val, right_val = float(y_left[i]), float(y_right[i])
            diff = right_val - left_val
            sel.annotation.set_text(f"{subj}\n{xtick_labels[0]}: {left_val:.3f}\n{xtick_labels[1]}: {right_val:.3f}\nΔ:
{diff:+.3f}")
    elif enable_hover and not HAVE_MPLCURSORS:
        warnings.warn("mplcursors non installato: tooltips disabilitati. Installa con: pip install mplcursors")

```

```python
# ------------------------- main -------------------------
def compute_x_order(x_order_arg: str, class_declared_order):
    """
    Determina l'ordine (sinistra, destra) delle condizioni.
    Ritorna:
      - order: tuple in lower ('rest','task') o ('task','rest')
      - origin: 'manual' | 'auto(rest,task)' | 'auto(task,rest)' | 'fallback'
    """
    # Manuale
    if x_order_arg and x_order_arg.lower() != "auto":
        parts = [s.strip() for s in x_order_arg.split(",")]
        if len(parts) != 2:
            raise ValueError("--x-order deve essere 'auto' oppure 'Rest,Task' o 'Task,Rest'")
        a,b = parts[0].lower(), parts[1].lower()
        if {a,b} != {"rest","task"}:
            raise ValueError("--x-order manuale supporta solo Rest/Task per questo script")
        return (a,b), "manual"

    # Auto: leggi dall'ordine delle righe 'Class'
    decl = [c.lower() for c in class_declared_order]
    if "rest" in decl and "task" in decl:
        if decl.index("rest") < decl.index("task"):
            return ("rest","task"), "auto(rest,task)"
        else:
            return ("task","rest"), "auto(task,rest)"
    # fallback
    return ("rest","task"), "fallback"

def reconcile_xtick_labels(user_xticks: str, order_labels):
    """
    Allinea le etichette testo ai due slot (sinistra, destra) imposti da 'order_labels' (in lower).
    Ritorna: (labels_tuple, swapped_bool, custom_bool)
    """
    if user_xticks:
        parts = [s.strip() for s in user_xticks.split(",")]
        if len(parts) == 2:
            if tuple(order_labels) == ("task","rest"):
                return (parts[1], parts[0]), True, True
            else:
                return (parts[0], parts[1]), False, True
        else:
            warnings.warn("--xticks deve contenere due voci separate da virgola. Uso etichette di default.")
    # default: usa le label standard coerenti con order
    return (order_labels[0].title(), order_labels[1].title()), False, False

def main():
    ap = argparse.ArgumentParser(description="Plot Rest↔Task per uno o più vertici con pairing per NOME soggetto e controllo dell'ordine X.")
    ap.add_argument("--overlay", required=True, help="Percorso al file overlay (.mgh/.mgz)")
    ap.add_argument("--fsgd", required=True, help="Percorso al file .fsgd con Input e classi Rest/Task")
    ap.add_argument("--vertices", required=True, help="Indice/i dei vertici: '105805' oppure '12,34,56' oppure '100-110'")
    ap.add_argument("--title-base", default="Vertice", help="Testo base del titolo (default: 'Vertice')")
    ap.add_argument("--xlabel", default="Condizione", help="Etichetta asse X (default: 'Condizione')")
    ap.add_argument("--ylabel", default="FLAIR cortical intensity (a.u.)", help="Etichetta asse Y (default: 'FLAIR cortical intensity (a.u.)')")
    ap.add_argument("--xticks", default="Rest,Task", help="Etichette dei tick X separate da virgola (default: 'Rest,Task')")
    ap.add_argument("--no-hover", action="store_true", help="Disattiva i tooltip al passaggio del mouse")
    # Modalità di controllo
    ap.add_argument("--check-pairs", action="store_true", help="Stampa l'accoppiamento REST↔TASK per soggetto")
    ap.add_argument("--only-check", action="store_true", help="Esegue solo la stampa di controllo e termina (niente grafici)")
    ap.add_argument("--check-vertex", type=int, default=None, help="(Opz.) Stampa anche i valori Rest/Task per questo vertice")
    # Export CSV
    ap.add_argument("--check-out", default=None, help="(Opz.) Percorso file CSV per esportare le coppie e, se --check-vertex, anche i valori per quel vertice")
    ap.add_argument("--csv-sep", default=";", help="Separatore di campo per CSV (default: ';')")
    ap.add_argument("--csv-dec", default=",", help="Separatore decimale per CSV (default: ',')")
    # Pairing per NOME
    ap.add_argument("--pair-by", choices=["auto","exact","regex"], default="auto", help="Strategia di pairing per nome soggetto (default: auto)")
    ap.add_argument("--key-regex", default=None, help="Regex per estrarre la chiave quando --pair-by=regex (usa il 1° gruppo di cattura se presente)")
    ap.add_argument("--fail-on-duplicates", action="store_true", help="Se presente, i duplicati per la stessa chiave causano errore invece di warning")
    # Nuovo: ordine X
    ap.add_argument("--x-order", default="auto", help="Ordine X: 'auto' (da FSGD) oppure 'Rest,Task' o 'Task,Rest'")
    args = ap.parse_args()

    # Caricamento dati
    img = nib.load(args.overlay)
    data = extract_data_array(img)
    inputs, classes, class_decl = load_fsgd(args.fsgd)
    hemi = infer_hemisphere_from_path(args.overlay)

    # Pairing PER NOME (non per ordine!)
    pairs = build_pairs(inputs, classes, pair_by=args.pair_by, key_regex=args.key_regex, fail_on_duplicates=args.fail_on_duplicates)
    if not pairs:
        sys.exit("Nessuna coppia REST↔TASK trovata con chiavi compatibili. Controlla il tuo FSGD / la regex.")
```

```
351
352     # Ordine X e label coerenti (con log)
353     order_lower, order_origin = compute_x_order(args.x_order, class_decl)
354     xt, swapped, custom_xt = reconcile_xtick_labels(args.xticks, order_lower)
355
356     # LOG informativi
357     if order_origin.startswith("auto"):
358         print(f"[INFO] --x-order auto → rilevato ordine Class nel FSGD: {order_lower[0].title()},{order_lower[1].title()}")
359     elif order_origin == "manual":
360         print(f"[INFO] --x-order manuale → ordine fissato a: {order_lower[0].title()},{order_lower[1].title()}")
361     else:
362         print(f"[INFO] --x-order fallback → uso: {order_lower[0].title()},{order_lower[1].title()}")
363
364     if custom_xt and swapped:
365         print(f"[WARN] --xticks riordinate per rispettare --x-order: {xt[0]} (x=0), {xt[1]} (x=1)")
366
367     # Modalità di controllo / CSV
368     if args.check_pairs or args.only_check or args.check_vertex is not None or args.check_out:
369         print_pairs_report(
370             pairs, inputs, classes,
371             data if args.check_vertex is not None else None,
372             args.check_vertex,
373             order=order_lower, xtick_labels=xt
374         )
375         if args.check_out:
376             write_pairs_csv(
377                 pairs, inputs, classes, args.check_out,
378                 data if args.check_vertex is not None else None,
379                 args.check_vertex,
380                 order=order_lower, xtick_labels=xt,
381                 csv_sep=args.csv_sep, csv_dec=args.csv_dec
382             )
383             print(f"[INFO] CSV scritto in: {args.check_out}")
384         if args.only_check:
385             return
386
387     # Plotting
388     vertices = parse_vertices(args.vertices)
389     for v in vertices:
390         if v < 0 or v >= data.shape[0]:
391             raise IndexError(f"Vertex {v} fuori dai limiti [0..{data.shape[0]-1}]")
392         plot_for_vertex(
393             data, v, pairs, args.title_base, hemi, args.xlabel, args.ylabel,
394             order=order_lower, xtick_labels=xt, enable_hover=(not args.no_hover)
395         )
396
397     plt.show()
398
399 if __name__ == "__main__":
400     main()
401
```

APPENDIX II – A BRIEF INTERVIEW ON SUPR-FLAIR

Question: What does the acronym SUPR-FLAIR stand for?

Answer: SUPR-FLAIR stands for SUrface-PRojected FLAIR. It denotes the projection of voxelwise FLAIR signal intensity onto a reconstructed cortical surface to obtain vertex-wise maps of cortical FLAIR intensity.

Question: What does this method consist of?

Answer: The method consists of: (i) co-registering the subject's FLAIR volume to a high-resolution T1-weighted dataset; (ii) normalizing FLAIR intensity (in our implementation, by dividing voxel intensities by the median white-matter signal); and (iii) sampling the normalized FLAIR signal along the cortical ribbon and projecting the resulting values onto the cortical surface (pial, GWMI, or inflated). The output is a surface "painting" that allows rapid visualization of cortical FLAIR patterns in anatomically meaningful space.

Question: How, when, and by whom was the SUPR-FLAIR method developed?

Answer: SUPR-FLAIR was developed within the presurgical imaging workflow of the "Claudio Munari" Center for Epilepsy Surgery (ASST GOM Niguarda, Milan). It originated from the practical need to integrate FLAIR information into multimodal 3D surgical planning scenes built with FreeSurfer-derived surfaces and 3D Slicer. The initial implementation was created by Francesco Cardinale and collaborators, and subsequently refined through iterative clinical use and methodological development over the following years.

Question: What was the original goal for which SUPR-FLAIR was developed?

Answer: The original goal was surgical planning: to delineate, in a rapid and nearly automatic manner, the topography and extent of MRI-visible cortical lesions that appear hyperintense on FLAIR, avoiding time-consuming manual slice-by-slice contouring and enabling seamless inclusion of lesion-related information in multimodal 3D scenes for SEEG implantation and resective/disconnective procedures.

Question: What is the SUPR-FLAIR-sa method?

Answer: SUPR-FLAIR-sa is the statistical extension of SUPR-FLAIR ("sa" = statistical analysis). It applies surface-based, vertex-wise statistical modeling (typically within a GLM framework) to compare an individual patient's SUPR-FLAIR map against a normative/control dataset, thereby generating significance maps that highlight vertices or clusters where cortical FLAIR intensity differs from the reference population.

Question: What is the main purpose of SUPR-FLAIR-sa?

Answer: Its main purpose is to increase sensitivity to subtle cortical abnormalities, particularly when conventional MRI inspection is negative or equivocal. By providing a statistically grounded "second look," SUPR-FLAIR-sa helps refine topographic hypotheses and can support decisions in advanced diagnostics and presurgical planning (e.g., selection of suspicious regions for SEEG sampling or targeted resection).

Question: Which software tools were used for the SUPR-FLAIR and SUPR-FLAIR-sa methods?

Answer: The SUPR-FLAIR / SUPR-FLAIR-sa workflow relies on a combination of widely used neuroimaging packages plus in-house scripting:

- FreeSurfer: for automated cortical surface reconstruction (recon-all), sampling/projection of FLAIR intensity onto the surface (mri_vol2surf), and surface-based vertex-wise statistics (e.g., mri_glmfit and/or the GUI tool QDEC).
- FSL: for linear intra-subject image registration (FLIRT) and intensity/algebra/statistics operations used during normalization (fslmaths, fslstats, and in some cases fsl-anat/FAST for tissue segmentation support).
- 3D Slicer (including specific extensions when needed): for assembling multimodal 3D scenes and surgical planning (integration of MRI/PET, vasculature, and SEEG electrode models).
- In-house scripts (e.g., a bash-based pipeline such as PHANTOMS): to automate file conversion, registrations, normalization steps, surface sampling calls, and the generation of 3D planning scenes and analysis outputs.

In short, FreeSurfer provides surfaces + vertex-wise mapping/statistics, FSL provides registration and intensity processing, 3D Slicer provides multimodal visualization and planning, and custom scripting glues the pipeline into an end-to-end workflow.

Question: Has a diagnostic performance study of SUPR-FLAIR-sa been performed?

Answer: Yes. A retrospective cohort study was conducted in MRI-negative patients undergoing temporal surgery, assessing the method's performance under prespecified criteria (including definitions of test positivity relative to the resection zone and seizure outcome). While the results indicate clinically meaningful signal, they also highlight limitations related to sample size, reference standard constraints, and control selection.

Question: Can SUPR-FLAIR-sa be used only to study FCD?

Answer: No. Although FCD is a primary target, because subtle dysplastic cortex may produce mild, spatially restricted FLAIR signal changes, the method is not intrinsically lesion-specific. SUPR-FLAIR-sa can be applied to any condition in which cortical FLAIR intensity is expected to deviate from normative patterns, including other epileptogenic substrates and potentially broader neuroinflammatory or network-related processes.

Question: Does SUPR-FLAIR-sa highlight only epileptogenic lesions?

Answer: Not necessarily. SUPR-FLAIR-sa highlights statistical deviations in cortical FLAIR intensity, which may reflect the epileptogenic lesion itself but can also reveal extra-lesional abnormalities. These may reflect network-level pathophysiology, state-dependent effects, postoperative changes, scanner-related biases, or other non-lesional factors. Therefore, results must always be interpreted in clinical context and integrated with electrophysiology and multimodal imaging.

Question: Can SUPR-FLAIR-sa be used to study specific anatomo-functional organizations of the cerebral hemispheres? If so, which ones?

Answer: Yes—at least at an exploratory level. Surface-based analysis of cortical FLAIR patterns in healthy subjects suggests associations with inter-individual functional traits, including language lateralization and manual dominance/dexterity. These findings support the hypothesis that a fraction of cortical FLAIR intensity reflects underlying anatomo-functional organization rather than purely static structure.

Question: Can SUPR-FLAIR-sa be used to study acute cortical FLAIR signal changes?

Answer: Potentially, yes. "Within-subject", paired designs (task vs rest; eyes-open vs eyes-closed conditions) suggest that SUPR-FLAIR-sa can detect small short-timescale modulations in expected

networks (e.g., sensorimotor cortex during finger tapping; visual cortex during eyes-open). While preliminary, these findings indicate that cortical FLAIR may contain a state-dependent component.

Question: Ultimately, is the FLAIR signal exclusively structural?
Answer: The evidence suggests no. FLAIR is strongly influenced by tissue microstructure and water content, but several observations, including extra-lesional signal patterns, postoperative dynamics, and task/state-related modulations, support the view that cortical FLAIR also reflects dynamic physiological and pathophysiological processes (e.g., interstitial water shifts, microvascular exchange, glial metabolism), at least in part.

Question: Can SUPR-FLAIR-sa be used with images acquired on 3T scanners?
Answer: Yes, in principle. The approach is not field-strength dependent. However, its practical applicability depends on data quality, robust surface reconstruction, and, critically, scanner/protocol specificity of the normative dataset. Reliable statistical comparisons require that patients and controls be acquired with sufficiently matched hardware and acquisition settings (and often even comparable software releases).

Question: What are the possible future developments of SUPR-FLAIR-sa?
Answer: Future developments include:

- Improved harmonization across scanners and software versions (e.g., calibration phantoms, advanced normalization, or learning-based harmonization).
- Larger normative datasets (including age-stratified controls and multi-center cohorts).
- Integration with multimodal features (FLAIR + T1/T2-derived morphometry + diffusion/PET) and classifier-based approaches.
- Prospective validation in presurgical pathways, including standardized decision-impact analyses.
- Extension to functional/state paradigms, testing whether FLAIR can serve as a complementary “structural-functional” sensor of cortical physiology on short timescales.
- Incorporation of negative deviations (hypointensities) and bidirectional modeling, rather than focusing only on hyperintensity.

APPENDIX III – SUPR-FLAIR-SA OF A PHD-STUDENT

The final example we wish to illustrate concerns a colleague, M.R., herself a neurosurgeon at the "Claudio Munari" Center for Epilepsy Surgery and a PhD student at the CNR in Parma.

From a technical standpoint, this observation is useful to demonstrate that the SUPR-FLAIR-sa method is also applicable to FLAIR images acquired on a 3T scanner. Indeed, we briefly present the case of a healthy subject who underwent high-field MRI on a 3T scanner (Siemens MAGNETOM Vida, Erlangen, Germany), as did the other 63 healthy subjects used as the control group.

The peculiarity M.R. is that she is an exceptionally fast talker. SUPR-FLAIR-sa reveals numerous areas of relative cortical hyperintensity that clearly involve, among others, key language-related regions. Of particular interest, the distribution of cortical FLAIR hyperintensities largely mirrors the localization of areas activated by two simple fMRI paradigms for language mapping. (Figure 53).

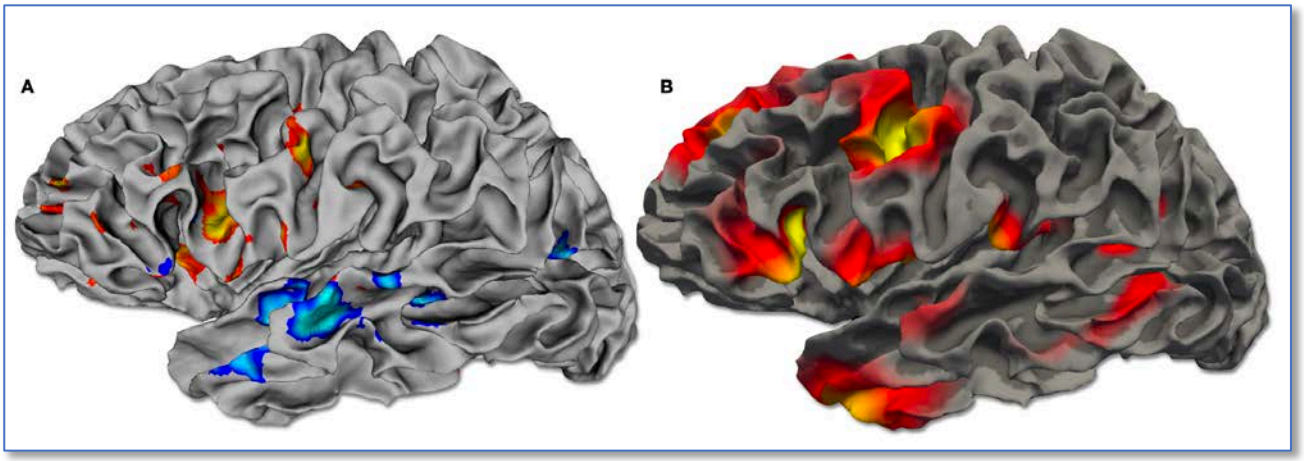

Figure 53: Comparison between language f-MRI and SUPR-FLAIR-sa (subject = M.R.).
(A) Projection onto the GWMI surface of the most significant activation blobs obtained with conventional model-based f-MRI during a phonemic/semantic fluency paradigm (warm colors) and a text-comprehension paradigm (cool colors).
(B) SUPR-FLAIR-sa: multiple fronto-temporal regions of cortical FLAIR hyperintensity overlap with the activation areas identified by -fMRI.

In light of this analysis, which clearly reflects an underlying anatomo-functional organization consistent with the subject's peculiar characteristics, we propose that M.R. attempt a Guinness

World Records contest in the Fastest Talker (English) category[12], thereby bringing visibility to our research groups and increasing the chances of disseminating the work carried out (Figure 54).

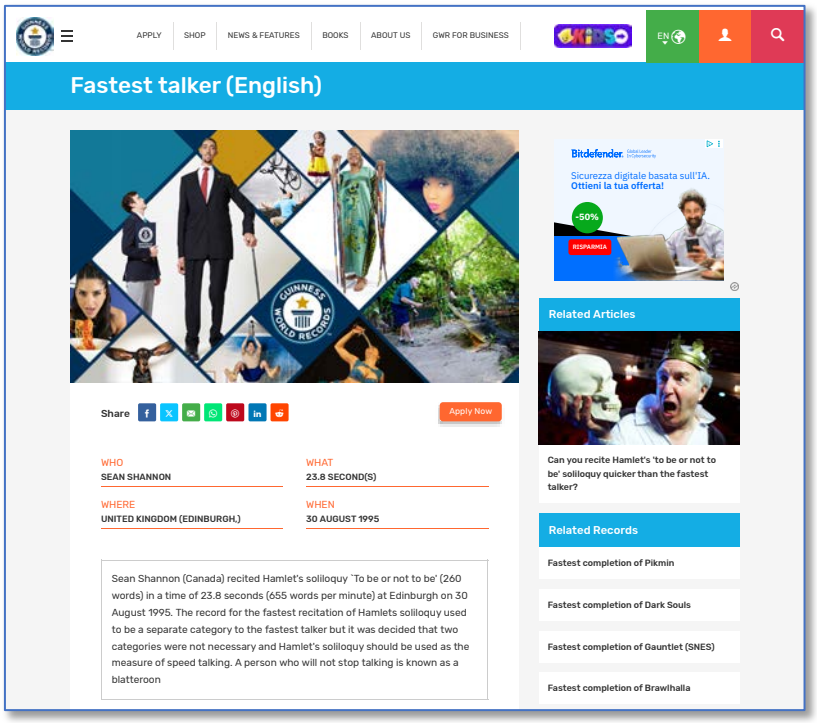

Figure 54: website of Guinness World Records contest in the Fastest Talker (English) category

[12] https://www.guinnessworldrecords.com/world-records/358936-fastest-talker

REFERENCES

1. Abarrategui B, Mariani V, Rizzi M, Berta L, Scarpa P, Zauli FM, Squarza S, Banfi P, D'Orio P, Cardinale F, Del Vecchio M, Caruana F, Avanzini P, Sartori I. Language lateralization mapping (reversibly) masked by nondominant focal epilepsy: a case report. Front Hum Neurosci. 2023;17:1254779.
2. Adler S, Wagstyl K, Gunny R, Ronan L, Bériault S, Cross JH, Fletcher PC, Baldeweg T. Novel surface features for automated detection of focal cortical dysplasias in paediatric epilepsy. NeuroImage Clin. 2017;14:18–27.
3. Adler S, Blackwood M, Northam GB, Gunny R, Hong S-J, Bernhardt BC, Bernasconi A, Bernasconi N, Jacques TS, Tisdall MM, Carmichael DW, Cross JH, Baldeweg T. Multimodal computational neocortical anatomy in pediatric hippocampal sclerosis. Ann Clin Transl Neurol. 2018a;5(10):1200–10.
4. Adler S, Hong S-J, Liu M, Baldeweg T, Cross JH, Bernasconi A, Bernhardt BC, Bernasconi N. Topographic principles of cortical fluid-attenuated inversion recovery signal in temporal lobe epilepsy. Epilepsia. 2018b;59:627–35.
5. Ahmed B, Brodley CE, Blackmon KE, Kuzniecky RI, Barash G, Carlson CE, Quinn BT, Doyle WK, French JA, Devinsky O, Thesen T. Cortical feature analysis and machine learning improves detection of "MRI-negative" focal cortical dysplasia. Epilepsy Behav. 2015;48:21–8.
6. Amunts K, Schlaug G, Schleicher A, Steinmetz H, Dabringhaus A, Roland PE, Zilles K. Asymmetry in the human motor cortex and handedness. Neuroimage. 1996;4(3):216–22.
7. Bai R, Springer CS, Plenz D, Basser PJ. Brain active transmembrane water cycling measured by MR is associated with neuronal activity. Magn Reson Med. 2019;81(2):1280–95.
8. Bernasconi A, Bernasconi N, Bernhardt BC, Schrader D. Advances in MRI for "cryptogenic" epilepsies. Nat Rev Neurol. 2011 Mar;7(2):99–108.
9. Bunyaratavej K, Siwanuwatn R. Three-Dimensional Cortical Surface Reconstruction Versus Operative Findings: Their Similarity and Applications. World Neurosurg. 2017;107:809–19.
10. Cardinale F, Miserocchi A, Moscato A, Cossu M, Castana L, Schiariti MP, Gozzo F, Pero G, Quilici L, Citterio A, Minella M, Torresin A, Lo Russo G. Talairach Methodology in the Multimodal Imaging and Robotics Era. In: Scarabin J-M, editor. Stereotaxy and Epilepsy Surgery. Montrouge: John Libbey Eurotext; 2012. p. 245–72.

11. Cardinale F, Cossu M, Castana L, Casaceli G, Schiariti MP, Miserocchi A, Fuschillo D, Moscato A, Caborni C, Arnulfo G, Lo Russo G. Stereoelectroencephalography: surgical methodology, safety, and stereotactic application accuracy in 500 procedures. Neurosurgery. 2013 Mar;72(3):353–66.
12. Cardinale F, Chinnici G, Bramerio M, Mai R, Sartori I, Cossu M, Lo Russo G, Castana L, Colombo N, Caborni C, De Momi E, Ferrigno G. Validation of FreeSurfer-Estimated Brain Cortical Thickness: Comparison with Histologic Measurements. Neuroinformatics. 2014 May 2;12:535–42.
13. Cardinale F, Pero G, Quilici L, Piano M, Colombo PE, Moscato A, Castana L, Casaceli G, Fuschillo D, Gennari L, Cenzato M, Lo Russo G, Cossu M. Cerebral angiography for multimodal surgical planning in epilepsy surgery: description of a new three-dimensional technique and literature review. World Neurosurg. 2015;84(2):358–67.
14. Chabardès S, Kahane P, Minotti L, Tassi L, Grand S, Hoffmann D, Benabid AL. The temporopolar cortex plays a pivotal role in temporal lobe seizures. Brain. 2005;128(Pt 8):1818–31.
15. Chen J-G, Han K-W, Zhang D-F, Li Z-X, Li Y-M, Hou L-J. Presurgical Planning for Supratentorial Lesions with Free Slicer Software and Sina App. World Neurosurg. 2017;106:193–7.
16. Chepkoech J-L, Walhovd KB, Grydeland H, Fjell AM. Effects of change in FreeSurfer version on classification accuracy of patients with Alzheimer's disease and mild cognitive impairment. Hum Brain Mapp. 2016;37(5):1831–41.
17. Cohen-Adad J. What can we learn from T2* maps of the cortex? Neuroimage. 2014;93:189–200.
18. Cohen NT, You X, Krishnamurthy M, Sepeta LN, Zhang A, Oluigbo CO, Whitehead MT, Gholipour T, Baldeweg T, Wagstyl K, Adler S, Gaillard WD, Ripart M, Whitaker K, Napolitano A, De Palma L, De Benedictis A, Foldes S, Humphreys Z, Zhang K, Hu W, Mo J, Likeman M, Davies S, Güttler C, Lenge M, Tang Y, Wang S, Chari A, Tisdall M, Bargallo N, Conde-Blanco E, Pariente JC, Pascual-Diaz S, Delgado-Martínez I, Pérez-Enríquez C, Lagorio I, Abela E, Mullatti N, O'Muircheartaigh J, Vecchiato K, Liu Y, Caligiuri ME, Sinclair B, Vivash L, Willard A, Kandasamy J, McLellan A, Sokol D, Semmelroch M, Kloster AG, Opheim G, Ribeiro L, Yasuda C, Rossi-Espagnet C, Hamandi K, Tietze A, Barba C, Guerrini R, Gaillard WD, Wang I, González-Ortiz S, Severino M, Striano P, Tortora D, Kälviäinen R, Gambardella A, Labate A, Desmond P, Lui E, O'Brien T, Shetty J, Jackson G, Duncan JS, Winston G, Pinborg LH, Cendes F, Cross JH.

Networks Underlie Temporal Onset of Dysplasia-Related Epilepsy: A MELD Study. Ann Neurol. 2022;92(3):503–11.

19. Colombo N, Tassi L, Deleo F, Citterio A, Bramerio M, Mai R, Sartori I, Cardinale F, Lo Russo G, Spreafico R. Focal cortical dysplasia type IIa and IIb: MRI aspects in 118 cases proven by histopathology. Neuroradiology. 2012 Oct;54(10):1065–77.
20. Dale AM, Fischl BR, Sereno MI. Cortical Surface-Based Analysis. I. Segmentation and Surface Reconstruction. Neuroimage. 1999;194:179–94.
21. Dassonville P, Zhu XH, Uğurbil K, Kim SG, Ashe J. Functional activation in motor cortex reflects the direction and the degree of handedness. Proc Natl Acad Sci U S A. 1997;94(25):14015–8.
22. Dorfer C, Widjaja E, Ochi A, Snead OC, Rutka JT. Epilepsy surgery: recent advances in brain mapping, neuroimaging and surgical procedures. J Neurosurg Sci. 2015;51(2):163–70.
23. d'Orio P, Monteiro P, Otayza JI, Rocca A, Revay M, Castana L, Cardinale F. Stereo-electro-encephalography (SEEG) methodology: technical nuances and insights into image-guided robot-assisted electrode implantation. Neurosurg Focus Video. 2024;11(July):V4.
24. Duncan JS. Imaging in the surgical treatment of epilepsy. Nat Rev Neurol. 2010;6(10):537–50.
25. Duncan JS, Winston GP, Koepp MJ, Ourselin S. Brain imaging in the assessment for epilepsy surgery. Lancet Neurol. 2016;4422(15):1–14.
26. Engel J Jr, Van Ness PC, Rasmussen TB, Ojemann LM. Outcome with respect to epileptic seizures. In: Engel J Jr., editor. Surgical Treatment of the Epilepsies. Second Edition. New York: Raven Press, Ltd.; 1993. p. 609–21.
27. Fedorov A, Beichel R, Kalpathy-Cramer J, Finet J, Fillion-Robin JC, Pujol S, Bauer C, Jennings D, Fennessy F, Sonka M, Buatti J, Aylward S, Miller J V, Pieper S, Kikinis R. 3D Slicer as an image computing platform for the Quantitative Imaging Network. Magn Reson Imaging. 2012;30(9):1323–41.
28. Fischl BR, van der Kouwe AJ, Destrieux C, Halgren E, Ségonne F, Salat DH, Busa E, Seidman LJ, Goldstein J, Kennedy D, Caviness V, Makris N, Rosen BR, Dale AM. Automatically Parcellating the Human Cerebral Cortex. Cereb Cortex. 2004 Jan 1;14(1):11–22.
29. Fischl BR. FreeSurfer. Neuroimage. 2012 Jan 10;62:774–81.
30. Focke NK, Symms MR, Burdett JL, Duncan JS. Voxel-based analysis of whole brain FLAIR at 3T detects focal cortical dysplasia. Epilepsia. 2008;49(5):786–93.

31. Focke NK, Bonelli SB, Yogarajah M, Scott C, Symms MR, Duncan JS. Automated normalized FLAIR imaging in MRI-negative patients with refractory focal epilepsy. Epilepsia. 2009;50(6):1484–90.
32. Foundas AL, Hong K, Leonard CM, Heilman KM. Hand Preference and Magnetic Resonance Imaging Asymmetries of the Central Sulcus. Neuropsychiatry, Neuropsychol Behav Neurol. 1998;11(2):65–71.
33. Garbelli R, Milesi G, Medici V, Villani F, Didato G, Deleo F, D'Incerti L, Morbin M, Mazzoleni G, Giovagnoli AR, Parente A, Zucca I, Mastropietro A, Spreafico R. Blurring in patients with temporal lobe epilepsy: clinical, high-field imaging and ultrastructural study. Brain. 2012 Aug;135(Pt 8):2337–49.
34. Genovese M, Arcasensa A, Morbelli S, Lenge M, Barba C, Mirandola L, Caligiuri ME, Caulo M, Panzica F, Cardinale F, Rossi-Espagnet C, Tortora D, Vaudano AE. SWANe: Standardized workflow for advanced neuroimaging in epilepsy. SoftwareX. 2024;26(April):101703.
35. Geschwind N, Levitsky W. Human brain: Left-right asymmetries in temporal speech region. Science. 1968;161(3837):186–7.
36. Giovagnoli AR, Parisi A. Fifty Years of Handedness Research: A Neurological and Methodological Update. Brain Sci. 2024;14:418.
37. Good CD, Johnsrude I, Ashburner J, Henson RN, Friston KJ, Frackowiak RS. Cerebral asymmetry and the effects of sex and handedness on brain structure: A voxel-based morphometric analysis of 465 normal adult human brains. Neuroimage. 2001;14(3):685–700.
38. Grabowska A, Gut M, Binder M, Forsberg L, Rymarczyk K, Urbanik A. Switching handedness: fMRI study of hand motor control in right-handers, left-handers and converted left-handers. Acta Neurobiol Exp (Wars). 2012;72(4):439–51.
39. Gronenschild EH, Habets P, Jacobs H IL, Mengelers R, Rozendaal N, van Os J, Marcelis M. The Effects of FreeSurfer Version, Workstation Type, and Macintosh Operating System Version on Anatomical Volume and Cortical Thickness Measurements. PLoS One. 2012 Jun 1;7(6):e38234.
40. Guadalupe T, Willems RM, Zwiers MP, Arias Vasquez A, Hoogman M, Hagoort P, Fernandez G, Buitelaar J, Franke B, Fisher SE, Francks C. Differences in cerebral cortical anatomy of left- and right-handers. Front Psychol. 2014;5(MAR):1–8.
41. Haller S, Kövari E, Herrmann FR, Cuvinciuc V, Tomm AM, Zulian GB, Lovblad KO, Giannakopoulos P, Bouras C. Do brain T2/FLAIR white matter hyperintensities correspond to

myelin loss in normal aging? A radiologic-neuropathologic correlation study. Acta Neuropathol Commun. 2013;1:14.

42. Hajnal JV, Collins AG, White SJ, Pennock JM, Oatridge A, Baudouin CJ, Young IR, Bydder GM. Imaging of human brain activity at 0.15 T using fluid attenuated inversion recovery (FLAIR) pulse sequences. Magn Reson Med. 1993;30(5):650–3.
43. Hamilton LS, Narr KL, Lüders E, Szeszko PR, Thompson PM, Bilder RM, Toga AW. Asymmetries of cortical thickness: Effects of handedness, sex, and schizophrenia. Neuroreport. 2007;18(14):1427–31.
44. Hervé PY, Mazoyer B, Crivello F, Perchey G, Tzourio-Mazoyer N. Finger tapping, handedness and grey matter amount in the Rolando's genu area. Neuroimage. 2005;25(4):1133–45.
45. Hong S-J, Kim H, Schrader D, Bernasconi N, Bernhardt BC, Bernasconi A. Automated detection of cortical dysplasia type II in MRI-negative epilepsy. Neurology. 2014;83:48–55.
46. Huppertz H-J, Grimm C, Fauser S, Kassubek J, Mader I, Hochmuth A, Spreer J, Schulze-Bonhage A. Enhanced visualization of blurred gray-white matter junctions in focal cortical dysplasia by voxel-based 3D MRI analysis. Epilepsy Res. 2005;67(1–2):35–50.
47. Huppertz H-J, Wagner J, Weber B, House PM, Urbach H. Automated quantitative FLAIR analysis in hippocampal sclerosis. Epilepsy Res. 2011;97(1–2):146–56.
48. Jang H, Lee JY, Lee K Il, Park KM. Are there differences in brain morphology according to handedness? Brain Behav. 2017;7:e00730.
49. Jenkinson M, Smith SM. A global optimisation method for robust affine registration of brain images. Med Image Anal. 2001 Jun;5(2):143–56.
50. Jenkinson M, Beckmann CF, Behrens TE, Woolrich MW, Smith SM. Fsl. Neuroimage. 2012 Aug 15;62(2):782–90.
51. Karaarslan E, Arslan A. Perirolandic cortex of the normal brain: Low signal intensity on turbo FLAIR MR images. Radiology. 2003;227(2):538–41.
52. Karlsson EM, Ocklenburg S. Leftward asymmetry of the planum temporale and its association with language. Brain Struct Funct. 2025;230(6).
53. Kedarasetti RT, Turner KL, Echagarruga C, Gluckman BJ, Drew PJ, Costanzo F. Functional hyperemia drives fluid exchange in the paravascular space. Fluids Barriers CNS. 2020;17:52.
54. Klöppel S, van Eimeren T, Glauche V, Vongerichten A, Münchau A, Frackowiak RS, Büchel C, Weiller C, Siebner HR. The effect of handedness on cortical motor activation during simple bilateral movements. Neuroimage. 2007;34(1):274–80.

55. Le Bihan D, Urayama SI, Aso T, Hanakawa T, Fukuyama H. Direct and fast detection of neuronal activation in the human brain with diffusion MRI. Proc Natl Acad Sci USA. 2006;103(21):8263–8.
56. LeMay M, Culebras A. Human Brain — Morphologic Differences in the Hemispheres Demonstrable by Carotid Arteriography. N Engl J Med. 1972;287(4):168–70.
57. Lüders E, Cherbuin N, Thompson PM, Gutman B, Anstey KJ, Sachdev P, Toga AW. When more is less: Associations between corpus callosum size and handedness lateralization. Neuroimage. 2010;52(1):43–9.
58. Månsson KN, Cortes DS, Manzouri A, Li T-Q, Hau S, Fischer H. Enlargement in the Human Visual Cortex. Cereb Cortex. 2020;30:851–7.
59. Minkin K, Gabrowsky K, Penkov M, Todorov Y, Tanova R, Milenova Y, Romansky K, Dimova P. Stereoelectroencephalography Using Magnetic Resonance Angiography for Avascular Trajectory Planning: Technical Report. Neurosurgery. 2017;81(4):688–95.
60. Munari C, Bancaud J. The role of stereo-electroencephalography (SEEG) in the evaluation of partial epileptic seizures. In: Porter RJ, Morselli PL, editors. The Epilepsies. Bodmin: Butterworth & Co. (Publishers) Ltd; 1985. p. 267–306.
61. Nierhaus T, Vidaurre C, Sannelli C, Mueller K-R, Villringer A. Immediate brain plasticity after one hour of brain–computer interface (BCI). J Physiol. 2021;599(9):2435–51.
62. Nowell M, Rodionov R, Zombori G, Sparks R, Winston GP, Kinghorn J, Diehl B, Wehner T, Miserocchi A, McEvoy AW, Ourselin S, Duncan JS. Utility of 3D multimodality imaging in the implantation of intracranial electrodes in epilepsy. Epilepsia. 2015;56(3):403–13.
63. Ocklenburg S, Friedrich P, Fraenz C, Schlüter C, Beste C, Güntürkün O, Genç E. Neurite architecture of the planum temporale predicts neurophysiological processing of auditory speech. Sci Adv. 2018;4(7):1–8.
64. Ocklenburg S, Mundorf A, Peterburs J, Paracchini S. Genetics of human handedness: microtubules and beyond. Trends Genet. 2025;41(6):497–505.
65. Olivo G, Lövdén M, Manzouri A, Terlau L, Jenner B, Jafari A, Petersson S, Li T-Q, Fischer H, Månsson KN. Estimated gray matter volume rapidly changes after a short motor task. Cereb Cortex. 2022;32:4356–69.
66. Pieper S, Halle M, Kikinis R. 3D Slicer. In: 2004 2nd IEEE International Symposium on Biomedical Imaging: Macro to Nano. Ieee; 2004. p. 632–5.

67. Powell JL, Kemp GJ, Roberts N, García-Finaña M. Sulcal morphology and volume of Broca's area linked to handedness and sex. Brain Lang. 2012;121(3):206–18.
68. Qin P, Bi Q, Guo Z, Yang L, Li H, Li P, Liang X, Luo J, Kong X, Xiong Y, Sun B, Ocklenburg S, Gong G. Microstructural asymmetries of the planum temporale predict functional lateralization of auditory-language processing. Elife. 2024;13:RP95547.
69. Repanshek Z, Haneef Z, Vendrame M, Jacobson M, Azizi A. Transient brain MRI changes after prolonged seizures. In: American Epilepsy Society 2007 Annual Meeting. 2007. p. 1084.
70. Ripart M, Spitzer H, Williams LZ, Walger L, Chen A, Napolitano A, Rossi-Espagnet C, Foldes ST, Hu W, Mo J, Likeman M, Rüber T, Caligiuri ME, Gambardella A, Guttler C, Tietze A, Lenge M, Guerrini R, Cohen NT, Wang I, Kloster A, Pinborg LH, Hamandi K, Jackson G, Tortora D, Tisdall M, Conde-Blanco E, Pariente JC, Perez-Enriquez C, Gonzalez-Ortiz S, Mullatti N, Vecchiato K, Liu Y, Kalviainen R, Sokol D, Shetty J, Sinclair B, Vivash L, Willard A, Winston GP, Yasuda CL, Cendes F, Shinohara RT, Duncan JS, Cross JH, Baldeweg T, Robinson EC, Iglesias JE, Adler S, Wagstyl K. Detection of Epileptogenic Focal Cortical Dysplasia Using Graph Neural Networks A MELD Study. JAMA Neurol. 2025;82(4):397–406.
71. Rosas HD, Liu A, Hersch SM, Glessner M, Ferrante R, Salat DH, van der Kouwe AJ, Jenkins B, Dale AM, Fischl BR. Regional and progressive thinning of the cortical ribbon in Huntington's disease. Neurology. 2002;58:695–701.
72. Scorza D, El Hadji S, Cortés C, Bertelsen A, Cardinale F, Baselli G, Essert C, De Momi E. Surgical planning assistance in keyhole and percutaneous surgery: a systematic review. Med Image Anal. 2021;67:101820.
73. Sha Z, Pepe A, Schijven D, Carrion-Castillo A, Roe JM, Westerhausen R, Joliot M, Fisher SE, Crivello F, Francks C. Handedness and its genetic influences are associated with structural asymmetries of the cerebral cortex in 31,864 individuals. Proc Natl Acad Sci USA. 2021;118(47):e2113095118.
74. Shadlen MN, Kandel ER. Nerve cells, neural circuitry, and behavior. In: Kandel ER, Koester JD, Mack SH, Siegelbaum SA, editors. Principles of Neural Science. 6th ed. McGraw-Hill; 2021.
75. Singh LN, Higano S, Takahashi S, Kurihara N, Furuta S, Tamura H, Shimanuki Y, Mugikura S, Fujii T, Yamadori A, Sakamoto M, Yamada S. Comparison of ipsilateral activation between right and left handers: A functional MR imaging study. Neuroreport. 1998;9(8):1861–6.
76. Solodkin A, Hlustik P, Noll D, Small S. Lateralization of motor circuits and handedness during finger movements. Eur J Neurol. 2001;8(5):425–34.

77. Sone D, Beheshti I. Clinical Application of Machine Learning Models for Brain Imaging in Epilepsy: A Review. Front Neurosci. 2021;15(June):684825.
78. Sparks R, Vakharia VN, Rodionov R, Vos SB, Diehl B, Wehner T, Miserocchi A, McEvoy AW, Duncan JS, Ourselin S. Anatomy-driven multiple trajectory planning (ADMTP) of intracranial electrodes for epilepsy surgery. Int J Comput Assist Radiol Surg. 2017;12:1245–55.
79. Spencer SS, Huh L. Outcomes of epilepsy surgery in adults and children. Lancet Neurol. 2008 Jun;7(6):525–37.
80. Spitzer H, Ripart M, Whitaker K, D'Arco F, Mankad K, Chen AA, Napolitano A, De Palma L, De Benedictis A, Foldes S, Humphreys Z, Zhang K, Hu W, Mo J, Likeman M, Davies S, Güttler C, Lenge M, Cohen NT, Tang Y, Wang S, Chari A, Tisdall MM, Bargallo N, Conde-Blanco E, Pariente JC, Pascual-Diaz S, Delgado-Martínez I, Pérez-Enríquez C, Lagorio I, Abela E, Mullatti N, O'Muircheartaigh J, Vecchiato K, Liu Y, Caligiuri ME, Sinclair B, Vivash L, Willard A, Kandasamy J, McLellan A, Sokol D, Semmelroch M, Kloster AG, Opheim G, Ribeiro L, Yasuda CL, Rossi-Espagnet C, Hamandi K, Tietze A, Barba C, Guerrini R, Gaillard WD, You X, Wang I, González-Ortiz S, Severino M, Striano P, Tortora D, Kälviäinen R, Gambardella A, Labate A, Desmond P, Lui E, O'Brien T, Shetty J, Jackson GD, Duncan JS, Winston GP, Pinborg LH, Cendes F, Theis FJ, Shinohara RT, Cross JH, Baldeweg T, Adler S, Wagstyl K. Interpretable surface-based detection of focal cortical dysplasias: a Multi-centre Epilepsy Lesion Detection study. Brain. 2022;145(11):3859–71.
81. Taubert M, Draganski B, Anwander A, Müller K, Horstmann A, Villringer A, Ragert P. Dynamic properties of human brain structure: Learning-related changes in cortical areas and associated fiber connections. J Neurosci. 2010;30(35):11670–7.
82. Téllez-Zenteno JF, Ronquillo LH, Moien-Afshari F, Wiebe S. Surgical outcomes in lesional and non-lesional epilepsy: A systematic review and meta-analysis. Epilepsy Res. 2010;89(2–3):310–8.
83. Thesen T, Quinn BT, Carlson CE, Devinsky O, DuBois J, McDonald CR, French JA, Leventer R, Felsovalyi O, Wang X, Halgren E, Kuzniecky RI. Detection of epileptogenic cortical malformations with surface-based MRI morphometry. PLoS One. 2011 Jan;6(2):e16430.
84. Tringali G, Bono B, Dones I, Cordella R, Didato G, Villani F, Prada F. Multimodal Approach For Radical Excision Of Focal Cortical Dysplasia By Combining Advanced MRI Data To Intraoperative Ultrasound, Electrocorticography And Cortical Stimulation: A Preliminary Experience. World Neurosurg. 2018;113:E738–46.

85. Tzourio-Mazoyer N, Crivello F, Mazoyer B. Is the planum temporale surface area a marker of hemispheric or regional language lateralization? Brain Struct Funct. 2018;223(3):1217–28.
86. Uhlig M, Reinelt JD, Lauckner ME, Kumral D, Schaare HL, Mildner T, Babayan A, Möller HE, Engert V, Villringer A, Gaebler M. NeuroImage Rapid volumetric brain changes after acute psychosocial stress. Neuroimage. 2023;265:119760.
87. Van Essen DC. A Population-Average, Landmark- and Surface-based (PALS) atlas of human cerebral cortex. Neuroimage. 2005;28(3):635–62.
88. Van Essen DC, Glasser MF, Dierker DL, Harwell J, Coalson TS. Parcellations and hemispheric asymmetries of human cerebral cortex analyzed on surface-based atlases. Cereb Cortex. 2012;22(10):2241–62.
89. Van Essen DC, Glasser MF. In vivo architectonics: A cortico-centric perspective. Neuroimage. 2014;93:157–64.
90. Volkmann J, Schnitzler A, Witte O, Freund H. Handedness and asymmetry of hand representation in human motor cortex. J Neurophysiol. 1998;79(4):2149–54.
91. Vollmar C, Noachtar S, Winkler PA. Multimodal image processing in pre-surgical planning. In: Lüders HO, editor. Textbook of Epilepsy Surgery. Second Edition. London: informa healthcare; 2008. p. 771–7.
92. Wagstyl K, Adler S, Pimpel B, Chari A, Seunarine K, Lorio S, Thornton RC, Baldeweg T, Tisdall MM. Planning stereoelectroencephalography using automated lesion detection: Retrospective feasibility study. Epilepsia. 2020;61(7):1406–16.
93. Wagstyl K, Whitaker K, Raznahan A, Seidlitz J, Vértes PE, Foldes S, Humphreys Z, Hu W, Mo J, Likeman M, Davies S, Lenge M, Cohen NT, Tang Y, Wang S, Ripart M, Chari A, Tisdall MM, Bargalló N, Conde-Blanco E, Pariente JC, Pascual-Diaz S, Delgado-Martínez I, Pérez-Enríquez C, Lagorio I, Abela E, Mullatti N, O'Muircheartaigh J, Vecchiato K, Liu Y, Caligiuri ME, Sinclair B, Vivash L, Willard A, Kandasamy J, McLellan A, Sokol D, Semmelroch M, Kloster A, Opheim G, Yasuda CL, Zhang K, Hamandi K, Barba C, Guerrini R, Gaillard WD, You X, Wang ZI, González-Ortiz S, Severino M, Striano P, Tortora D, Kalviainen R, Gambardella A, Labate A, Desmond P, Lui E, O'Brien T, Shetty J, Jackson GD, Duncan JS, Winston GP, Pinborg LH, Cendes F, Cross JH, Baldeweg T, Adler S. Atlas of lesion locations and postsurgical seizure freedom in focal cortical dysplasia: A MELD study. Epilepsia. 2022;63:61–74.
94. Walch E, Fiacco TA. Honey, I shrunk the extracellular space: Measurements and mechanisms of astrocyte swelling. Glia. 2022;70(11):2013–31.

95. Wang ZI, Alexopoulos A V, Jones SE, Jaisani Z, Najm IM, Prayson RA. The pathology of magnetic-resonance-imaging-negative epilepsy. Mod Pathol. 2013;26(8):1051–8.
96. Wasserthal C, Brechmann A, Stadler J, Fischl BR, Engel K. Localizing the human primary auditory cortex in vivo using structural MRI. Neuroimage. 2014;93:237–51.
97. Wiebe S, Blume WT, Girvin JP, Eliasziw M. A randomized, controlled trial of surgery for temporal-lobe epilepsy. N Engl J Med. 2001;345(5):311–8.
98. Witelson SF. The Brain Connection: The Corpus Callosum Is Larger in Left-Handers. Science (80-). 1985;229:665–8.
99. Yeo BTT, Krienen FM, Sepulcre J, Sabuncu MR, Lashkari D, Hollinshead M, Roffman JL, Smoller JW, Zollei L, Polimeni JR, Fischl BR, Liu H, Buckner RL. The organization of the human cerebral cortex estimated by intrinsic functional connectivity. J Neurophysiol. 2011;106:1125–65.
100. Zaretskaya N, Fink E, Arsenovic A, Ischebeck A. Fast and functionally specific cortical thickness changes induced by visual stimulation. Cereb Cortex. 2023;33(6):2823–37.
101. Zhao B, Zhang C, Wang X, Wang Y, Liu C, Mo J, Zheng Z, Zhang K, Shao X-Q, Hu W, Zhang J. Sulcus-centered resection for focal cortical dysplasia type II: surgical techniques and outcomes. J Neurosurg. 2021;135(July):266–72.